SYNTHESIS AND BIOLOGICAL EVALUATION OF ENANTIOPURE SUBSTITUTED TITANOCENE COMPLEXES

MELCHIOR CINI, M.Sc.

Thesis submitted to the University of Nottingham for the degree of Doctor of Philosophy

JULY 2015

Abstract

Tolerated by normal tissues, implementation of anti-cancer therapies based on titanium compounds is limited by low efficacy/selectivity, lack of understanding of their mode(s) of action and access to the most active chiral variants. This thesis reports the synthesis, characterization and biological evaluation of a novel class of chiral substituted titanocenes from novel chiral cyclopentadienyl ligands, themselves accessible from substituted pentafulvenes.

After an introductory chapter, the second chapter describes the synthesis and biological evaluation of substituted (*rac*/*meso*)-mixtures of $TiCl_2\{\eta\text{-}C_5H_4CHEt(phenyl)\}_2$ (abbreviated $Cp^R{}_2TiCl_2$). Addition of a substituted pentafulvene to alkyl/branched-alkyl/phenyl Grignard solutions with catalytic copper catalyst resulted in the formation of novel racemic/tautomeric cyclopentadienyl ligands in yields of up to 92%. The deprotonation of the racemic substituted cyclopentadienyl ligands with *n*-butyllithium and subsequent transmetallation with titanium(IV) tetrachloride resulted in the formation of novel substituted titanocene complexes in yields up to 81%. The antiproliferative activities of the (*rac*/*meso*)-mixtures of titanocenes in comparison to the simple benzyl-substituted titanocene analogue, titanocene dichloride and cisplatin were then evaluated *in vitro* against HCT-116, MiaPaCa-2 and MDA-MB-468 carcinoma cell lines, which represented intractable cancers from three different organ sites. All chiral substituted titanocenes were micromolar active against all the studied cancer cell lines. Finally, cyclic voltammetry studies using chiral substituted titanocenes were carried which confirmed a close to optimal fit of the chiral substituted ethyl titanocene.

The third chapter reports the synthesis and biological evaluation of single enantiomers of $TiCl_2\{\eta\text{-}C_5H_4CHEt(2\text{-}MeOPh)\}_2$ (abbreviated $Cp^R{}_2TiCl_2$), attained through unprecedented asymmetric copper-catalysed addition of $ZnEt_2$ to the C=C bond of substituted pentafulvenes $C_5H_4(=CHAr)$ (Ar = 2-MeOPh and related species). Such enantioselective reaction resulted in enantiomerically enriched (up to 93:7 *e.r.*) cyclopentadienyl ligands. Copper catalyst promotion with both chiral phosphoramidite ligands and a phosphate additive was vital in realizing both acceptable enantioselectivies and reaction rates. Chloride hydrolysis of the enantiopure titanocene to $[Cp^R{}_2Ti(OH)]^+$ can be detected by NMR, GCMS and LCMS *in vitro* under near therapeutic conditions. The anti-cancer potency of (*S,S*)-$Cp^R{}_2TiCl_2$ was twice that of other stereoisomers, selective for cancer cells, and the kinetics of formation of the soluble hydroxy species correlate with the latter being the biologically active species. Extensive cytoplasmic vacuolization, endoplasmic reticulum (ER) swelling and activation of MAPKinase signal transduction were consistent with ligand-induced paraptosis (type III cell death), which is morphologically distinct from, and independent of, caspase-mediated apoptosis in MDA-MB-468 and HCT-116 cells.

Table of Contents

Abstract 2

Table of contents 5

Acknowledgements 7

Abbreviations 8

Chapter 1 - Introduction 10

1.1 Cancer - the unmet need for new therapies 10

1.2 Why chiral enantiopure drugs? 12

1.3 Platinum complexes as antitumor drugs 14

1.3.1 Cisplatin mode of action 14

1.3.2 Cisplatin resistance 16

1.3.3 Derivatives of cisplatin 18

1.4 Titanocene complexes as antitumor drugs 19

1.4.1 Cancerostatic activity of titanocene dichloride 19

1.4.2 Titanocenes mode of action 21

1.5 Chiral substituted bis(η5-cyclopentadienyl)titanium 27

1.5.1 Metallocene formation 27

1.5.2 Pentafulvene derived titanocene complexes 29

1.6 Thesis aims 35

Chapter 2 - (*rac*/*meso)*-titanocenes 36

2.1 Introduction 36

2.2 Literature approaches - racemic cyclopentadienyl ligands 36

2.3 Proposed route 39

2.4 Synthesis of racemic substituted cyclopentadienyl ligands 40

2.5 Synthesis of chiral rac/meso substituted titanocene complexes 44

2.6 Growth inhibitory studies 49

2.7 Electrochemical study 52

Chapter 3 - Enantiopure titanocenes 56

3.1 Introduction 56

3.2 Enantio-enriched substituted cyclopentadienyl ligands 61

3.2.1 Grignard reagent trials 61

3.2.2 Organolithium trials 64

3.2.3 Organozinc/organoaluminium trials 64

3.2.4 Scope of reaction 76

3.3 Synthesis of enantiopure titanocenes 79

3.4 Biological studies 83

3.4.1 MTT analysis 83

3.4.2 Clonogenic Assay 87

3.4.3 Hydrolysis studies $Cp^{R}_{2}Ti(IV)$ speciation 90

3.4.3.1 Mass Spectrometry 90

3.4.3.2 NMR Spectroscopy 92

3.4.3.3 Comparison with literature results 94

3.4.4 Dual cell cycle / DNA damage 96

3.4.5 Dual annexin V-FITC/PI 99

3.4.6 Paraptosis (type III cell death) 102

3.4.6.1 Microscopy Imaging 102

3.4.6.2 MAPK pathway - kinase screening 109

3.5 Conclusion 112

Chapter 4 - Experimental 114

4.1 Chemistry Section 114

4.1.1 General experimental 114

4.1.2 Preparation of pentafulvene derivatives 115

4.1.3 Preparation of chiral cyclopentadienyl derivatives 131

4.1.4 Preparation of chiral titanocene derivatives 162

4.2 Biology section 171

4.2.1 Cell culture 171

4.2.2 Growth inhibitory studies *in vitro* 171

4.2.3 Clonogenic assays 171

4.2.4 Annexin V-FITC/PI apoptosis assay 173

4.2.5 Cell cycle & Dual DNA damage (γh2ax) / cell cycle analysis 174

4.2.6 Confocal microscopy - live imaging 176

4.2.7 Relative protein phosphorylation 176

4.2.8 Western Blot Analysis 176

4.2.9 ICP-MS studies 178

4.3 TEM studies 179

4.3.1 Instrument / cell culture 179

References 181

Acknowledgements

First and foremost I should like to thank my supervisor, Professor Simon Woodward for his continuous support throughout the course of this work. I greatly appreciate his continuous encouragement, dedication, enthusiasm and availability, in this fascinating yet challenging project. My gratitude also extends to my co-supervisor, Assistant Professor Tracey Bradshaw for her honest thoughts and advice.

Particular thanks goes to Dr. William Lewis, Dr. Huw Williams, Denise McLean and Dr. Scott Young for their assistance with X-ray crystallography, NMR facilities, TEM sectioning and ICP-MS respectively. Thanks also goes to to the technical and analytical staff namely: Shazad, Kevin, Dane, Eric, Chris and Jim. I'd also like to sincerely thank the University of Nottingham and the Edith Johnson Bequest for funding this PhD project.

I should also like to acknowledge past and present members of the Woodward group and Bradshaw group, most notably Laurence Burroughs, Benoit Wahl, Darren Willcox, Lee Eccleshare, Phil Andrews, Christopher M. Latham, Vijay Raja, Anchala Kuruppu, Mohannad Al-kazzaz and Mohammed Al-Hayali.

Last but not least, a big thanks goes to my family and friends for their constant support and encouragement.

Abbreviations

CpR	substituted cyclopentadienyl, η^5-C_5H_4R
MAPK	mitogen-activated protein kinase
ERK1/2	extracellular signal-regulated kinase 1 and 2
mrp-2	multidrug resistance-associated protein 2
chk1	checkpoint kinase 1
Gadd45a	Growth arrest and DNA-damage 45a
NCI	National Cancer Institute
pKa	acid dissociation constant
PK/PD	Pharmacokinetic/Pharmacodynamic
ADME	Absorption, distribution, metabolism and excretion
IC_{50}	half maximal inhibitory concentration
GI_{50}	concentration that inhibits cell proliferation by 50%
MTT	3-(4,5-dimethylthiazol-2-yl)-2,5-diphenyltetrazolium bromide
er	enantiomeric ratio
dr	diastereomeric ratio
COSY	Correlation Spectroscopy
HMQC	Heteronuclear Multiple-Quantum Correlation
HMBC	Heteronuclear Multiple-Bond Correlation
DEPT	Distortionless Enhancement by Polarization Transfer
MTBE	methyl *tert*-butyl ether
EI	electron impact
ER	endoplasmic reticulum
BINAP	2,2'-bis(diphenylphosphino)-1,1'-binaphthyl

TMEDA	*N*,*N*-tetramethylethylene diamine
PS	phosphatidyl serine
PI	propidium iodide
ZVAD-FMK	carbobenzoxy-valyl-alanyl-aspartyl-[O-methyl]-fluoromethylketone
TEM	Transmission electron microscopy
EDX	Energy-dispersive X-ray spectroscopy
EELS	Electron energy loss spectroscopy

Chapter 1 - Introduction

1.1 Cancer – the unmet need for new therapies

Cancer is defined as the collection of related diseases involving abnormal cell growth and division forming tumors. Malignant cancerous cells that spread into or invade nearby tissues are called invasive whilst those cells that migrate to other parts of the body to form new tumors are called metastatic. Unlike malignant tumors, some tumors are neither invasive nor metastatic and are therefore benign.[1] According to WHO estimates for 2011, mortality caused by cancer now surpasses that through coronary heart diseases and strokes.[2] Worldwide cancer incidence and mortality estimates in 2012 revealed 14.1 million new cases and 8.2 million deaths (Figure 1). It is estimated that 20 million new cancer cases will be expected annually throughout the world in 2025.[2] The most common cancer in the world in 2012 was lung cancer, both in terms of new cases (1.8 million, 12.9% total) and deaths (1.6 million, 19.4% total). The second most common cancer is breast cancer (1.7 million cases, 11.9% total) but since it has a relatively better prognosis, it ranks 5th in cancer related death (0.5 million, 6.4% total). Triple negative (basal-like) breast cancers do not express estrogen receptor, progesterone receptor or human epidermal growth factor receptor 2, tend to affect younger women, are aggressive and more resistant to therapy.[3] Colorectal cancer had the third most common incidence rate (1.4 million, 9.7% total) with a death rate of 0.7 million cases in 2012. Pancreatic cancer has a very poor prognosis (mortality:incidence ratio of 0.98). In fact, the mortality rate (seventh most common cause of cancer death) is relatively higher than its incidence rate (twelfth). The primary cause of this pattern worldwide seems to relate to under diagnosis and the unmet need which is development of new therapies.[2]

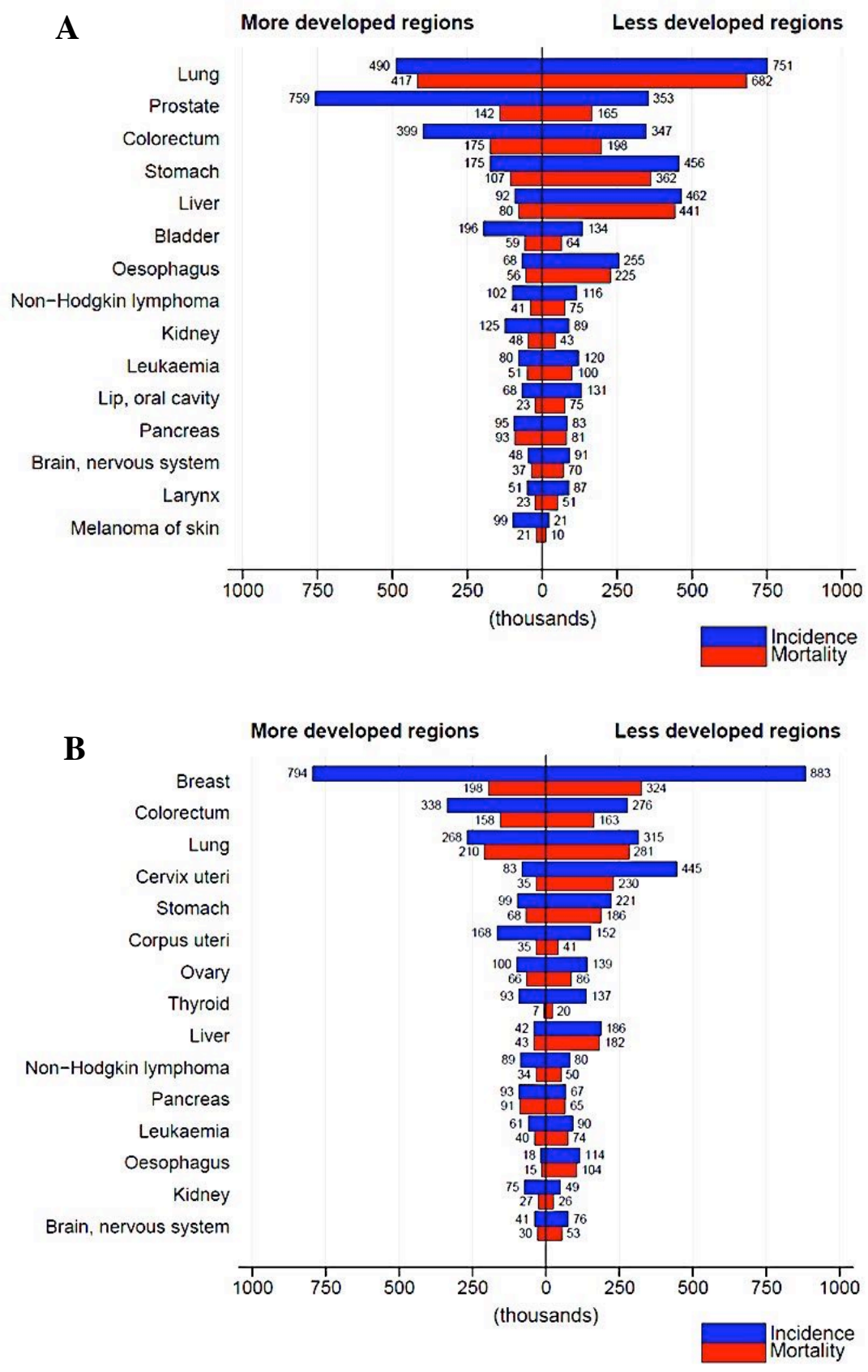


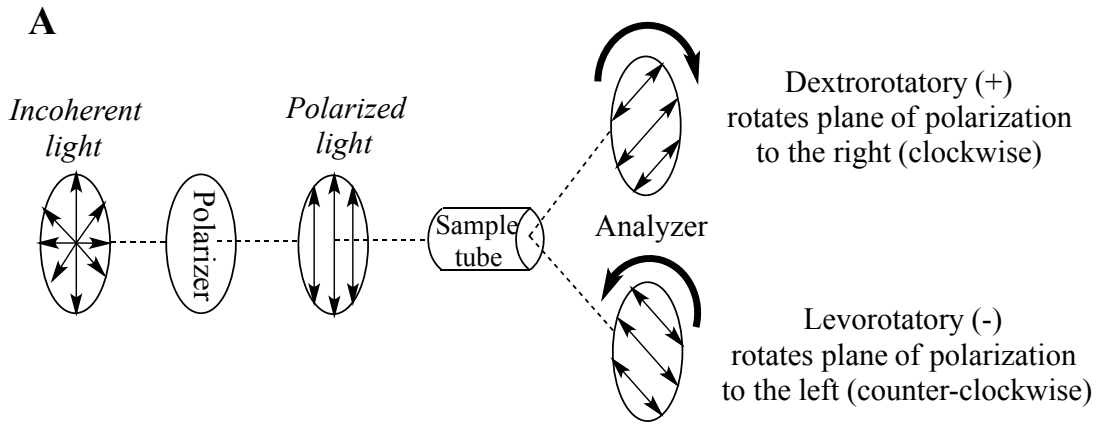
Figure 1. Estimated numbers (thousands) of new cancer incidence and mortality in more developed and less developed regions of the world in men (a) and women (b) in 2012.[2]

1.2 Why chiral enantiopure drugs?

Chirality is ubiquitous in nature and is of fundamental importance in the design, discovery and development of new drugs.[4] Enantiomeric drugs are classified as either racemic or single enantiomers with one or more chiral centers. A pharmaceutical racemate contains an equimolar mixture of two non-superimposable mirror image enantiomers whilst an enantiopure drug is available in one specific purified enantiomeric form. Each enantiomer affects plane polarized light differently; its optical rotation is measured by a polarimeter (Figure 2A).[5] Living organisms are made up of chiral enantiopure compounds. All 21 essential amino acids possess a (-)-configuration whilst most carbohydrates have a (+)-configuration.[4]

Development of a new chiral drug can result from two scenarios; *de novo* synthesis of an enantiomerically pure drug or a switch from an existing racemic drug to one of its enantiomers in a pure form.[4] The latter scenario can offer both potential enhanced therapy and a marketing strategy to further profitability due to patent extension benefits.[4]

Enantiomers in a racemate drug can behave differently in biological environments. Apart from selectivity for receptors, transporters and enzymes, two enantiomers can also significantly differ in the bioavailability, rate of metabolism, metabolites, excretion, potency and toxicity (Figure 2B).[6] A striking example is in the chiral drug Ethambutol **1**. The two enantiomers of this drug had an entirely different interaction with their biological target. The (+)-enantiomer is a bacteriostatic drug prescribed to treat tuberculosis whilst the other (-)-enantiomer causes blindness.[7] Another example is in the development of the anti-cancer chiral platinum drugs, which is detailed in Section 1.3.

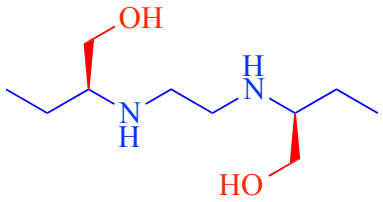


B

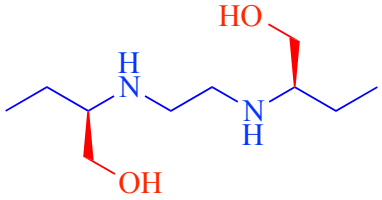
Potential advantages of chiral enantiopure drugs;

- Less complex, more selective pharmacodynamic profile
- Potential for an improved therapeutic index
- Less complex pharmacokinetic profile
- Reduced potential for complex drug interaction
- Less complex relationship between plasma concentration and effect

treatment of tubercolosis;

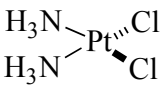


(+)-(*S*,*S*)-**1** - Tuberculostatic

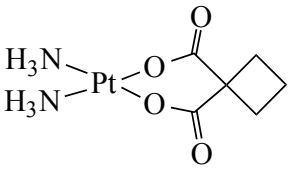


(-)-(*R*,*R*)-**1** - Causes blindness

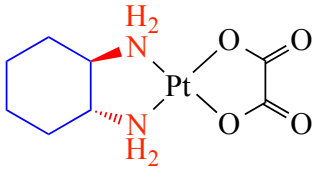
anticancer therapy;



cisplatin **2**
First-generation
Pt drug



carboplatin **3**
Second-generation
Pt drug



oxaliplatin **4**
Third-generation Pt drug
trans isomer (1*R*,2*R*) more effective than *trans* (1*S*,1*S*) and *cis* (1*R*,2*S*) isomer

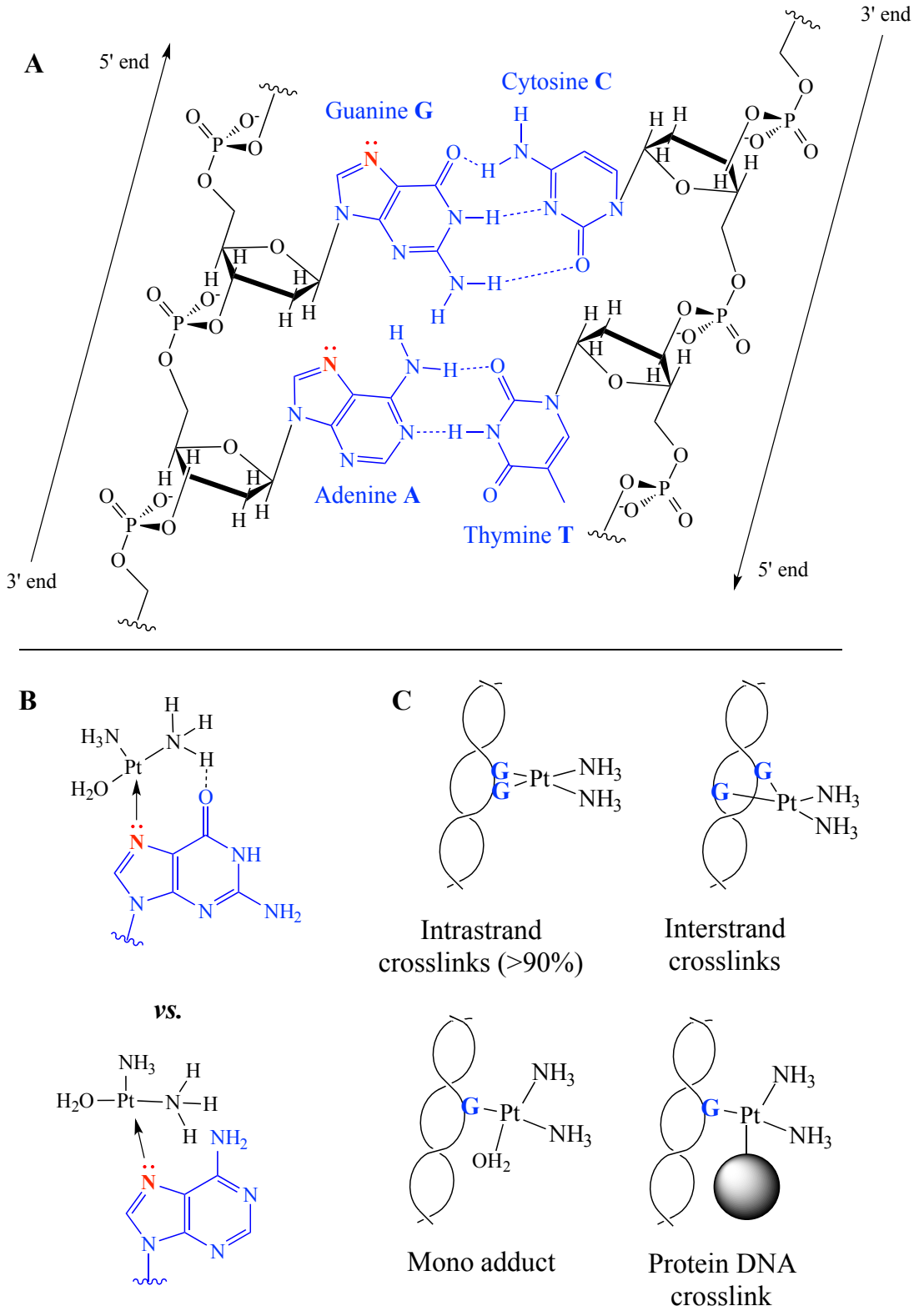
Figure 2: Chiral enantiopure drugs **A** Measurement of optical rotation through polarimetry.[5] **B** Potential advantages of chiral enantiopure drugs.[8]

Cisplatin **2**, the first generation of platinum drugs discovered serendipitously by Rosenberg in the late 1960s, is used as an adjuvant therapy for the treatment of a range of tumors, and is a lead compound in anticancer research.[9] The drug works by inducing DNA damage, resulting in inhibition of DNA synthesis, suppression of RNA transcription and effects on the cell cycle, ultimately leading to apoptosis. Cisplatin offered excellent initial response (≤70%) to ovarian cancer patients although tumors become resistant to therapy quite rapidly (patient 5-year survival rate of only 15-20%).[10] Unfortunately, tumors resistant to cisplatin are often also cross-resistant to diverse unrelated antitumor drugs.[11] Cisplatin limitations also include a broad range of toxicity and detrimental kidney toxicity.[12]

1.3 Platinum complexes as antitumor drugs

1.3.1 Cisplatin mode of action

Cisplatin hydrolysis occurs spontaneously upon hydration with water ligands. The highly reactive mono-aquated species is rate limited by the interaction and potential vulnerability to many endogenous nucleophiles such as glutathione, methionine, metallothionein and other proteins.[13] Aquated cisplatin species exerts its cytotoxicity by interaction with nucleophilic *N*7-sites of purine bases in DNA to form DNA-protein and DNA-DNA intra and interstrand crosslinks (Scheme 1).[14] Intrastrand crosslinks account for more than 90% of total lesions. Platinum binds more rapidly to guanine purine bases than adenine due to its higher pKa basicity and by hydrogen bonding of the amine-NH to the *O*6 of guanosine as evidenced in Scheme 1.[15] In fact, about two thirds of all platinum was reported to bind at guanine-guanine purines in intrastrand crosslinks.[16] A linear correlation was reported between the amount of DNA bound to platinum and its cytotoxicity.



Scheme 1: A Platinum binds to DNA at *N*7 sites of guanine and to a lesser extent adenosine, resulting in a kink in the DNA which disrupts DNA replication and transcription. **B** Platinum binding to Guanine is kinetically favored due to hydrogen bonding between the amine NH of platinum and ketone *O*6 of guanine. **C** More than 90% of platinum binding to DNA results in intrastrand crosslinks.

Recognition of intrastrand DNA damage by over 20 individual proteins starts a cascade, which ultimately results in apoptosis.[17] Cell cycle activation checkpoints are reported to occur as a result of cisplatin induced DNA damage. A transient S-phase arrest is induced temporally followed by a long-lasting G2/M arrest due to inhibition of the Cdc2-cyclin A or B kinase.[18,19] Activation of the p53 tumor suppressor protein is also a direct consequence of DNA damage. DNA damage recognition proteins activate ATR kinase, which phosphorylates and activates p53 at serine 15.[20] Various genes are transactivated by p53 after cisplatin exposure, including the CDK inhibitor p21 and the DNA damage-inducible Gadd45a gene. The Gadd45a protein enhances the nucleotide excision repair (NER) complex to repair the DNA and hence promotes cell survival. Apoptosis is activated when the DNA damage is beyond repair.[21] ATR kinase protein also activates other downstream targets such as CHK1 kinase and the MAPKinase pathway. All three major subfamily MAPK kinases (including the extracellular signal-regulated kinases (ERK), the c-Jun N-terminal kinases (JNK) and the p38 kinases) (Figure 3) are activated following tumor cell exposure to cisplatin resulting in regulation of cell proliferation, differentiation, survival and death.[22]

1.3.2 Cisplatin resistance

Cisplatin resistance occurs as a result of intracellular changes that reduce the drug's ability to either interact and damage the DNA or interfere with DNA damaging signals.[23,24] These intracellular changes can be attributed to either an inhibition in the drug uptake or an increase in drug efflux, or both. Resistant cells contain increased levels of the transporter multidrug resistant protein MRP2. Cells overexpressing the MRP2 protein following MRP2 gene transfection resulted in a 10-fold increase in cisplatin resistance.[25] Conversely, an increase in cisplatin sensitivity was observed

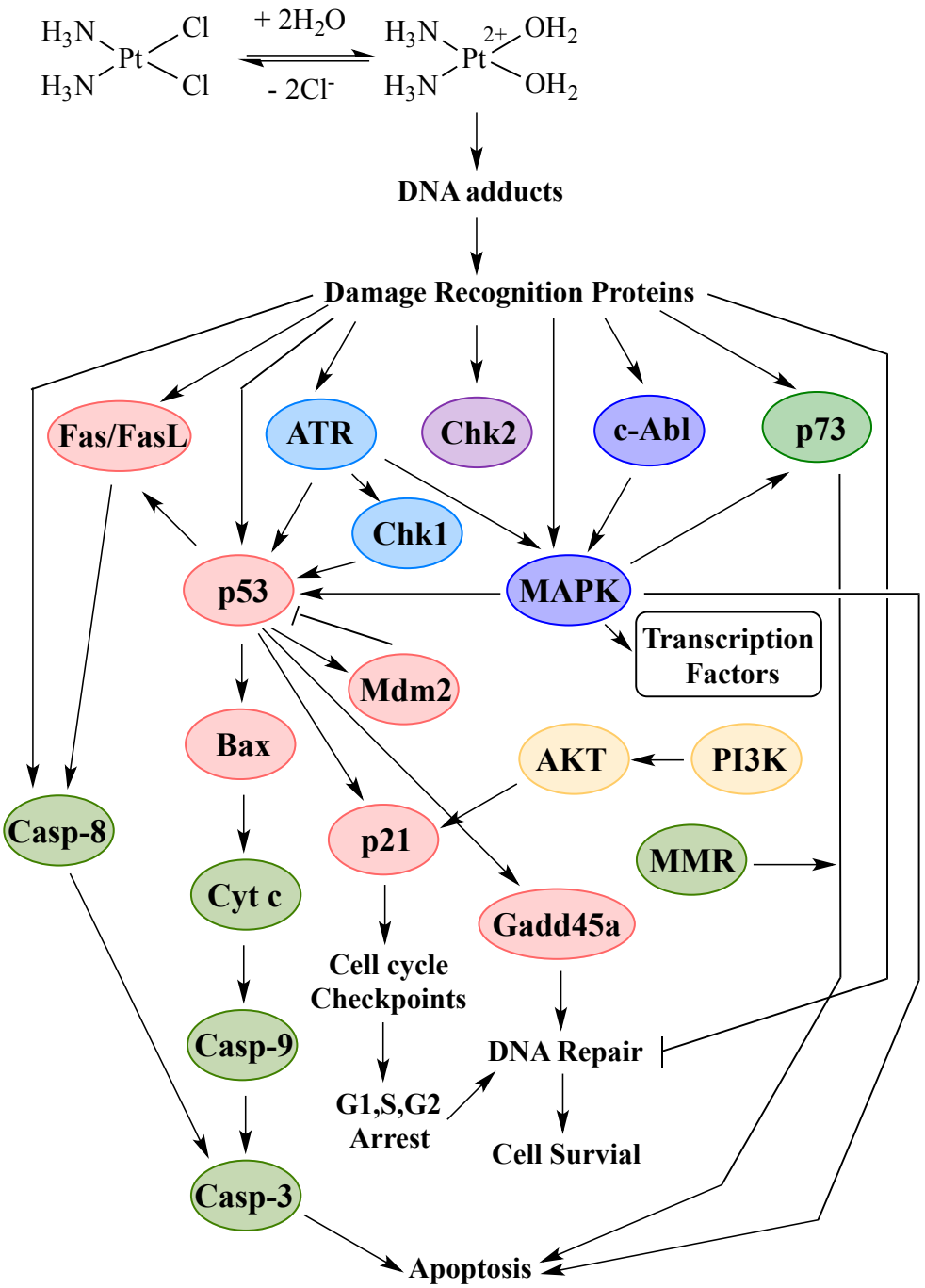


Figure 3: An overview of the pathways involved in mediating cisplatin-induced cellular effects.[13]

by transfection of tumor cells with an MRP2 antisense expression vector.[26] The overexpression of both ATP7A and ATP7B copper-transporting P-type ATPase proteins in cisplatin resistant tumor cells has been attributed to enhanced cisplatin efflux.[27]

1.3.3 Derivatives of cisplatin

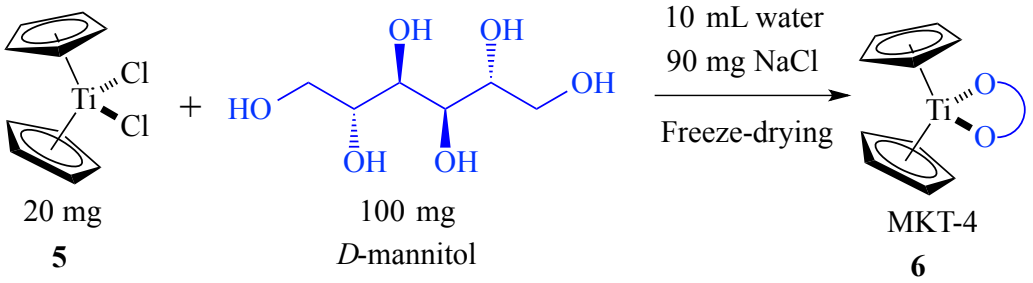
Replacement of the chlorine ligands with carboxylates led to the formation of carboplatin **3** – a more water-soluble derivative. Carboplatin managed to reduce some of the toxic side effects of cisplatin without compromising activity. However, carboplatin is only active against the same range of tumors as cisplatin.[12] The turning point in the generation of effective platinum drugs was platinum ligation with a single enantiomer of (*R,R*)-1,2-diaminocyclohexane forming oxaloplatin **4**. The trans (1*R*,2*R*) isomer was found to have a much higher activity than the trans (1*S*,2*S*) and achiral cis (1*R*,2*S*) isomers in leukemia, colon and melanoma tumor cell subpanels whist the achiral cis (1*R*,2*S*) exhibited greater activity towards leukemia, lung and ovary tumor cell subpanels.[28] Oxaliplatin also provided lower toxic side effects than cisplatin, had positive outcomes against cisplatin resistant cell lines and showed antitumor activity against colorectal carcinoma.[12] Non cross-resistance of the hydrophobic and bulkier oxaliplatin with respect to the two amines of cisplatin is proposed to occur *via* different recognition by various cellular proteins (mismatch repair proteins), DNA polymerases and DNA damage recognition proteins.[28] Although, *in vitro* cisplatin-resistant tumor cell lines obtained through continuous exposure of increasing drug concentrations are quite different from clinically resistant phenotypes. In fact, a recent systematic literature survey has shown that oxaliplatin is cross-resistant to cisplatin in low-level resistant cell lines and in patients with cisplatin resistant cancers.[29]

1.4 Titanocene complexes as antitumor drugs

1.4.1 Cytostatic activity of titanocene dichloride

The 'bent sandwich' metallocene dichloridobis(η^5-cyclopentadienyl)titanium (titanocene dichloride) **5** is a clinically trialed anti-cancer agent of lower *in vivo* tissue toxicity than the more commonly encountered Pt-based drugs (cisplatin, carboplatin). Köpf and Köpf Meier in 1979, first reported the cancerostatic activity of **5** on mice injected with tumor cells.[30] Extensive anti-tumor investigations were carried out on **5** against various experimental tumor systems transplanted in mice. These included leukemias L1210 and P388[31], Lewis lung carcinomas[32], colon 38 carcinoma and B16 melanoma[33], solid sarcoma 180[34], fluid and solid Ehrich ascites tumors in CF1 mice[35] and xenografted human tumors of the colon, rectum, stomach, lung, breast head and neck.[32,33,36] Survival of 80-90% of CF1 mice with Ehrlich ascites tumor without any tumor re-manifestation was obtained with a single intraperitoneal injection of titanocene **5**.[35] Also, significant growth inhibition of up to 90% was observed against a range of human gastrointestinal carcinomas and a growth inhibition of up to 80% in colon and Lewis lung carcinoma and B16 melanoma.[32] Having shown that titanocene **5** had medium antiproliferative activity *in vitro* but promising results *in vivo*, the compound was clinically trialed. Two separate Phase I clinical trials were reported in 1998.[37,38] In the first Phase I clinical trial, twenty patients with advanced cancer were given a weekly dose of a lyophilized form of titanocene **5** dissolved in a malate buffer (MKT5). Freeze-drying in a pH 3.2 malate buffer was carried out in order to prevent hydrolytic instability of **5**. Escalating doses from 70 to 185 mg/m^2 of MKT5 were administered to patients in order to determine the maximum tolerated dose and the dose-limiting toxicities. The maximum tolerated dose recommended for Phase II clinical trials was found to be

140 mg/m^2/wk.[37] In the second Phase I study, forty patients with refractory solid malignancies were treated every three weeks with a dose-escalation clinical trial of a lyophilized form of **5** (MKT4) (Scheme 2). Two minor responses for bladder carcinoma and non-small cell lung cancer were observed. Hepatotoxicity was observed in only three out of thirty-nine assessable patients, which was linked to rapidly progressive liver metastases. In addition, other adverse effects attributed to MKT4 lyophilized titanocene **6** included metallic taste, anorexia, nausea, vomiting and pain during infusion. The maximum tolerated dose was found to be 315 mg/m^2 and the recommended dose for Phase II evaluation, was found to be 240 mg/m^2, given every three weeks, with isotonic saline hydration to reduce renal toxicity.[38]



Scheme 2: Preparation of lyophilized titanocene MKT-4.[39]

Phase II clinical evaluation of the cytostatic agent **6** was conducted in fifteen patients with metastatic breast cancer. Unfortunately, an intravenous administration of **6** at a dose of 240-270 mg/m^2 every three weeks was not effective for these patients and only two patients received a minor positive response. Apart from no objective remission, patients also suffered from drug-related toxicities.[40] In another Phase II clinical study, fourteen patients with metastatic renal-cell carcinoma received 270 mg/m^2 titanocene dichloride every three weeks for six weeks. Although mild to moderate toxicity and side effects were reported, no partial or complete response to the treatment were detectable.[41]

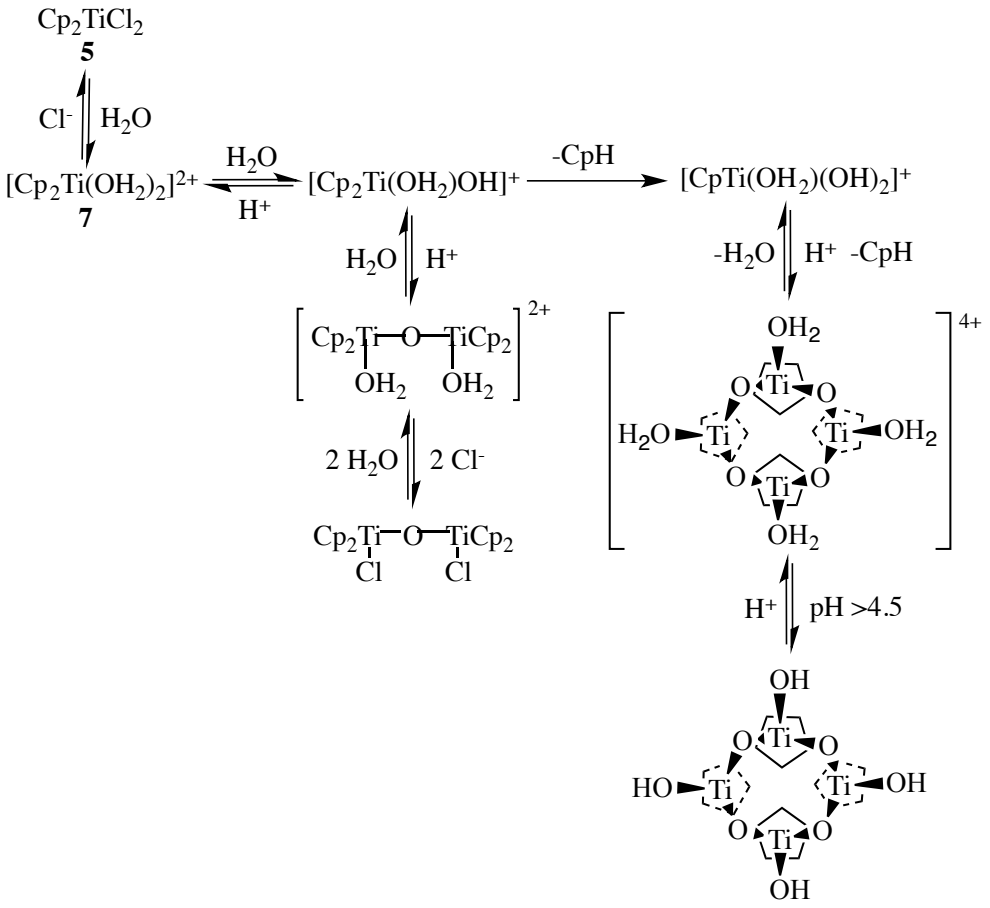
1.4.2 Titanocene modes of action

Tolerated by normal tissues, implementation of anti-cancer therapies based on titanium compounds is still limited by the lack of understanding of the active species and its mode(s) of action, low efficacy/selectivity and access to the most chiral variants. Although often suggested to be DNA binders,[42] the mode of action of titanocenes is clearly distinct from cisplatin, as evidenced by the lack of cross-resistance, nucleic acid metabolism and differences in their anti-tumor profiles against the NCI 60 cell line panel.[42]

The main anti-tumor activity exerted by titanocene complexes is suggested to occur *via* accumulation in nucleic acid rich regions of the nucleus, which in turn inhibits the synthesis of RNA and DNA.[43,44] This is particularly evidenced by the early reports of Köpf Maier whereby TEM samples of Ehrlich ascites tumor cells treated with titanocene **5** were EELS analyzed, revealing intracellular titanium localization, particularly within the nucleic chromatin.[45,46] However, although both cisplatin and titanocene **5** share a common MCl_2 unit, only weak binding of titanocene **5** to DNA nucleotides was reported at physiological pH, possibly due to extensive hydrolysis of titanocene **5** at pH 7.[47] The introduction of methyl substituents on Cp rings of titanocene **5** greatly enhanced the stability of mononucleotide adducts at physiological pH 7, partly due to a drastic decrease in substitued-Cp hydrolysis.[48]

The hydrolysis of the parent titanocene **5** has been extensively reported.[47,48,49] Hydrolysis of the chloro ligands occurs very rapidly in aqueous solutions resulting in the formation of aqua-, hydroxo-, μ-hydroxo- or μ-oxo-bridged species, depending on the pH value and concentration (Scheme 4). In unbuffered water containing 0.32 M KNO_3 at 37 ºC, titanocene **5** undergoes reversible rapid hydrolysis of the first

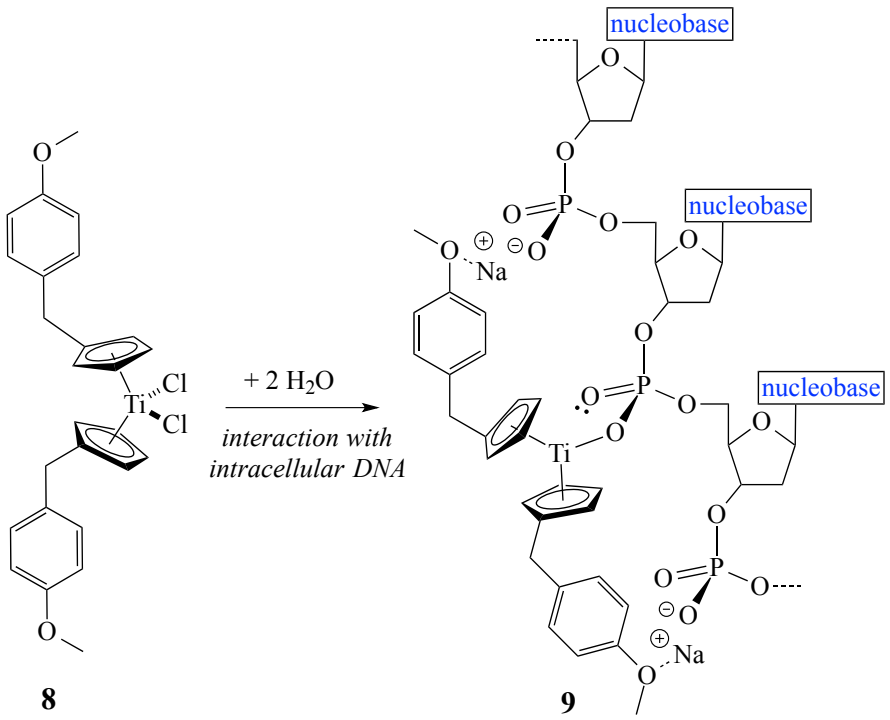
chloride ligand followed by a slower dissociation of second chloride ($t_{1/2} \approx 50$ min), leading to the diaqua species **7**. In contrast to cisplatin, titanocene **5** is also susceptible to ligand (cyclopentadienide) loss, resulting in insoluble uncharacterizable precipitates. The half-life for the loss of cyclopentadienide from **5** was reported to be 57 ± 0.9 h at 37 °C showing approximately first-order kinetics.[49]



Scheme 3: The complex equilibria resulting from dissolution of titanocene in water at physiological pH.[50]

A hydrolysis experiment was also carried out on the anti-cancer active substituted achiral Titanocene Y **8**.[51] At a pD of 2.5, (1 mM, DMSO/D_2O 1:4) over the course of 72 h, the signals intensities of titanocene Y **8** were found to decrease resulting in uncharacterized species. At a pD of 4.4, (1 mM, DMSO/D_2O 1:4), significant amounts of precipitate occurred immediately. No signals of **8** were found after 20 h at pD 4.4.[51]

Computational studies on the interaction of aqueous titanocene Y **9** ((η^5-C_5H_4-CH_2-C_6H_4-OCH_3)$_2$$Ti^{2+}$ cation) revealed titanium bound to phosphate diester groups. The two *p*-methoxybenzyl groups of the diaqua species were computationally found to interact with two sodium counterions bound to two neighbouring phosphate groups in the DNA.[52] The fact that titanium(IV) is a hard lewis acid suggests that the negatively charged oxygen atoms on the phosphate group of polymeric DNA might be a good interaction site. Extensive evidence of the binding interaction between titanocene and nucleotides has been reported, although such studies are arguably not a true representation for polymeric DNA. In fact, such results might not be relevant to the true interactions that take place between the compound and DNA in the cell.[44] Other alternative targets have been proposed for titanocene **5** including inhibition of enzymes kinase C (regulates cellular proliferation)[53] and human topoisomerase II (regulates DNA replication),[54] binding to protein transferrin and/or serum albumin.

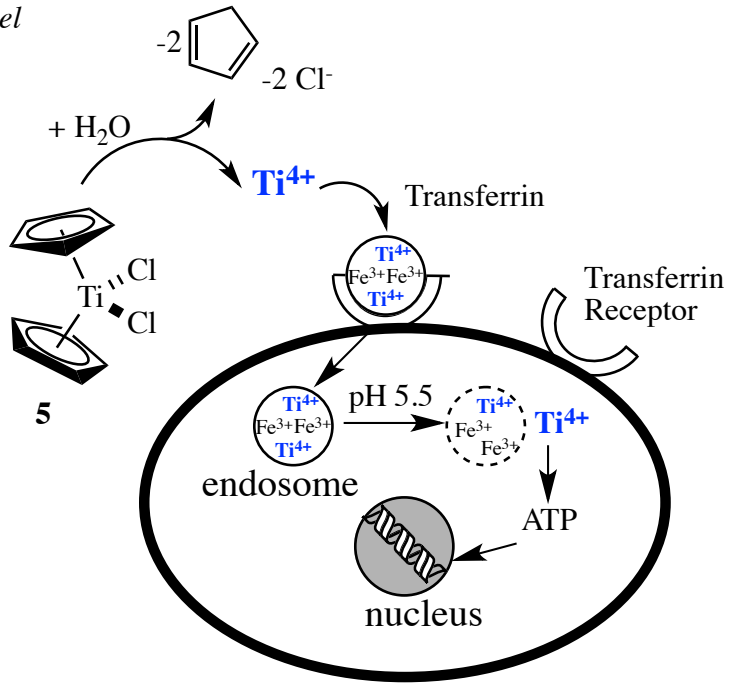


Scheme 4: Schematic view of the possible coordination mode of the (η^5-C_5H_4-CH_2-C_6H_4-OCH_3)$_2$$Ti^{2+}$ cation (Titanocene **7**) with DNA phospho diester groups.[51]

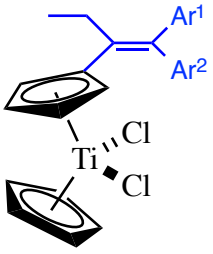
Two antagonistic pools of experimental data have built up in the last fifteen years regarding cellular uptake of hydrolyzed titanocenes. Sadler elegantly showed that titanocene **5** is sequestered by apo-transferrin under physiological conditions of 100 mM NaCl, 25 mM hydrogencarbonate and 4 mM phosphate, pH 7.4 at 25 ^{o}C resulting in both chloride and cyclopentadienyl loss leading to a Ti^{4+} species. It is thought that transferrin provides a 'Trojan horse' for the delivery of this Ti^{4+} species to 'iron hungry' cancer cells (Scheme 5A).[55,56,57] NMR transferrin metal-induced conformational changes studies confirm this theory; Ti^{4+} from titanocene **5** is first loaded to the C-lobe of transferrin followed by the N-lobe, resulting in a stable Ti_2-Tf complex. This Ti_2-Tf complex is then intracellularly transported in endosomal membrane-bounded compartments leading to release of both Ti^{4+} ions when in contact with ATP, followed by binding to DNA nucleic acid regions.[43,58] Sadler and his co-workers also showed that titanium loaded transferrin binds to the transferrin receptor on the surface of the cell as Ti_2-Tf blocked the uptake of radioactive ^{59}Fe-Tf into BeWo cells.[58]

However, several studies demonstrate that the addition of transferrin to cell-viability assays did not improve the cytotoxicity of a range of Ti^{4+} complexes in several cell lines, albeit with titanocene **5**, in some cases (Scheme 5B).[59-62] Also, metabolic hydrolysis of cyclopentadienyl ligands in electron-rich substituted titanocenes is known to be slower than **5** and transferrin binding of these has not been comprehensively documented.[56,57] If the Sadler 'naked' Ti^{4+} model operates alone for the growth inhibitory activity of all titanocenes, the extreme range of biological activity (IC_{50} 5-1000+ μM) of Cp-substituted titanocenes is hard to rationalise. For example, a particular substituted titanocene with a tamoxifen-derived substitutent on the cyclopentadienyl ligand **10** promoted cancer proliferation in the hormone

A - *Sadler model*



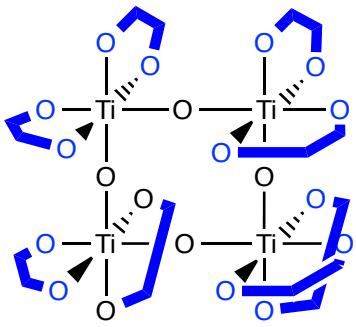
B - *Non Sadler model*



Titanocifen

10

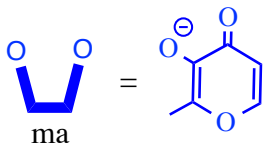
promotes hormone dependent breast cancer proliferation



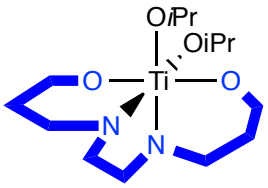
$[Ti_4(ma)_8(\mu\text{-}O)_4]\ 18H_2O$

11

where ma*;*



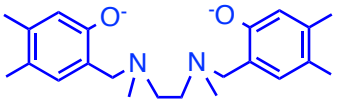
ma

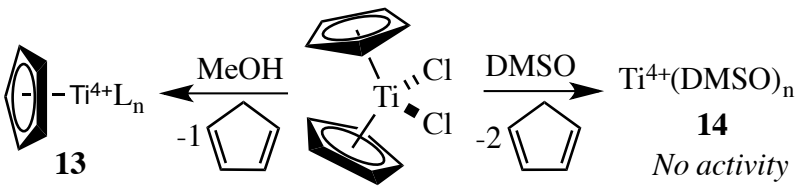


cis-$[Ti(L^3)(O\mathit{i}Pr)_2]$

12

where L^3 =





13

Increased activity

14

No activity

Scheme 5: A While there is good evidence that all of the 'Cp' and 'Cl' units of titanocene **5** can be hydrolyzed and uptake by transferrin into the cell, this is complicated by conflicting evidence **B**.

dependent breast cell line MCF7.[55] The oxo-bridged maltolate soluble $Ti(\mu\text{-}O)_4(ma)_8$ **11** is reported not to transfer titanium(IV) to apo-transferrin, but is still cytotoxic towards HT-29 colon cancer cells. Similarly, for the highly cytotoxic titanium(IV) salan **12** only low binding to apo-transferrin and DNA has been reported.[43,63] The mono-Cp titanocene **13** obtained from hydrolytic pre-treatment of **5** with methanol also increases the activity of **5**, but not under conditions promoting complete chloride/cyclopentadienyl loss **14**.[64]

Reversible binding of antitumor drugs to albumin can offer an alternative for titanium uptake as cancer cells are known to be leaky for albumin. Research showed that titanocene Y **8** has a cytotoxic effect only in the presence of serum albumin when tested on the estrogen-dependent breast cancer cell line MCF-7.[65] Drug uptake is potentially facilitated across the endothelial cell wall of blood vessels of tumors through the albumin receptor-mediated transport pathway.[65] Recent molecular docking experiments on a range of benzyl and heteroaryl substituted titanocenes has evidenced this binding to either of the human serum albumin primary drug binding sites I or II. Potential binding results from hydrogen bonding and/or van der Waals interactions between the amino acid residues and the substituted cyclopentadienyl polar groups.[66]

Such conflicting evidence has led to alternative modes of action being suggested for titanocenes. The rational design of *in vivo* titanocene agents is significantly hindered by these ambiguities. Currently before agents are introduced into the clinic, mechanism(s) of action need to be well understood, allowing subsequent *in vivo* efficacy, stability, PK/PD and ADME studies to be performed.

1.5 Chiral substituted bis(η^5-cyclopentadienyl)titanium complexes

1.5.1 Metallocene formation

Titanocene **5** and its derivatives belong to a group of compounds in organometallic chemistry called metallocenes. Metallocenes can be defined as those complexes having one or two η^5-cyclopentadienyl rings coordinated to a central metal ion.[67] Examples include: the planar sandwich **15**, half sandwich **16**, multidecker sandwich **17** and bent sandwich complexes such as titanocene **5** (Figure 4).[67]

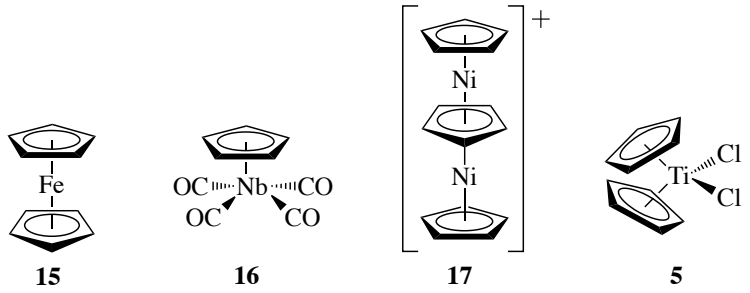
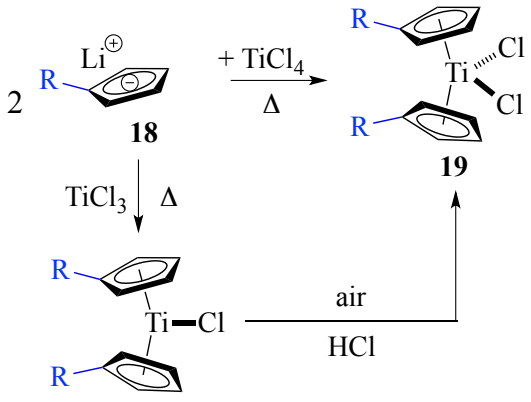


Figure 4: Different sandwich types of metallocene complexes.

The bent metallocene dichlorides of group 4 metals (Ti, Zr, Hf) have been extensively studied.[68] The transmetallation reaction between a substituted cyclopentadienide salt **18** and titanium tetrachloride in an ethereal solvent results in the formation of the bent dichloridobis(η^5-substituted-cyclopentadienyl)titanium **19**. Improved yields of **19** can often be attained by the use of titanium trichloride with **18** followed by oxidation using hydrochloric acid in air (Scheme 16).[68]



Scheme 6: Transmetallation reaction.

Cyclopentadienyl ligands are particularly attractive as they can be used as a support for introducing chirality in a metallocene.[69] There are three different types of cyclopentadienyl ligand-derived chirality. These result from the two stereotopic faces of such ligands.[69] The homotopic faces in **20-21** are equivalent, either due to the presence of a C_2 axis of symmetry between the two faces or due to interchange by free rotation around a C_2 axis. The enantiotopic faces **22** occur through interconversion of cyclopentadienyl ligand faces by reflection through a mirror plane. The diastereotopic faces **23** possess non-interconvertable cyclopentadienyl ligand faces[69] (Figure 5).

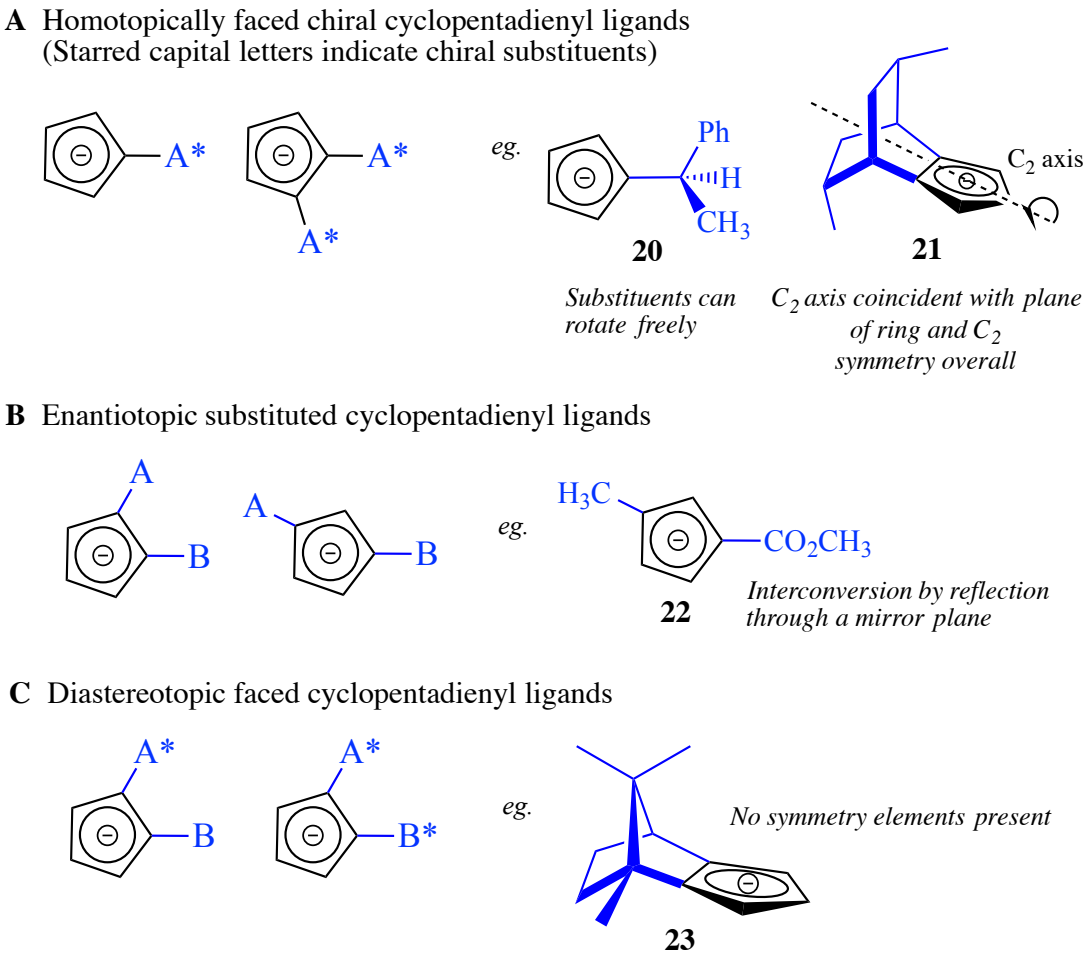
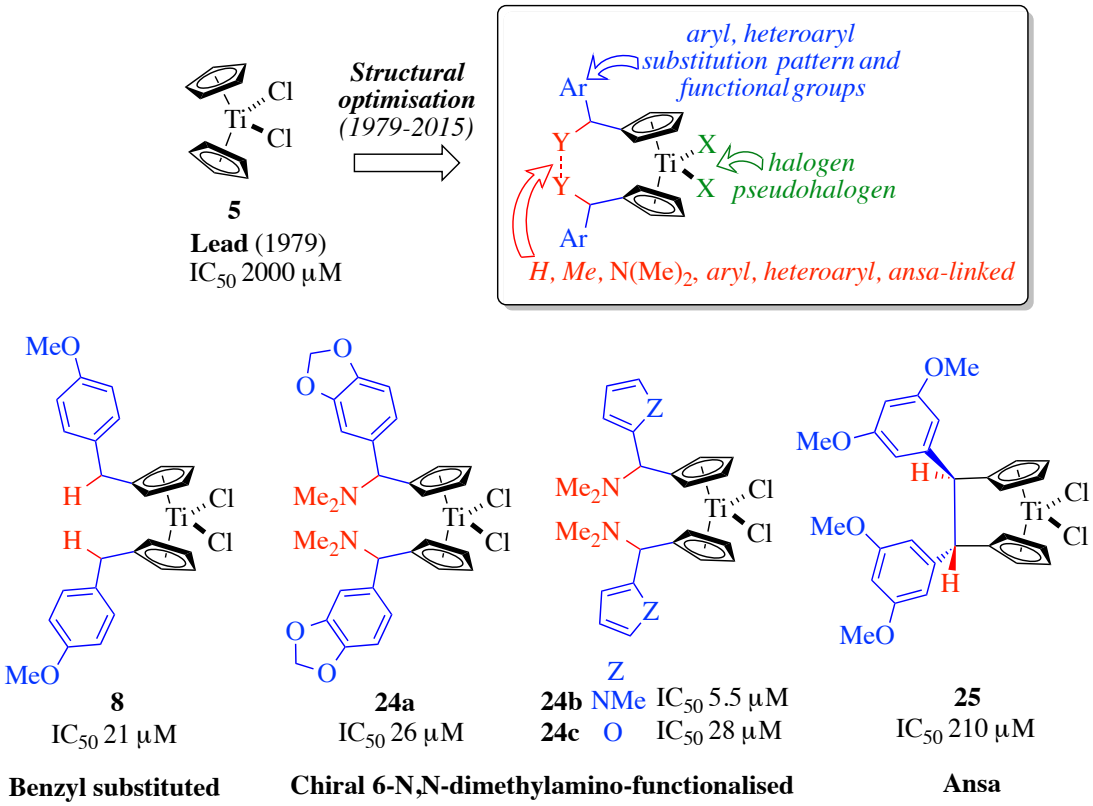


Figure 5: Different types of chiral cyclopentadienyl ligands.

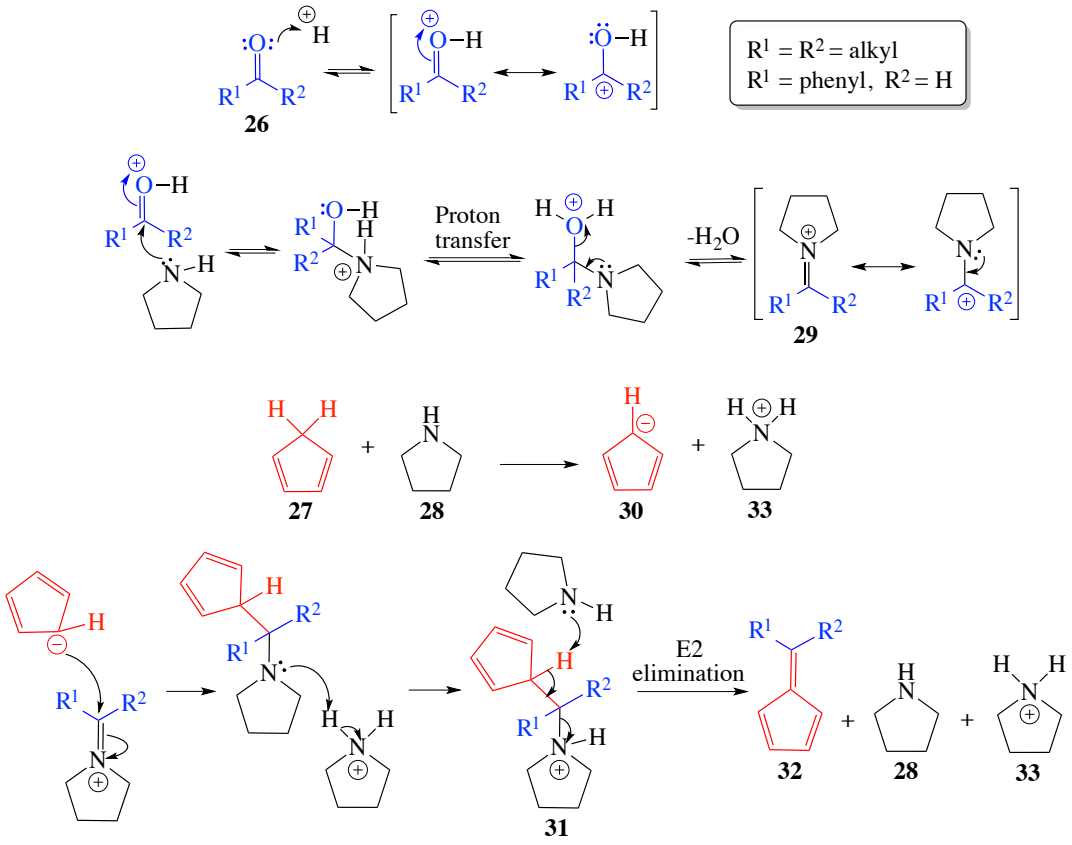
1.5.2 Pentfulvene derived bis(η^5-cyclopentadienyl)titanium complexes

During the past 30 years, achiral and chiral derivatives of titanocene dichloride **5** have attracted considerable attention as potential alternative chemotherapeutic agents to cisplatin **2**.[70,71] McGowan's elegant synthesis of ring-substituted cationic titanocene dichloride derivatives provided water-soluble compounds, which showed significant activity against ovarian cancer.[72] However, in the past 10 years, several synthetic methods based upon novel pentafulvene derived titanocenes were reported by Tacke and his co-workers. These include: benzyl substituted titanocenes and chiral 6-*N*,*N*-dimethylamino-functionalized titanocenes and *ansa*-titanocenes. This led to the identification of titanocene structures in Scheme 7, with **8** and **24a-c** showing high potency in the low micromolar range whilst **25** exhibited modest potency within a medium micromolar range.[71]



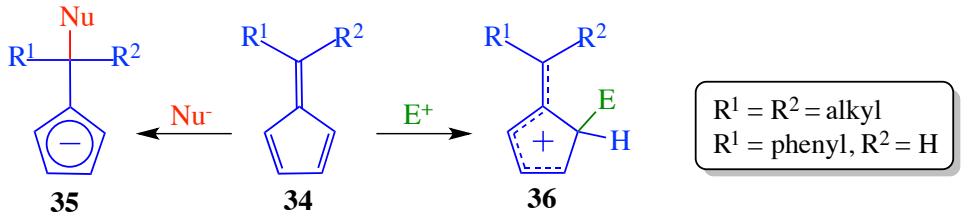
Scheme 7: Lead and titanocene structural optimization. Biological activities against pig kidney cancer LLC-PK cells for which cisplatin gives an IC_{50} value of 3.3 μM.

Substituted pentafulvenes have been extensively used as starting materials to synthesize biologically active substituted titanocenes. Pentafulvenes can be defined as cyclic cross-conjugated molecules having an exocyclic double bond and an odd number of carbons (five) in the ring.[73] Stone and Little achieved a versatile, simple and high yield method for the synthesis of 6-substituted / 6,6-disubstituted pentafulvenes.[74] The method involved the dissolution of aliphatic carbonyl compounds or aromatic aldehydes **26** and cyclopentadiene **27** in methanol, followed by subsequent addition of pyrrolidine **28**.[74] Their approach was to pre-form an iminium ion **29** in a Mannich-type manner which can then serve as an acceptor towards cyclopentadienide **30**, giving aminomethylcyclopentadiene **31**.[73] An E2 elimination of this species results in the formation of the substituted pentafulvene product **32**, pyrrolidine **28** and pyrrolidium ion **33**, as shown in Scheme 8.



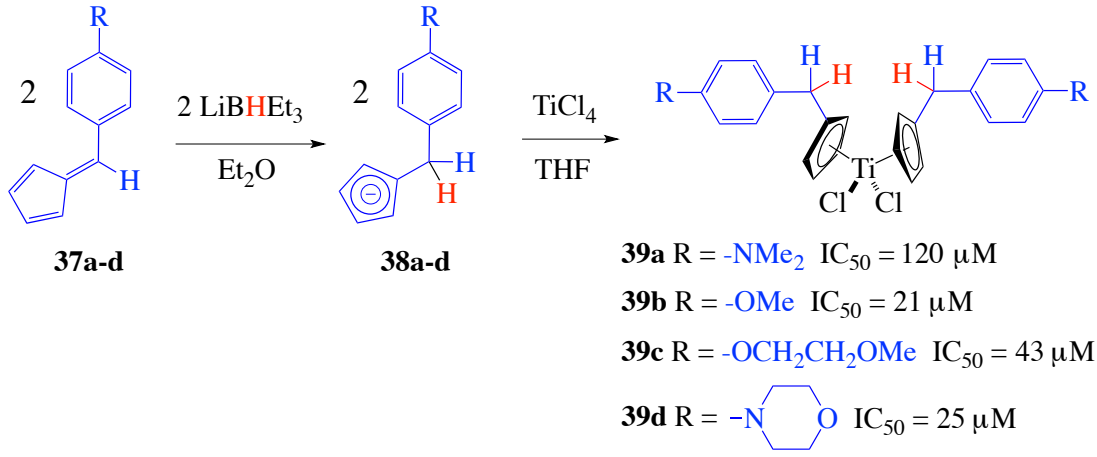
Scheme 8: Mannich type addition, E2 elimination and product formation.

Substituted pentafulvenes **34** can be reacted with both nucleophiles and electrophiles, as shown in Scheme 9. Nucleophiles, characterized by a high energy HOMO, preferentially attack the LUMO of the pentafulvenes. Nucleophilic attack occurs at C-6 since it has the largest Hückel coefficient and results in the formation of carbanions **35**.[73] These compounds are highly stable due to the formation of the aromatic sextet of electrons, in accordance with Hückel's rule. On the other hand, electrophiles, being characterized by a low energy LUMO, bind to the HOMO of the pentafulvenes. According to Hückel coefficients, electrophilic attack occurs at the C-1/C-4 of the ring. Electrophilic attack gives rise to delocalized carbocations **36**.[73]



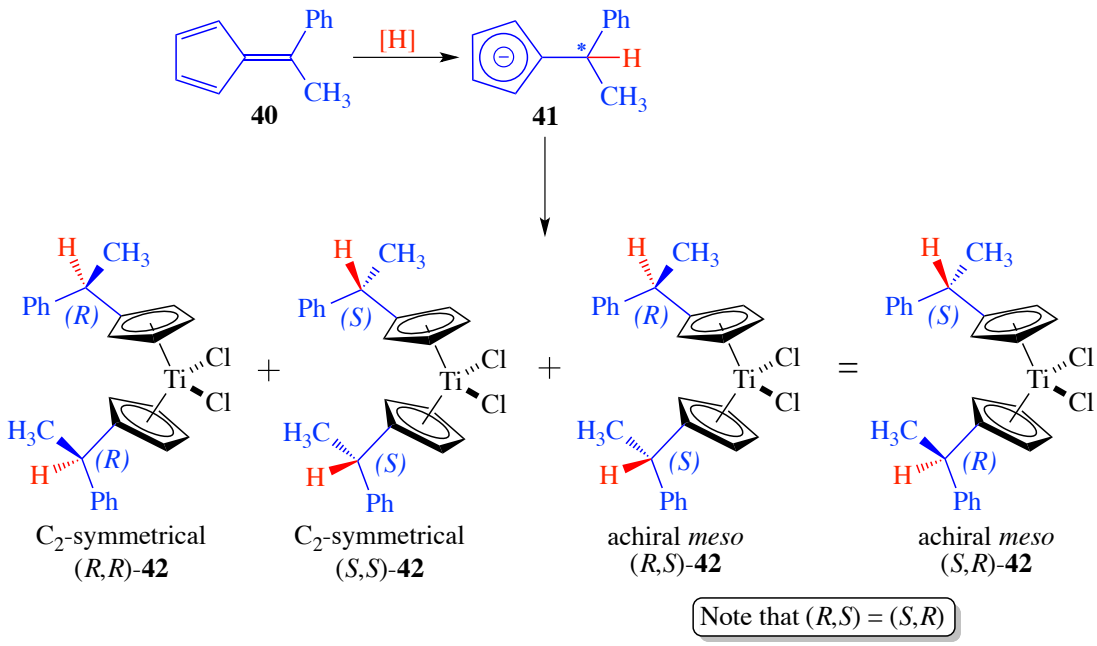
Scheme 9: Substituted pentafulvene reactions with nucleophiles and electrophiles.

The nucleophilic hydride transfer reaction from lithium triethylborohydride (super hydride®) to the exocyclic double bond of 6-arylsubstituted pentafulvenes **37a-d** results in the formation of lithium cyclopentadienide species **38a-d** (Scheme 10).[71] Selective nucleophilic attack occurs at the exocyclic double bond of pentafulvenes rather than the diene component due to an increased polarity of the exocyclic double bond through inductive effects of their respective aryl groups. Subsequent transmetallation of the hydrolithation product **38a-d** with titanium tetrachloride led to the synthesis of benzyl-substituted titanocenes **39a-d**. The *in vitro* cytotoxicity of the benzyl-substituted titanocenes such as **39a-d** was determined against LLC-PK cells, as can be seen in Scheme 10.[71]



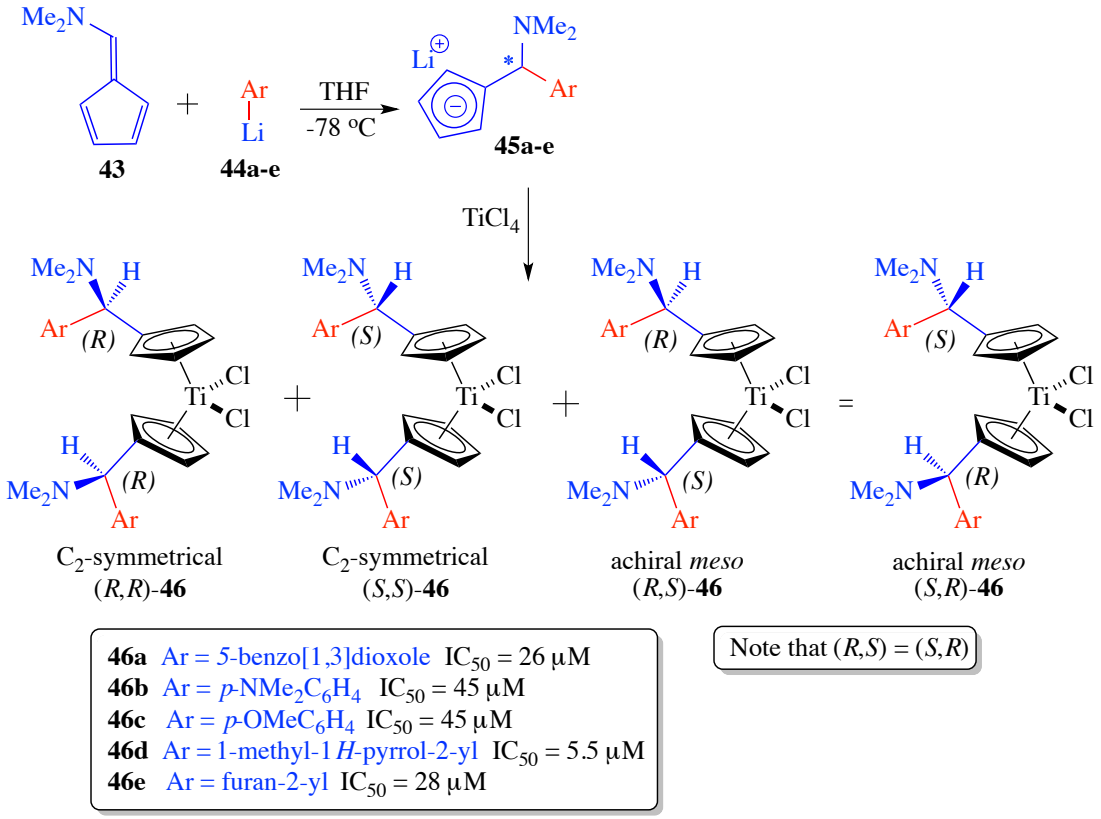
Scheme 10: Synthesis and biological activity of benzyl substituted titanocenes.

Unsymmetrical 6,6-disubstituted pentafulvenes such as **40** have been reduced by β-hydride transfer from isobutyllithium[69] or with lithium aluminium hydride,[75] forming racemic cyclopentadienyl anions **41**, followed by transmetallation with titanium tetrachloride. This led to a mixture of chiral racemic and achiral *meso* diastereoisomer **42** (Scheme 11). Through repeated recrystallizations, the chiral racemic C_2-symmetrical enantiomers (*R*,*R* and *S*,*S*) can be obtained from a mixture of racemic stereoisomers and *meso* stereoisomer.[75]



Scheme 11: Chiral titanocenes *via* hydrolithation.

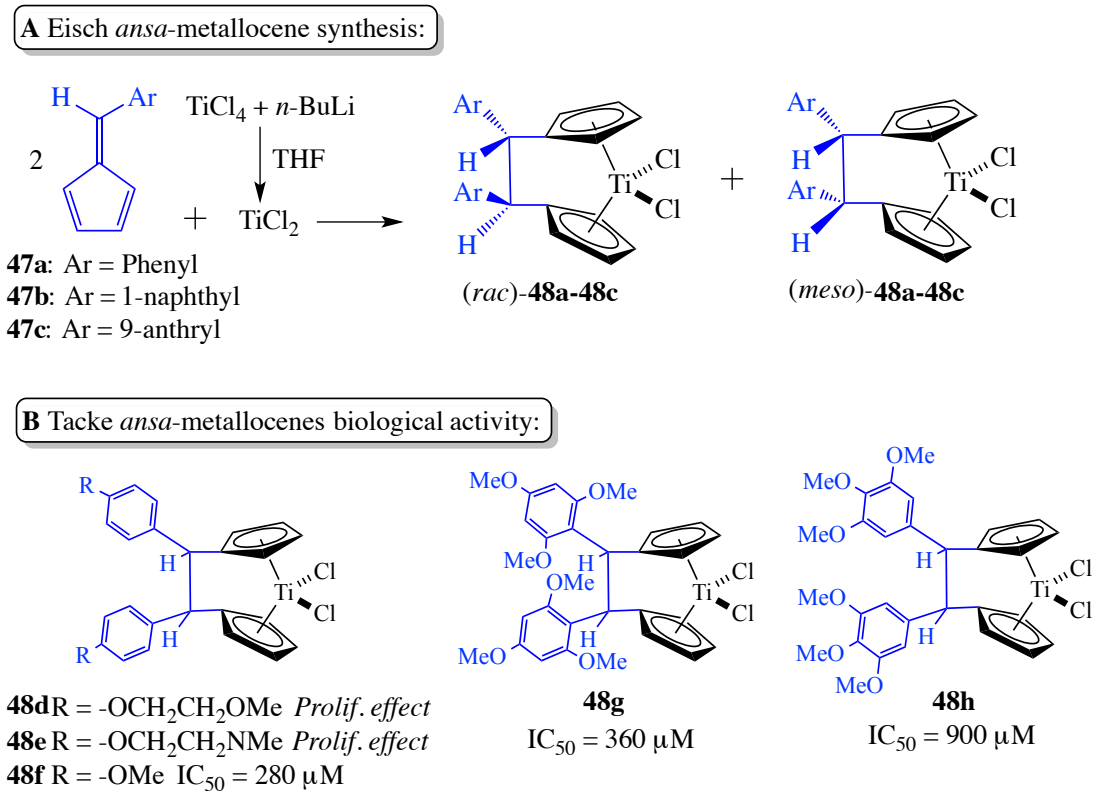
The carbolithation reaction of 1-(cyclopenta-2,4-dien-1-ylidene)-*N*,*N*-dimethylmethanamine **43** with aryl or heteroaryl lithium species **44a-e**, resulted in the formation of the chiral cyclopentadienyl ligands **45a-e.** Subsequent transmetallation of two equivalents of **45a-e** with titanium tetrachloride led to an equimolar mixture of chiral racemic and achiral *meso* titanocenes **46a-e**. The *in vitro* cytotoxicity of chiral dimethylamino-functionalised titanocenes such as **46a-d** was determined against LLC-PK cells, as can be seen in Scheme 12.[70,71,76] The carbolithation reaction provided highly cytotoxic chiral titanocenes, although, disentangling the relative biological activities of such mixtures is not possible preventing their advancement to clinical trials.[71]



Scheme 12: Chiral mixtures of titanocenes *via* carbolithation.

The preparation of *ansa*-metallocenes has been desirable in two ways: their practical synthetic method and the possibility of isolation and subsequent interpretation of

stereoisomers.[69] These compounds are characterized by an interannular bridge connecting the two cyclopentadienyl ligands, as can be seen in Scheme 10. This bridge restricts the conformation of the cyclopentadienyl ligands, which brings about a change in electronic behavior at the metal centre.[77] The method of preparation of *ansa*-metallocenes first involves the synthesis of a low valent group 4 metal halide (e.g. $TiCl_2$), by reacting the corresponding metal tetrahalide with *n*-butyllithium in THF, followed by the addition of two equivalents of substituted pentafulvene units **47a-c.** This results in a reductive dimerization process, yielding *ansa*-metallocenes **48**. Pentafulvenes having two different substitutents at the C6 position can lead to C_2 symmetrical chiral ansa-metallocenes (Scheme 13).[77]



Scheme 13: A Eisch ansa-metallocene synthesis. **B** IC_{50} values showing the effects of titanocenes **38-43** on the viability of LLC-PK cells.

A series of *ansa*-titanocenes were evaluated against LLC-PK cells, as can be seen in Scheme 10B. Surprisingly, cytotoxic analysis of the soluble 4-(2-

methoxyethoxy)phenyl and bis-(2-methoxyethyl)amino substituted *ansa*-titanocenes **48d-e** showed proliferative effects, in contrast to the anti-proliferative effects observed with *ansa*-titanocenes **48f-h**.[78-81]

1.6 Thesis aims

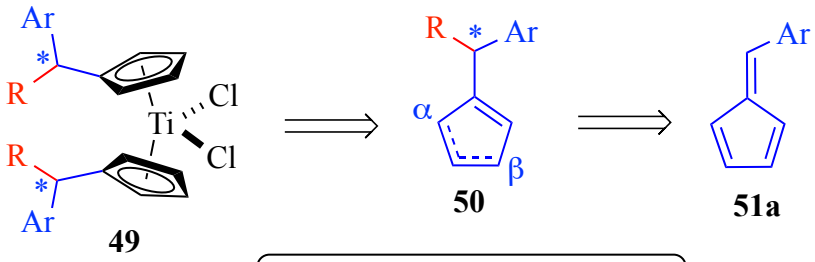
The primary objective behind this research was to synthesize and fully characterize novel single enantiomer chiral substituted titanocenes, from novel chiral substituted cyclopentadienyl ligands, themselves accessible from 6-substituted pentafulvenes.

The research herein aims to develop a new organometallic addition to substituted fulvenes, other than the carbolithation method. The hypothesis behind this idea was to explore the addition of transition metal compounds such as copper salts/complexes, so as to 'soften' the 'hard' organometallic nucleophile. This idea may result in attaining two other novel research aims: the nucleophilic organo-addition reaction between 6-substituted pentafulvenes and unreactive or reductive primary alkyl or branched alkyl organometallics with β-hydride ability, and the development of a subsequent catalytic enantioselective nucleophilic addition process. Transmetallation of the cyclopentadienide products with titanium tetrachloride will ultimately lead to the synthesis of chiral *rac*/*meso* titanocenes and chiral enantiopure titanocenes. The current research also aimed to test these chiral substituted titanocene complexes as anti-tumor agents and to explore their mode of action.

Chapter 2 – (*Rac*/*meso*)-titanocenes

2.1 Introduction

This chapter details the synthesis of substituted titanocenes of type **49** (Scheme 1) as potential anti-cancer agents and their biological activity. These species are to be accessed *via* disconnection to the racemic/tautomeric cyclopentadienyl derivatives of types **50**, themselves accessible from substituted pentafulvene **51a**.

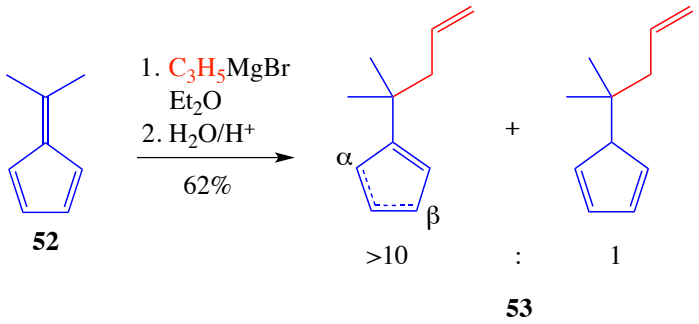


Scheme 14: Preparation of substituted titanocenes.

It is therefore appropriate in this chapter to review key activity in areas relevant to such complexes and their precursors, and this is discussed in the following sections.

2.2 Literature Approaches – racemic cyclopentadienyl ligands

The nucleophilic addition of allylmagnesium bromide to the dialkyl pentafulvene 5-(propan-2-ylidine)cyclopenta-1,3-diene **52** has been reported twice.[82,83] The dialkyl pentafulvene **52** was treated with excess allyl magnesium bromide in ether at room temperature, which resulted in the formation of a tautomeric mixture (62% yield) of substituted cyclopentadienes **53** (Scheme 15).[82] Based on the reaction mechanism between carbonyl compounds and organolithium/magnesium, it has been proposed that the organo species adds to the C6 carbon of the pentafulvene and the magnesium halide coordinates to the cyclopentadienide anion.[83]

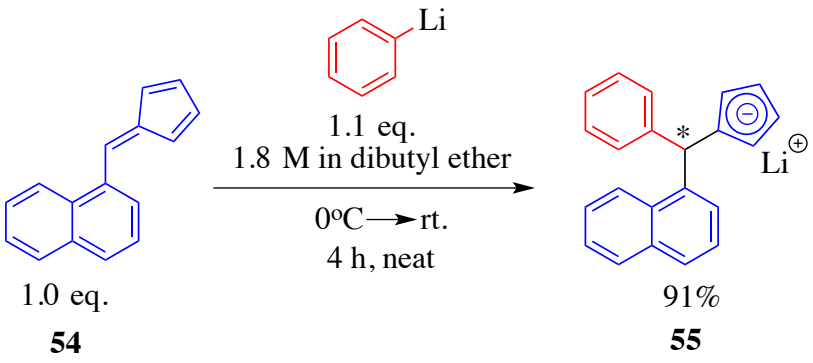


Scheme 15: Allylic Grignard addition to a disubstituted pentafulvene.

However, the reaction of cyclopentadienyl magnesium bromide with di-substituted pentafulvenes results in the formation of a reduction product.[83] It was proposed that this reaction proceeds through a free radical reaction but these authors are unclear about the source of the H-atom and necessary studies should be carried out.[83] Other Grignard reagents such as ethylmagnesium bromide, *n*-butylmagnesium bromide, phenylmagnesium bromide, benzylmagnesium chloride, cyclopentadienyl lithium and cylopentadienyl sodium have also been tried as nucleophilic reagents to a series of 6,6-dialkylfulvenes. Surprisingly, no addition product was observed.[83] Recently (2010), the nucleophilic addition of benzylmagnesium chloride to **52** was attained.[84] The organometallic reagent was added dropwise at room temperature to the disubstituted pentafulvene, stirred overnight and subsequently quenched with deionized water. A pale yellow liquid was obtained in 69% yield as a mixture of tautomers.[84]

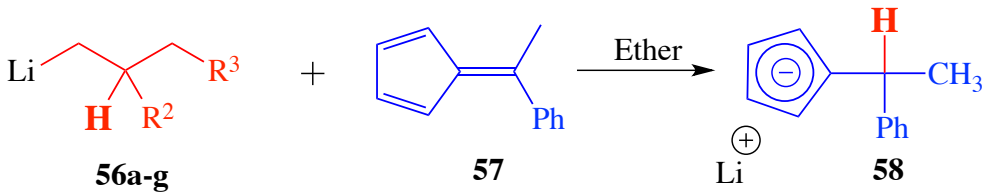
Organolithium reagents have also been used as nucleophilic reagents. The nucleophilic addition of methyllithium onto the exocyclic double bond of 6-substituted fulvenes was reported in 2007.[85] The organometallic reagent was added to an ether solution of 6-substituted fulvene at -78 ^{o}C, warmed to room temperature and left to stir for 6 h. A free-flowing powder of chiral racemic substituted cyclopentadienide lithium product was obtained in 50-65% yield.[85] In 2012, the

nucleophilic addition of phenyllithium onto the exocyclic double bond of 1-(cyclopenta-2,4-dien-1-ylidenemethyl)naphthalene **54** was reported (Scheme 16).[86] The organolithium reagent was added dropwise to **54** at 0 °C, warmed to room temperature and stirred for 4 h. A white solid of lithium cyclopentadienide product **55** was obtained in 91% yield.



Scheme 16: Phenyllithium addition to 6-substituted fulvene.

Erker (1991) noted that treatment of a wide variety of suitably branched alkyllithium reagents **56a-g** to (1-(cyclopenta-2,4-dien-1-ylidene)ethyl)benzene **57** resulted in high β-hydride transfer (60% with isobutyllithium compared to 20-30% when using unbranched alkyllithium reagents with β-hydride transfer ability) forming the lithium cyclopentadienide anion **58** (Scheme 17).[87] The β-hydride transfer reaction was explained through deuterium-labelling experiment through the use of 2,2-dideuterio-1-lithiobutane. An attempt to perform an asymmetric β-hydride transfer to form enantiomerically pure chiral cyclopentadienyl ligands failed.[87] Optically active lithium reagents such as (*S*-)-1-lithio-2-phenylpropane, (*S*)-1-lithio-2-cyclohexylpropane and (*R*)-1-lithio-2-phenylbutane were reacted with **57** to give the chiral reduction products in good yield. Subsequent reaction of the cyclopentadienyl ligands with zirconium tetrachloride *bis* THF led to the observation of almost identical *meso*:*rac* metallocene product ratios.[87]



	R^2	R^3
a	H	Me
b	H	H
c	Me	H
d	Ph	H
e	Cy	H
f	Ph	Me
g	D	Me

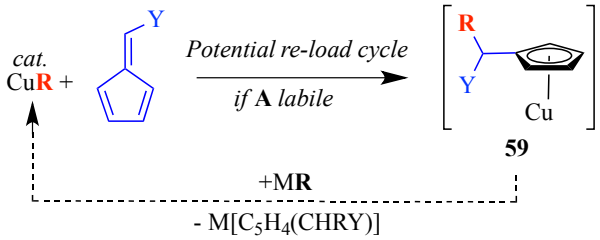
Scheme 17: Alkyl organolithium addition to 6,6-disubstituted pentafulvene.

2.3: Proposed route

The secondary centres in **24** and the proximal oxygen atom of **24c** suggested to us that species containing [η^5 –C_5H_4CHR(2-MeOPh)] units might be good candidates for therapeutic screening. However, these were notably absent in the current titanocene dichloride compound library. As highlighted in Scheme 17, a closer look at the literature reveals that additions of RLi or RMgX to 6-substituted pentafulvenes (the normal optimal route) suffer badly from competing hydride transfer (unless R = Me or Ar).[83,87] This synthetic deficiency has left the -CHAlkylAr motif rather underrepresented in substituted cyclopentadienyl chemistry, for which, in addition to any biological use, a wide range of additional applications in organic synthesis and catalysis has also been identified.[69]

Based on previous experiences in the Woodward group,[88-90] we speculated that hydride transfer would be avoided if a "Michael-like" organocopper addition to yield **59** was to be employed (Scheme 14). Cyclopentadienyl groups are widely regarded as "nontransferable" from transition metal ions, but $CpCu^I$ complexes are some of the most labile.[91-94] We reasoned that with a suitably nucleophilic terminal

organometallic species, it should prove possible to close the catalytic cycle of Scheme 18.



Scheme 18: Proposed use of fulvene substrates in copper-catalysed addition of terminal organometallics.

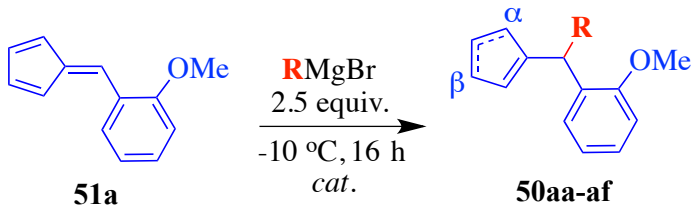
Thus, the primary objective behind this research was to synthesize and fully characterize novel chiral racemic cyclopentadienyl ligands through a new catalytic system as shown in Scheme 18, followed by transmetallation with titanium tetrachloride to form novel chiral substituted titanocenes. These chiral substituted titanocene complexes were then screened for anti-tumor activity.

2.4: Synthesis of racemic substituted cyclopentadienyl ligands

1-(Cyclopenta-2,4-dien-1-ylidenemethyl)2-methoxybenzene **51a** was selected for our trials and prepared by literature procedures from cyclopentadiene and 2-methoxybenzaldehyde.[95] The initial addition of **51a** to a 5-fold excess of a stoichiometric cuprate prepared from CuI/LiBr/EtMgBr in tetrahydrofuran (THF) at –10 °C produced the ethyl addition product **50aa** in modest yield (43 %) after 16 h - no hydride-transfer byproducts were detected. Higher yields of **50aa** were achieved through the use of a catalytic version of the highly reactive cyanoGilman type organocuprate (Table 1). Ethylmagnesium bromide (2.5 equiv.) was added to a THF solution of catalytic copper(I) cyanide (10 mol%) and lithium chloride (10 mol%) at -10 ^{o}C, followed by the addition of a THF solution of **51a** (1.0 equiv.). The reaction was left to stir for 16 h at -10 ^{o}C. Workup involved the quenching of aqueous

cyanide residues with a sodium hypochlorite solution (bleach), to oxidize residual cyanide ions into less harmful cyanates. Quantitative conversion of **50aa** was determined by ^{1}H NMR spectroscopy, with a yield after purification of 88% (Table 1). A background reaction using ethylmagnesium bromide (2.5 equiv.) followed by the addition of **51a** (1.0 equiv.) at -10 °C for 16 h did not provide any yield of **50aa**. Thus, we were able to demonstrate that the soft organocuprate species formed from 10 mol% catalytic species (copper(I) cyanide and lithium chloride) and excess Grignard reagent to **51a** had a dramatic effect on the reaction rate. In order to limit the use of copper cyanide, due to safety issues, we turned our attention to the use of other copper additives (Table 1).

Table 1. Development of catalytic procedure for RMgBr additions to **51a**.[a]



51a **50aa-af**

Run	CuI (mol %)	Additive (mol %)	R	Solvent	Yield (%)
1	CuCN (10)	LiCl (10)	Et **50aa**	THF	88
2	CuBr•SMe_2 (10)	-	Et **50aa**	THF	85
3	CuBr•SMe_2 (10)	-	*n*Bu[b] **50ab**	THF	87
4	CuBr•SMe_2 (10)	-	*i*Bu **50ac**	THF	92
5	CuBr•SMe_2 (10)	-	allyl **50ad**	THF	91
6	CuBr•SMe_2 (10)	-	Me **50ae**	THF	27[c]
7	CuBr•SMe_2 (10)	-	Ph **50af**	THF	24[c]
8	CuI (8)	PPh_3 (10)	Me **50ae**	*t*BuOMe	91[d]
9	CuI (8)	PPh_3 (10)	Ph **50af**	*t*BuOMe	66

[a] Performed with **51a** on a 1-10 mmol scale, isolated yields except where noted. [b] *n*BuMgCl used. [c] Conversion of **51a**. [d] Isolated from 77% conversion (10 mmol scale).

The aim was to develop a simple and effective method for the synthesis of chiral substituted cyclopentadienyls without compromising the yield. The copper catalyst CuBr•SMe_2 (10 mol %) was dissolved in THF followed by the addition of the alkyl, branched alkyl or phenyl Grignard reagents at -10 ^{o}C and a solution of **51a**. Excellent yields of up to 92% on at least 2 g scale were obtained after column chromatography, yielding compounds **50aa-ad** using commercially available CuBr•SMe_2. One limitation of the CuBr•SMe_2 catalyst system was that it would not provide the methyl and phenyl derivatives **50ae-af** in good yield; only partial conversions were attained (Table 1, Runs 6–7). These deficiencies could be overcome through the use of *t*BuOMe (MTBE) and PPh_3 (Table 1, Runs 8–9). Presumably, the lower coordination ability of MTBE leads to a more Lewis-acidic cuprate, which can overcome the slower transmetallation rates from these Grignard reagents from "$CpCu^{I}$" (**59**, Scheme 18). Some support is given to this idea by the observation that MeMgBr (Mg–C ≈ 60 kcal mol^{-1})[96] is the slowest reacting system.

All of the isolated cyclopentadiene products **50** are colourless oils and show the expected spectroscopic properties. All are isolated as close to 1:1 mixtures of α/β [1,5] hydrogen shift tautomers. In particular, two overlapping multiplets at δ_H = 1.81–2.08 ppm in the ^{1}H NMR spectrum of **50aa** (Figure 6), confirmed the presence of diastereotopic methylene groups. Additionally, two broadened signals at δ_H = 2.85 and 3.00 ppm in a 0.8:1.2 ratio also indicated the presence of two [1,5] hydrogen shift tautomers, in which the CH_2 group is either α or β to the *ipso*-cyclopentadienyl carbon atom. Through 2D NMR spectroscopy [COSY (Figure 7), HMQC and HMBC], near full assignment of the two sets of tautomeric signals could be made; however, they could not be independently distinguished.

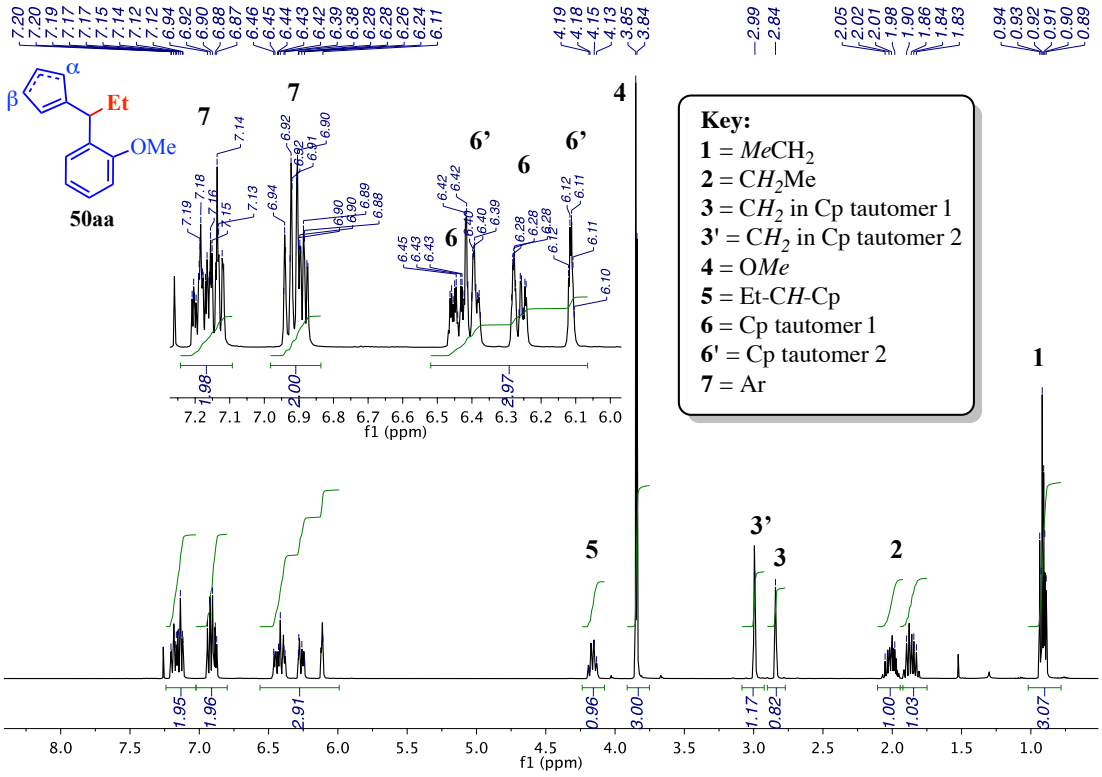


Figure 6: ^{1}H NMR spectrum of **50aa**.

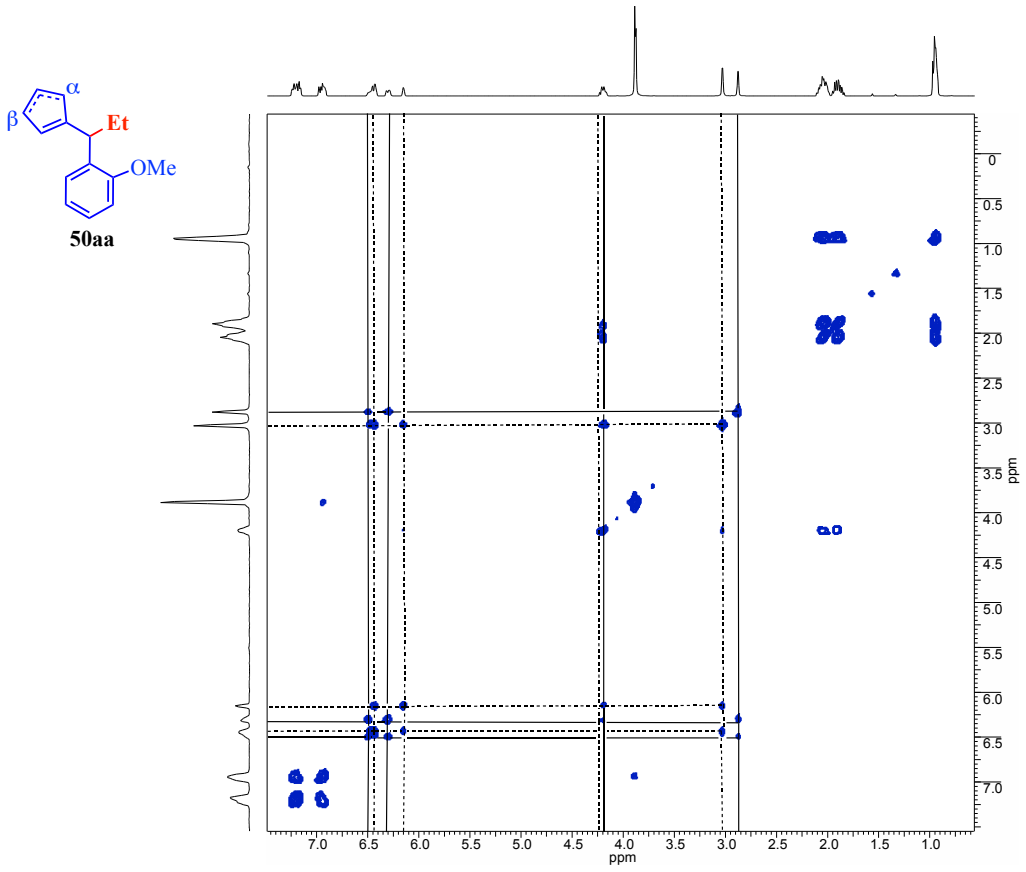
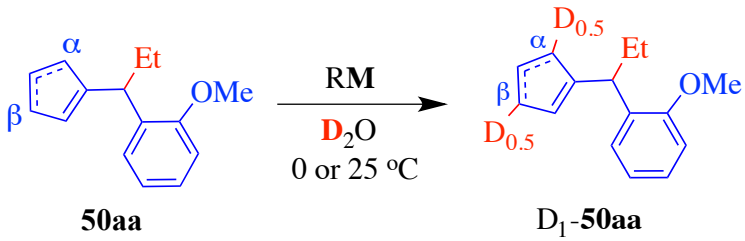


Figure 7: ^{1}H COSY spectrum of **50aa**.

2.5 Synthesis of chiral (*rac*/*meso*) substituted titanocene complexes

With an efficient route to **50** in hand, we focused our attention on the preparation of the derived titanocenes **49**. The aim was to obtain metal cyclopentadienide solids in good yields that could then be filtered under argon, followed by the transmetallation reaction with titanium tetrachloride. Optimization of the cyclopentadienyl deprotonation step was first carried out. Several conventional bases such as sodium hydride (NaH), sodium bis(trimethylsilyl)amide (NaHDMS) and *n*-butyllithium were utilised in the optimization of the cyclopentadienyl **50aa** deprotonation step, as shown in Table 2.

Table 2: Optimization of cyclopentadienyl deprotonation.[a]

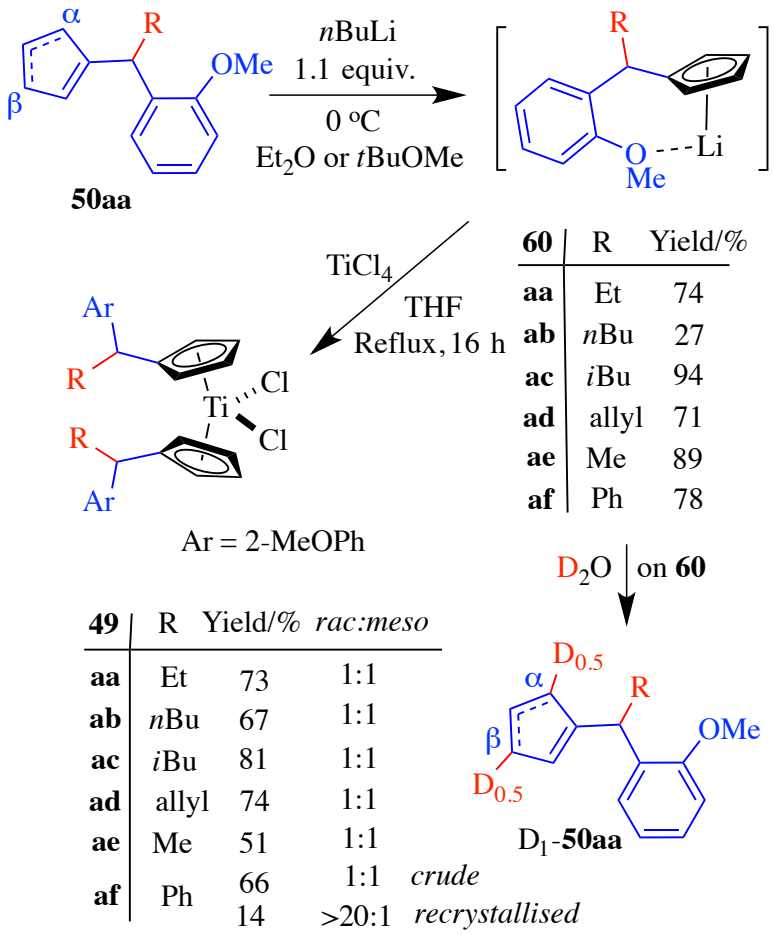


50aa D_1-**50aa**

Run	Solvent	Base	Temp (°C)	Time (min)	% D[d]
1	THF	NaH	0 to 25	90[b]	10
2	Ether	NaH	0 to 25	90[b]	0
3	THF	NaH	0 to 25	960[c]	20
4	Ether	NaH	0 to 25	960[c]	0
5	Ether	NaHDMS	0	30	90
6	THF	*n*-BuLi	0	5	93
7	THF	*n*-BuLi	0	30	100
8	Ether	*n*-BuLi	0	30	100
9	MTBE	*n*-BuLi	0	30	100

[a] A racemic-tautomeric mixture was used as the source of cyclopentadienyl starting material **50aa** (53.5 mg, 0.25 mmol, 1.0 equiv.) and (0.28 mmol, 1.1 equiv.) of base. [b] 10 min at 0 °C followed by 80 min at 25 °C. [c] 10 min at 0 °C followed by 950 min at 25 °C. [d] Determined by ^{1}H NMR by monitoring the deuterium incorporation in the acidic proton of the cyclopentadienyl.

Rapid quantitative deprotonation of **50aa** by *n*BuLi (1.1 equiv.) in THF, Et_2O or MTBE at 0 °C was confirmed by quenching the reaction with D_2O which led to **D_1-50aa** as an α/β isomer mix. Having identified a method for the formation of the lithium substituted cyclopentadienides **60**, a trial synthesis of the substituted titanocene product was carried out in a one-pot method by first deprotonating **50aa** with *n*BuLi (1.1 equiv.) in THF followed by the subsequent transmetallation with titanium tetrachloride. Unfortunately, the direct use of these reaction mixtures with either $TiCl_4$ or $TiCl_4(THF)_2$ led only to intractable mixtures. As has been found before,[97] synthesis of the lithium intermediate in ether followed by filtration of the precipitate and drying of the resultant organolithium species **60aa-af** is required to attain chemoselective preparation of titanocenes **49aa-af** (Scheme 15).



60	R	Yield/%
aa	Et	74
ab	*n*Bu	27
ac	*i*Bu	94
ad	allyl	71
ae	Me	89
af	Ph	78

49	R	Yield/%	*rac:meso*	
aa	Et	73	1:1	
ab	*n*Bu	67	1:1	
ac	*i*Bu	81	1:1	
ad	allyl	74	1:1	
ae	Me	51	1:1	
af	Ph	66	1:1	*crude*
		14	>20:1	*recrystallised*

Scheme 19. Preparation of titanocene dichlorides **49**.

The lower yield of **60ab** is caused by its higher solubility in hydrocarbons containing trace *t*BuOMe. Recrystallization of the crude titanocene reaction mixtures containing **49** allowed the isolation of analytically pure red-orange/brown powders containing 1:1 mixtures of *rac*/*meso* diastereomers for **49aa-ae** from CH_2Cl_2/pentane.

The ^{1}H NMR spectrum of the *rac*- and *meso*-**49aa** is representative of the class (Figure 8). A triplet at δ_H = 0.76 ppm is attributed to the methyl group of one diastereomer and shows a typical $^3J_{H,H}$ of 7.5 Hz. This signal is overlapped by the equivalent methyl group of the other diastereomer at δ_H = 0.77 ppm.

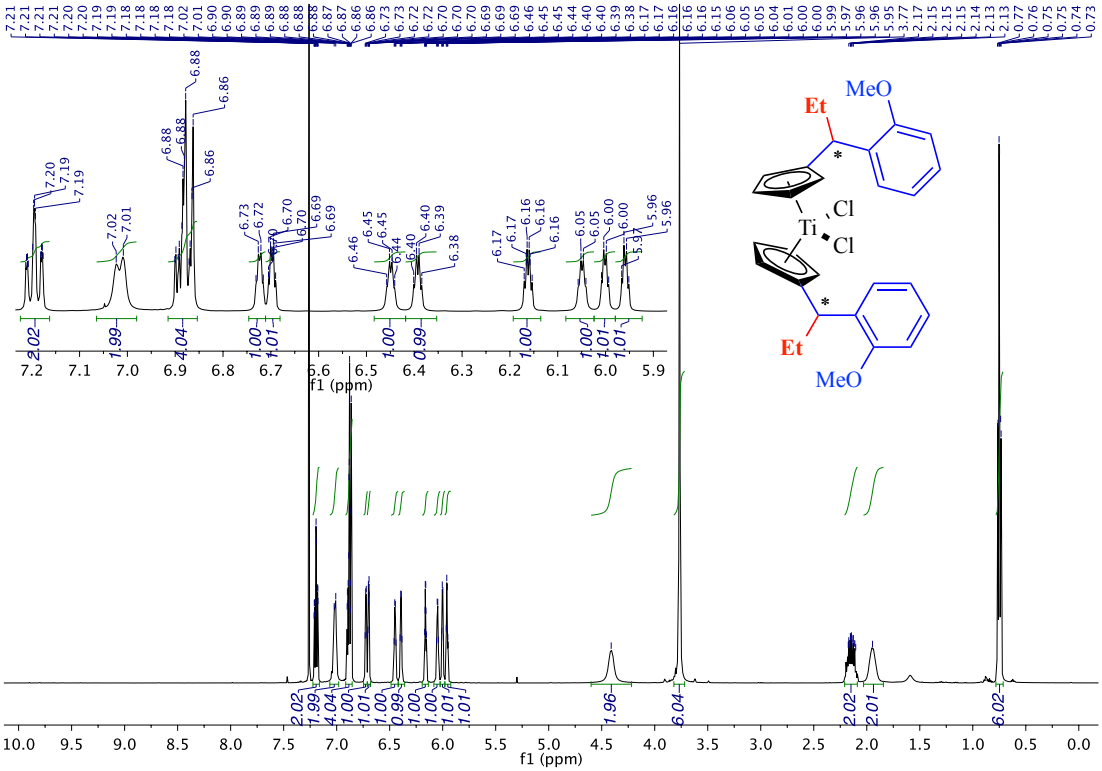


Figure 8: ^{1}H NMR spectrum of **49aa**.

A broad signal at δ_H = 1.96 ppm and an associated multiplet at δ_H = 2.08– 2.23 ppm (integrating to 4 H) are assigned to the overlapping diastereomeric signals of the CH_2 groups, whereas the methoxy and α-CH groups of the two stereoisomers are coincident at δ_H = 3.78 and 4.42 ppm, respectively. The broadness of the latter

indicates restricted rotation within the molecule, most likely about the Cp–CHEtAr bond. The chemical shift region between δ_H = 5.97 to 6.73 ppm contains two sets of signals from diastereotopic cyclopentadienyl methine protons.

The ^{1}H-^{1}H COSY spectrum of the aromatic region allows assignment of two sets of four magnetically inequivalent protons (δ_H = 5.97, 6.06, 6.46 and 6.73 and δ_H = 6.01, 6.17, 6.40 and 6.71 ppm) for the C_5H_4R units of the two diastereomers. The phenylene signals are badly overlapped with only slight separation on the 4-H Ar (δ_H = 7.22 and 7.23 ppm) and 5-H Ar (δ_H = 6.90 and 6.91ppm) signals of the diastereomers. The *rac*/*meso* signals of 3-H Ar at δ = 6.91 ppm and 6-H Ar at δ = 7.04 ppm are essentially coincident, and the latter signal is appreciably broadened at ambient temperature.

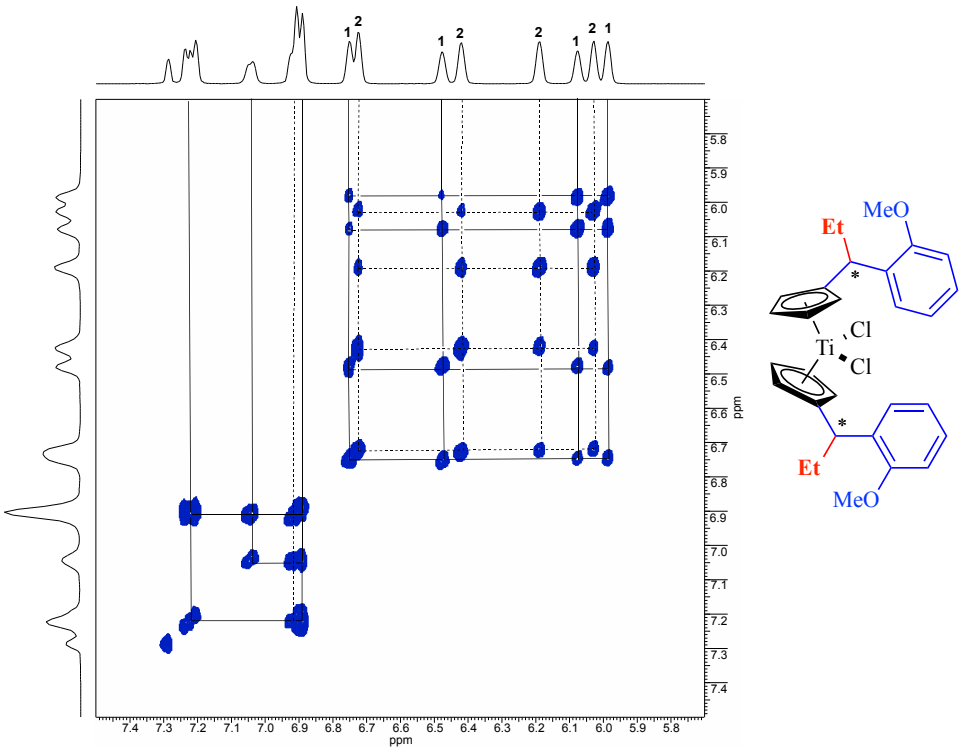


Figure 9: ^{1}H:^{1}H COSY spectrum (aromatic region) of **49aa**.

For **9af**, only small initial crops of crystalline *rac*-**9af** were isolated from chloroform/hexane, but the *meso* form could not be isolated in a pure form from the mother liquor (which provided only sticky intractable *rac*/*meso* mixtures). The relative *rac* stereochemistry of **9af** was confirmed by X-ray crystallography (Figure 10).

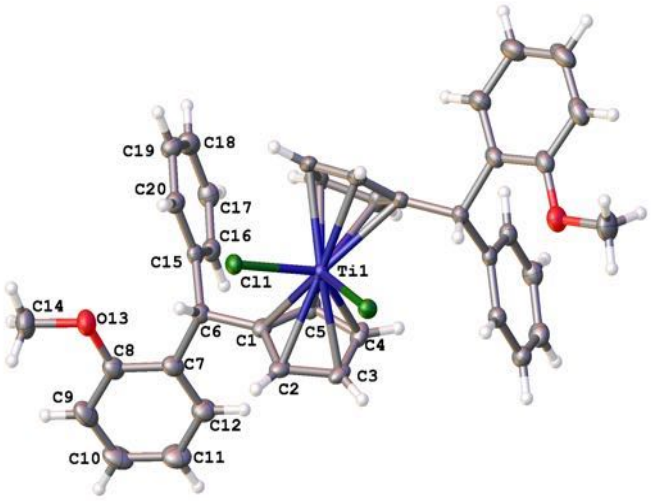
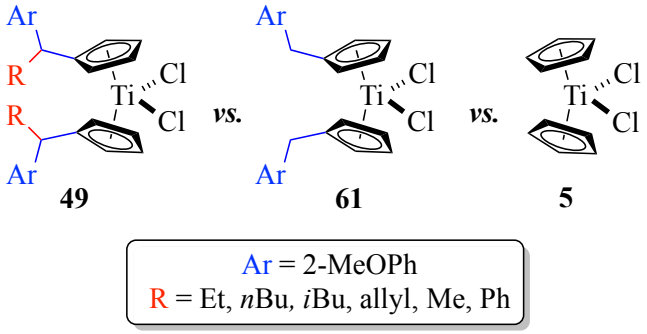


Figure 10: Molecular structure of *rac*-**49af**.

The Ti–Cl and Ti–C(Cp_{ave}) bond lengths in *rac*-**49af** are 2.335 and 2.392 Å respectively which compare well with those of typical dichloridobis(η^5-cyclopentadienyl)titanium structures bearing a Cp-CHAr unit in the Cambridge Crystallographic Database.[98] These monosubstituted titanocene dichlorides show Ti–Cl and Ti–C(Cp_{ave}) bond lengths of 2.31–2.37 and 2.39–2.45 Å, respectively. Often the Ti–C bond length associated with the point of substitution in such complexes is appreciably lengthened (2.40–2.49 Å) and this is the case in *rac*-4**9af**, which shows 2.442 Å for Ti–C(1). The origin of the restricted rotation in **49** is also clear from the structure of *rac*-**49af**, for which the C(2)–C(7) and C(5)–C(15) distances (3.28 and 3.00 Å respectively) are close to the expected C···C van der Waals contact ranges.

2.6 Growth Inhibitory Studies

The antiproliferative activities of the RCHAr-substituted titanocenes **49**, in comparison to the simple benzyl-substituted titanocene analogue **61**, *97* dichloridobis(η^5-cyclopentadienyl)titanium **5** (Scheme 20) and cisplatin **2** evaluated *in vitro* against HCT-116 (colorectal), MiaPaCa-2 (pancreatic) and MDA-MB-468 (triple negative breast) carcinoma cell lines, which represent intractable cancers from three different organ sites.



Scheme 20: Species compared with cisplain in growth inhibitory studies.

The compound concentrations that inhibit cell growth by 50% (GI_{50} values) after 72 h exposure of cells to agents **49**, **61, 5** and cisplatin were obtained by standard MTT [3-(4,5-dimethylthiazol-2-yl)-2,5-diphenyltetrazolium bromide] assay and are shown in Table 3. Compound stocks (10 mM) were prepared in dimethyl sulfoxide (DMSO) and diluted in nutrient medium immediately prior to use. All of the complexes **(1)** were assayed as 1:1 *rac*/*meso* mixtures of stereoisomers except for rac-**49af**, which was assigned as a single *rac* diastereomer.

As can be deduced from Table 3, all chiral-substituted titanocenes **49** are active against all the studied cancer cell lines in the examined concentration range (0.01–100 μM). The dose–response relationships of **49aa** and **49ae** in HCT-116, MiaPaCa-2 and MDA-MB-468 carcinoma cell lines are highlighted in Figure 11.

Table 3: Growth inhibitory assays. GI_{50} values as mean standard error of mean (SEM) of three independent experiments (n = 4 per experiment).

	Mean GI_{50} (μM)		
Compound	HCT-116	MiaPaCa-2	MDA-MB-468
49aa	12.2 ± 3.9	7.5 ± 0.4	5.3 ± 1.7
49ab	42.4 ± 4.8	34.7 ± 3.1	14.6 ± 4.2
49ac	24.6 ± 3.5	22.4 ± 3.9	32.3 ± 1.7
49ad	28.6 ± 2.9	24.8 ± 1.0	26.7 ± 0.5
49ae	5.7 ± 2.8	6.6 ± 1.0	7.7 ± 2.6
rac-**49af**	25.0 ± 0.5	11.4 ± 2.6	27.5 ± 0.5
61	73.4 ± 3.9	22.7 ± 1.5	76.2 ± 2.6
5	>100	>100	>100
cisplatin	7.9 ± 0.5	5.8 ± 0.7	2.1 ± 0.6

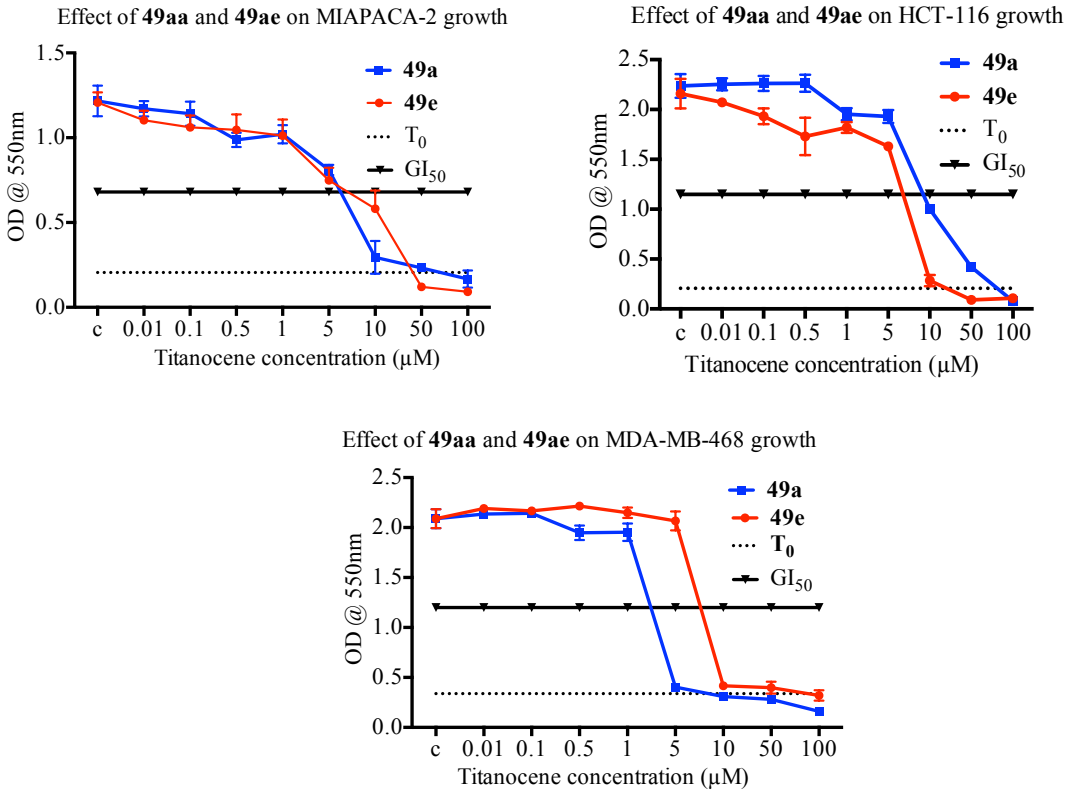


Figure 11: MTT assay profiles for inhibition of MIaPaCa-2, HCT-116 and MDA-MB-468 growth by **49aa** and **49ae**.

Duplicate DMSO (vehicle) controls were performed on all three cell lines, representative of DMSO content over the whole range of concentrations; growth of cells was not significantly inhibited (DMSO <1%). On direct comparison of **49** with **61** and **5**, it can be deduced that all chiral complexes **49** are much more active than their titanocene reference counterparts. Of particular note are **49aa** and **49ae** with GI_{50} values ≤10 μM in all three cell lines, which makes them some of the most active titanocenes reported in this area and directly comparable to cisplatin (particularly against HCT-116 and MiaPaCa-2 cells). This can be correlated to the presence of their –CHRAr substituents, which might lead to a significant increase in inhibitory activity, as has been seen before.[70,71] MDA-MB 468 demonstrates greater sensitivity towards **49aa**, **49ab** and cisplatin. MiaPaCa-2 is relatively more sensitive to the growth inhibitory properties of *rac*-**49af** and **61**. Titanocenes **49ad** and **49ae** demonstrate approximately equiactivity in all three cell lines. In an *in vitro* cytotoxicity study performed with benzyl-substituted titanocenes such as Titanocene Y **8** against 36 human tumour cell lines from 14 different organ sites, it was found that the cytotoxicity of **8** relative to cisplatin was comparatively much lower in colon carcinoma cell lines. However, it was comparable to cisplatin pancreas and breast carcinoma cell lines.[99]

Of particular note is the effect of chain length on the growth inhibitory activity of family **49**. As can be seen in Table 3, the longer the chain length, the lower the growth inhibitory values obtained. As the chain length increases, the growth inhibitory activity diminishes by a factor of approximately six from a C_1/C_2 side chain to an *n*-butyl chain. Optimal results were obtained for titanocenes with an ethyl sidechain **49aa**, showing GI_{50} values of 12.2 μM for HCT-116, 7.5 μM for MiaPaCa-2 and 5.3 μM for MDA-MB-468, or a methyl side chain **49ae**, which has GI_{50} values

of 5.7 μM for HCT-116, 6.6 μM for MiaPaCa-2 and 7.7 μM for MDA-MB-468. These two titanocenes show almost identical activity with uniform growth inhibitory responses in all three cancer cell lines, which are similar to the activity of standard cisplatin (GI_{50} values of 7.9 μM for HCT-116, 5.8 μM for MiaPaCa-2 and 2.1 μM for MDA-MB-468). The growth inhibitory range shown by the *n*- and *iso*- butyl derivatives (**1c** and **1d**) across HCT-116 and MDA-MB-468 cell lines also deserves comment. Complex **49ac** is statistically ($P < 0.05$) less active towards HCT-116 than MDA-468, whereas for **49ad**, the trend is reversed. It has been proposed[100,101] that the cyclopentadienyl ligands are removed in the cytotoxic events associated with dichloridobis(η^5-cyclopentadienyl)titanium therapeutics, and the role of the cyclopentadienyl ligand is limited to pharmacokinetics. Therefore, the activity profiles of **49ac** and **49ad** are somewhat unexpected in light of the rather close structural similarity of these complexes. This might indicate significant molecular recognition at some point in the mode of action rather than simple pharmokinetic effects. Finally, we also note the significantly increased growth inhibition evoked by class **49** in comparison with titanocene-Y **8** in colon carcinoma cell lines.[99]

2.7 Electrochemical studies

In order to better understand the observed growth inhibitory differences between different side chains on the chiral RCHAr-substituted titanocenes **49**, in comparison to the simple benzyl-substituted titanocene analogue **61** and dichloridobis(η^5-cyclopentadienyl)titanium **5**, a cyclic voltammetry study for each titanocene was carried out. As can be seen in Figure 12, the $E_{1/2}$ potential for each titanocene was calculated in dichloromethane against ferrocene Fc/Fc^+ as the internal standard. A platinum electrode was utilised and tetrabutylammonium hexafluorophosphate was

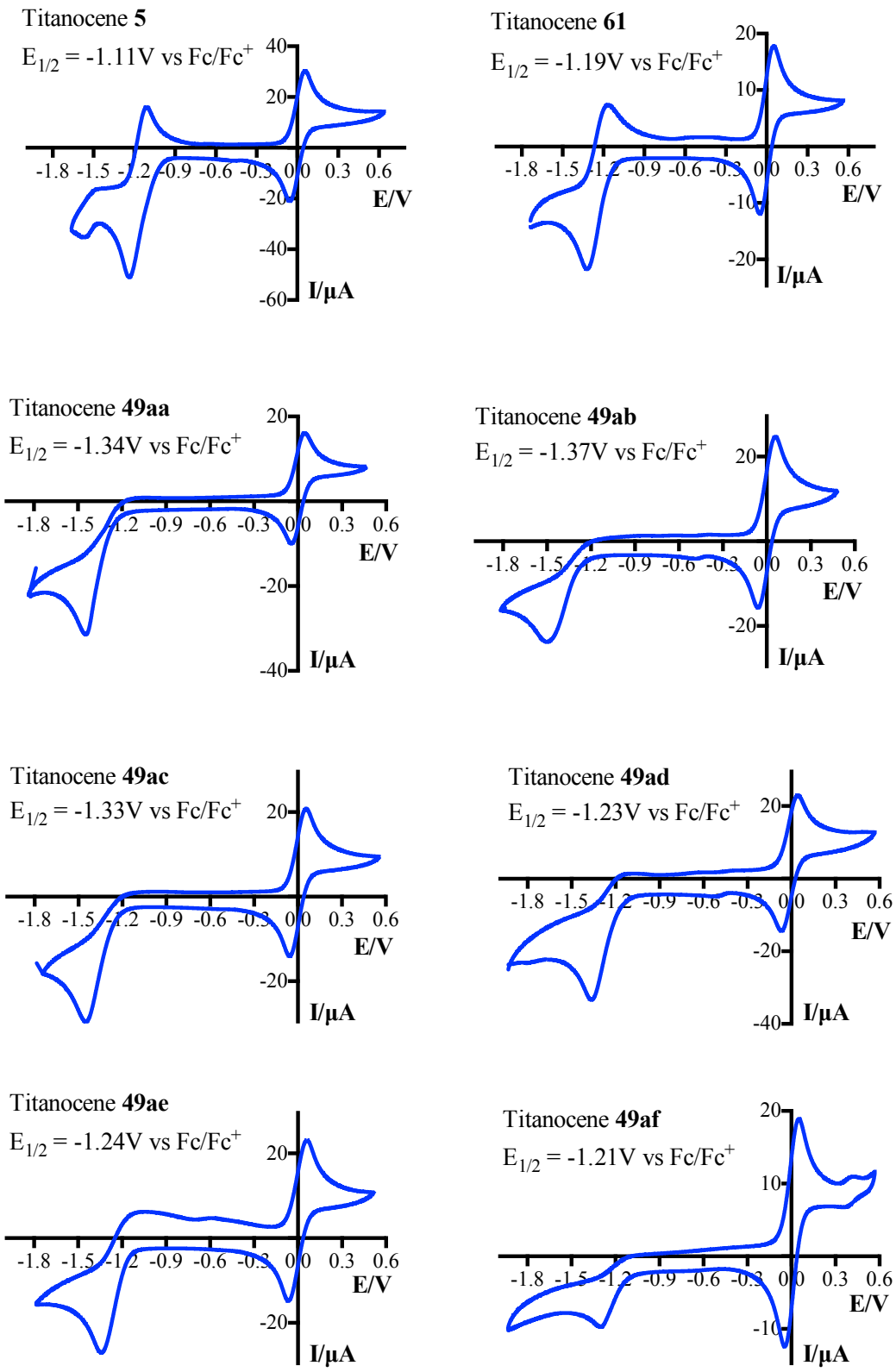


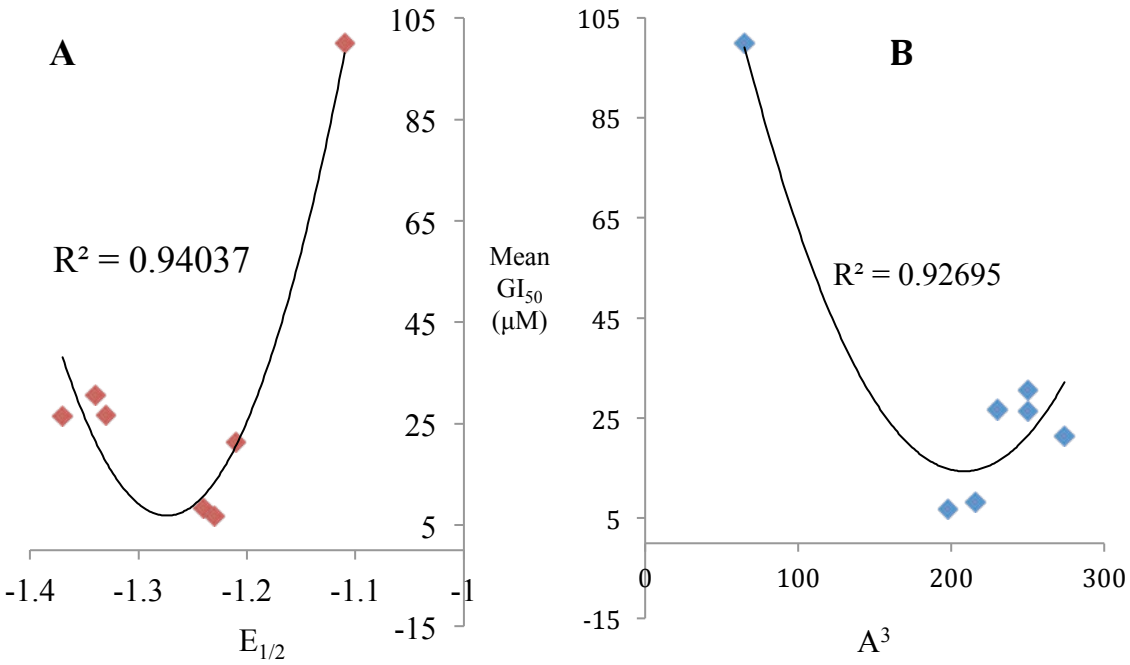
Figure 12: Cyclic voltammetry of titanocene dichloride and titanocene derivatives in dichloromethane.

used as the electrolyte. For titanocene complex **5**, with no substituents on the cyclopentadienyl ring, it is possible to visualize a considerable reduction peak at -1.26V from Fc/Fc^+ and a weaker corresponding oxidation peak at -1.08V from Fc/Fc^+. The $E_{1/2}$ potential for this semi-reversible redox reaction was found to be that of -1.1V with respect to Fc/Fc^+. The achiral benzyl-substituted titanocene analogue **61** evidenced similar cyclic voltagram with respect to titanocene **5**, albeit greater $E_{1/2}$ potential. A considerable reduction peak at -1.34 V from Fc/Fc^+ and a weaker corresponding oxidation peak at -1.12 V from Fc/Fc^+ were obtained for titanocene **61**. The $E_{1/2}$ potential for this semi-reversible redox reaction was found to be that of -1.19V with respect to Fc/Fc^+. On contrary, the voltagramms of chiral RCHAr-substituted titanocenes **49** exhibit a reduction peak and no oxidation peak thus indicating high redox stability for these compounds. The voltagramms for these titanocenes **49** show a complete irreversible system due to the lack of an oxidation peak for the metal center. The $E_{1/2}$ potentials for the chiral RCHAr-substituted titanocenes **49** correlate with the length of the side chain as can be seen in Table 3, ranging from -1.24V with respect to Fc/Fc^+ for titanocene **49aa** to -1.37V with respect to Fc/Fc^+ for titanocene **49ac**.

In the absence of an explicit mode of action for compounds **49** in our cell lines we took a holistic approach to confirming that **49aa** was close to optimal. Correlations of the averaged GI_{50} values to both the $E_{1/2}$ and the cyclopentadienyl ligand volumes A^3 were made (Table 4). A literature method was used to estimate the latter.[102] While the correlations were not perfect (R^2 = 0.93 and 0.94), they do suggest that **49aa** is close to optimal and so this was selected for progression to asymmetric synthesis studies.

Table 4: Growth inhibitory assays. GI_{50} values as mean standard error of mean (SEM) of three independent experiments (n = 4 per experiment) *vs.* reduction potential **A** and substituent volume **B**.

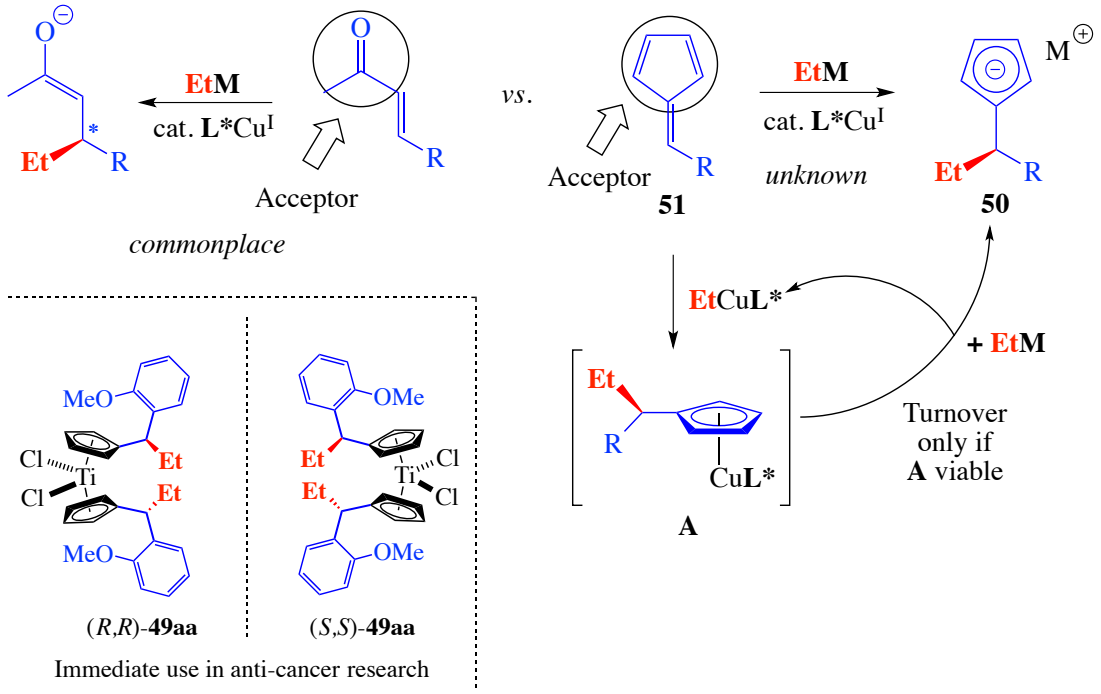
			Mean GI_{50} (μM)			Mean GI_{50} (μM)
Compound	$E_{1/2}$	A^3	HCT-116	MiaPaCa-2	MDA-MB-468	Average for three cell lines
49aa	-1.24	216	12.2	7.5	5.3	8.3
49ab	-1.34	250	42.4	34.7	14.6	30.6
49ac	-1.37	250	24.6	22.4	32.3	26.4
49ad	-1.33	230	28.6	24.8	26.7	26.7
49ae	-1.23	198	5.7	6.6	7.7	6.7
***rac*-49af**	-1.21	274	25	11.4	27.5	21.3
5	-1.11	60	>100	>100	>100	>100



Chapter 3 – Enantiopure titanocenes

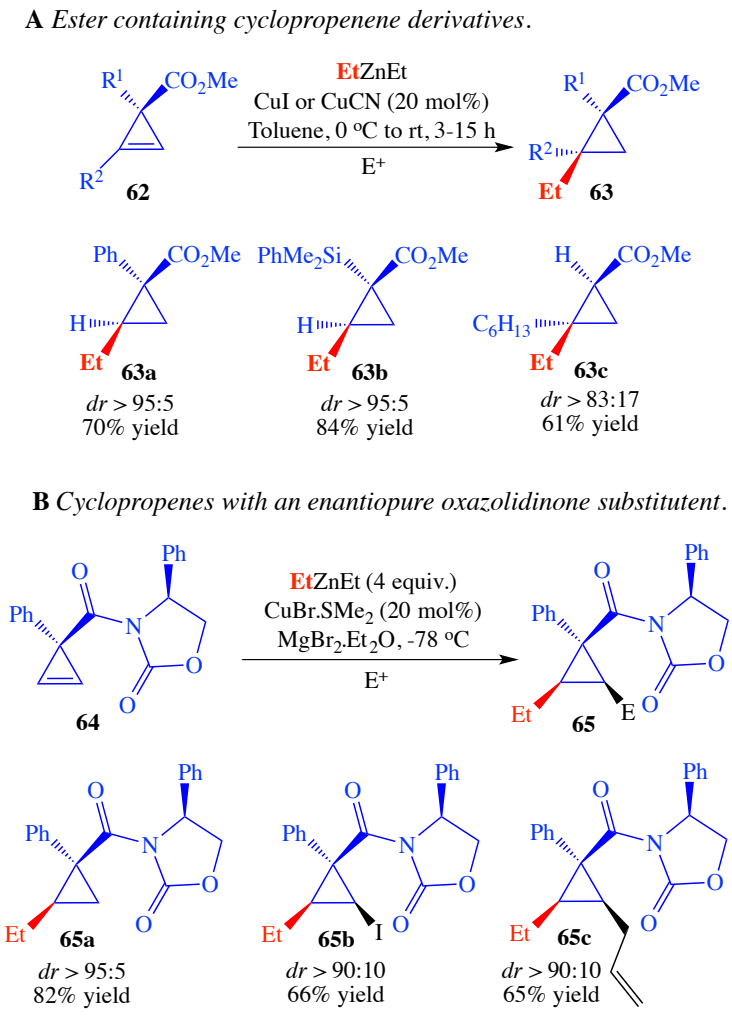
3.1 Introduction

Copper-catalysed asymmetric additions to Michael acceptors (EWG = COR, NO_2, *etc*.) have become commonplace in the last 10 years (Scheme 1).[103] However, equivalent additions to pentafulvenes **51** containing an equally powerful anion stabilising Cp group are unknown (Scheme 1). This unprecedented methodology would allow the synthesis of enantio-enriched cyclopentadienyl ligands **50aa**, which would have immediate application. For example, the active anti-cancer titanocene *rac*/*meso*-**49aa** would be accessible as single enantiomers (*R*,*R*)-**49aa** and (*S*,*S*)-**49aa** favouring its development towards clinical trials. Similarly, many metal cyclopentadienyl complexes are vitally important catalysts in polymerisation and an increasing number of fine chemical transformations.[104]



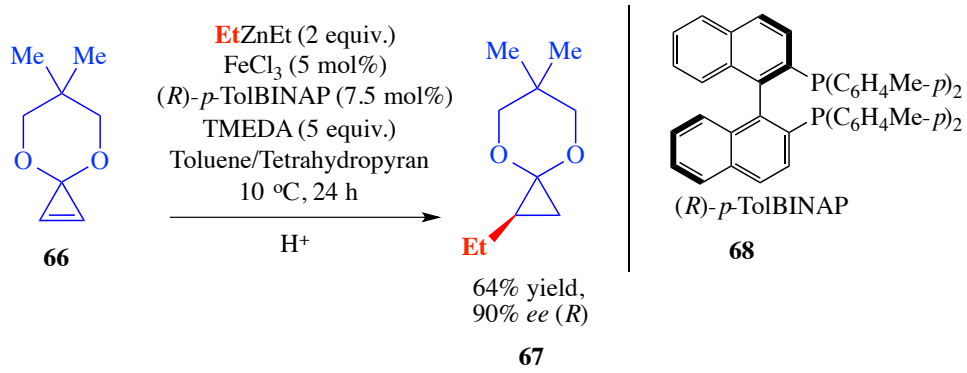
Scheme 21: Copper-catalysed enantioselective additions in electron-deficient alkenes *vs*. pentafulvenes.

Asymmetric copper-catalysed carbometallation reactions are highly challenging, owing to the difficulty in controlling addition of the organocopper to unactivated double bonds.[105] Most known examples relate to the carbometallation of strained double bonds. There are currently two stereoselective alkene copper-catalysed carbozincation reactions. The first is of ester-containing cyclopropene derivatives **62** to give substituted cyclopropanes **63** with high diastereoselectivity (Scheme 22a) whilst the second is the use of cyclopropenes with an enantiomerically pure oxazolidinone as a chiral auxiliary **64**. This results in substituted cyclopropane derivatives **65** with high diasteriomeric ratios due to excellent face discrimination of the double bond through a *syn*-chelated copper-catalysed carbozincation (Scheme 22b).[105]



Scheme 22: Copper catalysed carbozincation[105]

The use of iron salts as catalysts for carbozincation reactions is of particular interest; they are cheap, non-toxic and environmentally benign. Nakamura first reported the use of iron complexes as catalysts for the asymmetric olefin carbometalation of cyclopropenone acetal **66** to 2-substituted cyclopropanone acetal **67** (Scheme 23).[106] A ternary catalytic system involving ferric chloride, the chiral enantiopure diphosphine ligand (*R*)-*p*-TolBINAP **68** and the bidentate achiral diammine TMEDA were utilised. The reaction was run in a toluene/tetrahydropyran mixture as the enantioselectivity was heavily reduced when THF was utilised. Also, when the achiral TMEDA additive was absent in the reaction, only racemic products were obtained.[106]

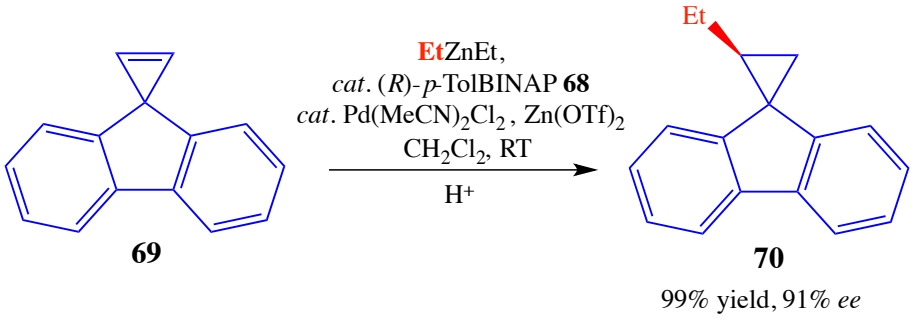


Scheme 23: Enantioselective iron catalysed carbozincation.[106]

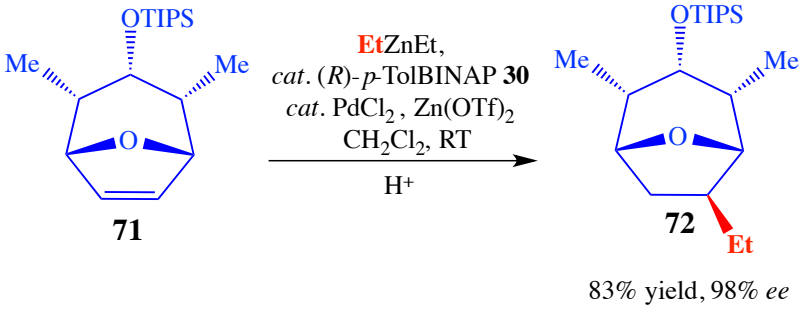
In 2011, Lautens reported a highly enantioselective palladium catalysed carbozincation of cyclopropenes using bis(acetonitrile)dichloropalladium(II) as catalyst and (*R*)-*p*-TolBINAP **68** as chiral ligand (Scheme 24a).[107] Treatment of the cyclopropene functionality **69** with diethylzinc in the presence of the palladium(II) salt, chiral ligand **68** and zinc triflate followed by subsequent quenching with water afforded **70** in 99% yield and 91% *ee*. The use of the zinc triflate additive is thought to help the formation of a more reactive cationic palladium(II) species.[107] Using the same conditions, Lautens also reported the palladium(II)-catalysed carbozincation of

oxabicycloalkenes **71** to the oxabicycloalkane **72** in 81% yield and 98% *ee* (Scheme 24b).[108]

A *Palladium(II) carbozincation of cyclopropenes*

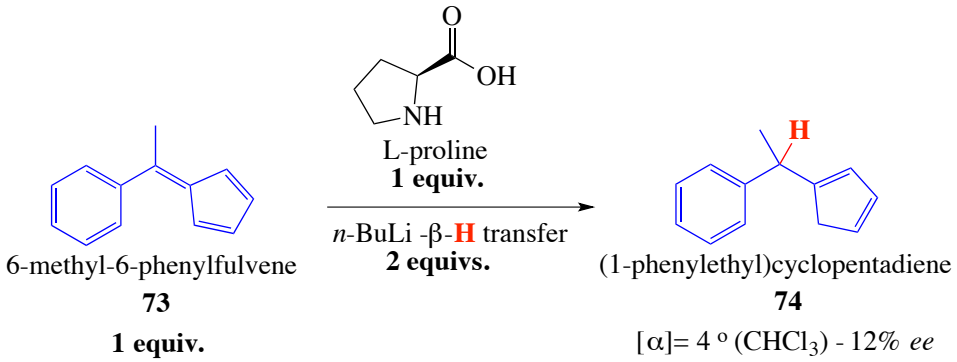


B *Palladium(II) carbozincation of oxabicycloalkenes*



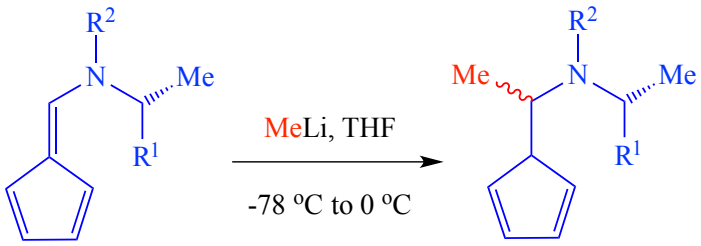
Scheme 24: Enantioselective palladium catalysed carbozincation.[107,108]

The reaction of 6-methyl-6-phenylfulvene **73** with an equivalent of the chiral auxiliary L-proline (1 equiv.) and *n*-BuLi (2 equivs.) results in the formation of (1-phenylethyl)cyclopentadiene **74** through β-hydride transfer with poor enantioselectivity (12% *ee*) (Scheme 12).[109]



Scheme 25: Mintz hydride transfer.[109]

Chiral cyclopentadienyl synthons have been prepared through diastereoselective addition of MeLi to optically active 6-(dialkylamino)fulvenes derived from (*R*)-(1-phenylethyl)amine, (*R*)-(1-cyclohexylethyl)amine and (1*R*,2*S*)-*O*-methylephedrine. ***110*** The addition of MeLi to these fulvenes **75a-e** resulted in the formation of the corresponding dialkyl(1-cyclopentadienylethyl)amines **76a-e** with high diastereoselectivity, up to 87:13 *dr* in the case of the fulvene derived from (*R*)-(1-cyclohexylethyl)amine (Scheme 11).

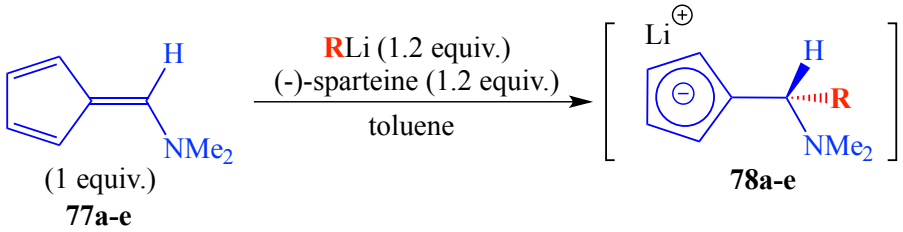


75a-e **76a-e**

Product	R^1	R^2	*dr* (%)
75a	Me	Ph	75:25
75b	Me	Cy	93:7
75c	Et	Cy	90:10
75d	CH_2Ph	Cy	83:17
75e	Me	(*S*)-CH(OMe)Ph	90:10

Table 5: Togni's diasterioselective addition.[110]

The only successful reported literature of a stoichiometric enantioselective organometallic addition to a pentafulvene entails the dropwise addition of 1-(cyclopenta-2,4-dien-1-ylidene)-*N*,*N*-dimethylmethanamine **77a-e** at -90 °C in a toluene solution of stoichiometric equivalents of (-)-sparteine and aryllithium (Scheme 13).[111] The mixture was warmed at -78 °C and stirred for 7 h yielding excellent yields of **78a-e** and in high enantiomeric excess. The use of a catalytic amount of the chiral base resulted in a much lower enantioselectivity.



	R	Yield (%)[a]	*ee* **40**/%[b]
a	Ph	93	51 (*R*)
b	2-MeC_6H_4	91	91 (*R*)
c[c]	2-MeC_6H_4	81	8 (*R*)
d	2-OMeC_6H_4	83	90 (*R*)
e	Naphtyl	92	83 (*R*)

[a] Isolated yield of rhodium complex obtained by subsequent reaction of **78a-e** with $[RhCl(norbornadiene)]_2$
[b] Determined by HPLC (Chiralcel OD-H) 100/1 hexane/2-propanol
[c] 20 mol% (-)-sparteine

Table 6: Hayashi's stoichiometric enantioselective addition to fulvenes.[111]

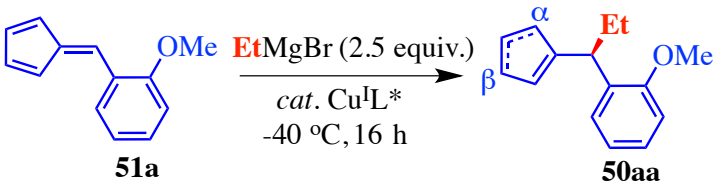
3.2 Enantio-enriched substituted cyclopentadienyl ligands

3.2.1 Grignard reagent trials

Our research aimed to develop a novel enantioselective catalysed organo-addition reaction to fulvenes, which would provide access to highly enantioenriched alkyl substituted chiral cyclopentadienyl ligands / titanocenes. Based on our previous work,[112] a range of alkyl/branched alkyl racemic cyclopentadienyl ligands were obtained in high yield, by the addition of organocuprates, to the electrophilic exocyclic double bond of the 6-substituted pentafulvene 1-(cyclopenta-2,4-dien-1-ylidenemethyl)-2-methoxybenzene **51a**.

We were interested to probe whether chiral ligands would deliver ligand-accelerated catalysis. As highlighted before in our previous work[112] the addition of chiral phosphanes and Grignard reagent (EtMgBr) to **51a** provided no evidence of any induced stereoselectivity (Table 7-8).

Table 7: Comparison of selected ligands in Grignard addition to **1**.



51a **50aa**

Entry	Cu(I) (3 mol%)	L* (5 mol%)	Yield **50aa** (%)[a]	Recovered **51a** (%)[a]	*er* ***50aa***[c]
1	-	-	0	56	50:50
2	CuBr•SMe_2	-	69	11	50:50
3	-	**79**	0	28	50:50
4	CuBr•SMe_2	**79**	55	5	50:50
5	-	**80**	0	51	50:50
6	CuBr•SMe_2	**80**	31	39	50:50
7	-	**81**	5 (4)[b]	114 (96)[b]	50:50
8	CuBr•SMe_2	**81**	92 (85)[b]	16 (15)[b]	50:50
9	CuI	**82**	3	36	50:50
10	CuBr•SMe_2	**82**	47	36	50:50
11	CuI	**83**	1	101	50:50
12	CuBr•SMe_2	**83**	63	2	50:50

[a] Yield by chiral GC on a CP-Chirasil-DEX CB column against internal standard
[b] Normalised GC yield [c] *er* by chiral GC on a CP-Chirasil-DEX CB column.

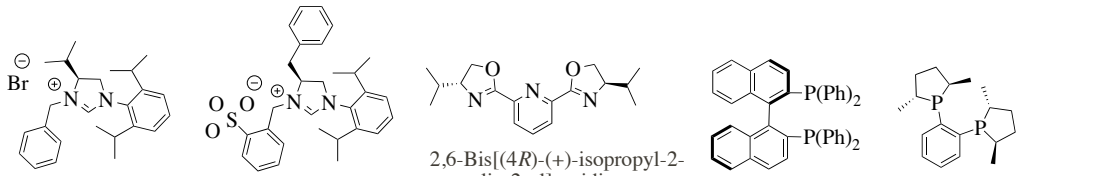
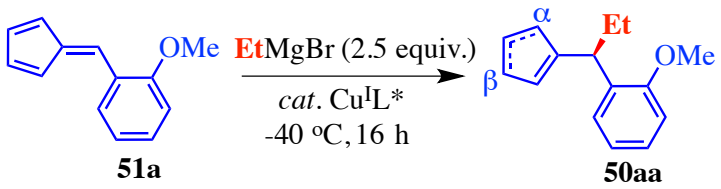


Figure 14: Initial chiral ligand screening with EtMgBr

A typical reaction involved the addition of the copper source and chiral ligand in ether (Table 7), MTBE or CH_2Cl_2 (Table 8) followed by the addition EtMgBr (2.5 equiv.) at -40 °C. The mixture was then left to stir at this temperature for 15 min followed by the dropwise addition of solvent solution (1.0 mL) of **51a** (0.5 mmol). The reaction was left at -40 °C for 16 h and was then quenched with NH_4Cl.

Table 8: Further comparison of selected ligands in Grignard addition to **1**.



51a **50aa**

Entry	Cu (5 mol%)	L* (6 mol%)	Solvent	Yield **50aa** (%)[a,b]	Recovered **51a** (%)[a,b]	*er* ***50aa***[c]
1	CuI	**68**	CH_2Cl_2	106 (81)	25 (19)	50:50
2	CuBr•SMe_2	**68**	MTBE	114 (81)	27 (19)	50:50
3	CuBr	**68**	MTBE	98 (79)	26 (21)	50:50
4	CuBr•SMe_2	**84**	MTBE	92 (80)	23 (20)	50:50
5	CuBr	**85**	CH_2Cl_2	23 (18)	104 (82)	51:49
6	CuBr•SMe_2	**86**	MTBE	94 (81)	22 (19)	51:49
7	CuCl	**87**	MTBE	7 (6)	124 (94)	51:49
8	CuCl	**85**	MTBE	87 (79)	23 (21)	50:50
9	CuBr•SMe_2	**88**	MTBE	69 (62)	42 (38)	50:50
10	CuBr	**89**	MTBE	85 (81)	20 (19)	50:50
11	CuBr•SMe_2	**89**	MTBE	95 (80)	24 (20)	50:50
12	$Cu(OAc)_2$	**90**	MTBE	106 (80)	26 (20)	50:50

[a] Yield by chiral GC on a CP-Chirasil-DEX CB column against internal standard [b] Normalised GC yields are presented in brackets on the basis that complete mass balance is attained [c] *er* by chiral GC on a CP-Chirasil-DEX CB column.

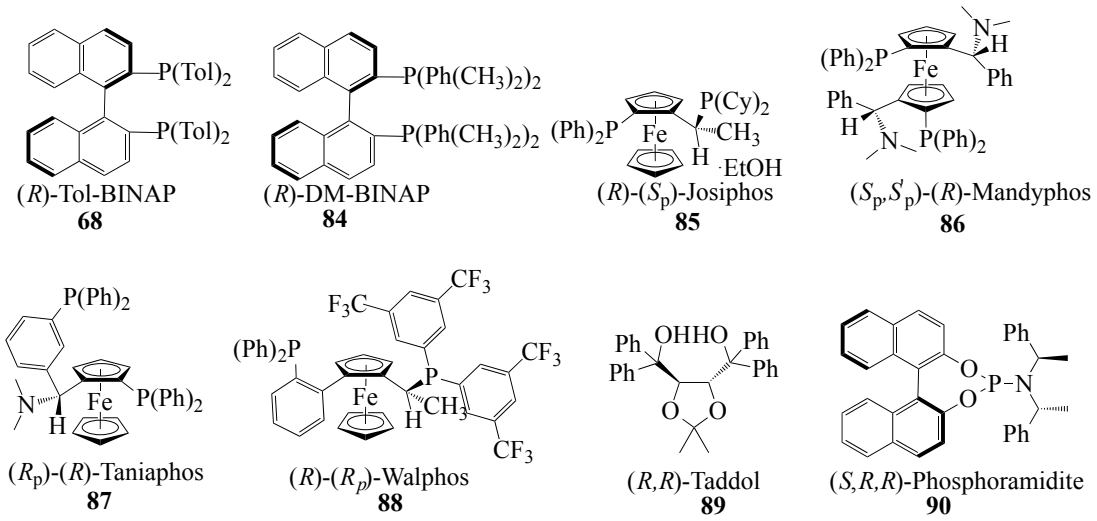
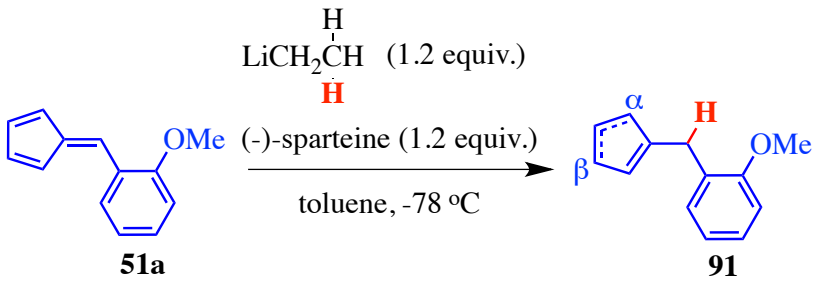


Figure 15: Further chiral ligand screening with EtMgBr.

3.2.2 Organolithium trials

The only successful literature example of an enantioselective organometallic addition to a fulvene entails the dropwise addition of 1-(cyclopenta-2,4-dien-1-ylidene)-*N*,*N*-dimethylmethanamine at -90 °C to a toluene solution of stoichiometric equivalents of (-)-sparteine and phenyllithium, providing excellent yields and enantiomeric excess.[111] Thus, a similar reaction was devised. To a solution of freshly distilled (-)-sparteine (0.11 mL, 112 mg, 0.48 mmol) in dry toluene (0.8 mL) was added a solution of ethyllithium in toluene (0.22 M, 2.18 mL, 0.48 mmol) at -78 °C. The solution was stirred for 10 min and then cooled to -90 °C followed by the dropwise addition over 10 min of **51a** (73.6 mg, 0.4 mmol) in dry toluene (0.4 mL). The reaction was left to stir at -78 °C for 7 h. Unfortunately, the desired product was not obtained. A different product was obtained in moderate yield. Analysis by GC-MS indicated that the product formed was a result of hydride transfer **91** (Scheme 14).

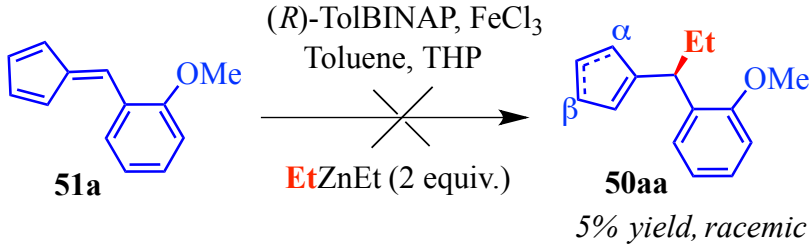


Scheme 26: EtLi addition to **51a**

3.2.3 Organozinc/organoaluminium trials

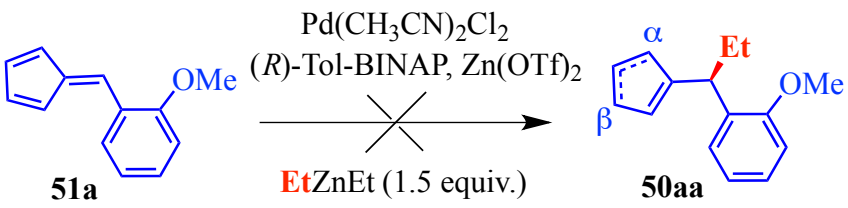
Next we turned our attention to the use of more covalent reagents (diethylzinc or triethylaluminium), so as to try and control the reaction. We rationalised that a a stronger M-O contact with **51a** would lead to a more ordered transition state providing **A** (see Scheme 21) and this should also maximise any enantiofacial selectivity by putative RCu^{I}**L***.

A similar reaction to Nakumara's iron catalysed olefin carbometalation of cyclopropenone acetals[106] was devised. To a mixture of (*R*)-Tol-BINAP (25.5 mg, 7.5 mol%) and Et_2Zn (1.25 mL, 0.8 M, 1 mmol) was added dropwise a 0.1 M tetrahydropyran (0.25 mL) solution of $FeCl_3$ (4.1 mg, 0.025 mmol) at 25 °C. The reaction was diluted with 2 mL toluene. A solution of **51a** was added (92.1 mg, 0.5 mmol) in 1 mL toluene over 2 h at 0 °C. The reaction was stirred at 5 °C for 48 h followed by quenching with NH_4Cl. A 5% yield of racemic product was obtained (Scheme 27).



Scheme 27: Nakamura Iron catalysed olefin carbometalation.

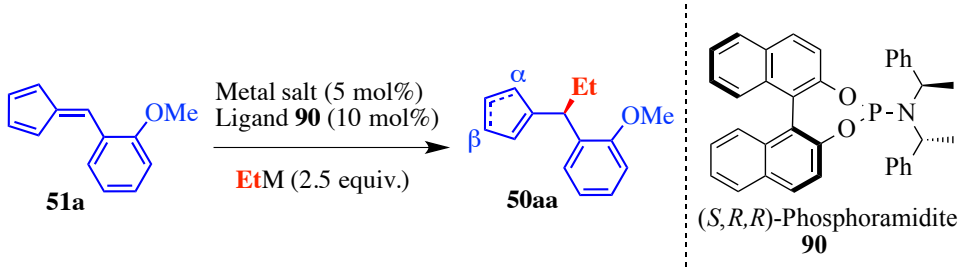
A palladium-catalysed enantioselective addition was then tried. Substituted pentafulvene **51a** (74 mg, 0.4 mmol), $Pd(CH_3CN)_2Cl_2$ (5.2 mg, 0.02 mmol), (*R*)-Tol-BINAP (16.2 mg, 0.024 mmol) and $Zn(OTf)_2$ (14.6 mg, 0.04 mmol) were placed in a dry Schlenk flask. Dichloromethane (3 mL) was added and the mixture was stirred for 1 h at 25 °C. Then the reaction was cooled at -78 °C and diethylzinc (0.6 mL, 1.5 equiv.) was added dropwise. The reaction was allowed to warm to 25 °C overnight. No product was obtained (Scheme 28).



Scheme 28: Pd catalysed enantioselective addition.

Inspired by the work led by Feringa, notably his conjugate addition to chalcones,[113] a set of reactions were carried out using ligand **90** (10 mol%), metal source (5 mol%) in toluene or diethyl ether (2.0 mL). The mixture was left to stir at 25 °C for 1 h, followed by the dropwise addition of a solvent solution of **51a** (0.5 mmol) (Table 5).

Table 9: Addition of orgamometallic - Metal screen with **90** – *Reaction at 0 °C.*



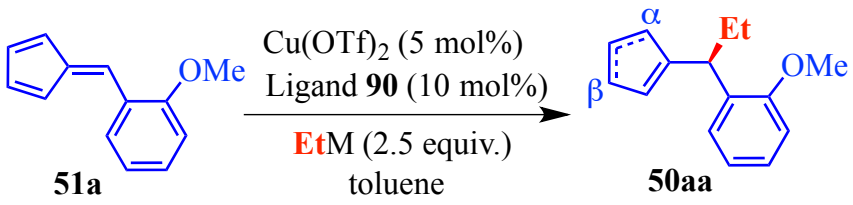
Entry	MX (5 mol%)	RM	Solvent	Yield **50aa** (%)[a]	Recovered **51a** (%)[a]	*er* %[b]
1	$Cu(OTf)_2$	Et_2Zn	Toluene	2	39	65:35
2[c]	$Cu(OTf)_2$	Et_2Zn	Toluene	6	45	67:33
3	$Cu(MeCN)_4BF_4$	Et_2Zn	Toluene	1	44	54:46
4	$Cu(MeCN)_4BF_4$	Et_2Zn	Ether	1	24	50:50
5	$FeCl_3$	Et_2Zn	Toluene	3	63	51:49
6	$MnCl_2$	Et_2Zn	Toluene	3	68	51:49
7	$Rh_2(OAc)_4$	Et_2Zn	Toluene	5	64	51:49
8	$FeCl_3$	Et_3Al	Toluene	3	98	53:47
9	$Ni(OAc)_2$	Et_3Al	Ether	0	44	50:50
10	$MnCl_2$	Et_3Al	Toluene	8	83	51:49

[a] Yield by chiral GC on a CP-Chirasil-DEX CB column against internal standard [b] *er* by chiral GC on a CP-Chirasil-DEX CB column [c] Addition of **51a** followed by diethylzinc

As shown in Table 9 using diethylzinc as the organometallic reagent, moderate to low enantioselectivies were obtained in Entries 1, 2 and 3. Although the product yield obtained is less than 6% in all cases, this demonstrates the first enantioselective carbozincation reaction to substituted pentafulvenes. The use of non-copper salts with diethylzinc or triethylaluminium resulted in poor or no yields and enantioselectivity.

As shown in Table 10, increasing the catalyst concentration (Entry 1-3) resulted in low yield (16%) and moderate *er*. A poor yield or no reaction at all was attained when screening other metal salts. The use of a stoichiometric amount of chiral ligand did not result in an increase in yield and *er* (Table 10, Entry 4). Changing the metal source with ligand **90** resulted in poor yield, racemic product (Entry 6-11) or low *er* (Entry 12).

Table 10: Addition of diethylzinc - Metal salt screen with **52**[a] – *Reaction at 0 °C*.



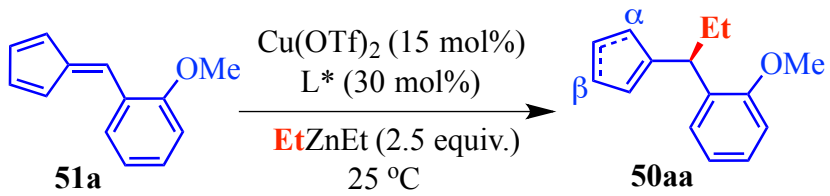
51a **50aa**

Entry	MX	L	Yield **50aa** (%)[b]	Rec. **51a** (%)[b]	*er* **50aa**[c]
1	$Cu(OTf)_2$ 15 mol%	30 mol%	7	93	63:37
2	$Cu(OTf)_2$ 25 mol%	50 mol%	16	84	71:29
3	$Cu(OTf)_2$ 5 mol%	10 mol%	6	94	58:42
4	$Cu(OTf)_2$ 5 mol%	1 equiv.	3	97	53:47
5[d]	$Cu(OTf)_2$ 5 mol%	10 mol%	/	/	/
6	$CuBr•SMe_2$ 10mol%	n/a	4	96	50:50
7	Li(OTf) 5 mol%	10 mol%	1	99	51:49
8	In(OTf)3 5 mol%	10 mol%	2	98	50:50
9	CuTC 5 mol%	10 mol%	2	98	50:50
10	Mn(III) acac 5 mol%	10 mol%	2	98	50:50
11	$Sn(OTf)_2$ 5 mol%	10 mol%	3	97	50:50
12	Co(II) acac 5 mol%	10 mol%	2	98	54:46[e]

[a] Addition of metal source (x mol%) and Ligand **90** (x mol%) in toluene (2.0 mL). The mixture was left to stir for 1 h followed by the addition of a toluene solution (1.0 mL) of **1** (0.5 mmol). Mixture left to stir for 10 min followed by the dropwise addition of diethylzinc (2.5 equiv.) at 0 °C. Left for 16 h. [b] Normalised yield by chiral GC on a CP-Chirasil-DEX CB column against internal standard [c] *er* by chiral GC on a CP-Chirasil-DEX CB column [d] Tetrahydrofuran used as solvent rather than toluene [e] Addition of 2.5 equiv. TMSCl. [f] opposite enantiomer.

As the Lewis acidic $Cu(OTf)_2$ was the most effective precursor, we turned our attention to the effect of solvent / chiral ligand in the reaction (Table 11). The use of $Cu(OTf)_2$ (15 mol%) and chiral ligand **90** (30 mol%) in MTBE (Entry 1), resulted in a high *er* (88:12) but low yield (20%). Changing the solvent to Me-THF (Entry 2) resulted in no reaction at all whilst in toluene (Entry 3) a massive drop in *er* (64:36) and yield (10%) was observed. Of particular note is the use of the chiral amine **91**. A high yield (76%) but essentially racemic product was attained in MTBE (Entry 4). The use of imidazolium ligands resulted in poor to no yields (Entries 7-12).

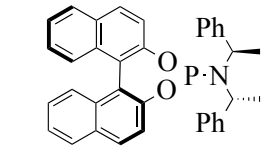
Table 11: Effect of solvent/ligand screen[a] – *Reaction at 25 °C.*



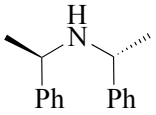
51a **50aa**

Entry	L*	Solvent	Yield **50aa** (%)[b]	Rec. **51a** (%)[b]	*er* **50aa**[c]
1	**90**	MTBE	20	18	88:12
2	**90**	Me-THF	1	76	50:50
3	**90**	Toluene	10	63	64:36
4	**91**	MTBE	76	22	52:48
5	**91**	Me-THF	5	95	53:47
6	**92**	MTBE	6	72	50:50
7	**92**	Me-THF	2	98	50:50
8	**92**	Toluene	0	36	50:50
9	**93**	MTBE	9	84	50:50
10	**93**	Me-THF	1	69	50:50
11	**93**	Toluene	3	97	50:50

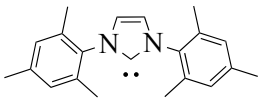
[a] Addition of $Cu(OTf)_2$ (15 mol%) and Ligand (30 mol%) in solvent (2.0 mL). The mixture was left to stir for 1 h at 25 °C followed by the addition of a solvent solution (1.0 mL) of **51a** (0.5 mmol). Mixture left to stir for 10 min followed by the dropwise addition of diethylzinc (2.5 equiv.) at 25 °C. Left for 16 h. [b] Yield by chiral GC on a CP-Chirasil-DEX CB column against internal standard [c] *er* by chiral GC on a CP-Chirasil-DEX CB column.



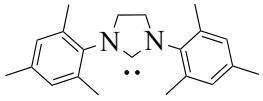
(*S,R,R*)-Phosphoramidite
90



(*R*)-bis((*R*)-1-phenylethyl)amine
91



1,3-dimesityl-1 *H*-imidazol-3-ium-2-ide
IMes
92

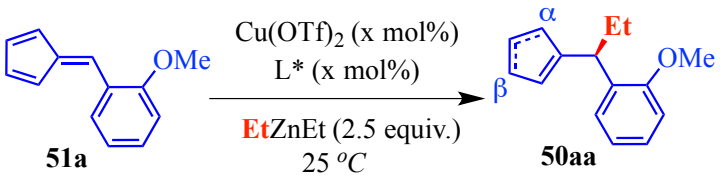


1,3-dimesityl-4,5-dihydro-1 *H*-imidazol-3-ium-2-ide
SIMes
93

Figure 16: Initial chiral ligand screening with Et_2Zn

As can be seen in Table 12, increasing the catalyst concentration up to 20 mol% copper(II) triflate and 40 mol% ligand **90** in MTBE resulted in a high *er* (89:11) but still with low yield (24%) (Entry 3). Increasing the catalyst loading up to 30 mol% copper(II) triflate and 60% ligand did not result in an increase in *er* (Entry 4-5) whilst changing the stoichiometry of the metal/ligand resulted in no yield (Entry 6-7). Exploration of a small phosphoramidite library (Table 12) provided a range of *er* values but no significant increase in activity except Entry 12 when compared to Entry 1. The use of ligand **94** (Entry 8), having an electron donating methoxy group at the *ortho*-position resulted in a higher yield than Entry 1 but lower *er*. Changing the bulky binapthyl core to a biphenol, or 3,5-dimethylphenol and the use of electronically/bulky chiral amines **95-97** (Entry 9-11) resulted in at most very small enantiomeric excess. The binaphthol ligand/2-naphthylethylamine counterpart **98** (Entry 12) showed promise when compared to Entry 1 as it showed higher yield (23%) whilst retaining the same *er* (75:25). The use of the bulky phosphoramidite having an octahydrobinaphtyl and 2-naphtylethylamine **99** (Entry 13) resulted in higher yields but lower *er* than Entry 3.

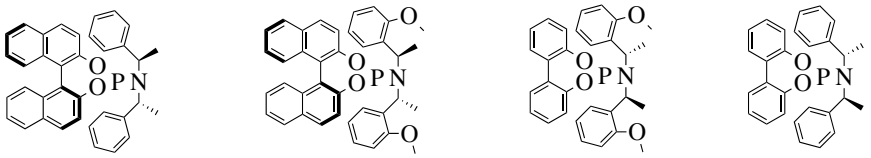
Table 12: $Cu(OTf)_2$ with ligand screen[a] – *Reaction at 25 °C.*



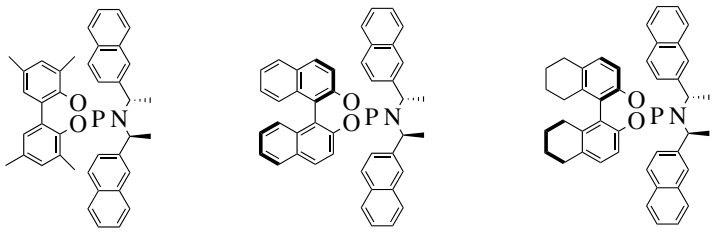
51a **50aa**

Entry	$Cu(OTf)_2$ (x mol%)	L*	Yield **50aa** (%)[b]	Recovered **51a** (%)[b]	*er* %[c]
1	10	**90** – 20 mol%	14	31	76:24
2	15	**90** – 30 mol%	27	58	87:13
3	20	**90** – 40 mol%	24	52	89:11
4	25	**90** – 50 mol%	15	34	88:12
5	30	**90** – 60 mol%	14	41	88:12
6	15	**90** – 20 mol%	2	74	/
7	15	**90** – 7.5 mol%	0	/	/
8	10	**94** – 20 mol%	24	47	68:32
9	4.2	**95** – 8.4 mol%	37	31	50:50
10	10	**96** – 20 mol%	8	61	55:45
11	5	**97** – 10 mol%	3	40	50:50
12	8	**98** – 16 mol%	23	28	75:25
13	20	**99** – 40 mol%	39	41	73:27

[a] Addition of $Cu(OTf)_2$ (x mol%) and Ligand (x mol%) in MTBE (2.0 mL). The mixture was left to stir at 25 °C for 1 h followed by the addition of a MTBE solution (1.0 mL) of **51a** (0.5 mmol). Mixture left to stir for 10 min followed by the dropwise addition of diethylzinc (2.5 equiv.) at 25 °C. Left for 16 h at 25 °C [b] Yield by chiral GC on a CP-Chirasil-DEX CB column against internal standard [c] *er* by chiral GC on a CP-Chirasil-DEX CB column.



(*S*,*R*,*R*)-Phosphoramidite **90** (*S*,*R*,*R*)-Phosphoramidite **94** (*S*)-Phosphoramidite **95** (*S*)-Phosphoramidite **96**

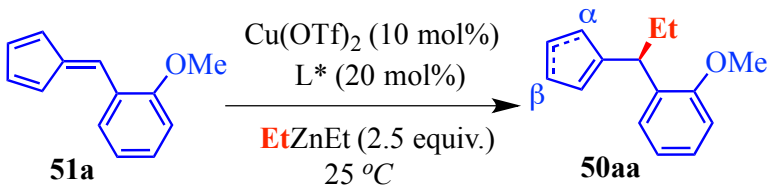


(*S*)-Phosphoramidite **97** (*R*,*S*,*S*)-Phosphoramidite **98** (*R*,*S*,*S*)-Phosphoramidite **99**

Figure 17: Chiral ligand screening with Et_2Zn.

Unfortunately, ligand classes other than phosphoramidite provided no enantioselectivity (Table 13, Figure 18). Negligible yields were obtained when ligands **100-103**, **104**, **106**, **108** and **83** were utilised. Moderate to high yield were obtained using the chiral oxazolipyridine **81**, chiral amino alcohols **105** and **109** and chiral amine **107**.

Table 13: Addition of diethylzinc – $Cu(OTf)_2$ with ligand screen[a] – *Reaction at 25 °C*.



Entry	L* (20 mol%)	Yield **50aa** (%)[b]	Recovered **51a** (%)[b]	*er* ***50aa*** [c]
1	**100**	7	40	50:50
2	**82**	0	65	50:50
3	**101**	3	62	50:50
4	**102**	7	31	50:50
5	**103**	33	53	50:50
6	**81**	62	38	50:50
7	**104**	5	114	50:50
8	**105**	68	32	50:50
9	**106**	0	n/a	50:50
10	**83**	28	52	50:50
11	**107**	57	48	50:50
12	**108**	0	102	50:50
13	**109**	50	38	50:50

[a] Addition of $Cu(OTf)_2$ (10 mol%) and Ligand (20 mol%) in MTBE (1.2 mL). The mixture was left to stir at 25 °C for 1 h followed by the addition of a MTBE solution (0.6 mL) of **51a** (0.3 mmol). Mixture left to stir for 10 min followed by the dropwise addition of diethylzinc (2.5 equiv.) at 25 °C. Left for 16 h at 25 °C [b] Yield by chiral GC on a CP-Chirasil-DEX CB column against internal standard [c] *ee* by chiral GC on a CP-Chirasil-DEX CB column.

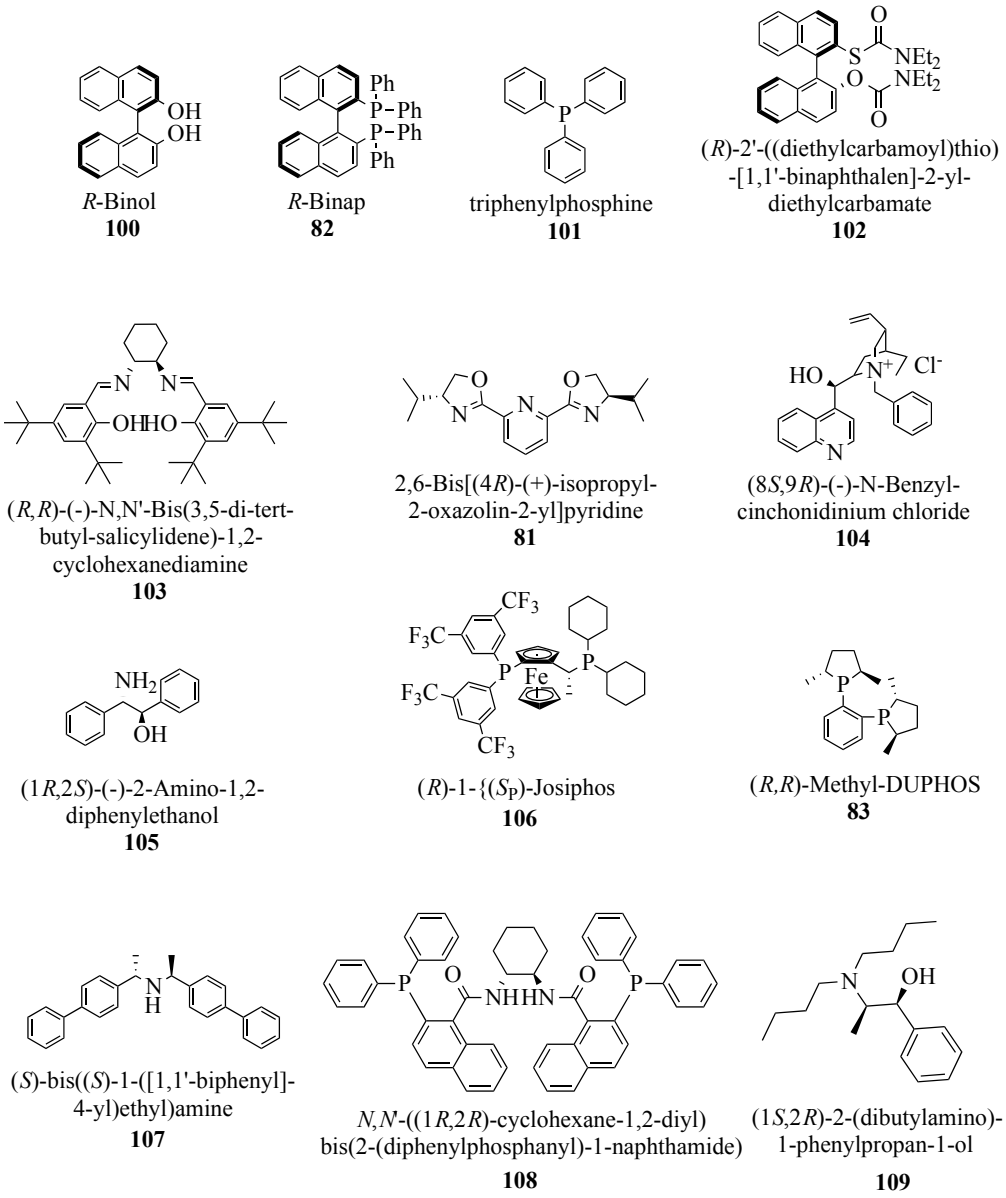
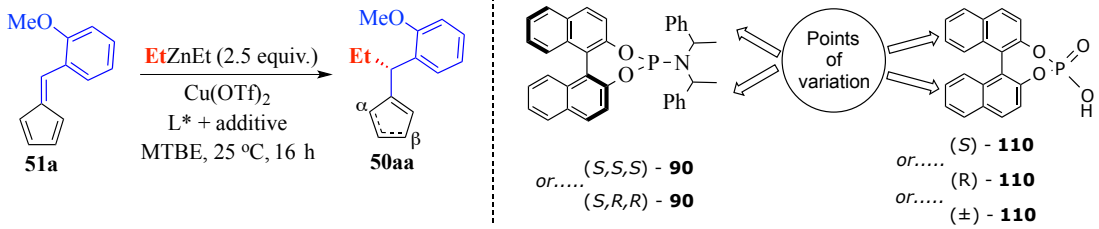


Figure 18: Chiral ligand screening

A screen of metal salts revealed that Lewis acidic $Cu(OTf)_2$ was the most effective precursor, so we sought for an additive that might improve its behaviour (Table 14). Bridging ligands are known to play a critical role in organising selective transition states in asymmetric copper(I) catalysis but are not normally modified to chiral units in copper catalysed asymmetric catalysis. To our delight, use of the simple commercial phosphoric acid **110** had a profound effect on both the rate and selectivity of the carbozincation. Using the conditions of Table 13 (run 12), a small library of phosphoric acid additives were then tested (Table 15, Figure 19).

Table 14. Additive effects in copper catalysed **90**/**110** $ZnEt_2$ additions to pentafulvene **51a**.[a]



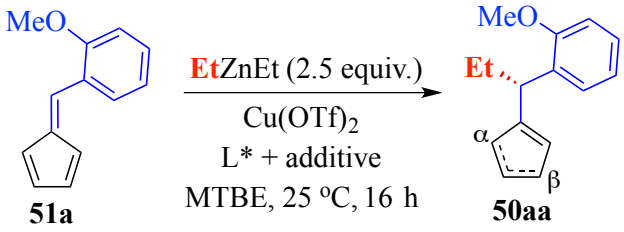
Entry	$Cu(OTf)_2$ (mol %)	L* (mol-%)	Additive (mol %)	Yield **50aa** %[b]	*er* **50aa**[b]
1	20	(*S,R,R*)- **90** (40)	/	24	89:11
2	20	(*S,R,R*)- **90** (20)	(*S*)- **110** (20)	2	88:12
3	20	(*S,R,R*)- **90** (30)	(*S*)- **110** (10)	1	86:14
4	20	(*S,R,R*)- **90** (30)	(*R*)- **110** (10)	2	86:14
5	20	(*S,S,S*)- **90** (40)	/	24	60:40
6	20	(*S,S,S*)- **90** (30)	(*S*)- **110** (10)	34	90:10
7	20	(*S,S,S*)- **90** (30)	(*R*)- **110** (10)	81	87:13
8	20	(*S,S,S*)- **90** (30)	(±)- **110** (10)	58	90:10
9	10	(*S,S,S*)- **90** (15)	(*R*)- **110** (10)	81	85:15
10	10	(*S,S,S*)- **90** (15)	(*R*)- **110** (15)	70	81:18
11	12	(*S,S,S*)- **90** (18)	(*S*)- **110** (13)	36	88:12
12	12	(*S,S,S*)- **90** (18)	(±)- **110** (13)	66	88:12

[a] Cu-source **L*** and additive in MTBE (1.2 mL) stirred for 1 h followed by **51a** (0.3 mmol) in MTBE (0.6 mL). After 10 min $ZnEt_2$ (2.5 equiv.) added dropwise and the mixture stirred (16 h). [b] Yield and *er* by chiral GC on a CP-Chirasil-DEX CB column against tridecane as internal standard.

As can be seen in Table 15, the displacement of the triflate anion with the achiral phenyl phosphinic acid and the octahydrobinol derived chiral phosphoric acid gave essentially racemic products in low to moderate yields. One the other hand, the use of the bulky BINOL derivatives at the 3,3' positions (SMe and 2,4,6-(^{i}Pr)$_3$C$_6$H$_2$) and VAPOL phosphoric acid led to moderate to high *er* values. This might imply that a bulky X^- is needed to have ligand accelerated catalysis and selectivity at the same time. The use of a pre-formed phosphate-Cu catalyst resulted in low yield and

racemic product indicating that the Lewis acidic triflate anion and the phosphate contribute in the enantioselective step.

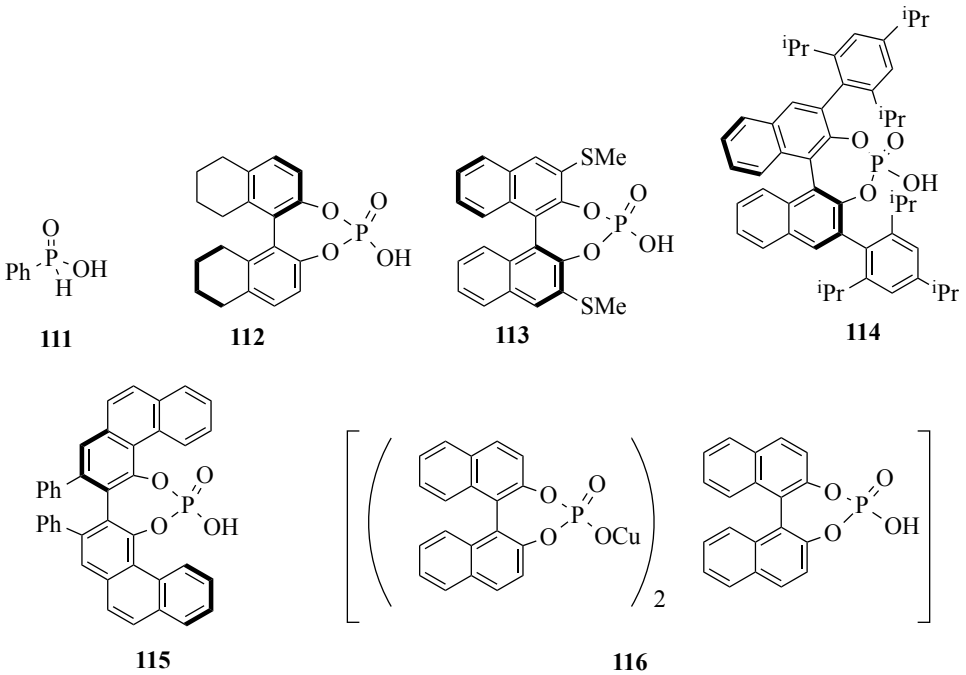
Table 15. Additive effects in copper catalysed L_A/L_B $ZnEt_2$ additions to pentafulvene **51a**.[a]



51a **50aa**

Run	$Cu(OTf)_2$ (mol %)	L* (18 mol %)	Additive (13 mol %)	Yield **50aa** %[b]	*er* **50aa**[b]
1	12	(*R,R,R*)- **90**	**111**	64	68:32
2	12	(*R,R,R*)- **90**	**112**	24	48:51
3	12	(*S,S,S*)- **90**	**113**	65	76:24
4	12	(*S,S,S*)- **90**	**114**	57	68:32
5	12	(*S,S,S*)- **90**	**115**	57	87:13
6	/	(*S,S,S*)- **90**	**116**	6	51:49

[a] Cu-source L* and additive in MTBE (1.2 mL) stirred for 1 h followed by **51a** (0.3 mmol) in MTBE (0.6 mL). After 10 min, $ZnEt_2$ (2.5 equiv.) added dropwise and the mixture stirred (16 h). [b] Yield and *er* by chiral GC on a CP-Chirasil-DEX CB column against tridecane as internal standard.

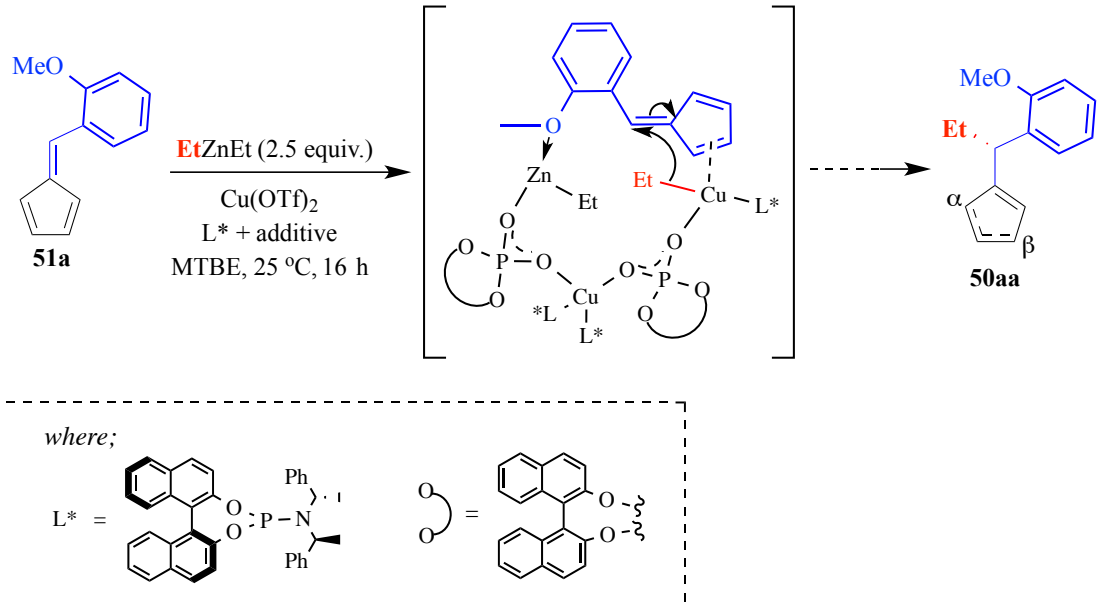


111 **112** **113** **114**

115 **116**

Figure 19: A screen of phosphoric acid additives

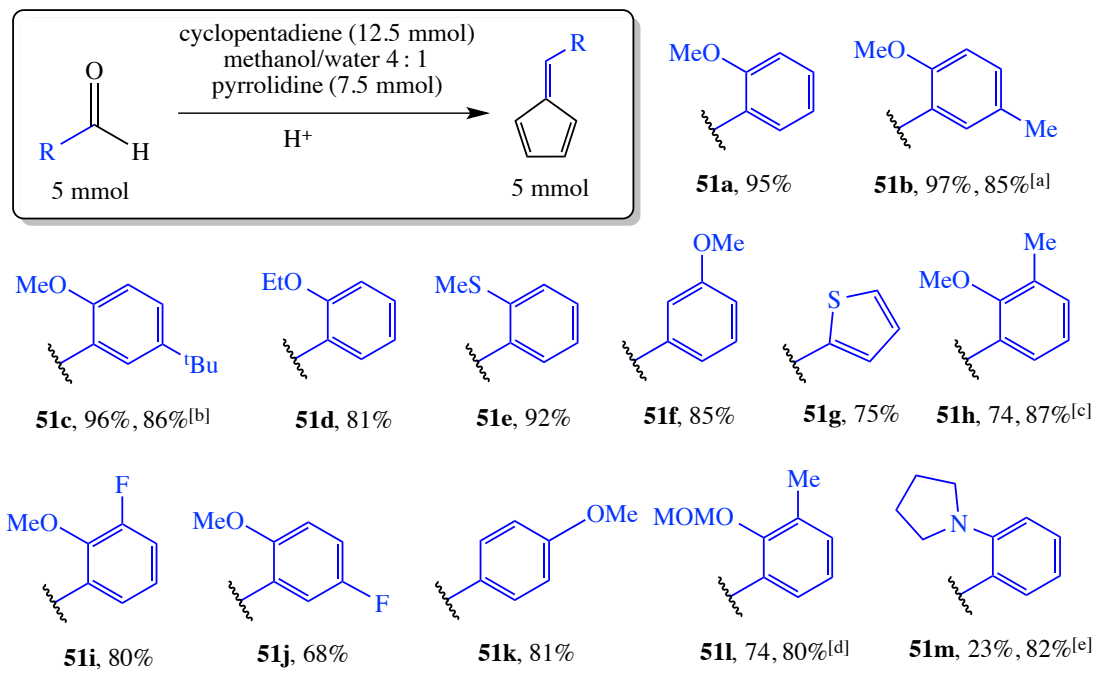
A tentative structure for the catalytic asymmetric $ZnEt_2$ addition method is proposed in Scheme 29, based on the optimal stoichiometry of the reactants. This could involve the interaction between the cuprate and the alkene component of the cyclopentadiene whilst the organo species adds to the C6 carbon of the substituted pentafulvene **51a**. The Lewis basic methoxy donor lone pair would also serve as a crucial anchor point to the Lewis acid zinc species thus holding the intermediate complex together.



Scheme 29: Proposed cuprate-ene π-complex interaction based on the optimal stoichiometry of the reactants.

3.2.4 Scope of the reaction

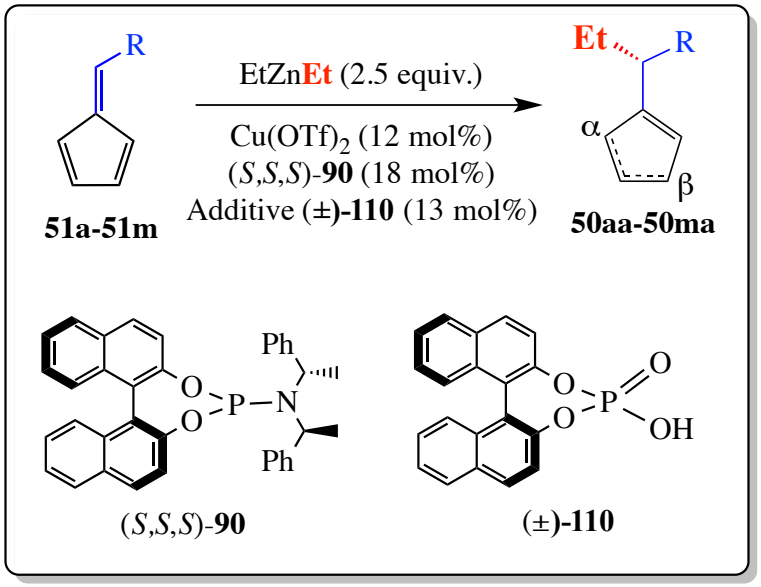
The catalytic asymmetric diethylzinc addition method for the preparation of enantio-enriched cyclopentadienyl ligands (*R*)- and (*S*)-**50aa** was devised for solution and biological studies of the derived titanocene **49aa**. However, the catalytic asymmetric diethylzinc addition is also of wider scope (*e*.g. for preparation of libraries of chiral Cp metal complexes). Having established the most suitable reaction conditions for the asymmetric ethyl addition to **51a**, several other 6-substituted pentafulvene starting materials containing lone pair donor groups on the aryl or heteroaryl ring were prepared in excellent yields (Scheme 30).

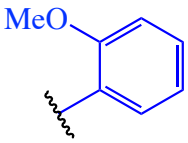


Scheme 30: Synthesis of 6-substituted pentafulvenes. [a] Synthesis of the intermediate afforded 1-(cyclopenta-2,4-dien-2-ylidenemethyl)-5-methylphenol in 97% yield. Subsequent methylation with iodomethane afforded **51b** in 85% yield. [b] Methylation of the aldehyde 5-(*tert*-butyl)-2-hydroxybenzaldehyde with iodomethane afforded the aldehyde precursor 5-*tert*-butyl-2-hydroxybenzaldehyde in 96% yield. Subsequent formation of **51c** was obtained in 86% yield. [c] Synthesis of the intermediate afforded 1-(cyclopenta-2,4-dien-2-ylidenemethyl)-3-methylphenol in 74% yield. Subsequent methylation with iodomethane afforded **51h** in 87% yield. [d] Synthesis of the same intermediate as [c] followed by subsequent protection with chloromethyl methyl ether afforded **51l** in 80% yield. [e] Synthesis of the aldehyde precursor afforded 2-(pyrrolidin-1-yl)benzaldehyde in 23% yield. Subsequent formation of **51m** was obtained in 82% yield.

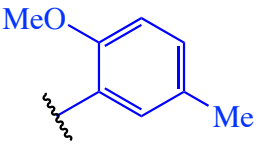
The choice of the 6-substituted pentafulvene substrates was limited to pentafulvenes with electron-donating substitutents, as these were reported to be much more stable at room temperature (lower rate of dimerisation) than pentafulvenes with electron-withdrawing substituents.[73] Additionally, aldehydes with electron donating substituents were found to have an appreciably higher rate of pentafulvene formation than those with electron withdrawing substituents.[114]

Screening of the 6-substituted pentafulvenes **51aa-5lma** in the catalytic asymmetric diethylzinc addition method revealed noteworthy considerations. Based on the correlation attained for **50aa** an (*S*) configuration for the major enantiomer attained from (*S,S,S*)-$\mathbf{L_A}$ is predicted for **50ab-51m**. Addition of dibutylzinc provided the butyl analogue **50ab** with 56% yield and *er* 90:10. A range 6-substituted pentafulvenes **51ba-51ia** can also be accommodated in this catalytic asymmetric addition reaction, providing **50ba-50ia** with *er* values ranging from 63:37 to 93:7. Substrates **50ba** and **50ca** having alkyl electron donating substituents situated on the other side of the aryl ring and **50da** bearing an ethoxy substituent, led to an increase in the enantioselectivity of the reaction. It is unclear whether this has arisen from steric and/or electronic effects. Unfortunately, substrates **50ha**, **50ia** and **50la** having *meta*-substitutents next to the *ortho*-methoxy group suffer from enantioselectivity with respect to parent **50aa**. The presence of a proximal coordinating group is vital to the success of the reaction; Ar = 2-MeOPh **50aa** led to *er* 86:14, Ar = 3-MeOPh **50f** led to *er* 63:37 whilst Ar = 4-MeOPh **50ka** led to racemic addition. The para-methoxy analogue **50k** is far away from the exocyclic double bond hence does not lock the copper-zinc transition state well enough to induce any stereoselectivity. The presence of sulfur or nitrogen groups for chelation-controlled reactions gave moderate **50ea**, **50ga** to low enantioselectivity **50ma**.

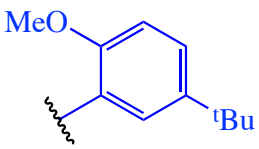




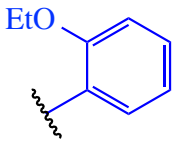
56% yield
50aa *er* 86:14 (**Et**)
50ab *er* 90:10 (**Bu**)



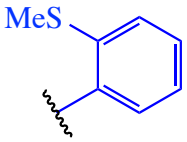
57% yield
50ba *er* 92:8



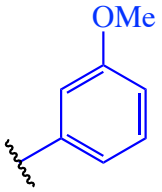
62% yield
50ca *er* 93:7



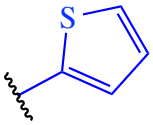
66% yield
50da *er* 87:13



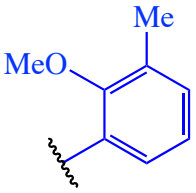
42% yield
50ea *er* 66:34



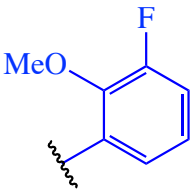
54% yield
50fa *er* 63:37



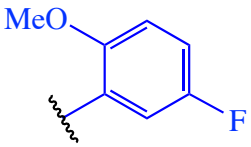
30% yield
50ga *er* 77:23



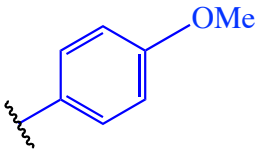
43% yield
50ha *er* 67:33



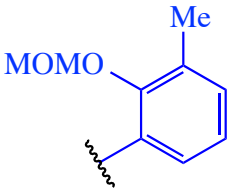
39% yield
50ia *er* 79:21



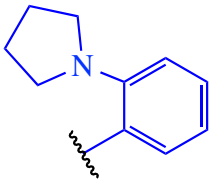
69% yield
50ja *er* 67:33



73% yield
50ka *er* 50:50



15% yield
50la *er* 67:37



38% yield
50ma *er* 56:44

Scheme 31: Enantiomerically enriched cyclopentadienyl ligands. Catalytic asymmetric organometallic addition to pentafulvenes **51a-51m** affords the enantio-enriched **51aa-51mm** (as a mixture of α/β double bond tautomers) needed for titanocene synthesis.

3.3 Synthesis of enantiopure titanocenes

Having identified the conditions for the synthesis of the enantio-enriched cyclopentadienyl ligands, the reaction was scaled up to 2.5 mmol. The substituted pentafulvene **51aa** (1 equiv.), $Cu(OTf)_2$ (12 mol%), ligand (*S*,*S*,*S*)-**90** (18 mol%) and additive (±)-**110** (13 mol%) gave the (*S*)-enantio-enriched cyclopentadienyl (*S*)-**50aa** in 57% yield and 86:14 *er*. The same reaction was carried out using ligand (*R*,*R*,*R*)-**90** instead of (*S*,*S*,*S*)-**90** which gave the opposite (*R*)-enantio-enriched cyclopentadienyl (*R*)-**50aa** in 61% yield and 13:87 *er*. With an efficient route to (*S*)-**50aa** and (*R*)-**50aa** in hand, we focused our attention on the preparation of the derived enantio-enriched titanocenes (*R*,*R*)-**49aa** and (*S*,*S*)-**49aa**. Rapid quantitative deprotonation of (*S*)-**50aa** by *n*BuLi (1.1 equiv.) in Et_2O at 0 °C led to the formation of the lithium substituted cyclopentadienide which was then cannula filtered, dried and weighed under argon. Transmetallation with titanium tetrachloride in refluxling THF for 16 h led to the formation of the enantio-enriched (*R*,*R*)-**49aa**.

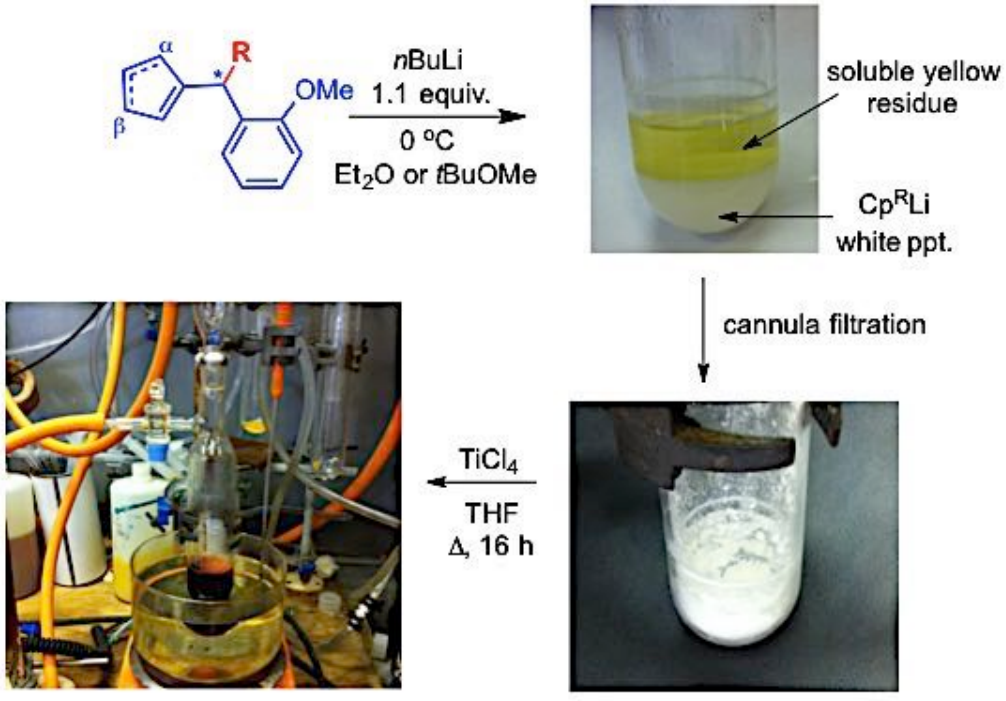
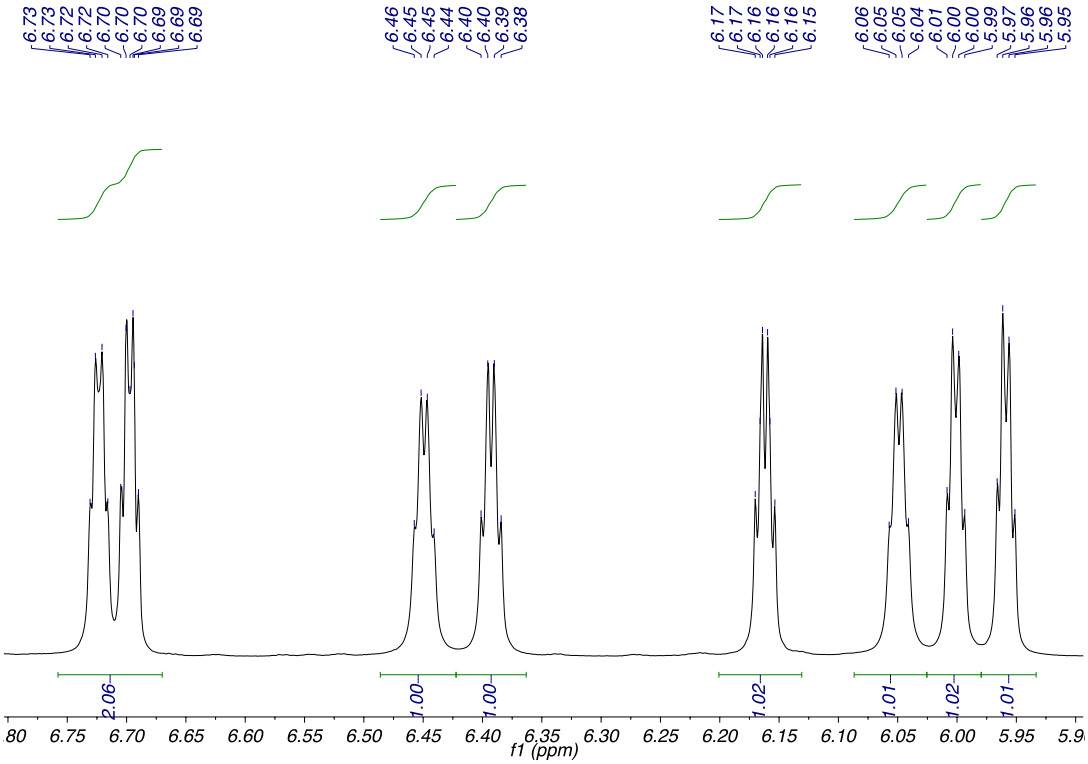


Figure 20: Titanocene synthesis in a snapshot.

A (*Rac*/*Meso*)-**49aa** - ^{1}H NMR Cp region - 4 diasterotopic *rac* protons and 4 *meso* protons.



B (*R*,*R*)-**49aa** - ^{1}H NMR Cp region - 4 diasterotopic *rac* protons with minor *meso* impurity

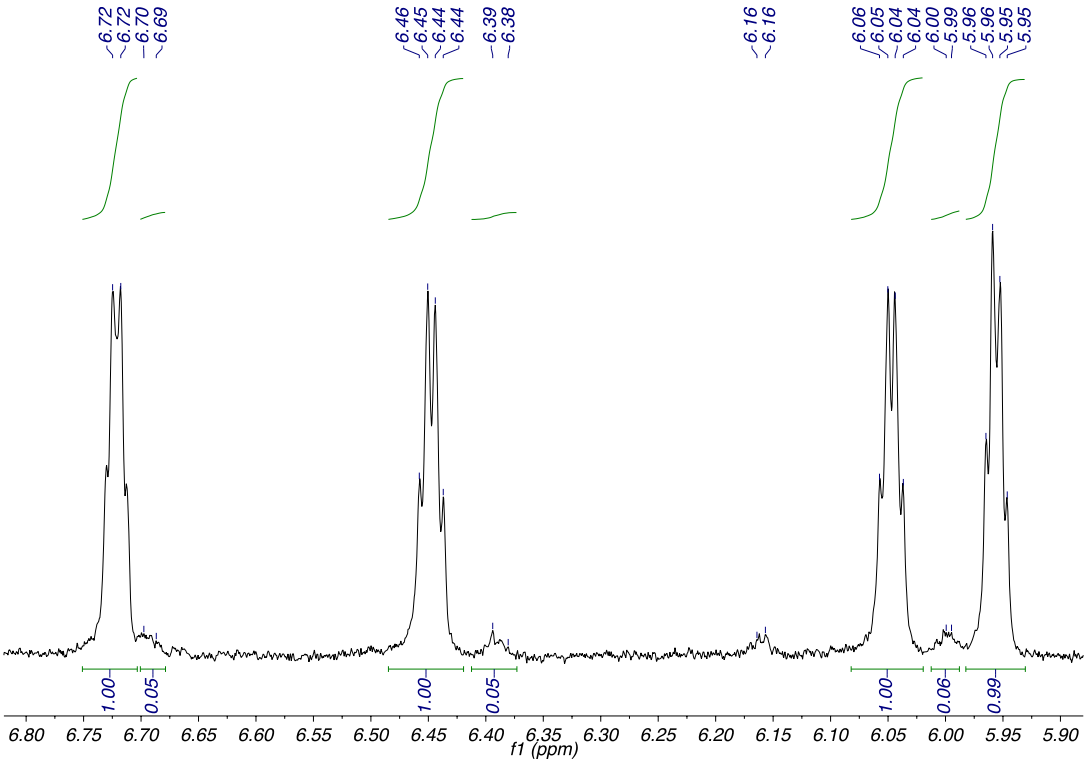


Figure 21: ^{1}H NMR Cp region of (*rac*/*meso*)-**49aa** and enantiopure (*R*,*R*)-**49aa**.

Recrystallisation of the crude titanocene reaction mixtures allowed the isolation (*R*,*R*)-**49aa**, red-orange crystals of enantiomeric purity (>99% *ee* – measured by HPLC) and a diastereomeric ratio of 0.92 (*R*,*R*) : 0.08 *meso*. Using the same protocol, the (*S*,*S*)-**49aa** was isolated in 99% *ee* and a diastereomeric ratio of 0.88 (*R*,*R*) : 0.12 *meso*.

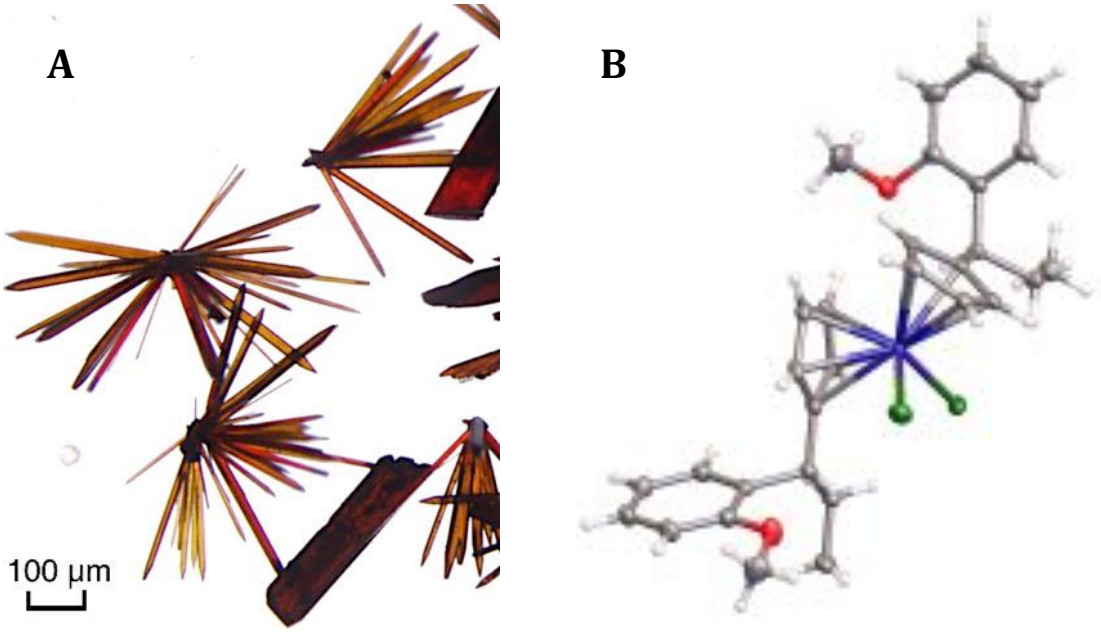


Figure 22: **A** Fan-shaped red-orange crystals of (*R*,*R*)-**49aa** under light microscope. **B** X-ray crystal structure for (*R*,*R*)-**49aa**.

A sample of **50aa** showing $[a]_D^{25}$ of -52.3 (*c* = 1.0, $CHCl_3$) provides an *er* of 86:14 by chiral GC (>110 °C, Chirasil-DEX-CB). Under these GC conditions 1,5-sigmatropic interconversion of the α/β tautomers of **50aa** is rapid, simplifying the assay. As explained above, (*S*)-**50aa** is converted to (*R*,*R*)-49**aa**. Two consecutive recrystallisations of the crude material afforded single crystals of (*R*,*R*)-49**aa** which was based on anomalous dispersion effect (Flack) tests. Thus, the initially eluted isomer GC cyclopentadiene is (-)-(*S*)-**50aa** and the latter the (+)-(*R*) isomer. The inversion of the stereochemical descriptor of cyclopentadiene (*S*)-**50aa** providing titanocene (*R,R*)-**49aa** is due only to the vagaries of Cahn-Ingold-Prelog assignment

rules. All stereoisomers of **49aa** could also be separated by chiral HPLC (Chiracel OD) but this was a less convenient approach.

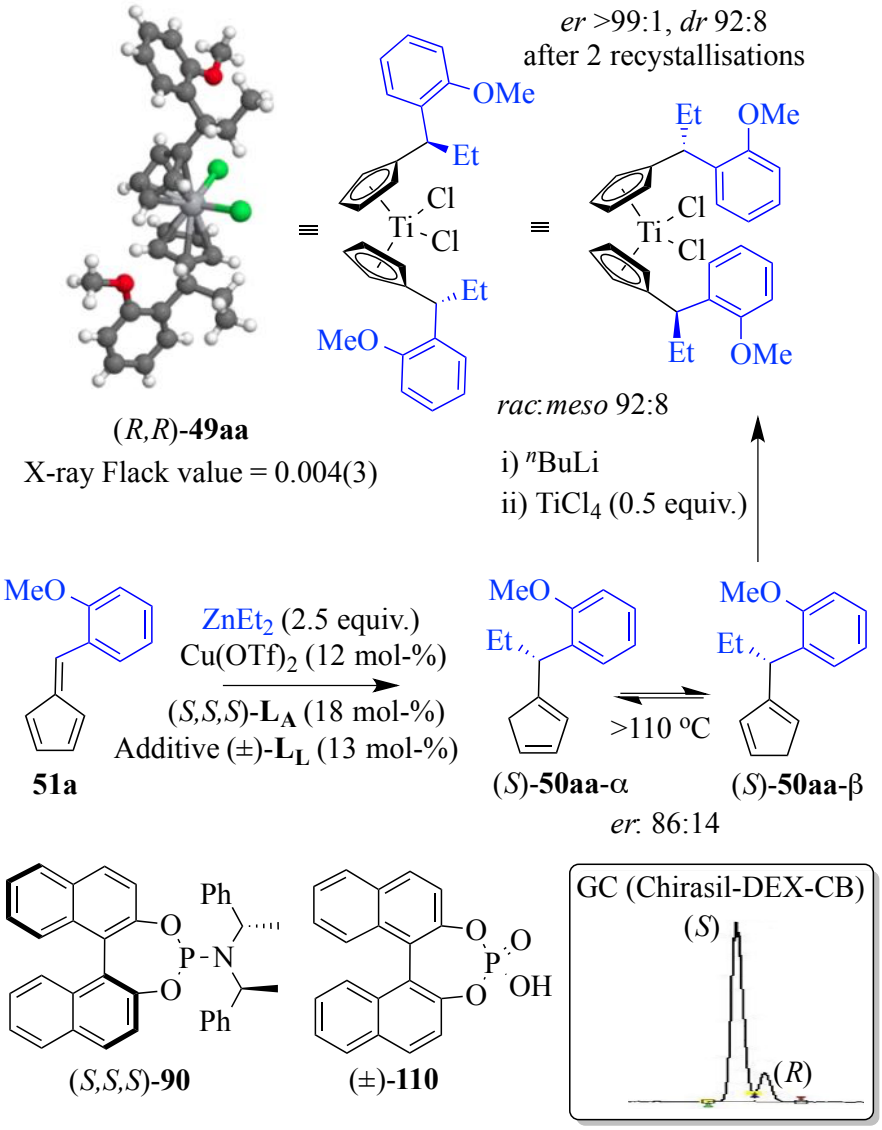


Figure 23: Molecular structure of (*R,R*)-**4** and derived stereochemical correlation to the asymmetric carbozincation process providing (*S*)-**6c**.

3.4. Biological studies

3.4.1 MTT analysis

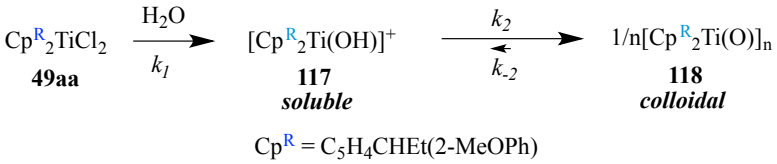
The antiproliferative activities of the enantiopure titanocenes (*R,R*)-**49aa**, (*S,S*)-**49aa** in comparison to the (*rac*/*meso*)-**49aa**, titanocene soluble derivative (*rac*/*meso*)-**119** and cisplatin **2** were evaluated *in vitro* at 24 h and 72 h (**119** only 72 h) against normal fibroblasts MRC5 and carcinoma cell lines HCT-116 (colorectal), MiaPaCa-2 (pancreatic) and MDA-MB-468 (breast). The soluble acid derivative (*rac*/*meso*)-**119** was synthesised using a literature method[115] involving a simple anionic exchange reaction between the chlorides in (*rac*/*meso*)-**49aa** and the oxalate in silver oxalate.

Hydrolytic instability of (*rac*/*meso*)-**49aa** to initial loss of chloride, and potential C_5H_4R cleavage, can provide a cocktail of species, which is further complicated when chiral substrates are present. Disentangling the relative biological activities of such mixtures was not possible, preventing their advancement to clinical trial. This sub-chapter aims to show modest suggestions for new tools of use in future detection of a correct mechanism of action *via* molecular chirality. The separated enantiomers (*S,S*)-**49aa** and (*R,R*)-**49aa**, were utilised as useful mechanistic probes in elucidating possible biological modes of action.

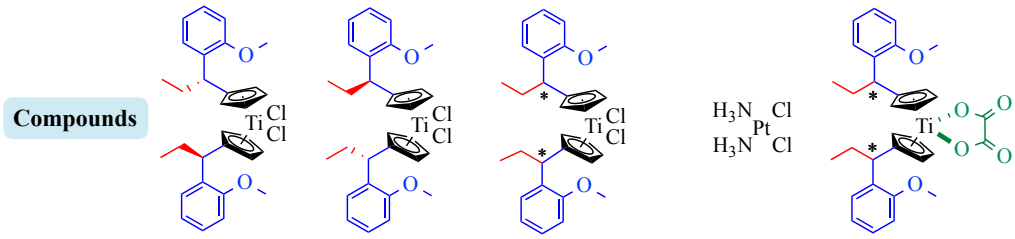
As can be seen in Figures 24-26 statistically significant ($P<0.05$) differential biological activity was observed in cancer cell lines for the enantiomers of **49aa**, within the first 24 h of exposure. This is not the case with normal fibroblasts MRC-5 where both (*R,R*)-**49aa** and (*S,S*)-**49aa** enantiomers possess similar, non-statistically different ($P>0.05$) GI_{50} activities. This preliminary investigation might reveal a chiral docking system sensitivity for carcinoma cell lines which seems to be less of a significance or even absent with normal cell lines. Furthermore, single enantiomer (*S,S*)-**49aa** showed selective activity (Figure 26) against representative carcinoma

cell lines *vs.* non-carcinogenic fibrobasts (P<0.05) whilst the antiproliferative effects of (*R,R*)-**49aa** are slightly more pronounced towards the normal cell line.

A



B



Cell line	(*R,R*)-**49aa**	(*S,S*)-**49aa**	*rac/meso*-**49aa**	cisplatin-**5**	*rac/meso*-**119**
24 h	(soluble homogenous titanium species at **1-24 h**)				
cancer Mia PaCa-2	42.5 ± 0.5	19.9 ± 3.5	32.3 ± 2.8	35.4 ± 1.4	
cancer MDA-MB-468	22.8 ± 2.8	11.5 ± 1.2	23.6 ± 0.4	7.4 ± 2.8	
cancer HCT-116	31.3 ± 1.6	14.8 ± 1.7	31.6 ± 3.9	34.9 ± 3.0	
normal MRC-5	21.4 ± 2.2	22.9 ± 3.4	17.0 ± 0.7	25.6 ± 3.6	
72 h	(colloidal titanium species **>24 h**)				
cancer Mia PaCa-2	7.3 ± 0.5	5.7 ± 1.3	7.5 ± 0.4	5.8 ± 0.7	17.9 ± 2.1
cancer MDA-MB-468	5.6 ± 1.8	5.4 ± 1.3	5.3 ± 1.7	2.1 ± 0.6	7.9 ± 0.9
cancer HCT-116	14.0 ± 2.1	9.4 ± 1.2	12.2 ± 3.9	7.9 ± 0.5	19.0 ± 0.8
normal MRC-5	25.1 ± 3.5	28.3 ± 5.0	28.6 ± 3.7	8.3 ± 3.1	70.3 ± 3.9

Figure 24: Correlation of speciation and biological activity. (A) Hydrolysis of enantiomerically pure **49aa** (200 μM) in aqueous DMSO (1% v/v). Kinetic model of observed (800 MHz NMR) intermediate **117** and MS detected product **118**. This model simulates [**117**] *vs*. time well (R^2 0.98). **(B)** Cell growth inhibition after 24 and 72 h determined by MTT assay (GI_{50} in μM) in cancer *vs*. a normal cell line for the enantiopure titanocenes **49aa**, the *rac*/*meso* mixture of stereoisomeric **49aa**, cisplatin **2** and the soluble acid titanocene derivative (*rac*/*meso*)-**119**. GI_{50} values are represented as mean standard error of mean (SEM) of at least three independent experiments (n = 4 per experiment). Compound stocks (20 mM) were prepared in dimethyl sulfoxide (DMSO) and diluted in nutrient medium immediately prior to use. Compounds were weighed using an analytical microbalance and cisplatin was used as positive control in each experiment throughout the whole study.

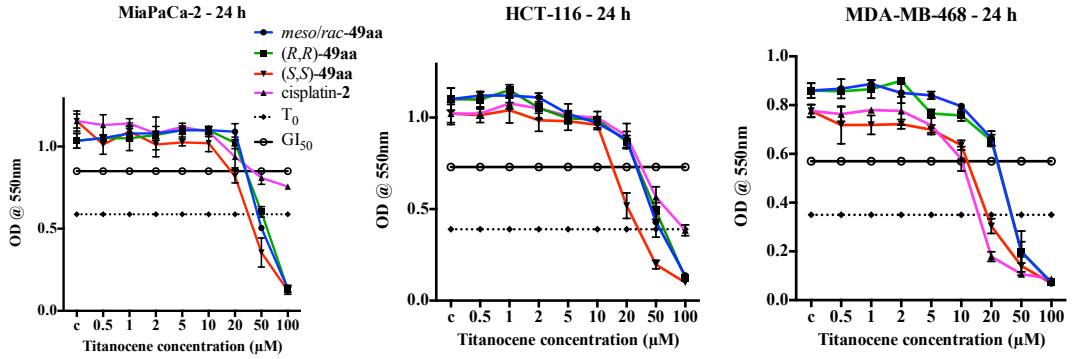


Figure 25: MTT assay profiles demonstrating dose-dependent growth inhibition of Mia PaCa-2, HCT-116 and MDA-MB-468 growth by (*rac*/*meso*)-**49aa**, (*R*,*R*)-**49aa**, (*S*,*S*)-**49aa** and cisplatin **2** after 24 h from agent addition.

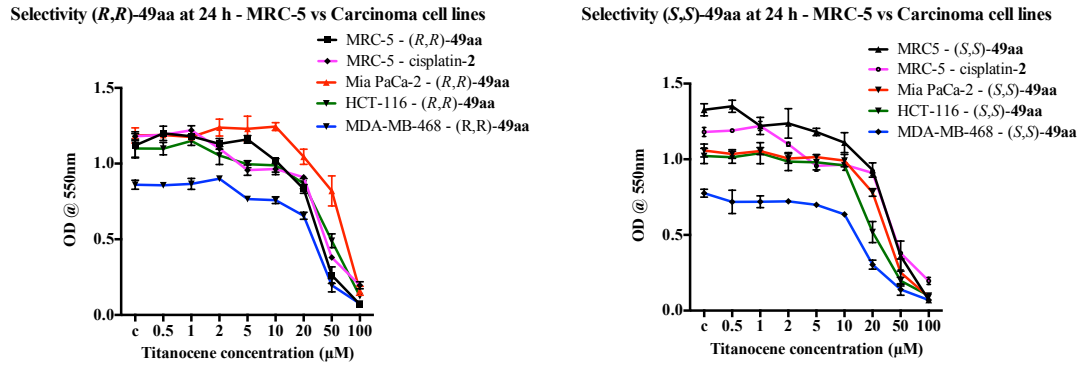


Figure 26: MTT selectivity assay profiles for dose-dependent inhibition of MRC-5, Mia PaCa-2, HCT-116 and MDA-MB-468 growth by (*R*,*R*)-**49aa**, (*S*,*S*)-**49aa** and cisplatin **2** after 24 h exposure.

When compared to cisplatin, (*S*,*S*)-**49aa** shows the same activity towards normal cells but intriguingly is > 2-fold more active than cisplatin against colon carcinoma, almost twice as active as cisplatin in pancreatic carcinoma whilst on the other hand, cisplatin is almost 2x more active than (*S*,*S*)-**49aa** in breast carcinoma at 24 h. Also, as can be seen from the dose-response relationships of titanocenes **49aa** and cisplatin (Figure 25, 26), cisplatin percentage inhibition might be dependent on the cancer type whereas titanocenes seem to have highly similar dose dependent curve with the highest concentration constituting almost 100% cytotoxicity.

All of the above might indicate that although titanocenes and cisplatin share a common MCl_2 unit, titanocene (*S,S*)-**49aa** does not have the same mode of action as cisplatin – in fact their anti-cancer targets are not well defined and their mode of action might be structure dependent.

Finally, after 72 h treatment, cisplatin **2** showed no statistically valid (P>0.05) selectivity towards cancer cells (equipotency against Mia PaCa-2, HCT-116 carcinoma cells and MRC-5 fibroblasts; with GI_{50} 6-8 μM; Figure 24B, 72 h) whereas all stereoisomers of **49aa** and soluble derivative **119** have in fact demonstrated significant selectivity towards cancer cells over normal fibroblasts (Figures 24B, 27, 28). With respect to **49aa**, 2- and 5-fold cancer cell line selectivity versus normal cell line was noted, whereas with **119**, 4- and 9-fold cancer cell selectivity versus normal cell line was noted (P<0.05). Indeed, at 50 μM, **119** caused negligible MRC5 growth inhibition; in stark contrast total growth inhibition and cytotoxicity were observed in all cancer cell lines exposed to 50 μM, **119**.

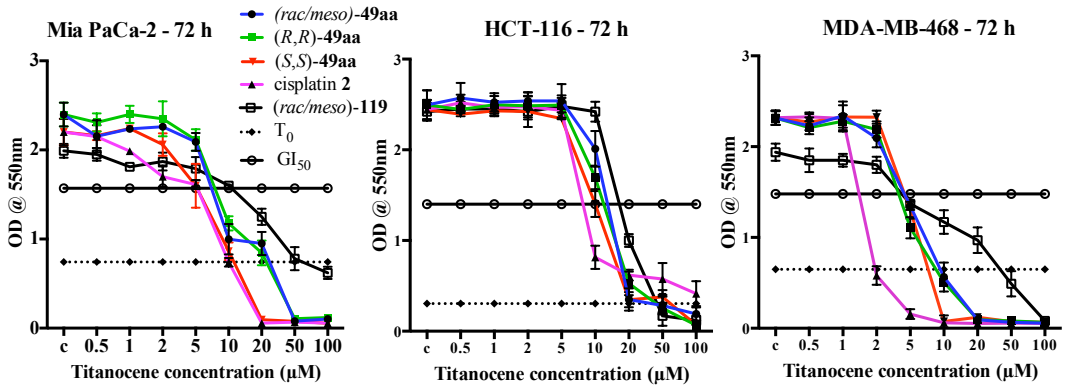


Figure 27: MTT assay profiles for inhibition of Mia PaCa-2, HCT-116 and MDA-MB-468 growth by (*rac/meso)*-**49aa**, (*R,R*)-**49aa**, (*S,S*)-**49aa**, (*rac/meso)*-**119** and cisplatin **2** after 72 h exposure.

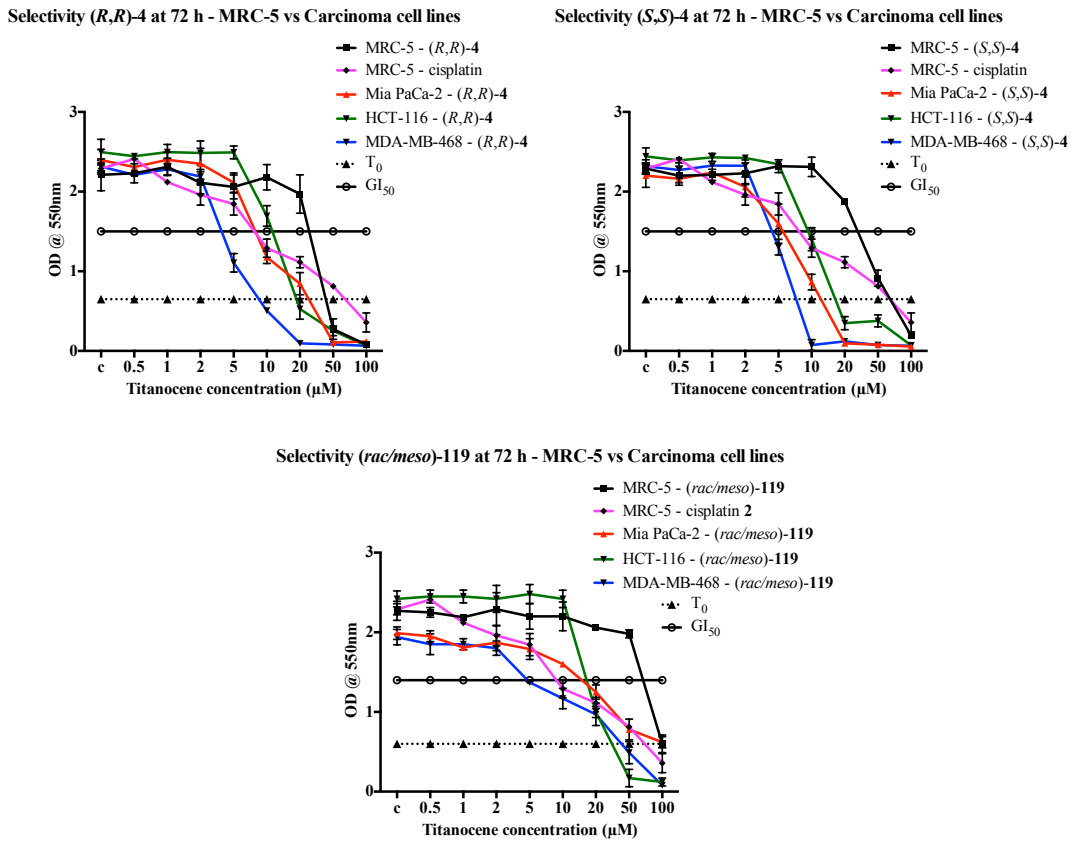


Figure 28: MTT selectivity assay profiles for inhibition of MRC-5, Mia PaCa-2, HCT-116 and MDA-MB-468 growth by (*rac*/*meso)*-**49aa**, (*R*,*R*)-**49aa**, (*S*,*S*)-**49aa**, (*rac*/*meso)*-**119** and cisplatin **2** after 72 h exposure.

3.4.2 Clonogenic Assay

Clonogenic assay is an *in vitro* cell survival assay used to test the ability of carcinoma cells to survive and recover from a brief exposure to an anticancer agent and form colonies consisting of at least 50 cells. After 24 h exposure to the agent, the cells are washed with phosphate buffered saline (PBS) and fresh medium is introduced. The cells are then incubated at 37 ^{o}C and allowed to form colonies for a number of days, after which the colonies are fixed, stained and counted. The percentage of cells that survived the treatment and were able to form progeny colonies is then measured versus the control. Assays performed to assess subsequent colony growth after 24 h exposure of HCT-116 and Mia PaCa-2 cells to (*S,S*)-**49aa** or (*R,R*)-**49aa** support >2x differential enantiomer activity (20-50 µM **49aa**, Figures

29-31). There was a general reduction of colony growth in both cell lines with an increase in titanocene concentration. In the case of Mia PaCa-2, significant ($P<0.05$) inhibition in colony formation from the control samples was visible at 20 μM titanocene concentration, whilst in HCT-116, 10 μM of titanocene was found to cause significant ($P<0.05$) inhibition in colony formation. Also, (*S*,*S*)-**49aa** was found to be more effective than (*R*,*R*)-**49aa** and (*rac*/*meso*)-**49aa** at higher concentrations. Cisplatin had a profound effect on colony formation as very few cells were able to recover and proliferate to form colonies.

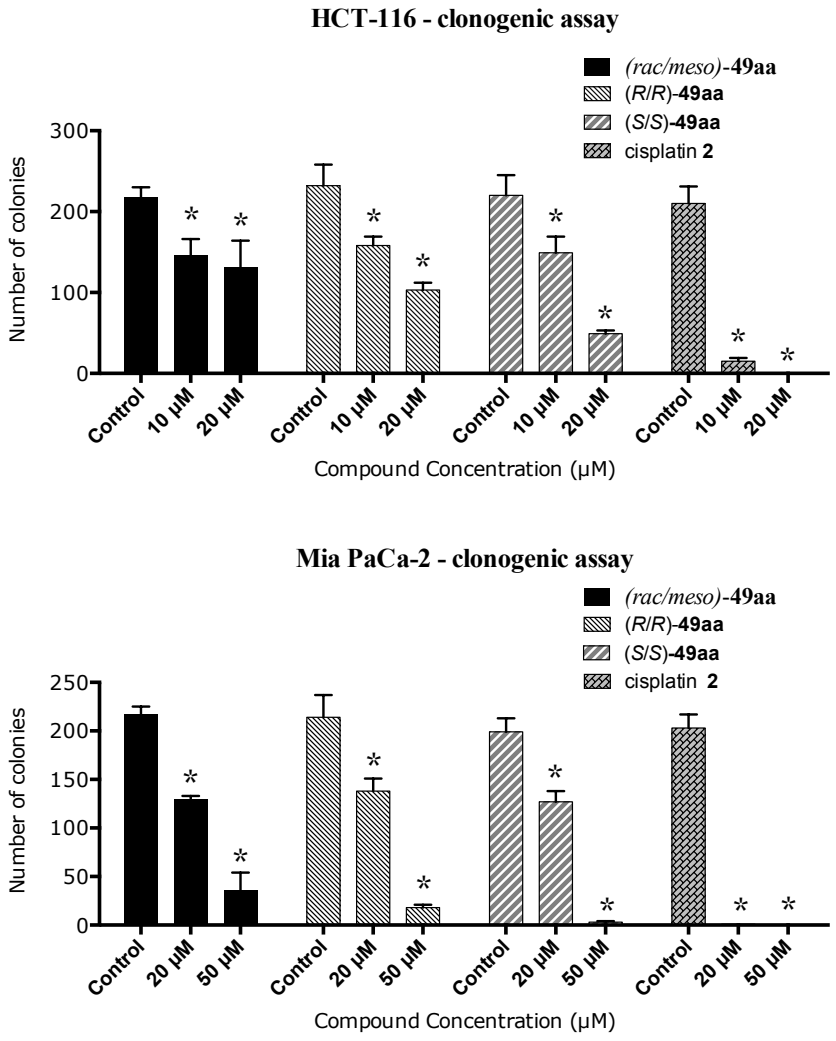


Figure 29: Effects of titanocene derivatives on clonogenic survival of Mia PaCa-2 and HCT-116 cell lines. Colonies were fixed, stained (methylene blue) and counted. Experiments were performed in triplicate, (n = 2 per experiment). Values are expressed as mean ± SD, *$P<0.05$ significantly different from control (untreated) using 2 way ANOVA – multiple comparisons.

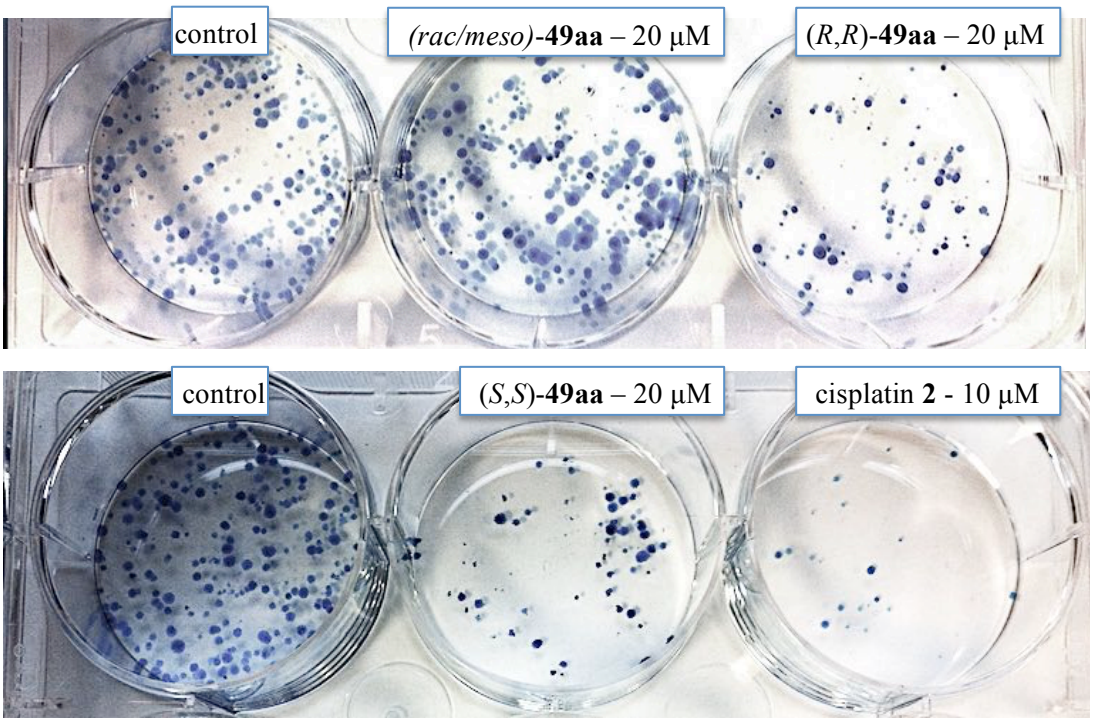


Figure 30: Representative effects of titanocene derivatives and cisplatin on clonogenic survival of HCT-116 cells.

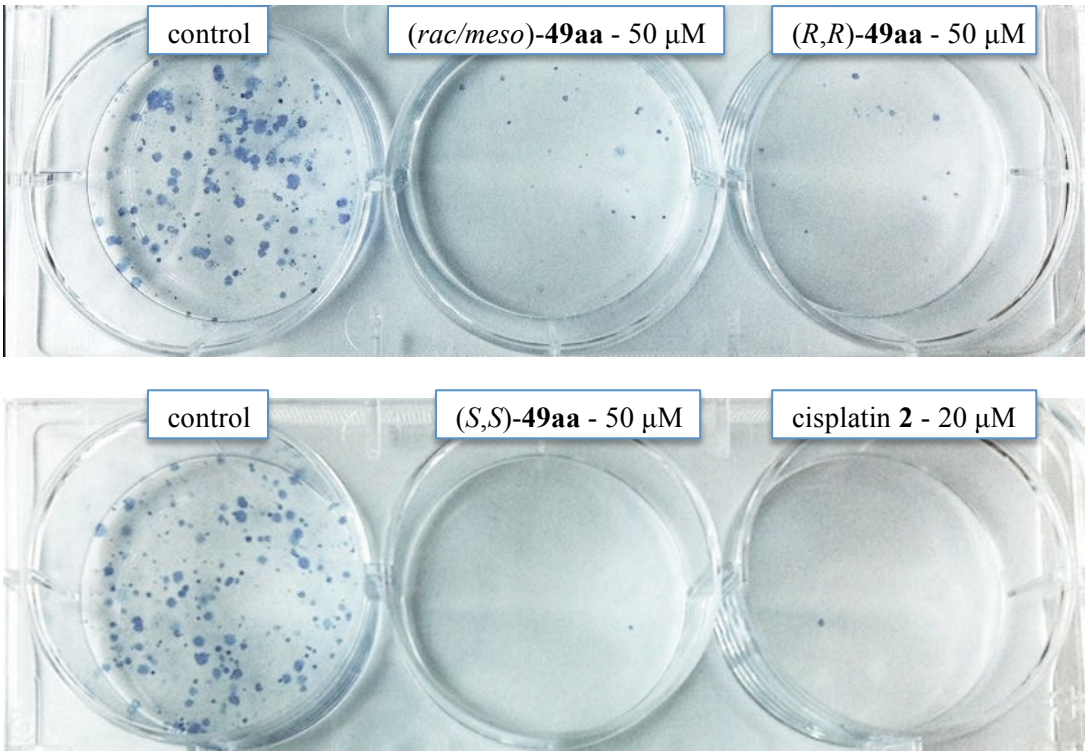


Figure 31: Representative effects of titanocene derivatives and cisplatin on clonogenic survival of Mia PaCa-2 cells.

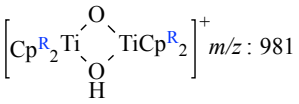
3.4.3 Hydrolysis studies – $Cp^R_2Ti(IV)$ speciation

3.4.3.1 – Mass Spectrometry

Sample dilutions (200μM) were prepared in RPMI-1640 (pH 6.9 to 7.2) using freshly prepared 20 mM DMSO top stock of (*S,S*)-**49aa**, in an identical manner those used in biological studies. Mass spectrometry provided insight into the species derived from (*S,S*)-**49aa**. Liquid Chromatography Mass Spectrometry (LCMS) assayed only truly homogeneous species (fine colloidal suspensions, even those apparently clear to the naked eye, are not eluted making this a powerful way to separate genuine solution Cp^RTi species from degradation events). Direct injection into Electrospray Mass Spectrometry (ESMS), assayed both homogeneous and colloidal species. Ions due to the latter could be identified by the presence of extra signals in the paired mass spectra. The ions detected by these two techniques during the starting material (colloidal), intermediate (truly homogeneous) and product (colloidal) phases of the hydrolyses of (*S,S*)-**49aa** are summarised in Figure 32. LCMS was carried out using an Agilent 1260 Infinity HPLC with a 6120 Quadrupole mass spectrometer Chromatography conditions: Waters Sunfire C18 3.5μm 2.1 x 30 mm column. Mobile phase 1: 0.1% formic acid in water, mobile phase 2 : 0.1% formic acid in acetonitrile. Method run at 40 ^oC with a flow rate of 0.8 mL min^{-1}, gradient of 5-95 % mobile phase 2 over 3.5 minutes with UV detection at 210-400 nm reported at 254 nm. MS ionisation by ESI operating in positive ion mode. Samples were collected every 10 min to 6 h depending on the rate of change in the speciation. Direct ESMS was conducted on a Bruker micrOTOF instrument in 1% DMSO in D_2O. In the period equivalent to that in our observation of paraptosis (microscopy studies of MDA-MB-468) soluble *m/z* 491 $[Cp^R_2Ti(OH)]^+$ **117** is the only cyclopentadienyl intermediate observed (>90% of total signal). No free ligand

m/z 214 was observed in our LCMS studies up to 24 h. Addition of MeOH to solutions containing m/z 491 $[Cp^R_2Ti(OH)]^+$ led to its rapid complete conversion to *m/z* 505 $[Cp^R_2Ti(OMe)]^+$.

A

Hydrolysis Period	Direct ESMS detects **both** *soluble* and *colloidal* species	LCMS detects only homogeneous *soluble* species
Induction period 0-1.5 h	$[Cp^R_2Ti(OH)]^+$ *m/z* : 491	$[Cp^R_2Ti(OH)]^+$ *m/z* : 491
	$[Cp^R_2TiCl]^+$ *m/z* (^{35}Cl): 509 **49aa** - $[M\text{-}Cl]^+$	
Intermediate maximised 2.4-4.1 h	$[Cp^R_2Ti(OH)]^+$ *m/z* : 491 **117**	$[Cp^R_2Ti(OH)]^+$ *m/z* : 491 *sole species* *>90% total ions present*
Product maximised >20 h	$[Cp^R_2Ti(O)] + H^+$ *m/z* : 491 **118**	
	 *m/z* : 981	*none detected*

B

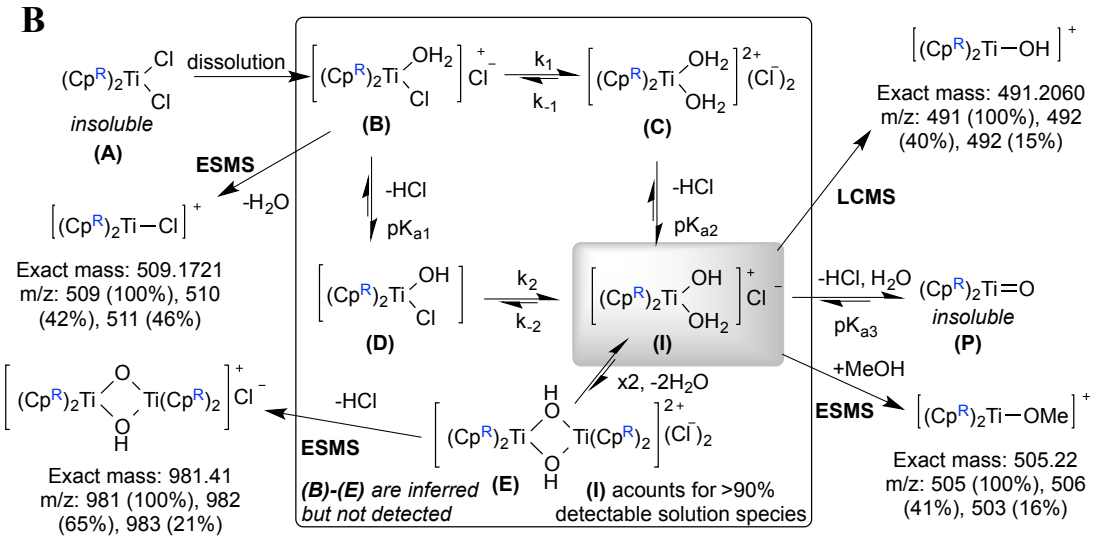


Figure 32: A Ions detected in the MS spectra of hydrolysing (*S,S*)-**49aa** in RPMI-1640 containing 1% v/v DMSO. In LCMS analysis $[Cp^R_2Ti(OH)]^+$ elutes at 3.0 min as the sole species present (>90% total signal) at 2.4-4.1 h. In the induction period we see traces of $[Cp^R_2TiCl]$ (≤10% total signal) 3.9 min indicative of (*S,S*)-**49aa** $[M\text{-}Cl]^+$, m/z (^{35}Cl): 509. No free ligand was detected. **B** ESMS (in 1% DMSO/99% D_2O) and LCMS studies (in 1% DMSO/99% D_2O or RPMI 1640 medium alone) point to a single major homogeneous species whose daughter ions are consistent with the presence of $[(Cp^R)_2Ti(OH)(OH_2)]Cl$ (**I**) being the major soluble intermediate attained upon dissolution of (*S,S*)-**49aa**.

3.4.3.2 – NMR spectroscopy

Samples of (*S,S*)- or (*R,R*)-**49aa** (200 μM in D_2O/d_6-DMSO, 99:1) for combined 800 MHz NMR were prepared in analogous manner to the preparation of stock solutions of **49aa** used in biological and MS studies, except that D_2O, not RPMI-1640, was used. Attempts to directly study samples in RPMI-1640 led to the observation of only very exchange broadened signals. For NMR studies (*R,R*)-**49aa** (0.6 mg, 1.1 mmol) was dissolved in spectroscopic grade d_6-DMSO (55 μL) to afford a nominal 20 mM top stock solution. An aliquot of this (15 μL, 0.3 μmol) was added to 1485 μL of a standard solution (67 μM) of Na-TMSP-d_4 [3-(trimethylsilyl)-2,2',3,3'-tetradeuteropropionic acid, sodium salt] in D_2O and the time noted. A sample of this nominal 200 μM solution of (*R,R*)-**49aa** containing Na-TMSP-d_4 internal standard (67 μM) was immediately transferred to the 800 MHz spectrometer and the latter set to attain ^{1}H NMR spectra every 25 min (probe temperature 25±0.2 ^oC). The limit of detection of soluble species in these experiment was ~1 μM. Controlled spiking experiments with Cp^RH showed that we would detect the free ligand at 1 μM, but none was seen in the period of observation (0-60 h).

Initially broad featureless data, associated with a colloidal insoluble starting material (**A**) were attained in an induction period (~100 mins) after dilution of the initial d_6-DMSO solution of (*R,R*)-**49aa**. After this period, rapid formation of homogenous intermediate (**I**) was observed which decayed ($t_{½}$ ~1.7 h) to a product (**P**), leaving some residual (**I**) in solution [**A** → **I** ⇌ **P**]. An optimal fit (R^2 0.98) to the [**A** → **I** ⇌ **P**] model was found using the equations of Moore and Pearson[116] and the fitting approach of Billo[117] (figure 33). Non-linear least squares analyses converged on: k_1 = 1.56(2) x 10^{-2} min^{-1}; k_2 = 1.50(2) x 10^{-2} min^{-1}; k_{-2} = 5.6(4) x 10^{-4} min^{-1}; $[\mathbf{A}]_0$

= 198(4) μM; $[\mathbf{I}]_{max}$ = 75(4) μM; $[\mathbf{I}]_{\infty}$ = 7(2) μM with a quality of fit R^2 of 0.98, where the identities of (**A**), (**I**) and (**P**) were correlated to (*R,R*)-**49aa**, **117**, and **118**. Other kinetic models: simple first or second order processes as either isolated or consecutive reactions gave inferior fit (R^2 0.90-0.95) to the observed full range data. Negligible back reaction from **117** to **49aa** was found (k_{-1} = 0) as the free chloride $[Cl^-]_{max}$ = 400 μM does not compete in the presence of excess water or DMSO: $[D_2O]$ >54 M; [DMSO] = 148 mM. LCMS analysis of the NMR samples at times when the intermediate's concentration is maximised showed only a single homogeneous species eluting at 3.0 min and ionising as *m/z* 491/492 $[Cp^R_2Ti(OH/D)]^+$.

The ability of the intermediate **I**, assigned to $[Cp^R_2Ti(OH)]^+$, to coordinate solvents was tested by use of increased DMSO concentration (20% v/v compared to the 1% v/v studies above; 2.82 M vs. 148 mM) keeping all other factors constant. Formation of the intermediate was rapid and k_1 could not be estimated accurately in 20% v/v DMSO but its decay from maximum concentration $[\mathbf{I}]_{max,obs}$ = 200 μM could be modelled by k_2 = 1.1(2) x 10^{-3} min^{-1}; k_{-2} = 1.5(2) x 10^{-4} min^{-1} (R^2 = 0.99). This is >150 times slower than in 1% v/v DMSO and indicates that the DMSO coordinated intermediate $[(Cp^R_2Ti(OH)(DMSO)]^+$ is much more stable than its aqua analogue.

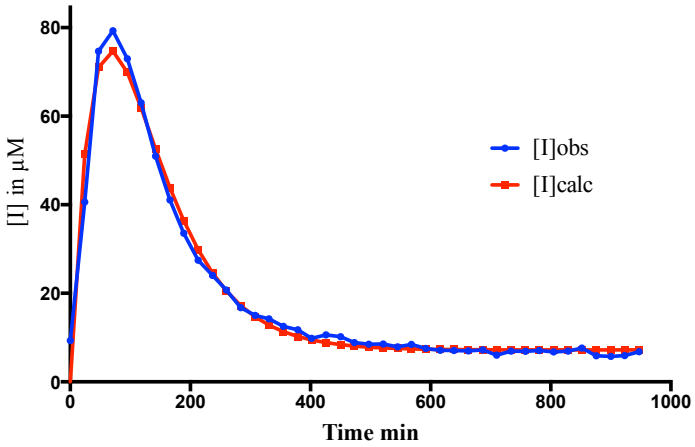


Figure 33: Hydrolysis chemistry of titanocene dichloride **49aa**. Simulated (red) vs. observed (blue) data for the growth of the soluble intermediate I assigned structure $[Cp^{R}{}_2Ti(OH)_2]^+$.

3.4.3.3: Comparison with literature results

Neutral titanocene compounds, such as Cp_2TiCl_2 **5** and **49aa**, are not soluble in aqueous media forming at best colloidal suspensions. Chloride ionisation is required to attain homogeneous aqueous solubility. The only previous study focused on the parent Cp_2TiCl_2. Here Marks[49] exposed finely ground Cp_2TiCl_2 to 0.32 M aqueous KNO_3 aiming for ~1 to 3.5 mM solutions in titanium (about 10× more concentrated than those in our own studies). This led to an induction period of *ca.* 50 min followed by dissolution. A chloride selective electrode was used to determine the overall rate of cleavage of both chlorides as $1.4(2) \times 10^{-2}$ min^{-1} based on initial rate data at 50 min. This is similar to the value we attain for complete chloride hydrolysis from **49aa** by NMR: $1.56(2) \times 10^{-2}$ min^{-1}. Marks' data is complicated by an estimated 7% Cp ligand hydrolysis during the overall dissolution. By titration Marks ***49*** determined the two pK_a ionisation constants of H_2O-complexed to Cp_2Ti^{2+} to be 3.5 and 4.35 respectively. This means that at pH values above 3.5 the major species present would

be $[Cp_2Ti(OH)]^+$ and this would readily deprotonate to neutral, and hence insoluble, $Cp_2Ti(O)$ at pH 7. Unfortunately, in the case of Cp_2TiCl_2, this behavior cannot be cleanly observed as with rising pH hydrolysis of the Cp groups also results, leading to complicated mixtures of species. Such poorly characterised mixtures have been nicely reviewed in detail by Potter.[118] In contrast to Cp_2TiCl_2, no Cp^R hydrolysis from **49aa** could be observed by either MS or ^1H NMR within 24 h (pH 7). Both techniques are in accord with formation of intermediate (**I**) of identity $[Cp^R_2Ti(OH)]^+$; as is the rapid exchange of (**I**) with methanol to provide $[Cp^R_2Ti(OMe)]^+$. Determination of the pK_a for $[Cp^R_2Ti(OH)]^+$ deprotonation is complicated by the presence of the multiple equilibria (see Figure 32). However at pH 7 and deprotonation to neutral insoluble $Cp^R_2Ti(O)$ is highly likely. Decay of $[Cp^R_2Ti(OH)]^+$ (**I**) is observed and the aqueous insolubility of its product is in accord with (**P**) being neutral $Cp^R_2Ti(O)$. MS studies of the crude colloidal product indicate the ions $[2 \times Cp^R_2Ti(O) + H^+]$ and $[Cp^R_2Ti(O) + H^+]$ also in accord with this proposal. An intermediate of $[Cp^R_2(OH)]^+$ is also consistent with the greater selectivity of (*S,S*)-**49aa** towards cancer cell lines *vs.* normal MRC-5. The high acidity of the cancer cell lines[119] is expected to lengthen the intermediate's lifetime in cancer cells. Exchange of $[Cp^R_2(OH)]^+$ to longer lived $[Cp^R_2Ti(OMe)]^+$ also provides a rational for the, otherwise poorly explained, increased toxicity of **5** when pre-treated with methanol.[120] Finally, slow endocytosis of colloidal $1/n[Cp^R_2Ti(O)]_n$ would also be fully concordant with the lack of enantiomer recognition we see at 72 h.

3.4.4 Dual cell cycle / DNA damage

The effects of (*R,R*)-**49aa**, (*S,S*)-**49aa** and cisplatin **2** on MDA-MB-468 and HCT-116 tumor cell cycle progression and DNA damage were analysed by flow cytometry. Examination of cell cycle distribution (MDA-MB-468 and HCT-116, 24 h and 72 h time points) revealed that in contrast to cisplatin **2**, which caused significant accumulation of pre-G1 phase events (>30 to 60%, 72 h, 10 or 25 μM; Figures 34-35), titanium complex (*S,S*)-**49aa** negligibly perturbed MDA-MB-468 or HCT 116 cell cycles (24 or 72 h; 10-30 μM, ±5% of control values, Figures 34-35). Titanocene Y **8** has been reported to reduce clonogenic survival, cause DNA damage and dose-dependent apoptosis in prostate cancer cells, but did not affect the cell cycle.[121] O`Connor *et al*. report that **8** caused significant prostate cell cycle effects and apoptosis.[122] However, these authors conclude a caspase-independent mode of cell death when the pan caspase inhibitor ZVAD-FMK failed to inhibit apoptosis. Titanocene dichloride **5** triggered A2780 ovarian carcinoma cell cycle arrest in late S, early G_2 cell cycle phase, formation of Ti-DNA adducts and apoptosis.[123]

To determine whether (*S,S*)-**49aa** caused DNA damage leading to double strand breaks (DSBs), we investigated generation of γH2AX. Histone H2AX is phosphorylated by kinases (such as ATM and ATR) at sites of DNA DSBs 1:1.[124] Distinct from cisplatin which clearly evokes H2AX phosphorylation ($P<0.05$); no statistical increase in γH2AX foci were detected following exposure of cells to **49aa** [figure 36, 20 or 30 mM **49aa** (either enantiomer) for 24 or 72 h)].

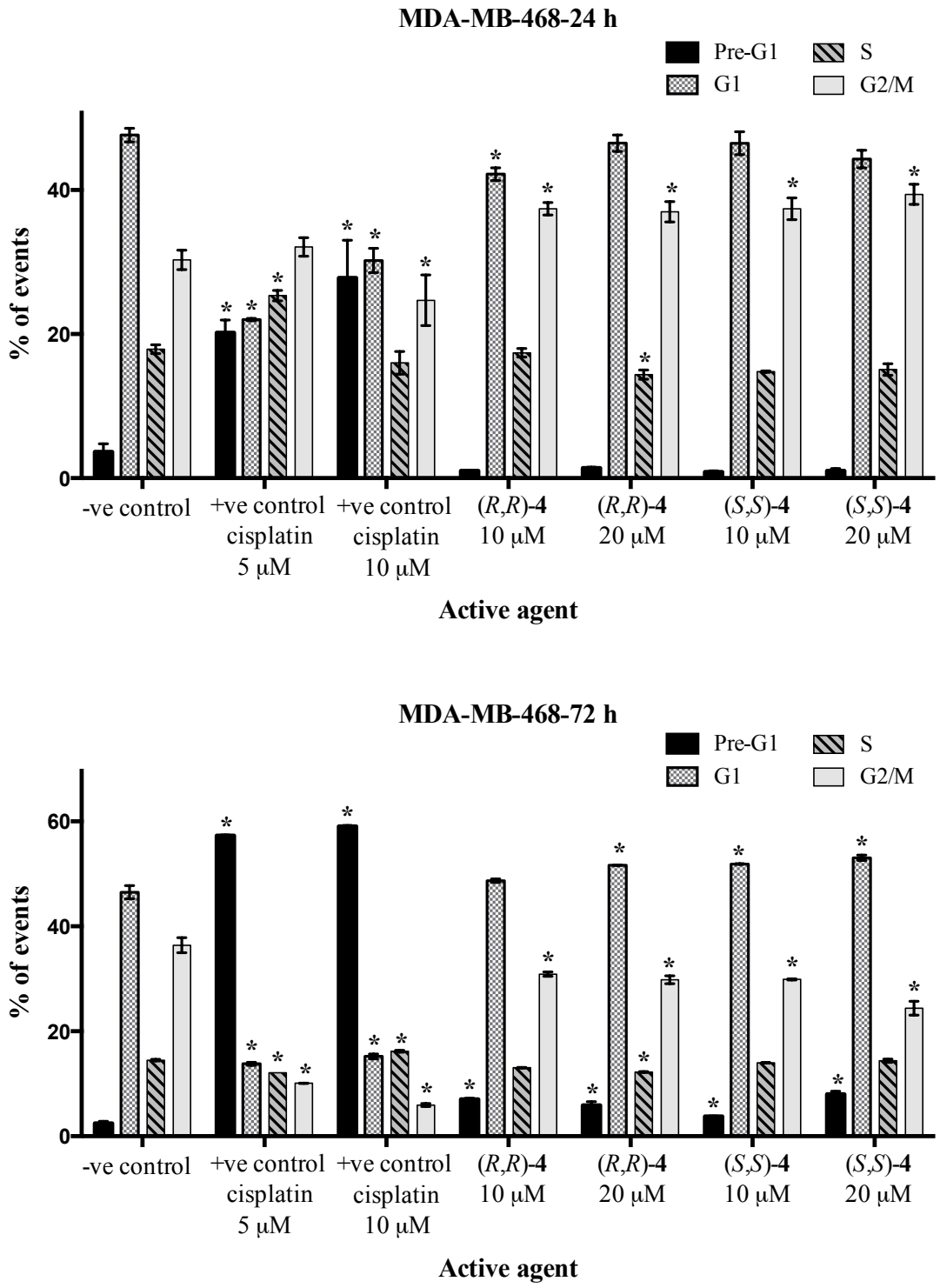


Figure 34: Cell cycle effects of cisplatin and titanocene derivatives on MDA-MB-468 cells 24 h and 72 h post-treatment. Data are representative of at least 3 independent trials. *P<0.05 significantly different from control (untreated) using 2 way ANOVA – multiple comparisons.

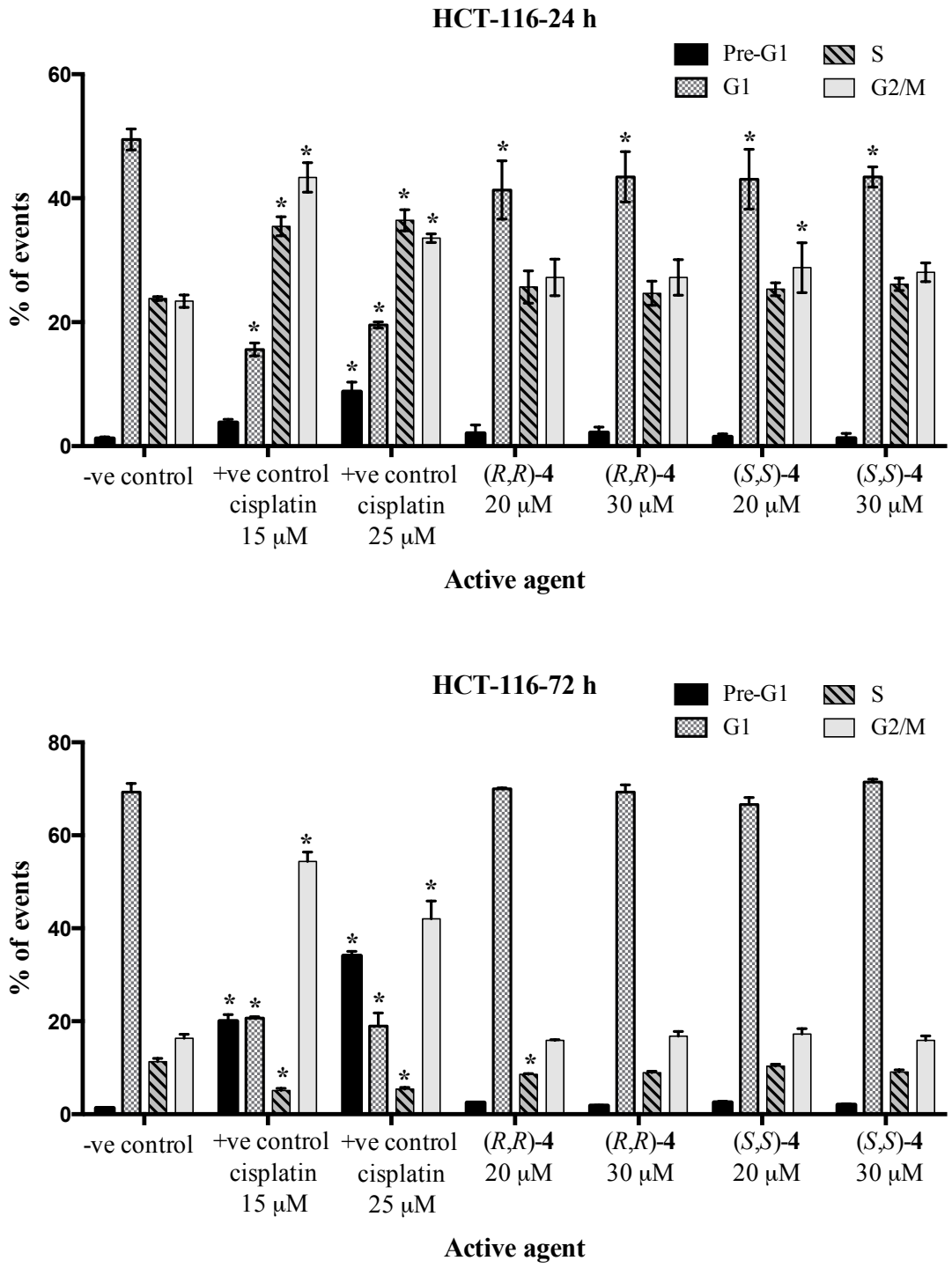


Figure 35: Cell cycle effects of cisplatin and titanocene derivatives on HCT-116 cells 24 h and 72 h post-treatment. Data are representative of at least 3 independent trials. *P<0.05 significantly different from control (untreated) using 2 way ANOVA – multiple comparisons.

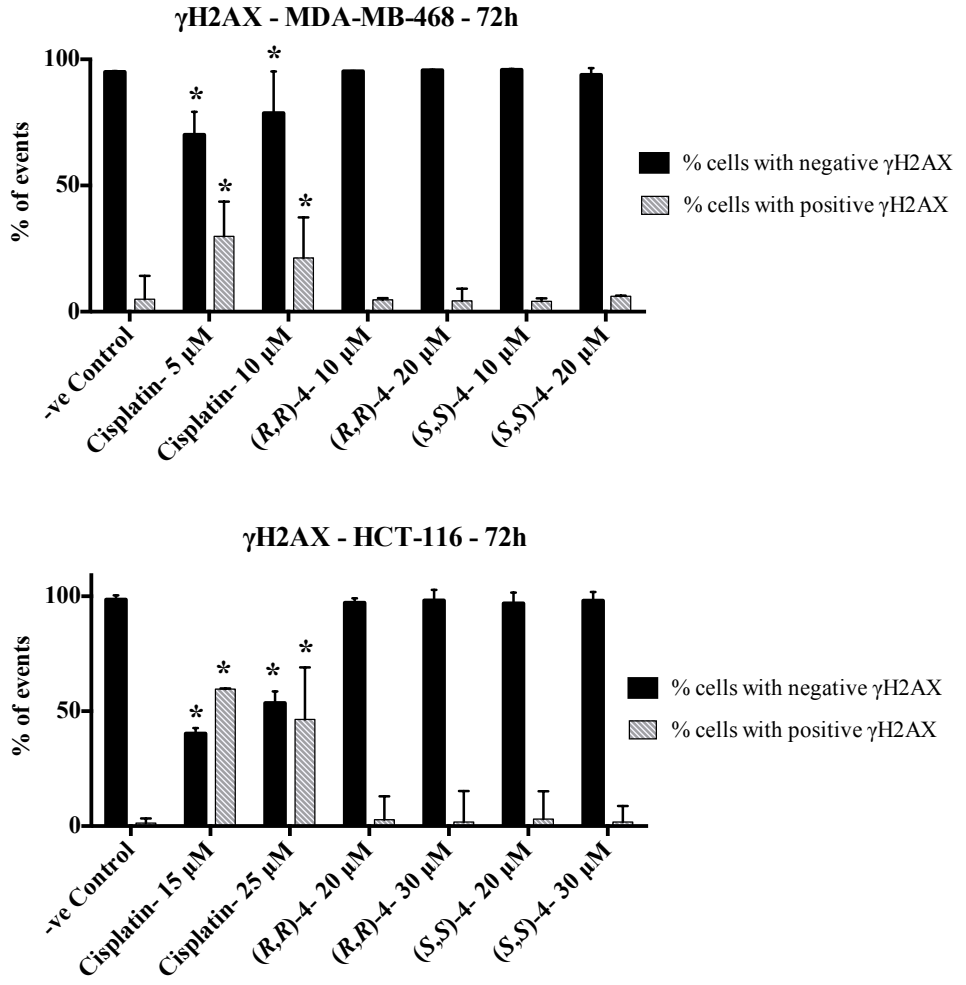


Figure 36: Measurement of DNA damage - double strand breaks. Percentage cells having phosphorylated γH2AX after addition of titanocene derivatives and cisplatin on MDA-MB-468 cells and HCT-116, 72 h post-treatment. Data are representative of at least 3 independent trials. At least 50,000 events per sample were analysed. *P<0.05 significantly different from control (untreated) using 2 way ANOVA – multiple comparisons.

3.4.5 Dual annexin V-FITC/PI

Stages of cellular apoptosis can be determined by a flow cytometry based assay using propidium iodide (PI) in conjunction with annexin V/FITC. This assay determines if cells are viable, early apoptotic, late apoptotic or necrotic via differences in plasma membrane asymmetry, integrity and peremeability.[125] During the early events of cellular apoptosis, the phosphatidylserine (PS) phospholipid translocates from the inner to the outer leaflet of the plasma membrane. The calcium

dependent phospholipid binding protein annexin V then binds tightly to PS. Annexin V is incorporated with the fluorochrome fluorescein isothiocyanate (FITC) which serves as a sensitive probe for flow cyctometric analysis of early apoptotic cells. The fluorescent molecule PI is also used as a DNA stain to determine cell viability.[126] Healthy cells with intact membranes exclude PI whereas PI can penetrate the membranes of dead cells. Thus, cellular apoptotic stages can be identified since viable cells are both annexin V and PI negative, early apoptotic ells are annexin V/FITC positive and PI negative whilst late apoptotic or necrotic dead cells are both annexin V and PI positive.

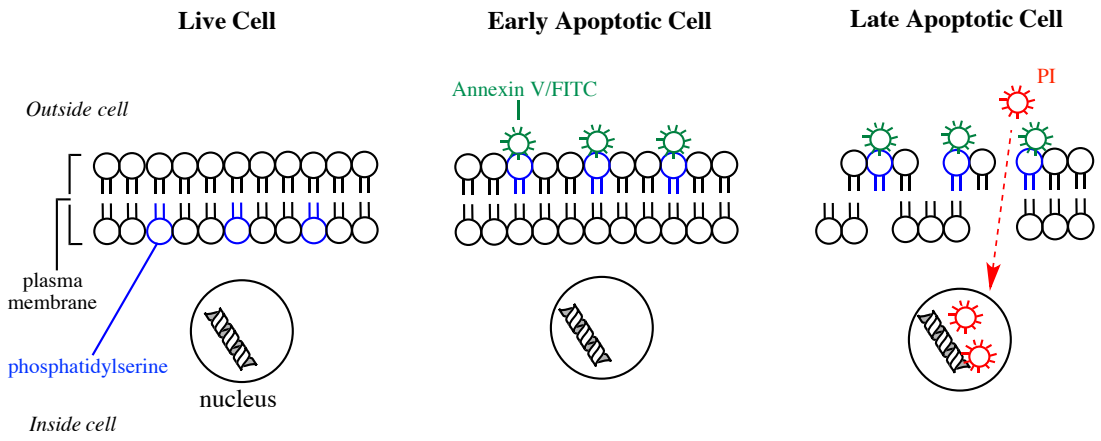


Figure 37: During early apoptosis, the phosphatidylserine (PS) phospholipid translocates from the inner to the outer leaflet of the plasma membrane, which can be detected using annexin V/FITC. During late apoptosis, PI also permeates the cell and intercalates DNA.

Dual annexin V-FITC/PI analysis revealed statistically significant ($P<0.05$) early and late apoptotic populations (A^+) following cellular exposure to cisplatin **2** (e.g. 5 μM; 24 h; MDA-MB-468 – 19% A^+; 5 μM; 72 h – 62% A^+). In contrast, cancer cells (MDA-MB-468 and HCT-116) treated with titanocenes (*R,R*)-**49aa** and (*S,S*)-**49aa** (10 and 20 μM; 24 h) revealed no A^+ populations; following 72 h exposure of MDA-MB 468 and HCT 115 cells to (*R,R*)-**4** and (*S,S*)-**4**, minimal (≤11% compared with ≤6% control) A+ populations were observed.

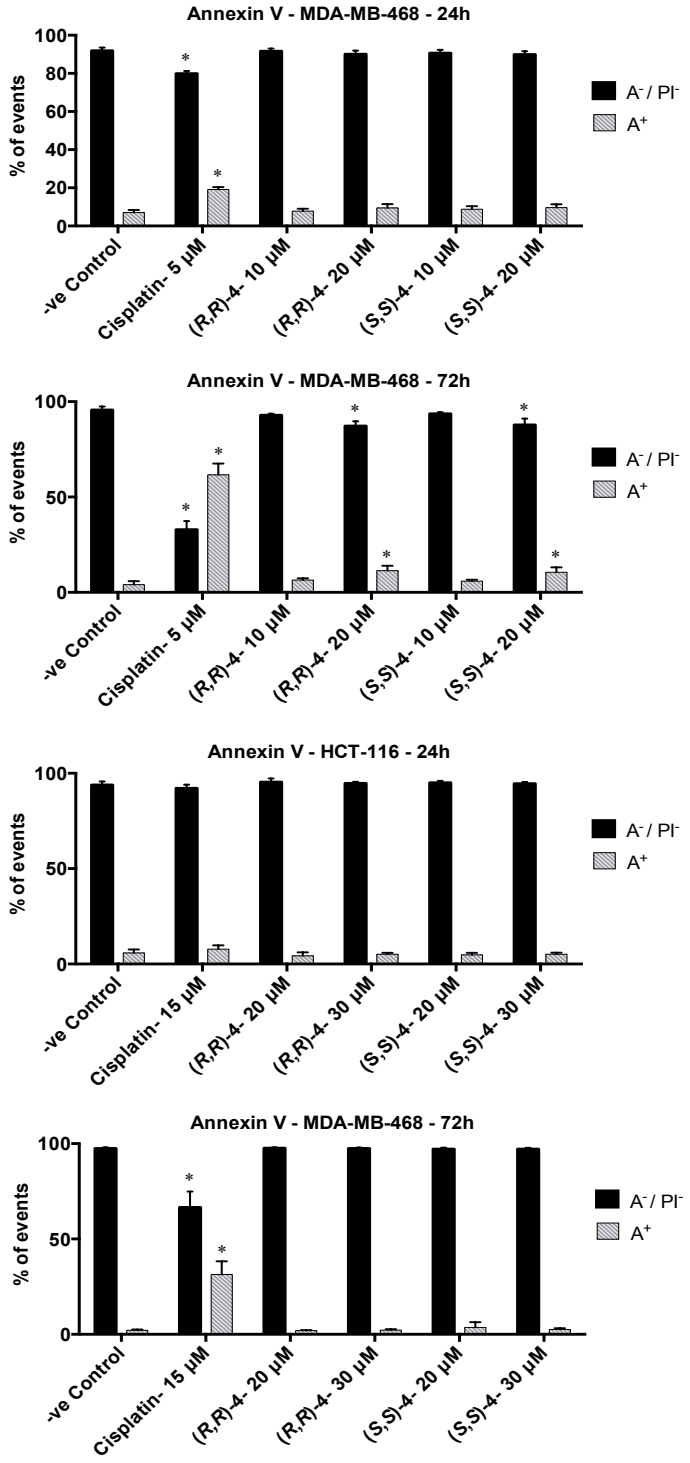


Figure 38: Effects of titanocene derivatives on apoptosis in MDA-MB-468 and HCT-116 cells. Cells were exposed to titanocene for 24 h or 72 h. Cells were analysed by annexin V/PI dual staining and flow cytometry. Titanocene derivatives induced negligible (insignificant) apoptosis whereas the positive control cisplatin induced apoptosis in a time-dependent manner. The percentage of cells undergoing apoptosis was defined as the sum of early apoptotic cells (annexin V-positive) and late apoptotic cells (annexin V-positive and PI-positive). Data are representative of at least 3 independent trials (n = 2 per experiment). *P<0.05 significantly different from control (untreated) using 2 way ANOVA – multiple comparisons.

3.4.6 Paraptosis (type III cell death)

3.4.6.1 Microscopy Imaging

Based on the experimental results in Section 3.52-3.53, the hypothesis that (*R,R*)-**49aa** and (*S,S*)-**49aa** evoke anticancer activity, DNA damage and cell death through apoptosis was rejected. Indeed, features characteristic of apoptosis – chromatin condensation, nuclear fragmentation, cytoplasmic shrinkage, apoptotic membrane blebbing and formation of apoptotic bodies were absent (TEM imaging, live cell confocal microscopy, Figures 39-40). However, as can be visualised in the mentioned figures, other dramatic cellular morphological modifications were induced by **49aa**, whose timing is concurrent with maximised concentrations of intermediate $[Cp^{R}_{2}Ti(OH)]^{+}$ (<6 h).

Transmission electron microscopy (TEM) is a microscopy technique that utilises an electron source instead of light. Since electrons have a much lower wavelength than visible light, much higher resolution (≥1000x) can be achieved than that of a light microscope.[127] Sample preparation for adherent cell microscopy imaging involves culturing cells in adherent treated coverslips, followed by fixation (gluteraldehyde in buffer) and postfixation (osmium tetraoxide). Samples are then washed with distilled water and then dehydrated with graded ethanol series. The coverslips containing adherent MDA-MB-468 cells were then washed with propylene oxide and embedded in resin in an oven for 48 h at 60 ^{o}C. Resin sections were mounted on a copper mesh grid and stained.[128] An electron source was then bombarded through an ultra-thin sample sections (70-200nm), interacting with it as it passes through, which was then analysed.[127]

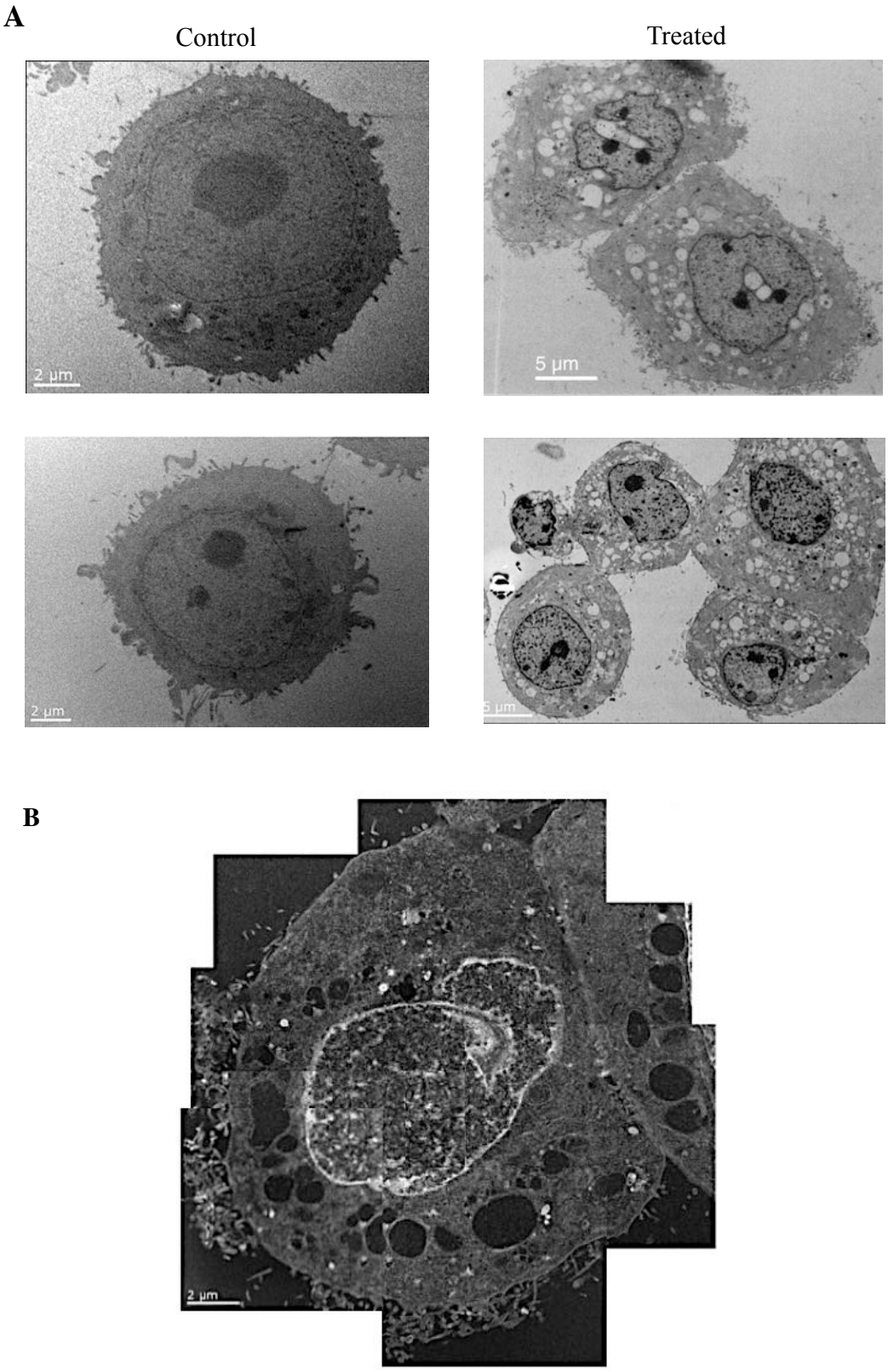


Figure 39: A TEM imaging of MDA-MB-468 cells before and after exposure to (*rac*/*meso*)-**49aa** (50 µM; 3-6 h), revealed extensive vacuolisation. **B** Dark Field Z-contrast montage after 3 h exposure to **49aa** (50 µM) revealed extensive low-density vacuoles.

As highly evident in Figure 39, TEM images of fixed and microtomed sections of MDA-MB-468 cells revealed high contrast subnanometer resolution of specific cell structures. TEM brightfield analysis of MDA-MB-468 control samples (no agent addition) revealed characteristic features of viable cells such as euchromatin (loosely packed – stains light), heterochromatin (densely packed – stains dark) and the nucleolus at the centre of the nucleus in the cell (densely packed – stains dark). TEM brightfield and Z-Contrast dark field imaging of sectioned MDA-MB-468 cells after the highest practical exposure to **49aa** (50 μM, 3-6 h) revealed the formation of extensive cytoplasmic vacuolarisation which is indicative of paraptosis, a characteristic feature of type III cell death. Negligible difference in the nuclear structure were noted.

Confocal microscopy time-image studies of live MDA-MB-468 cells after exposure to (*S,S*)-**49aa** (20 μM, Figure 39A) was carried out to better ascertain the type of cell death mechanism induced by the titanocene agent. ER-Tracker^{TM} Red dye, a cell-permeant live-cell fluorescent dye that selectively stains the endoplasmic reticulum (ER) was used to ascertain whether (*S,S*)-**49aa (**20 μM) induced vacuolarisation originated from the ER. Hoechst 33342 cell permeant nucleic acid stain was also used to ascertain whether live cell nuclei underwent pyknosis (irreversible condensation of chromatin in apoptotic or necrotic cells) after exposure to (*S,S*)-**49aa (**20 μM). Confocal microscopy time-image studies of live MDA-MB-468 cells exposed to (*S,S*)-**49aa** (20 μM) for 13 h, revealed ER swelling (0.33-4.6 h, Figure 40A) and crater-like cups on the cell surface (0.33-0.66 h, Figure 40B), similar to Vacquinol-1 treated glioblastoma cells, indicating an endocytic-like activity.[129] This

was followed by cytoplasmic vacuolisation, vacuole membrane rupture (osmotic lysis) and cell death.

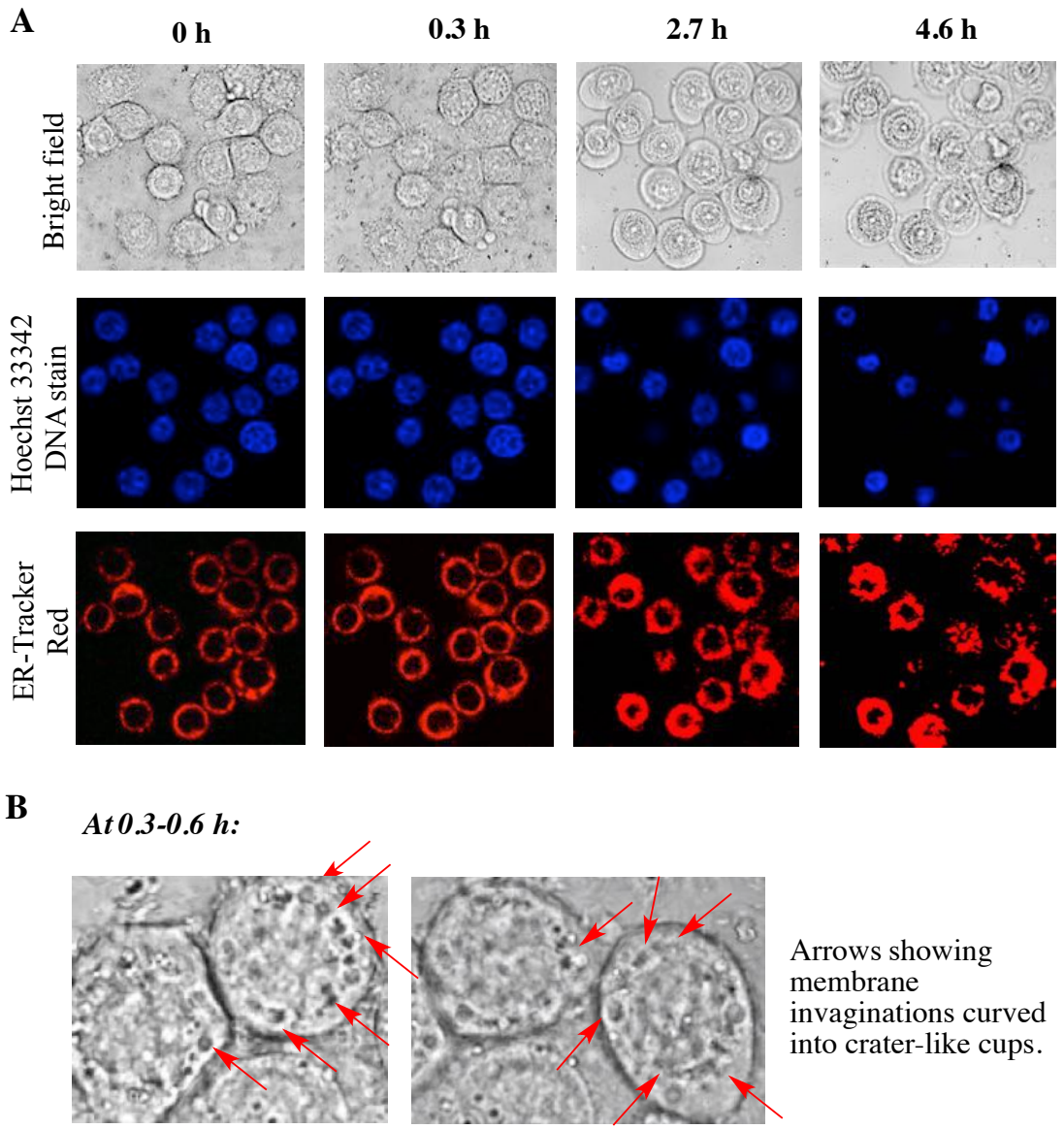


Figure 40: A Confocal microscopy MDA-MB-468 live cell imaging time-series studies after exposure to (*S,S*)-**49aa** (20 μM) revealed cytoplasmic vacuolization and ER swelling, followed by vacuole membrane rupture (osmotic lysis) and cell death. **B** Confocal microscopy MDA-MB-468 at 0.3-0.6 h revealed membrane invaginations curved into crater- like cups on the cell surface membrane indicating endocytic-like activity.

Intracellular titanium (Ti) in Ehrlich ascites tumor (EAT) cells has been previously reported through TEM analysis.[45,46] In the first example,[45] EAT cells from mice were harvested on day 6 after transplantation, fixed with buffer, post-fixed with osmium tetroxide and embedded in Mikropal (resin). Ultra-thin sections were then mounted on copper mesh, stained with uranyl acetate and lead citrate and then finally dipped for 15-30 min in 8000 μM titanocene dichloride **5**. Ti levels of a comparable intensity to the N levels were located in structures within the cell using EELS. The biological relevance of exposing dead sectioned cells to such vast excesses of strongly Lewis acidic **5** has unfortunately never been questioned. In their 1983 work,[46] EAT cells were cultured *in vitro* as a suspension culture cell line. Groups of 4 subcultures each containing about 5×10^6 EAT cells per 20 mL were exposed for 40 min to titanocene **5** in final concentrations of 1000 μM and 10000 μM (the GI_{50} of **5** was reported as 500 μM under these conditions). 'Semi-quantitative' EELS analysis again showed Ti levels of a comparable intensity to the N signal in certain intracellular structures. Although not discussed therein, the potential for hydrolysis of **5** to insoluble titanium species that would not have been removed by the saline wash used is significant.

In our own work, the more modern Gatan Tridiem detector for EELS and the state of the art Oxford Instruments detector for EDX were expected to show a significantly greater sensitivity to Ti, and would both be sufficient to detect Ti significantly below the levels reported above.[45,46] However, even a 40 min exposure to a very high concentration (1000 μM) did not reproducibly result in a detectable levels of Ti in the microtomed section by either EDX or EELS, despite an expected sensitivity of at least 0.1 at% and 1 at%, respectively given the section thickness and electron doses used in this work.

STEM-EDX mapping of the cells was performed to investigate any variance in Ti content across the cell. The work of Köpf-Maier and Krahl reported no Ti in mitochondria or lipids, but a remarkable level in other structures[45,46] comparable to the signal from N - maps in our work found the Ti signal remained at the level of background noise across the cell, while the N and O signals are clearly visible in Figure 41.

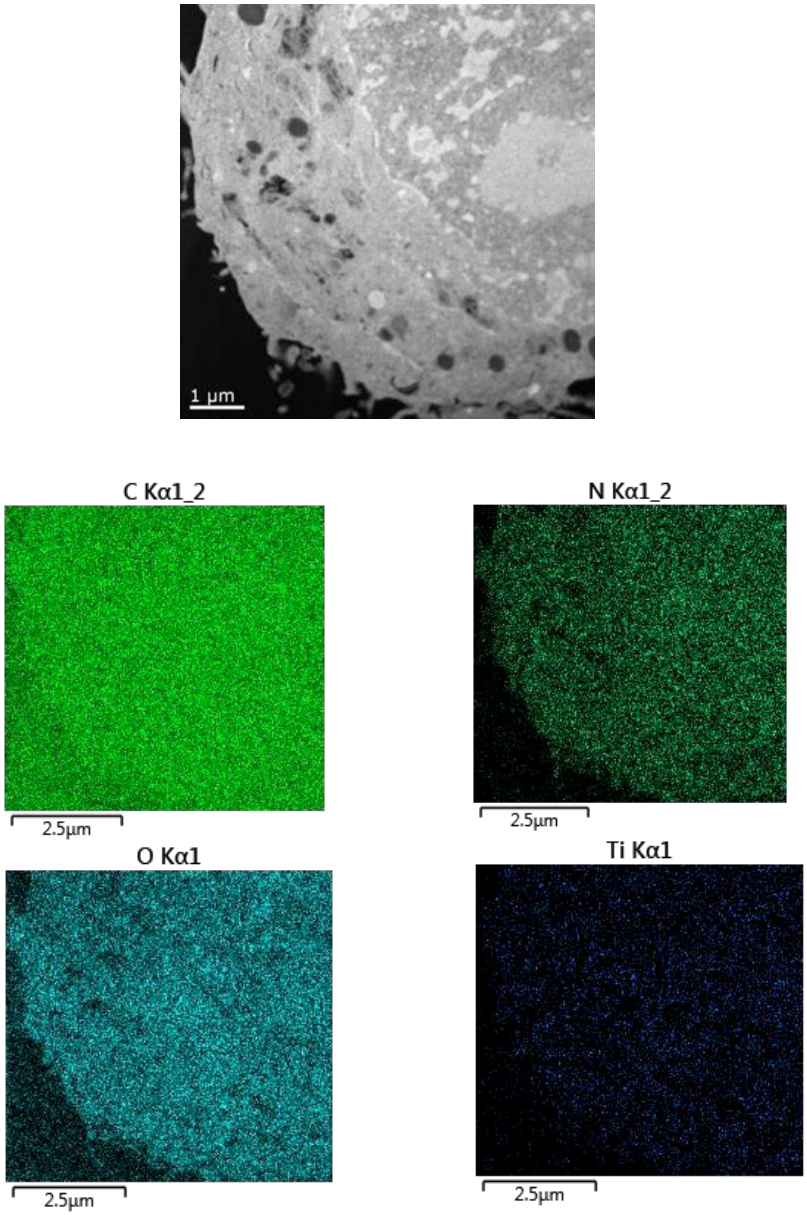


Figure 41: Annular dark field scanning TEM image and associated EDX elemental maps. N and O levels can be seen clearly; however the Ti signal is consistent with volume sensitive background noise only.

Similar results were obtained using EELS, once potential artefacts were subtracted. EELS analysis of low levels of Ti against a strong C background signal is compromised by a signal due to the carbon appearing in a range that overlaps the default Ti detection window used by the standard Gatan software (Figure 42A). The contribution of this artefact can be significantly increased by acquiring the signal in diffraction mode, which could lead to an incorrect identification of Ti (Figure 42B). Careful comparison of the signal observed in this region in this work indicates any deviation from the power law background as being likeliest to be due to the carbon contribution by comparison with a signal from an amorphous carbon film of similar thickness to the microtomed section.

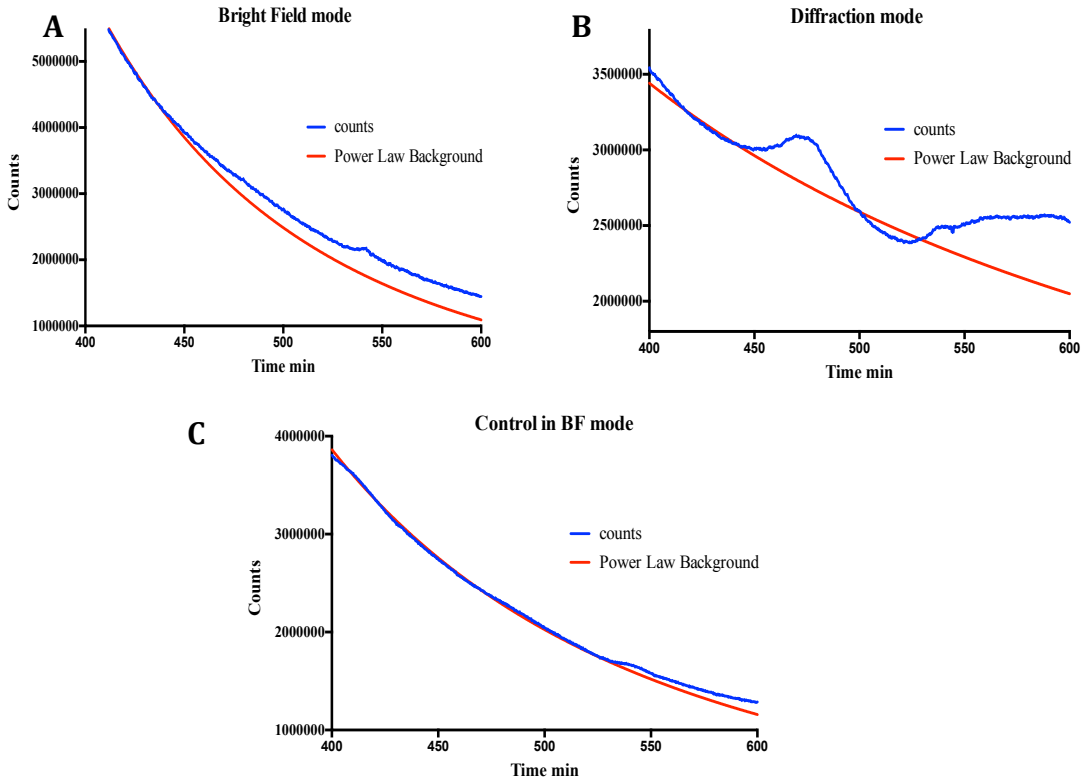


Figure 42: A EELS artefact producing a deviation from the power law background in the Ti region from a signal acquired in Bright Field mode from an amorphous carbon film – C and O content only. **B** EELS artefact producing a significant deviation in the Ti sensitive region from a signal acquired in Diffraction mode from an amorphous Carbon film – C and O content only. **C** EELS signal from a sample treated with **49aa** - Oxygen can be detected, no unambiguous Ti signal can be confirmed.

Reports in the literature describing endocytosis of TiO_2 20-30 nm nanospheres (at 24 h) in breast cancer SK-BR-3 cells resulted in average titanium concentrations of 28±5 picomols per cell as determined by ICP-MS, with some individual cells showing burdens >1000 picomol.[130] In comparison MDB-MB-468 breast cells treated with (*S*,*S*)-**49aa** (30 μM/4 h; the highest dose-time achievable without extensive lysis) had average titanium burdens per cell of only 3.3±0.3 femtomol, compared to 0.35 femtomol for control, untreated cells. Assuming hydrolysis to TiO_2, its known density (4.23 gcm^{-3}) and a homogeneous distribution of the Ti throughout the cell, there would have had to be $>10^7$ aggregates of less than 1-2 nm dimensions to be below our detector's threshold. Thus, the lack of free Cp^R in cultures containing **49aa**, very low Ti cellular concentrations and enantiomer dependent biology are not in accordance with significant accumulation of cyclopentadienyl free Ti^{4+} within our cell lines.

3.4.6.2 MAPK pathway – kinase screening

Based on the very low levels of titanium per cell that was detected by TEM/EDX/EELS and ICP-MS, the absence of detectable Ti-aggregates, the presence of cytoplasmic vacuolisation and endoplasmic reticulum stress, an alternative possible mechanism of action was investigated, involving homogeneous titanium-based paraptotic signal triggering.

Kinase screening of MDA-MB-468 provided evidence of signal transduction pathways activated to produce the cytoplasmic induced paraptosis observed with (*S*,*S*)-**49aa**. Strong up regulation of ERK is observed at 24 h in screening of (*S*,*S*)-**49aa** (20 μM) treated MDA-MB-468 against an array of key kinases (Figure 43).

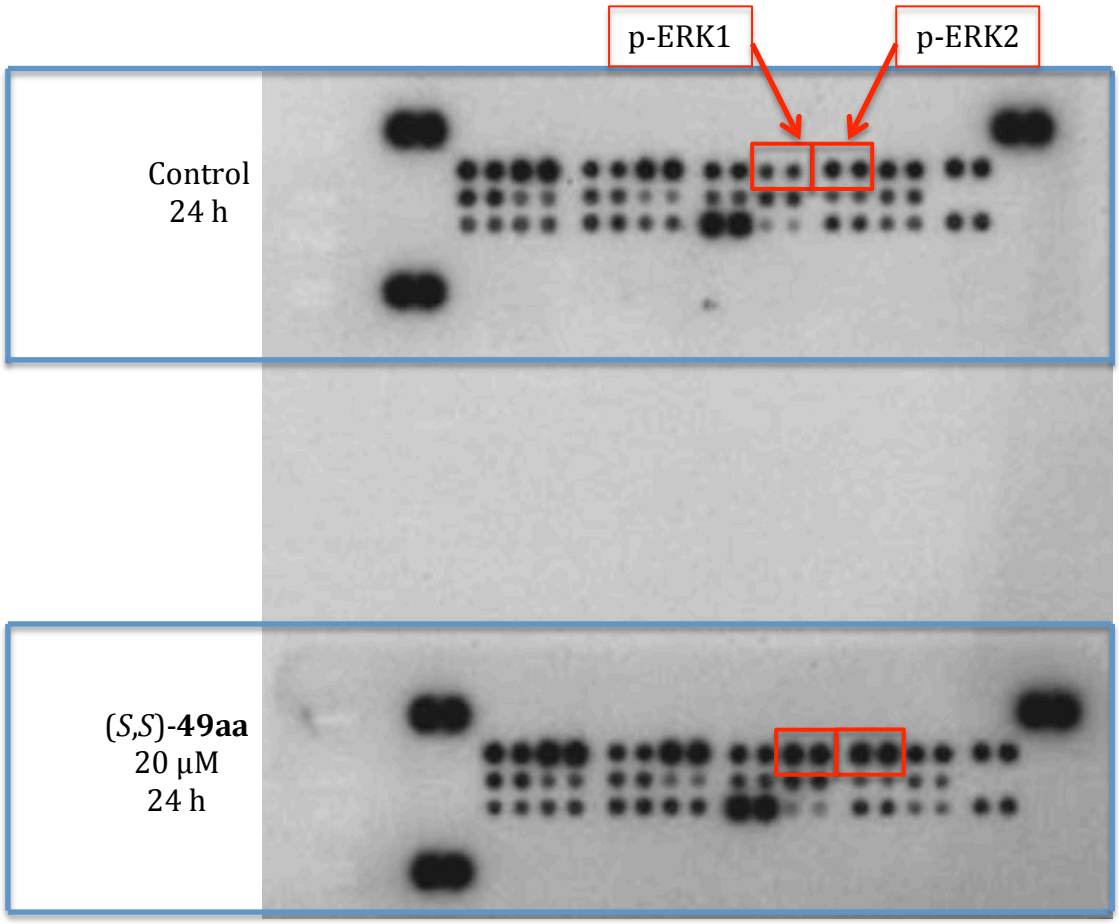


Figure 43: Human Phospho-MAPK Array screening of MDA-MB-468 provided further support for paraptosis. Strong up regulation of p-ERK was observed at 24 h (*S,S*)-**4** - 20 µM treated versus control.

Time dependent Western blot analyses of MDA-MB-468 and HCT-116 (Figure 44) confirm up regulation of the MAP (mitogen activated protein) kinase signaling pathway that cascades directly to ERK1/2. We observed clear up-regulation of epidermal growth factor receptor (EGFR) and phosphorylated EGFR expression. Resultant activation of EGFR signal transduction has been reported to lead directly to cell death through over production of the observed vacuoles and eventual membrane rupture. Such events leading to paraptotic cell death are known to be

triggered by selective activation of range of receptor-mediated pathways.[131-133] In HCT-116, AKT overexpression is observed in both cisplatin and titanocene **49aa** treated cells (24 h) which could be indicative of a survival mechanism in this cell line.[134] Over-expression of this proto-oncogene is a known early event during colon carcinogenesis.[135] The ERK cascade represents a central signaling pathway regulating distinct and opposing cellular processes.[136] Park et al. in 2014 reported vacuolisation, dilated ER and mitochondria in MH-S murine alveolar macrophages, by TiO_2 nanoparticles and conclude that induced paraptosis and late onset apoptosis are the modes of action.[137] This may to be related to the cellular toxicity we observe, at 72 h exposure for samples richer in insoluble titanium compounds, but cannot account fully for the selective toxicity we see for the soluble intermediate early on.

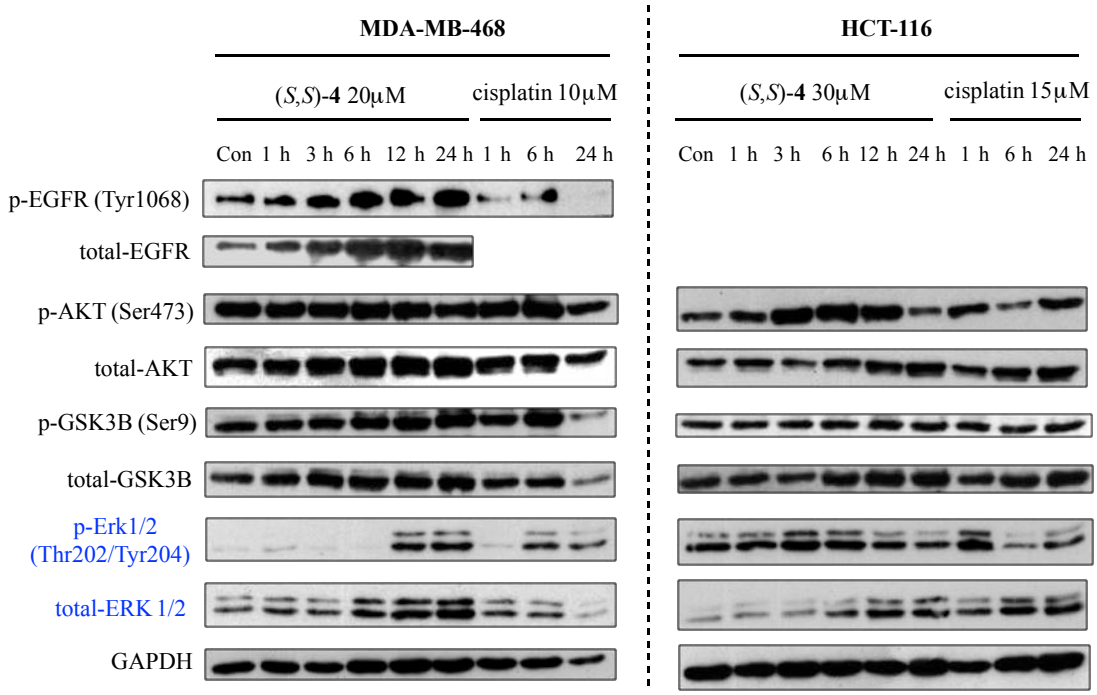


Figure 44: Western blot assays of MDA-MB-468 cells and HCT-116 treated with (*S,S*)-**49aa** (20 or 30 μM, 1-24 h) showed upregulation of total and p-ERK and total and p-EGFR *vs* control, a pattern which is distinct from cisplatin.

Conclusion

A protocol has been developed for the asymmetric copper-catalysed addition of ZnEt2 (ZnBu2) to exocyclic C=C bond of substituted pentafulvenes. Enantiomerically enriched (up to 93:7 *er*) cyclopentadienyl ligands were obtained, which provided rapid access to the unprecedented synthesis of enantiopure-substituted titanocenes. The (*S*,*S*) isomer proved to be at least twice active towards pancreatic, breast and colon cancer cell lines as its (*R*,*R*) enantiomer at 24 h. Unlike cisplatin, enantiopure titanocenes selectivity (2-5 fold) for cancer cell lines over MRC-5 fibroblasts was detected. In stark contrast to cisplatin, enantiopure substituted titanocenes negligibly perturbed MDA-MB-468 and HCT 116 cell cycle, did not cause DNA double strand breaks and failed to trigger significant apoptosis. Evidence strongly advocates cell death by paraptosis following treatment of cancer cells to enantiopure substituted titanocene; extensive cytoplasmic vacuolization accompanied by up-regulated expression of proteins integral to EGFR, MAP kinase and AKT signal transduction preceded membrane rupture and cell death. Appearance of these dramatic cellular morphological modifications is concurrent with maximized concentrations of intermediate $[Cp^{R}_{2}Ti(OH)]^{+}$ (<6 h).

The history of titanocene dichloride thereaputic agents is unfortunately populated with *ad hoc* suggestions for biological pathways that can be tangential to mode of action in particular cell lines and that are not always fully consistent with all experimental data. Unpicking the specific biological chaperone(s) that binds our key hydroxyl active intermediate triggering paraptosis will require extensive, systematic, correlation of target binding to cancer cell grow inhibition across a very wide family of enantiomeric substituted titanocenes to ensure complete veracity of the biological

target(s) involved. This is the next goal of our programme and this is beyond the scope of the present study. However, we conclude that the enantiomeric titanocenes disclosed herein are highly appropriate and powerful tools for this task, as well being of widespread use in many other areas where chiral cyclopentadienyl complexes are used.[138]

Chapter 4 - Experimental

4.1 Chemistry Section

4.1.1 General experimental

All reactions involving air sensitive reagents/intermediates were performed under an atmosphere of argon by using standard Schlenk techniques. Reaction solvents were distilled from appropriate drying agents under argon. Tetrahydrofuran, diethyl ether and methyl *tert*-butyl ether were dried and distilled from sodium/benzophenone. Grignard reagents and chiral catalysts were purchased from Acros and Sigma–Aldrich. All organolithium and Grignard reagents were titrated by using the Gilman double titration procedure before use. Organozinc and organoaluminium reagents were purchased from Acros and their concentration was tested via hydrogen gas evolution before use. All other solvents and reagents were used as received from commercial suppliers. Column chromatography was performed using Davisil silica gel 60, and TLC analysis was performed with Merck silica gel 60 F_{254nm}. NMR spectra (^{1}H, ^{13}C) were recorded with on Bruker AV400, DPX400, AV(III)400 or AV500 spectrometers with $CDCl_3$ as the deuterated solvent. Chemical shift values are reported in ppm, and solvent resonances were used as internal standards ($CHCl_3$: δ = 7.26 ppm for ^{1}H, δ = 77.16 ppm for ^{13}C). Coupling constants (J) are quoted in Hertz. Carbon NMR multiplicities and connectivities were assigned by using DEPT and HMQC experiments. IR spectra were recorded with a Nicolet Avatar FTIR spectrometer with a Nicolet Avatar 360 FTIR reflecting probe [attenuated total reflectance (ATR)] or a Perkin–Elmer 1600 FTIR spectrometer (thin films). HRMS were recorded with a Bruker ApexIV FT-ICRMS instrument (EI) or a Bruker MicroTOF LC-MS instrument (ESI). MS were recorded with a Bruker Ultraflex instrument (MALDI-TOF). GC analysis was carried out using a Varian 3400 with

CP400 autosampler instrument and HPLC assay was carried out using a Varian ProStar with UV detector. Elemental analyses were performed by using an Exeter Analytical CE-440 instrument. Melting points were determined with a Stuart Scientific SMP3 melting point apparatus. Optical rotation was recorded using an ADP 440 machine at 25 °C.

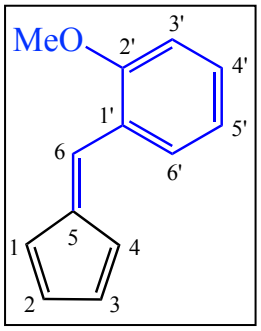
4.1.2 Preparation of pentafulvene derivatives

General Procedure A: Synthesis of Pentafulvenes

The appropriate aldehyde (5 mmol) and excess freshly fractioned cyclopentadiene (b.p. 38-40 °C, 1.1 mL, 12.5 mmol) were dissolved in methanol (4 mL) and water (1 mL) to give a colourless solution. On dropwise addition of pyrrolidine (0.65 mL, 7.5 mmol), the reaction changed colour to red. The reaction was stirred at room temperature and was monitored by TLC. Upon completion by TLC, acetic acid (0.3 mL, 5 mmol) was added to quench the reaction. The mixture was diluted with dichloromethane (5 mL) and deionized water (5 mL). After extraction from the aqueous layer and re-extraction with dichloromethane (5 mL), the combined organic portions were washed with brine (2 x 5 mL) and dried with anhydrous magnesium sulfate. The volatiles were evaporated in *vacuo*. The crude product was purified by flash chromatography using the same solvent mix as in the TLC yielding red oils or solids in moderate to high yield.

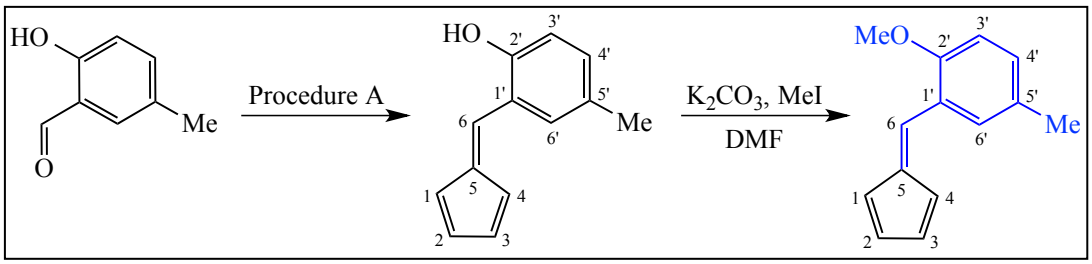
(**CARE!** Pentafulvenes are usually highly malodorous. Always work inside the fumehood, use protective equipment (marigold gloves, half-face mask) and quench any remaining pentafulvenes with bleach.

1-(Cyclopenta-2,4-dien-1-ylidenemethyl)-2-methoxybenzene 51a



Prepared according to general procedure A from 2-methoxybenzaldehyde (16.3 g, 0.12 mol) and excess freshly fractionated cyclopentadiene (25.2 mL, 0.30 mol) in methanol (120 mL) using pyrrolidine (15.0 mL, 0.18 mol) and acetic acid (18.0 mL, 0.32 mol) to yield the crude product. Flash column chromatography (pentane/CH_2Cl_2, 4:1) of the crude afforded the title compound as red oil (21.1 g, 95 %). (**CARE!** this compound is highly malodorous and has a tendency to undergo Diels-Alder dimerization. It should be handled only in a fume hood and stored in sealed flasks at -28 °C. $\mathbf{R_f}$ = 0.34 (pentane/CH_2Cl_2, 4:1). **^{1}H NMR** (400.1 MHz, $CDCl_3$, 25 °C): δ = 7.65 (dd, *J* = 7.7, 1.6 Hz, 1 H, H-6'), 7.61 (br., s, unresolved long range couplings, 1 H, H-6), 7.38 (ddd, *J* = 8.2, 7.5, 1.6 Hz, 1 H, H-4'), 7.05 (dddd, *J* = 7.7, 7.5, 1.6, 0.6 Hz, 1 H, H-5'), 6.94 (dd, *J* = 8.2, 0.6 Hz, 1 H, H-3'), 6.72-6.67 (m, 2 H, H-2 and H-3), 6.57 (app. ddd, *J* = 5.1, 1.8, 0.6 Hz, 1 H, H-1), 6.42 (app. dt, *J* = 5.1, 1.8 Hz, 1 H, H-4), 3.90 (s, 3H, OCH_3) ppm. **^{13}C NMR** (100.6 MHz, $CDCl_3$, 25 °C): δ = 158.6 (C-2'), 145.1 (C-5), 134.9 (C-2 or C-3), 133.9 (C-6), 132.5 (C-6'), 130.7 (C-1 or C-4'), 130.7 (C-1 or C-4'), 127.0 (C-4), 126.0 (C-1'), 120.7 (C-2 or C-3), 120.7 (C-5'), 110.7 (C-3'), 55.6 (OCH_3) ppm. **IR**($CHCl_3$): $\tilde{\nu}$ = 3070, 3002, 2937, 2836, 1622, 1597, 1489, 1464, 1339, 1302, 1249, 1109, 1049, 1027, 903, 842, 753, 624 cm^{-1}. **HRMS** (EI+): calcd. For $C_{13}H_{12}O$ $[M]^+$ 184.0888; found 184.0881. Data as in literature.[112]

1-(Cyclopenta-2,4-dien-1-ylidenemethyl)-2-methoxy-5-methylbenzene 51b

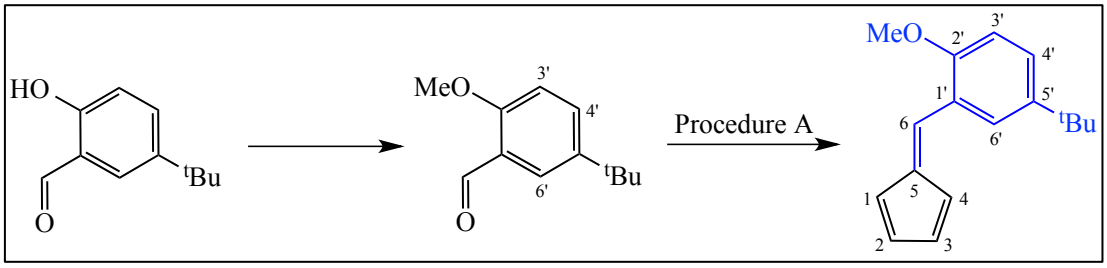


The required intermediate was prepared according to general procedure A from 2-hydroxy-5-methylbenzaldehyde (0.681 g, 5 mmol) to yield the crude intermediate. Flash column chromatography (pentane/Et_2O, 1:1) of the crude intermediate afforded 1-(cyclopenta-2,4-dien-2-ylidenemethyl)-5-methylphenol as a red oil (0.892 g, 97 %), which was stored at –28 °C. $\boldsymbol{R_f}$ = 0.46 (pentane/Et_2O, 1:1). The oil was found to be solvated in diethyl ether even after solvent evaporation in *vacuo* – further evaporation was found to lead to extensive decomposition of unsolvated phenolic intermediate. **^{1}H NMR** (400.1 MHz, $CDCl_3$, 25°C): δ = 7.42-7.37 (br., s, unresolved long range couplings, 1 H, H-6), 7.31 (d, J = 2.2 Hz, 1 H, H-6'), 7.05 (dd, J = 8.2, 2.2 Hz, 1 H, H-4'), 6.75 (d, J = 8.2 Hz, 1H, H-3'), 6.66 (ddt, J = 5.2, 2.0, 1.5 Hz, 1 H, H-2 or H-3), 6.60 (dddd, J = 5.2, 2.0, 1.3, 0.6 Hz, 1 H, H-2 or H-3), 6.52 (dddd, J = 5.2, 2.0, 1.3, 0.6 Hz, 1 H, H-1), 6.36 (dt, J = 5.2, 2.0 Hz, 1 H, H-4), 2.31 (s, *Me*-5', 3 H) ppm. **IR** ($CHCl_3$): $\tilde{\nu}$ = 3687, 3603, 3542, 3071, 2924, 1790, 1625, 1603, 1463, 1433, 1379, 1338, 1324, 1291, 1280, 1265, 1199, 1165, 1080, 1010, 990, 927, 918, 913. **HRMS** (EI+): calcd. For $C_{13}H_{12}O$ $[M]^+$ 184.0888; found 184.0887.

Subsequently, in a Schlenk flask, the pentafulvene intermediate (0.198 g, 1 mmol) was added in DMF (1 mL), followed by anhydrous potassium carbonate (0.280 g, 2 mmol) and methyl iodide (0.284 g, 2 mmol). The mixture was left to stir for 12 h at r.t. The reaction was then quenched with distilled water. After extraction with dichloromethane (2 x 5 mL), the combined organic portions were washed with brine

(2 x 5 mL) and dried with anhydrous magnesium sulfate. The volatiles were evaporated *in vacuo* to yield the crude product. Flash column chromatography (pentane/Et_2O, 1:1) of the crude afforded the title compound as a light red oil (0.169 g, 85 %), which was stored at –28 °C. $\boldsymbol{R_f}$ = 0.70 (pentane/Et_2O, 1:1). **^{1}H NMR** (400.1 MHz, $CDCl_3$, 25°C): δ = 7.54 (br., s, unresolved long range couplings, 1 H, H-6), 7.41 (d, J = 2.0 Hz, 1 H, H-6'), 7.15 (dd, J = 8.3, 2.0 Hz, 1 H, H-4'), 6.81 (d, J = 8.3 Hz, 1H, H-3'), 6.67-6.63 (m, 2 H, H-2 and H-3), 6.58 (ddd, J = 5.2, 1.6, 0.6 Hz, 1 H, H-1), 6.36 (dt, J = 5.2, 1.6Hz, 1 H, H-4), 3.85 (s, 3 H, -OCH_3), 2.33 (s, 3 H, *Me*-5') ppm. **^{13}C NMR** (100.6 MHz, $CDCl_3$, 25 °C): δ = 156.7 (C-2'), 144.9 (C-5), 134.8 (C-2 or C-3), 134.1 (C-6), 133.2 (C-6'), 131.2 (C-4'), 130.6 (C-1), 130.0, (C-5'), 127.1 (C-4), 125.8 (C-1'), 120.8 (C-2 or C-3), 110.7 (C-3'), 55.8 (OCH_3), 20.7 (Ar-CH_3) ppm. **IR**($CHCl_3$): $\tilde{\nu}$ = 3108, 3071, 3011, 2928, 2839, 1711, 1624, 1604, 1498, 1465, 1441, 1415, 1379, 1363, 1339, 1297, 1255, 1185, 1159, 1124, 1079, 1034, 1007, 991, 897. **HRMS** (EI+): calcd. For $C_{14}H_{14}O$ $[M]^+$ 198.1045; found 198.1045.

5-(*Tert*-butyl)-1-(cyclopenta-2,4-dien-1-ylidenemethyl)-2-methoxybenzene 51c

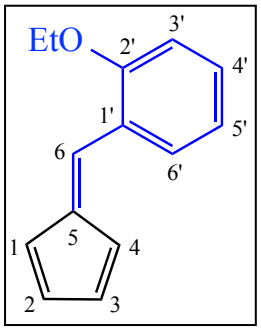


The aldehyde precursor 5-(*tert*-butyl)-2-methoxybenzaldehyde was prepared according to literature.[139] K_2CO_3 (1.08 g, 7 mmol) and iodomethane (0.5 mL, 7 mmol) were added to a solution of 5-*tert*-butyl-2-hydroxybenzaldehyde (1 g, 5.6 mmol) in DMF (11 mL). After it was stirred for 20 h at r.t., 12 mL of 0.5 M NaOH (aq.) was added to the solution and the reaction mixture was extracted with

diethyl ether (3 x 5 mL), washed with brine (2 x 5 mL) and the extracts dried with $MgSO_4$. Column chromatography of the crude intermediate (pentane/ethyl acetate 9:1) afforded 5-(*tert*-butyl)-2-methoxybenzaldehyde (1.034 g, 96%). **^{1}H NMR** (400.1 MHz, $CDCl_3$, 25°C): δ = 10.47 (d, J = 1.0 Hz, 1 H, CHO), 7.85 (d, J = 2.7 Hz, 1 H, H-6'), 7.59 (ddd, J = 8.7, 2.7, 1.0 Hz, 1 H, H-4'), 6.93 (d, J = 8.7 Hz, 1 H, H-3'), 3.91 (s, 3 H, O-CH_3), 1.31 (s, 9H, ^{t}Bu) ppm.

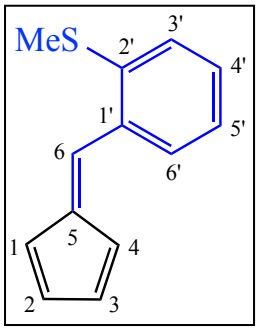
The title compound **51c** was then prepared according to general procedure A from 5-(*tert*-butyl)-2-methoxybenzaldehyde (0.96 g, 5 mmol), to yield the crude product. Flash column chromatography (pentane/Et_2O, 1:1) of the crude afforded the title compound as a light red oil (1.028 g, 86 %), which was stored at –28 °C. $\boldsymbol{R_f}$ = 0.74 (pentane/Et_2O, 1:1). **^{1}H NMR** (400.1 MHz, $CDCl_3$, 25°C): δ = 7.63 (d, J = 2.4 Hz, 1 H, H-6'), 7.58 (br., s, unresolved long range couplings, 1 H, H-6), 7.37 (dd, J = 8.6 Hz, 2.4 Hz, 1 H, H-4'), 1.35 (s, 9 H, ^{t}Bu), 6.85 (d, J = 8.6 Hz, 1 H, H-3'), 6.68-6.65 (m, 1 H, H-2 or H-3), 6.64-6.60 (m, 1 H, H-2 or H-3), 6.55-6.51 (m, 1 H, H-1), 6.39 (dt, J = 5.2, 1.6Hz, 1 H, H-4), 3.87 (s, 3 H, -OCH_3) ppm. **^{13}C NMR** (100.6 MHz, $CDCl_3$, 25 °C): δ = 156.6 (C-2'), 144.9 (C-5 or C-5'), 143.4 (C-5 or C-5'), 134.9 (C-2 or C-3), 134.7 (C-6), 130.6 (C-1), 130.0 (C-6'), 127.6 (C-4'), 127.1 (C-4), 125.4 (C-1'), 120.7 (C-2 or C-3), 110.3 (C-3'), 55.8 (OCH_3), 34.3 (-C(CH_3)$_3$), 31.6 (-C(CH_3)$_3$) ppm. **IR**($CHCl_3$): $\tilde{\nu}$ = 3071, 3011, 2965, 2906, 2870, 2839, 1624, 1604, 1499, 1464, 1441, 1395, 1380, 1365, 1338, 1298, 1283, 1254, 1181, 1159, 1135, 1107, 1079, 1032, 992, 940, 896. **HRMS** (EI+): calcd. For $C_{17}H_{20}O$ $[M]^+$ 240.1514; found 240.1513.

1-(Cyclopenta-2,4-dien-1-ylidenemethyl)-2-ethoxybenzene 51d



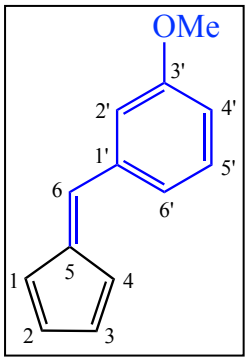
Prepared according to general procedure A from 2-ethoxybenzaldehyde (0.751 g, 5 mmol) to yield the crude product. Flash column chromatography (pentane/CH_2Cl_2, 8:1) afforded the title compound as a red oil (0.812 g, 81 %), which was stored at –28 °C. $\boldsymbol{R_f}$ = 0.34 (pentane/CH_2Cl_2, 8:1). **^{1}H NMR** (400.1 MHz, $CDCl_3$, 25 °C): δ = 7.61 (dd, J = 7.6, 1.6 Hz, 1 H, H-6'), 7.60 (br., s, unresolved long range couplings, 1 H, H-6), 7.33 (ddd, J = 8.2, 7.6, 1.6 Hz, 1 H, H-4'), 7.00 (dddd, J = 8.2, 7.6, 1.0, 0.6 Hz, 1 H, H-5'), 6.90 (dd, J = 8.2, 1.0 Hz, 1 H, H-3'), 6.68-6.63 (m, 2 H, H-2 and H-3), 6.55-6.51 (m, 1 H, H-1), 6.39 (dt, J = 5.2, 1.6 Hz, 1 H, H-4), 4.10 (q, J = 7.0 Hz, 2 H, -CH_2CH$_3$), 1.46 (t, J = 7.0 Hz, 3 H, -CH_3) ppm. **^{13}C NMR** (100.6 MHz, $CDCl_3$, 25 °C): δ = 158.2 (C-2') 144.9 (C-5), 134.8 (C-2 or C-3), 134.3 (C-6), 132.7 (C-6'), 130.7 (C-1 or C-4'), 130.6 (C-1 or C-4'), 127.1 (C-4), 126.2 (C-1'), 120.8 (C-2 or C-3), 120.6 (C-5'), 111.7 (C-3'), 64.1 (-OCH$_2$), 15.0 (-OCH$_2$$CH_3$) ppm. **IR**($CHCl_3$): $\tilde{\nu}$ = 3106, 3073, 3009, 2985, 2931, 2901, 2885, 2740, 2614, 2534, 2495, 2414, 2041, 1974, 1942, 1911, 1799, 1681, 1623, 1597, 1576, 1549, 1490, 1477, 1463, 1454, 1383, 1338, 1302, 1249, 1163, 1119, 1080, 1046, 990, 941, 928, 901, 853, 839. **HRMS** (EI+): calcd. for $C_{14}H_{14}O$ $[M]^+$ 198.1045; found 198.1045.

1-(cyclopenta-2,4-dien-1-ylidenemethyl)-2-(methylthio)benzene 51e



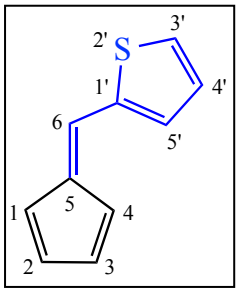
Prepared according to general procedure A from 2-(methylthio)benzaldehyde (0.760 g, 5 mmol) to yield the crude product. Flash column chromatography (pentane/Et_2O, 9:1) afforded the title compound as a red oil (0.746 g, 92 %), which was stored at –28 °C. R_f = 0.42 (pentane/Et_2O, 9:1). ^{1}H NMR (400.1 MHz, $CDCl_3$, 25 °C): δ = 7.54 (br., s, unresolved long range couplings, 1 H, H-6), 7.52-7.48 (m, 1 H, H-6'), 7.34-7.30 (m, 2 H, H-4' and H-5'), 7.24-7.20 (m, 1 H, H-3'), 6.65-6.62 (m, 1 H, H-2), 6.56-6.51 (m, 2 H, H-1 and H-3), 6.39 (dt, J = 5.2, 1.6Hz, 1 H, H-4), 2.48 (s, 3 H, -SCH_3) ppm. **^{13}C NMR** (100.6 MHz, $CDCl_3$, 25 °C): δ = 146.3 (C-2'), 139.7 (C-5), 135.8 (C-1'), 135.4 (C-6), 135.1 (C-6'), 132.3 (C-1 or C-4'), 131.5 (C-1 or C-4'), 129.4 (C-4), 126.6 (2C, C-2 and C-3), 125.3 (C-5'), 121.1 (C-3'), 16.5 (SCH_3) ppm. **IR**($CHCl_3$): $\tilde{\nu}$ = 3063, 3011, 2925, 1625, 1585, 1477, 1456, 1437, 1376, 1336, 1292, 1154, 1127, 1082, 1066, 1042, 989, 969, 901, 836, 625, 608 cm^{-1}. **HRMS** (EI+): calcd. for $C_{13}H_{12}S$ $[M]^+$ 200.0660; found 200.0663.

1-(Cyclopenta-2,4-dien-1-ylidenemethyl)-3-methoxybenzene 51f



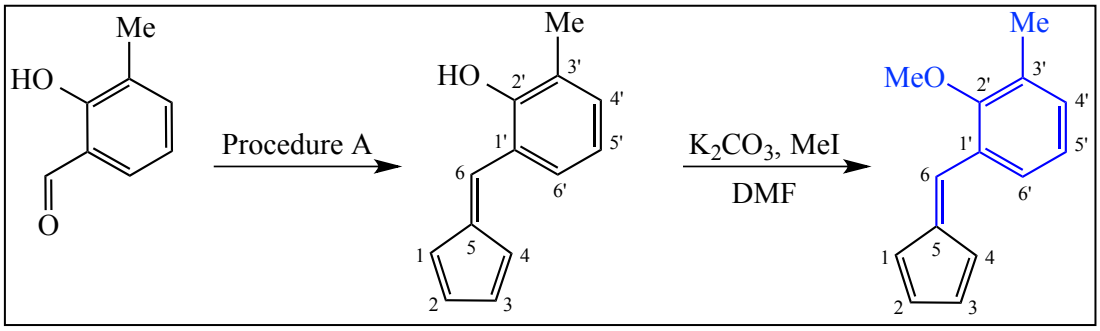
Prepared according to general procedure A from 3-methoxybenzaldehyde (0.681 g, 5 mmol) to yield the crude product. Flash column chromatography afforded the title compound as a light red oil (0.780 g, 85%), which was stored at –28 °C. $\boldsymbol{R_f}$ = 0.40 (pentane/CH_2Cl_2, 1:1). **^{1}H NMR** (400.1 MHz, $CDCl_3$, 25°C): δ = 7.36-7.29 (m, 1 H, H-6), 7.21-7.15 (m, 2 H, H-5' and H-6'), 7.12 (dd, J = 2.6, 1.6 Hz, 1 H, H-2'), 6.92 (ddd, J = 8.2, 2.6, 1.0 Hz, 1 H, H-4'), 6.73-6.64 (m, 1H, H-2), 6.54-6.49 (m, 2 H, H-1 and H-3), 6.32 (dt, J = 5.2, 1.8 Hz, 1 H, H-4), 3.85 (s, 1 H, -OCH_3) ppm. **^{13}C NMR** (100.6 MHz, $CDCl_3$, 25 °C): 159.9 (C-2'), 145.6 (C-5), 138.2 (C-1 and C-6), 135.6 (C-2 or C-3), 131.1 (C-6'), 129.8 (C-4'), 127.3 (C-4), 123.5 (C-1'), 120.5 (2C, C-2 or C-3), 115.8 (C-3' or C-5'), 115.1 (C-3' or C-5'), 55.5 (OCH_3) ppm. **HRMS** (EI+): calcd. for $C_{13}H_{12}O$ $[M]^+$ 184.0888; found 184.0879. These properties were in accordance with literature values.[97]

1-(Cyclopenta-2,4-dien-1-ylidenemethyl)-2-thiophene 51g



Prepared according to general procedure A from thiophene-2-carbaldehyde (0.561 g, 5 mmol) to yield the crude product. Flash column chromatography (pentane/Et_2O, 20:1) afforded the title compound as a red solid (0.598 g, 75 %), which was stored at –28 °C. $\boldsymbol{R_f}$ = 0.28 (pentane/Et_2O, 20:1). **^{1}H NMR** (400.1 MHz, $CDCl_3$, 25°C): δ = 7.50 (dt, J = 5.2 Hz, 1.0 Hz, 1 H, H-3'), 7.31 (dt, J = 4.0, 1.0 Hz, 1 H, H-5'), 7.26 (br., s, unresolved long range couplings, 1 H, H-6), 7.08 (dd, J = 5.2 Hz, 4.0 Hz, 1 H, H-4'), 6.91-6.88 (dddd, J = 5.6, 5.2, 1.6, 0.6 Hz, 1 H, H-2), 6.68-6.63 (m, 1 H, H-3), 6.48-6.46 (dddd, J = 5.2, 2.0, 1.6, 0.6 Hz, 1 H, H-1), 6.30 (dt, J = 5.6, 1.6 Hz, 1 H, H-4) ppm. **^{13}C NMR** (100.6 MHz, $CDCl_3$, 25 °C): δ = 142.6 (C-1'), 140.7 (C-5), 135.3 (C-5'), 133.3 (C-2 or C-3), 130.9 (C-2 or C-3), 130.6 (C-4'), 130.0 (C-3'), 127.8 (C-6), 127.4 (C-1), 119.6 (C-4) ppm. **HRMS** (EI+): calcd. for $C_{10}H_8S$ $[M]^+$ 160.0347; found 160.0340.

1-(Cyclopenta-2,4-dien-1-ylidenemethyl)-2-methoxy-3-methylbenzene 51h

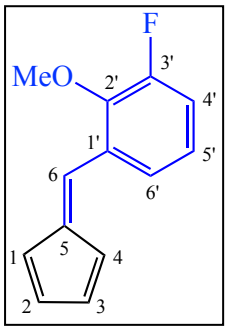


The crude intermediate was prepared according to general procedure A from 2-hydroxy-3-methylbenzaldehyde (0.681 g, 5 mmol). Flash column chromatography (pentane/Et_2O, 1:1) afforded 1-(cyclopenta-2,4-dien-2-ylidenemethyl)-3-methylphenol as a red oil (0.729 g, 74%), which was stored at –28 °C. $\boldsymbol{R_f}$ = 0.64 (pentane/Et_2O, 1:1). **^{1}H NMR** (400.1 MHz, $CDCl_3$, 25°C): δ = 7.45-7.42 (br., s, unresolved long range couplings, 1 H, H-6), 7.38-7.34 (m, 1 H, H-4' or H-6'), 7.21-7.15 (m, 1 H, H-4' or H-6'), 6.93 (t, J = 7.6 Hz, 1 H, H-5'), 6.68 (ddt, J = 5.2, 2.0, 1.5 Hz, 1 H, H-2), 6.61-6.58 (m, 1 H, H-3), 6.56 (dddd, J = 5.2, 2.0, 1.5, 0.6 Hz, 1 H, H-1), 6.40 (dt, J = 5.2, 2.0 Hz, 1H, H-4), 2.32 (s, 3 H , *Me*-3') ppm. **^{13}C NMR** (100.6 MHz, $CDCl_3$, 25 °C): δ = 152.6 (C-2'), 146.2 (C-3'), 133.5 (C-2 or C-3), 133.1 (C-6), 132.1 (C-6'), 131.4 (C-1 or C-4'), 130.1 (C-1 or C-4'), 126.7 (C-4), 124.1 (C-1' or C-5), 123.6 (C-1' or C-5), 120.7 (C-2 or C-3 or C-5'), 120.6 (C-2 or C-3 or C-5'), 16.0 (Ar-*C*H_3) ppm. **HRMS** (EI+): calcd. for $C_{13}H_{12}O$ $[M]^+$ 184.0888; found 184.0885.

Subsequently, in a Schlenk flask, the pentafulvene intermediate above (0.198 g, 1 mmol) was dissolved in DMF (1 mL), followed by the addition of potassium carbonate (0.280 g, 2 mmol) and methyl iodide (0.284g, 2 mmol). The mixture was left to stir for 12 h at r.t. The reaction was then quenched with distilled water. After

extraction with dichloromethane (2 x 5 mL), the combined organic portions were washed with brine (2 x 5 mL) and dried with anhydrous magnesium sulfate. The volatiles were evaporated *in vacuo* to yield the crude product. Flash column chromatography (pentane/Et_2O, 9:1) afforded the title compound as a light red oil (0.173 g, 87 %), which was stored at -28 °C. $\boldsymbol{R_f}$ = 0.44 (pentane/Et_2O, 9:1). **^{1}H NMR** (400.1 MHz, $CDCl_3$, 25°C): δ = 7.50 (br., s, unresolved long range couplings, 1 H, H-6), 7.46 (dd, J = 7.6, 1.8 Hz, 1 H, H-4'), 7.19-7.24 (m, 1 H, H-6'), 7.08 (t, 7.6 Hz, 1 H, H-5'), 6.66-6.65 (m, 2 H, H-3 and H-4), 6.56-6.53 (m, 1 H, H-1), 6.38 (dt, J = 5.2, 2.0Hz, 1 H, H-5), 3.75 (s, 3 H, -OCH_3), 2.32 (s, 3 H, 3'-*Me*), ppm. **^{13}C NMR** (100.6 MHz, $CDCl_3$, 25 °C): δ = 158.4 (C-2'), 145.7 (C-5), 135.1 (C-2 or C-3), 134.1 (C-6), 132.5 (C-6'), 131.5 (C-1' or C-3'), 131.1 (C-1 or C-4'), 130.6 (C-1 or C-4'), 130.4 (C-1' or C-3'), 127.1 (C-4), 124.2 (C-2 or C-3), 120.8 (C-5'), 61.7 (OCH_3), 16.1 (Ar-CH_3) ppm. **IR**($CHCl_3$): $\tilde{\nu}$ = 3073, 3011, 2958, 2937, 2872, 1625, 1587, 1465, 1418, 1374, 1337, 1259, 1173, 1095, 1080, 1078, 946, 909, 890. **HRMS** (EI+): calcd. for $C_{14}H_{14}O$ $[M]^+$ 198.1045; found 198.1043.

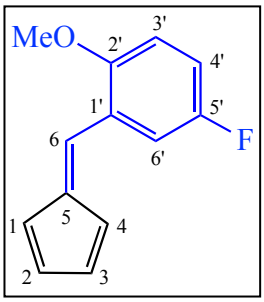
1-(Cyclopenta-2,4-dien-1-ylidenemethyl)-3-fluoro-2-methoxybenzene 51i



Prepared according to general procedure A from 3-fluoro-2-methoxybenzaldehyde (0.771 g, 5 mmol) to yield the crude product. Flash column chromatography (pentane/CH_2Cl_2, 4:1) afforded the title compound as a red oil (0.812 g, 80 %), which was stored at –28 °C. $\boldsymbol{R_f}$ = 0.36 (pentane/CH_2Cl_2, 4:1). **^{1}H NMR** (400.1 MHz,

$CDCl_3$, 25 °C): δ = 7.45 (br., s, unresolved long range couplings, 1 H, H-6), 7.40-7.35 (m, 1 H, H-4'), 7.15-7.01 (m, 2 H, H-5' and H-6'), 6.69-6.63 (m, 1 H, H-2 or H-3), 6.61-6.56 (m, 1 H, H-2 or H-3), 6.54 (dt, J = 5.2, 1.6 Hz, 1 H, H-1), 6.36 (dt, J = 5.2, 1.8 Hz, 1 H, 4-H), 3.97 (d, J = 1.8 Hz, 3 H, -OCH_3) ppm. **^{13}C NMR** (100.6 MHz, $CDCl_3$, 25 °C): δ = 155.5 (d, J = 247.0 Hz, C-3'), 147.0 (d, J = 10.7 Hz, C-2'), 146.4 (C-5), 135.7 (C-2 or C-3), 132.2 (C-6), 132.0 (d, J = 2.7 Hz, C-1'), 131.5 (C-1), 127.6 (d, J = 3.3 Hz, C-6'), 127.1 (C-4), 123.6 (d, J = 8.0 Hz, C-5'), 120.6 (C-2 or C-3), 117.7 (d, J = 19.5 Hz, C-4'), 62.0 (d, J = 5.9 Hz, -OCH$_3$) ppm. **^{19}F NMR** (376.6 MHz, $CDCl_3$) δ = -130.82 ppm. **IR**($CHCl_3$): $\tilde{\nu}$ = 3076, 3011, 2942, 2908, 2839, 1625, 1591, 1494, 1466, 1442, 1426, 1380, 1338, 1299, 1278, 1258, 1183, 1158, 1107, 1080, 1032, 992, 970, 898, 876, 821 cm^{-1}. **HRMS** (EI+): calcd. for $C_{13}H_{11}OF$ $[M]^+$ 202.0794; found 202.0800.

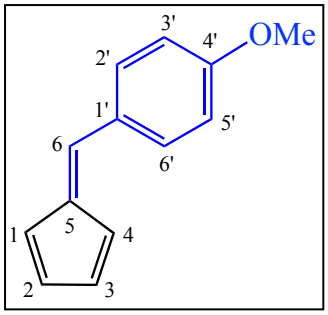
1-(Cyclopenta-2,4-dien-1-ylidenemethyl)-5-fluoro-2-methoxybenzene 51j



Prepared according to general procedure A from 5-fluoro-2-methoxybenzaldehyde (0.771 g, 5 mmol) to yield the crude product. Flash column chromatography (pentane/Et_2O, 6:1) afforded the title compound as a red oil (0.685 g, 68 %), which was stored at –28 °C. $\boldsymbol{R_f}$ = 0.48 (pentane/Et_2O, 6:1). **^{1}H NMR** (400.1 MHz, $CDCl_3$, 25 °C): δ = 7.45 (br., s, unresolved long range couplings, 1 H, H-6), 7.31 (dd, J = 9.0, 3.0, 0.6 Hz, 1 H, H-4'), 7.03 (ddd, J = 9.0, 8.0, 3.0 Hz, 1 H, H-6'), 6.84 (dd, J =

9.0, 4.4 Hz, 1 H, H-3'), 6.68-6.59 (m, 2 H, H-2 and H-3), 6.34 (dt, J = 4.8, 2.0Hz, 1 H, H-4), 6.54-6.51 (m, 1 H, H-1), 3.86 (s, 3 H, -OCH_3) ppm. **^{13}C NMR** (100.6 MHz, $CDCl_3$, 25 °C): δ = 155.9 (d, J = 238.6 Hz, C-5'), 154.8 (d, J = 2.0 Hz, C-2'), 145.9 (C-5), 135.7 (C-2 or C-3), 132.3 (d, J = 2.2 Hz, C-6), 131.3 (C-1), 127.2 (C-1'), 127.1 (C-4), 120.3 (C-2 or C-3), 118.6 (d, J = 23.6 Hz, C-6'), 116.6 (d, J = 23.6 Hz, C-4'), 111.7 (d, J = 8.0 Hz, C-3'), 56.3 (O*C*H_3) ppm. **^{19}F NMR** (376.6 MHz, $CDCl_3$) δ = -123.64 ppm. **IR**($CHCl_3$): $\tilde{\nu}$ = 3076, 3009, 2963, 2942, 2908, 2839, 1625, 1591, 1494, 1466, 1442, 1426, 1380, 1338, 1299, 1278, 1258, 1183, 1158, 1107, 1080, 1032, 992, 970, 898, 876, 821 cm^{-1}. **HRMS** (EI+): calcd. for $C_{13}H_{11}OF$ $[M]^+$ 202.0794; found 202.0794.

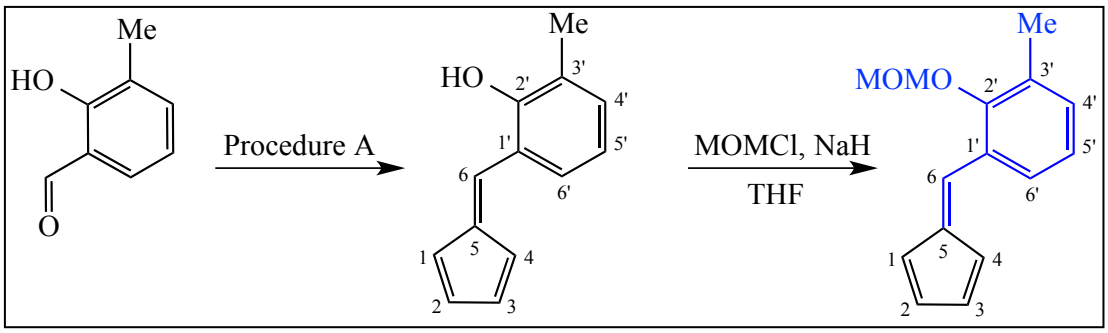
1-(Cyclopenta-2,4-dien-1-ylidenemethyl)-4-methoxybenzene 51k



Prepared according to general procedure A from 4-methoxybenzaldehyde (0.681 g, 5 mmol) to yield the crude product. Flash column chromatography (pentane/CH_2Cl_2, 4:1) afforded the title compound as an orange powder (0.789 g, 81%), which was stored at –28 °C. R_f = 0.42 (pentane/CH_2Cl_2, 4:1). **^{1}H NMR** (400.1 MHz, $CDCl_3$, 25 °C): δ = 7.57-7.61 (m, 2 H, H-2' and H-6'), 7.17 (br., s, unresolved long range couplings, 1 H, H-6), 6.98-6.92 (m, 2 H, H-3' and H-5'), 6.75-6.73 (m, 1 H, H-2 or H-3), 6.69-6.66 (m, 1 H, H-2 or H-3), 6.52-6.47 (m, 1 H, H-1), 6.33 (dt, J = 5.2, 1.8 Hz, 1 H, H-4), 3.86 (s, 3 H, -OCH_3), ppm. **^{13}C NMR** (100.6 MHz, $CDCl_3$, 25 °C): δ

= 160.8 (C-4'), 143.5 (C-5), 138.4 (C-2' or C-6'), 135.1 (C-2 or C-3), 132.6 (C-2' or C-6'), 129.9 (C-1), 129.7 (C-1'), 127.6 (C-4), 120.0 (C-2 or C-3), 114.4 (2C, C-3' and C-5'), 55.5 (OCH_3), ppm. **HRMS** (EI+): calcd. for $C_{13}H_{12}O$ $[M]^+$ 184.0888; found 184.0881. These properties were in accordance with literature values.[78]

1-(cyclopenta-2,4-dien-1-ylidenemethyl)-2-(methoxymethoxy)-3-methylbenzene 51l

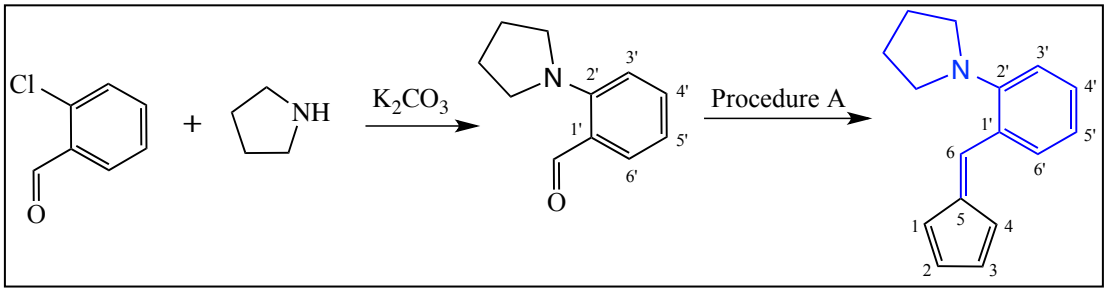


The crude intermediate was prepared according to general procedure A from 2-hydroxy-3-methylbenzaldehyde (0.681 g, 5 mmol). Flash column chromatography (pentane/Et_2O, 1:1) afforded 1-(cyclopenta-2,4-dien-2-ylidenemethyl)-3-methylphenol as a red oil (0.729 g, 74%), which was stored at –28 °C. $\boldsymbol{R_f}$ = 0.64 (pentane/Et_2O, 1:1). **^{1}H NMR** (400.1 MHz, $CDCl_3$, 25 °C): δ = 7.45-7.42 (br., s, unresolved long range couplings, 1 H, H-6), 7.38-7.34 (m, 1 H, H-4' or H-6'), 7.21-7.15 (m, 1 H, H-4' or H-6'), 6.93 (t, J = 7.6 Hz, 1 H, H-5'), 6.68 (ddt, J = 5.2, 2.0, 1.5 Hz, 1 H, H-2), 6.61-6.58 (m, 1 H, H-3), 6.56 (dddd, J = 5.2, 2.0, 1.5, 0.6 Hz, 1 H, H-1), 6.40 (dt, J = 5.2, 2.0 Hz, 1H, H-4), 2.32 (s, 3 H , *Me*-3') ppm. **^{13}C NMR** (100.6 MHz, $CDCl_3$, 25 °C): δ = 152.6 (C-2'), 146.2 (C-3'), 133.5 (C-2 or C-3), 133.1 (C-6), 132.1 (C-6'), 131.4 (C-1 or C-4'), 130.1 (C-1 or C-4'), 126.7 (C-4), 124.1 (C-1' or C-5), 123.6 (C-1' or C-5), 120.7 (C-2 or C-3 or C-5'), 120.6 (C-2 or C-3 or C-5'),

16.0 (Ar-*C*H_3) ppm. **HRMS** (EI+): calcd. for $C_{13}H_{12}O$ $[M]^+$ 184.0888; found 184.0885.

Subsequently, in a Schlenk flask, NaH 60% w/w in mineral oil (60.0 mg, 1.5 mmol) was washed with dry pentane (2 x 5 mL), followed by the addition of dry THF (2 mL). A THF solution (1 mL) of the pentafulvene intermediate (0.198 g, 1 mmol) was then added and the suspension was stirred at room temperature (1 h). Chloromethyl methyl ether (0.161 g, 2 mmol, 0.15 mL) was added dropwise at room temperature. The reaction was quenched after 2 h with distilled water (4 mL). After diethyl ether extraction (10 mL), the organic layer was then washed with water (2 x 10 mL), 5% NaOH (2 x 10 mL) and brine (2 x 10 mL). The organic layer was then dried with anhydrous magnesium sulfate followed by filtration. The volatiles were evaporated *in vacuo* to yield the crude product. Flash column chromatography (pentane/Et_2O, 1:1) afforded the title compound as a light red oil after column chromatography (0.182 g, 80 %), which was stored at –28 °C. $\boldsymbol{R_f}$ = 0.64 (pentane/Et_2O, 1:1). **^{1}H NMR** (400.1 MHz, $CDCl_3$, 25 °C): δ = 7.46 (br., s, unresolved long range couplings, 1 H, H-6), 7.43 (dd, J = 8.0, 7.6 Hz, 1 H, H-5'), 7.24-7.20 (m, 1 H, H-6'), 7.10-7.08 (m, 1 H, H-4'), 6.66-6.60 (m, 2 H, H-2 and H-3), 6.54-6.52 (m, 1 H, H-1), 6.35 (dt, J = 4.8, 2.0 Hz, 1 H, H-4), 4.98 (s, 2 H, -O-C*H*$_2$-O), 3.57 (s, 3 H, -OC*H*$_3$), 2.35 (s, 3 H, -CH_2-O-C*H*$_3$), ppm. **^{13}C NMR** (100.6 MHz, $CDCl_3$, 25 °C): δ = 155.8 (C-2'), 145.7 (C-3'), 135.1 (C-2 or C-3), 134.5 (C-6), 132.3 (C-6'), 131.8 (C-1' or C-5), 131.2 (C-6'), 130.7 (C-1), 126.8 (C-5'), 124.5 (C-4), 120.9 (C-2 or C-3), 100.3 (-O-*C*H_2-O-), 57.8 (O*C*H_3), 16.9 (Ar-*C*H_3) ppm. **IR**($CHCl_3$): $\tilde{\nu}$ = 3011, 2932, 1626, 1474, 1432, 1400, 1373, 1337, 1257, 1184, 1158, 1071, 971, 826, 889 cm^{-1}. MS (EI+): *m*/*z* (%) = calcd. for $C_{15}H_{16}O_2$ $[M]^+$ 228.1150; found 228.1155.

1-(2-(Cyclopenta-2,4-dien-1-ylidenemethyl)phenyl)pyrrolidine 51m



The aldehyde intermediate 2-(pyrrolidin-1-yl)benzaldehyde was prepared according to literature.[140] 2-Chlorobenzaldehyde (2.812 g, 20 mmol), pyrrolidine (1.96 mL, 24 mmol) and potassium carbonate (3.31 g, 24 mmol) were added in 15 mL of DMF, in a 50 mL round bottomed flask under argon and equipped with a reflux condenser. The reaction was heated to 80 °C for 24 h. After cooling, the mixture was added to saturated aqueous potassium carbonate solution (50 mL) and extracted with diethyl ether (3 x 50 mL). The extracts were dried over anhydrous magnesium sulfate and evaporated under reduced pressure to yield the crude intermediate. Flash column chromatography (pentane/MTBE, 9:1) afforded a yellow oil (0.799 g, 23 %). R_f = 0.30 (pentane/MTBE, 9:1). **^{1}H NMR** (400.1 MHz, $CDCl_3$, 25 °C): δ = 10.09 (s, 1 H), 7.71 (dd, J = 7.8, 1.8 Hz, 1 H, H-6'), 7.38 (ddd, J = 8.6, 7.0, 1.8 Hz, 1 H, H-4'), 6.89-6.76 (m, 2 H, H-3' and H-5'), 3.41-3.31 (m, 4 H, -CH_2-N-CH_2-), 2.04-1.94 (m, 4 H, -N-CH_2-CH_2-CH_2-) ppm. **^{13}C NMR** (100.6 MHz, $CDCl_3$, 25 °C): δ = 190.3 (C=O), 150.1 (C-2'), 134.3 (C-4' or C-6'), 133.3 (C-4' or C-6'), 123.1 (C-1'), 116.6 (C-3' or C-5'), 114.7 (C-3' or C-5'), 52.8 (-CH_2-N-CH_2-), 26.1 (-N-CH_2-CH_2-CH_2-) ppm. **HRMS** (EI+): calcd. for $C_{11}H_{13}NO$ $[M]^+$ 175.0997; found 175.0994.

The title compound was then prepared according to general procedure A from 2-(pyrrolidin-1-yl)benzaldehyde prepared above (0.876 g, 5 mmol), to yield the crude product. Flash column chromatography (pentane/MTBE, 9:1) afforded a red

oil (0.918 g, 82%), which was stored at –28 °C. R_f = 0.7 (pentane/MTBE, 9:1). **^{1}H NMR** (400.1 MHz, $CDCl_3$, 25°C): δ = 7.46-7.43 (m, 2 H, H-6 and H-6'), 7.28-7.22 (m, 1 H, H-4'), 6.90-6.85 (m, 2 H, H-3' and H-5'), 6.70-6.69 (m, 1 H, H-2), 6.65-6.63 (m, 1 H, H-3), 6.54 (dt, J = 4.6, 1.6 Hz, 1 H, H-1), 6.37 (dt, J = 5.2 Hz, 1.6 Hz, 1 H, H-4), 3.37-3.30 (m, 4 H, -CH_2-N-CH_2-), 2.00-1.91 (m, 4 H, -N-CH_2-CH_2-CH_2-) ppm. **^{13}C NMR** (100.6 MHz, $CDCl_3$, 25 °C): δ = 150.8 (C-2'), 142.6 (C-5), 139.7, 134.6, 133.8, 130.3, 129.7, 126.5, 126.3 (C-1'), 121.3, 119.0 (C-3' or C-5'), 114.8 (C-3' or C-5'), 52.6 (-CH$_2$-N-CH$_2$-), 25.6 (-N-CH_2-CH$_2$-CH$_2$-) ppm. **IR**($CHCl_3$): $\tilde{\nu}$ = 3068, 3011, 2973, 2875, 2834, 1622, 1612, 1594, 1482, 1460, 1450, 1378, 1355, 1337, 1298, 1272, 1164, 1142, 1080, 1052, 991, 955, 902, 836 cm^{-1}. **HRMS** (EI+): calcd. for $C_{16}H_{17}N$ $[M]^+$ 223.1361; found 223.1355.

4.1.3 Preparation of chiral cyclopentadienyl derivatives

General Procedure B - Synthesis of racemic substituted cyclopentadienyl compounds **50**

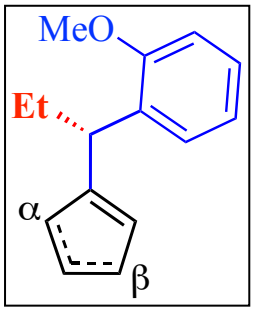
To a dry Schlenk tube, equipped with a magnetic stirrer and a septum, CuBr•SMe_2 (10.3 mg, 0.05 mmol, 10 mol%) was added to dry THF (1.5 mL) and left to stir at room temperature (15 min). The solution was cooled to -10 °C and ethylmagnesium bromide 0.80-0.90 M THF solution (1.25 mmol, 2.5 equiv.) was added dropwise and the reaction was left to stir (15 min) at -10 °C. A colour change from yellow to purple was noted. Neat pentafulvene **51a-m** (0.5 mmol, 1.0 equiv.) was dissolved in dry THF (0.5 mL) and added to the Grignard-cuprate solution dropwise. The reaction was then stirred for 16 h at -10 °C. Saturated aqueous NH_4Cl (3 mL) was added dropwise to quench the reaction, which was then allowed to warm to room temperature with rapid stirring. The reaction mixture was diluted with ether (3 mL)

and the organic phase extracted, washed with aqueous NH_4Cl solution (2 mL) and brine (2 x 2 mL). The organic layer was then dried over $MgSO_4$. All volatiles were removed under reduced pressure to yield the crude product, which was then purified by column chromatography using the same solvent mix as in the TLC to yield the racemic cyclopentadienyl ligands in 60-92% yields as colourless oils.

General Procedure C - Synthesis of enantio-enriched substituted cyclopentadienyl compounds (*S*)-**50**

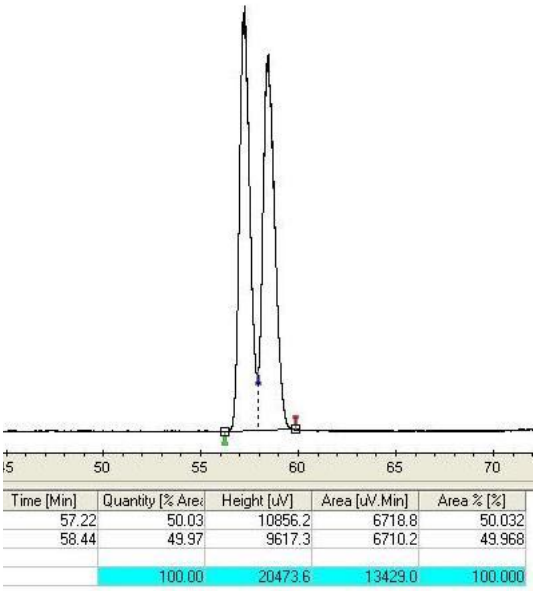
In a dry Schlenk tube equipped with a magnetic stirrer and a septum, $Cu(OTf)_2$ (13.0 mg, 12 mol%), ligand (*S,S,S*)-$\mathbf{L_A}$ (29.0 mg, 18 mol%) and additive (±)-$\mathbf{L_L}$ (13.6 mg, 13 mol%) was added in MTBE (1.2 mL). The mixture was left to stir at 25 ^oC for 1 h followed by the addition of a MTBE solution (0.6 mL) of **51a-m** (0.3 mmol). The mixture left to stir for 10 min followed by the dropwise addition of diethylzinc (0.8 mL, 2.5 equiv.) over 1 min at 25 ^oC. The mixture was left to stir for 16 h at 25 ^oC. Saturated NH_4Cl was added dropwise to quench the reaction, which was then warmed to room temperature with rapid stirring. Workup and purification as per general procedure B.

(*S*)-1-(1-(cyclopenta-1,3-dien-1-yl)propyl)-2-methoxybenzene and (*S*)-1-(1-(cyclopenta-1,4-dien-1-yl)propyl)-2-methoxybenzene (*S*)-51aa

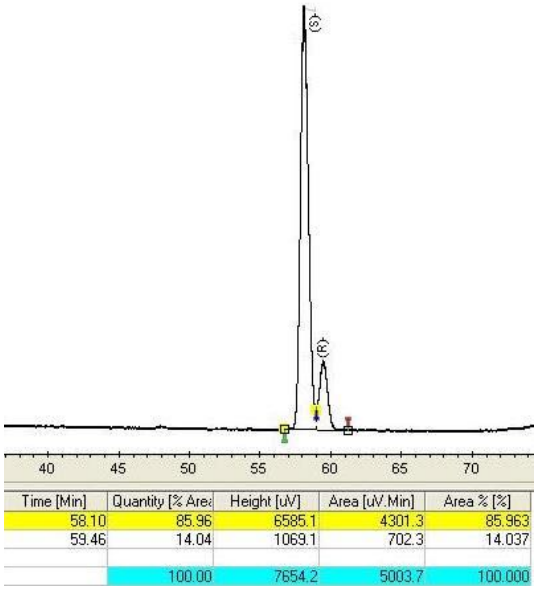


Prepared according to general procedure C (scaled up to 2.5 mmol) from 1-(cyclopenta-2,4-dien-1-ylidenemethyl)-2-methoxybenzene **51a** (0.46 g, 2.5 mmol), $Cu(OTf)_2$ (0.109 g, 12 mol%), ligand (*S*,*S*,*S*)-$\mathbf{L_A}$ (0.243 g, 18 mol%), additive (±)-$\mathbf{L_L}$ (0.113 g, 13 mol%) and diethylzinc (8 mL, 6.3 mmol, 2.5 equivs.) to yield the crude product. Column chromatography (pentane/CH_2Cl_2, 8:1) afforded the title compound as a colourless oil (0.365 g, 57%, 86:14 *er*). $\mathbf{R_f}$ = 0.32 (pentane/CH_2Cl_2, 8:1). The individual α/β tautomer (0.8 : 1.2 ratio) signals could not be uniquely identified and are referred to as tautomer 1 and tautomer 2 and integrated on this basis. **^{1}H NMR** (400.2 MHz, $CDCl_3$, 25 °C): δ = 7.23-7.11 (m, 2.0 H, Ar both tautomers), 6.96-6.87 (m, 2.0 H, Ar both tautomers), 6.48-6.45 (m, 0.4 H, Cp tautomer 1), 6.45-6.36 (m, 1.2 H, Cp tautomer 2), 6.31-6.23 (m, 0.8 H, Cp tautomer 1), 6.15-6.10 (m, 0.6 H, Cp tautomer 2), 4.22-4.12 (m, 1.0 H, *CH*Et both tautomers), 3.86 (s, 1.8 H, O*Me* tautomer 2) *overlapped by* 3.85 (s, 1.2 H, O*Me* tautomer 1), 3.02-2.98 (br, 1.2 H, CH_2 in Cp tautomer 2), 2.87-2.82 (br, 0.8 H, CH_2 in Cp tautomer 1), 2.08-1.81 (m, 2 H, CH_2Me both tautomers), 0.93 (t, 1.8 H, *J* = 7.3 Hz, CH_2*Me* tautomer 2) *overlapped by* 0.92 (t, 1.2 H, *J* = 7.3 Hz, CH_2*Me* tautomer 1) ppm. **^{13}C NMR** (100.6 MHz, $CDCl_3$, 25 °C): δ = 157.3 (*C*-O-Me tautomer 2). 157.1 (*C*-O-Me tautomer 1), 152.8 (Cp-*C*-CHEt tautomer 1), 149.9 (Cp-*C*-CHEt tautomer

2), 134.6 (Cp tautomer 2), 133.6 (Cp tautomer 1), 133.1 (Cp tautomer 1), 132.9 (Cp tautomer 2), 132.1 (Cp tautomer 2), 130.7 (Cp tautomer 1), 127.9 (Ar tautomer 1), 128.0 (Ar tautomer 2), 126.9 (Ar tautomer 2), 126.8 (Ar tautomer 1), 126.3 (Cp tautomer 1), 125.8 (Cp tautomer 2), 120.6 (Ar both tautomers), 110.6 (Ar both tautomers), 55.5 (O*Me* both tautomers), 42.6 (*C*H_2 in Cp tautomer 1), 41.0 (*C*H_2 in Cp tautomer 2), 40.4 (*C*HEt tautomer 1), 39.6 (*C*HEt tautomer 2), 27.8 (Me*C*H_2 tautomer 1), 27.3 (Me*C*H_2 tautomer 2), 12.5 (CH_2*Me* both tautomers) ppm. **IR** (thin film): $\tilde{\nu}$ = 3064, 2961, 2932, 2874, 2835, 1598, 1490, 1463, 1241, 1031, 899, 752 cm^{-1}. **HRMS** (EI^+): calcd. for $C_{15}H_{18}O$ $[M]^+$ 214.1358, found: 214.1360. **CHN** Anal. calcd. for $C_{15}H_{18}O$: C, 84.07; H, 8.47; found: C, 84.01; H, 8.67. **GC:** (Chirasil-DEX-CB); T_{inj} = 250 °C, T_{det} = 280 °C, flow = 2.0 mL min^{-1}, t_i = 110 °C (70 min), t_f = 170 °C (5.0 °C min^{-1}): (*S*)-enantiomer: t_R = 58.1 min, (*R*)-enantiomer: t_R = 59.5 min. **$[\alpha]_D^{25}$:** -52.2 (*c* = 1.0 in $CHCl_3$).

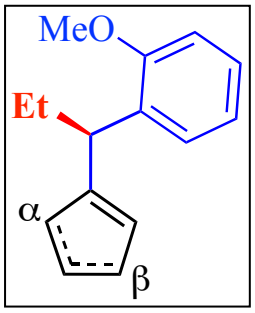


Time [Min]	Quantity [% Area]	Height [uV]	Area [uV.Min]	Area % [%]
57.22	50.03	10856.2	6718.8	50.032
58.44	49.97	9617.3	6710.2	49.968
	100.00	20473.6	13429.0	100.000

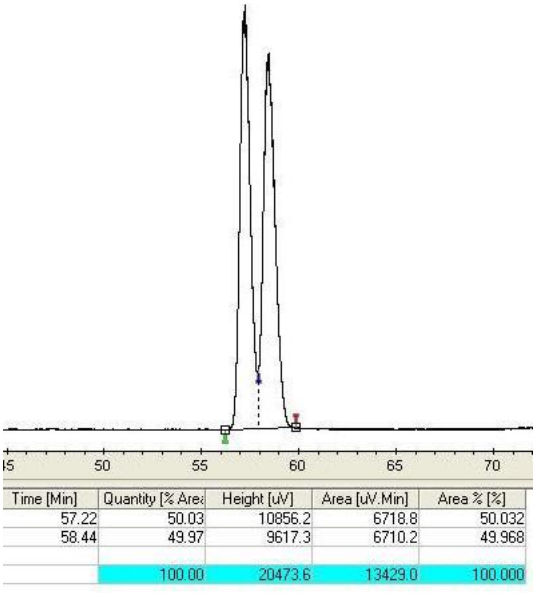


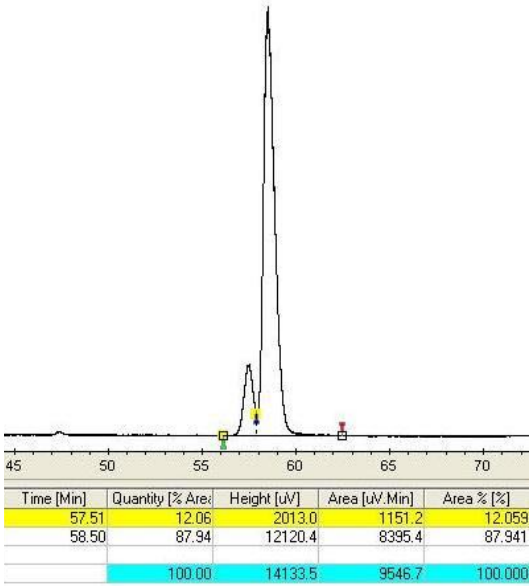
Time [Min]	Quantity [% Area]	Height [uV]	Area [uV.Min]	Area % [%]
58.10	85.96	6585.1	4301.3	85.963
59.46	14.04	1069.1	702.3	14.037
	100.00	7654.2	5003.7	100.000

(*R*)-1-(1-(cyclopenta-1,3-dien-1-yl)propyl)-2-methoxybenzene and (*R*)-1-(1-(cyclopenta-1,4-dien-1-yl)propyl)-2-methoxybenzene (*R*)-50aa

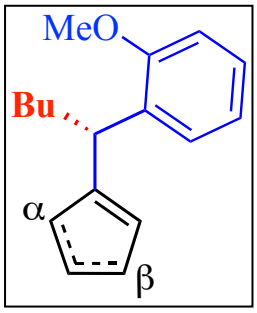


Prepared according to general procedure C (scaled up to 2.5 mmol) from 1-(cyclopenta-2,4-dien-1-ylidenemethyl)-2-methoxybenzene **51aa** (0.46 g, 2.5 mmol), $Cu(OTf)_2$ (0.109 g, 12 mol%), ligand (*R*,*R*,*R*)-$\mathbf{L_A}$ (0.243 g, 18 mol%) additive (±)-$\mathbf{L_L}$ (0.113 g, 13 mol%) and diethylzinc (8 mL, 6.3 mmol, 2.5 equivs.) to yield the crude product. Column chromatography (pentane/CH_2Cl_2, 8:1) afforded the title compound as a colourless oil as a colourless oil (0.395g, 61%, 13:87 *er*). **GC:** (Chirasil-DEX-CB); T_{inj} = 250 °C, T_{det} = 280 °C, flow = 2.0 mL min^{-1}, t_i = 110 °C (70 min), t_f = 170 °C (5.0 °C min^{-1}): (*S*)-enantiomer: t_R = 57.5 min, (*R*)-enantiomer: t_R = 58.5 min. **$[\alpha]_D^{25}$:** +55.1 (*c* = 1.0 in $CHCl_3$).





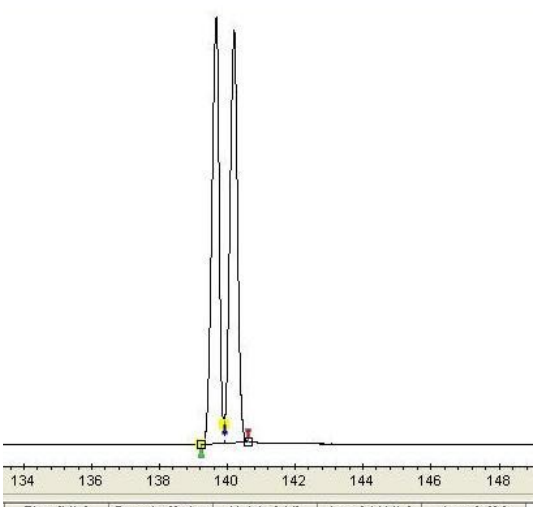
(*S*)-1-(1-(cyclopenta-1,3-dien-1-yl)pentyl)-2-methoxybenzene and (*S*)-1-(1-(cyclopenta-1,4-dien-1-yl)pentyl)-2-methoxybenzene (*S*)-50ab



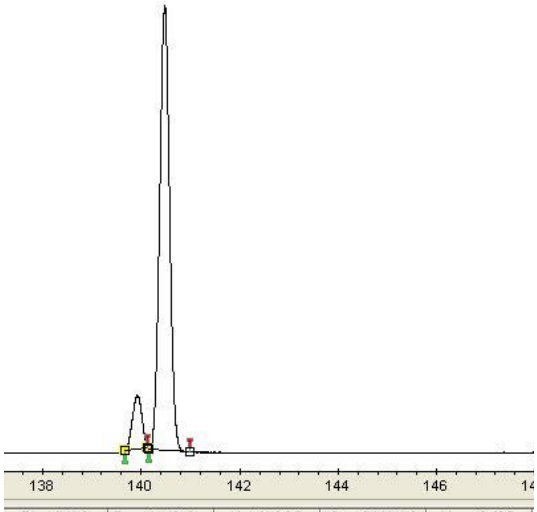
To a Schlenk flask equipped with a magnetic stirrer was added dry $ZnCl_2$ (0.574g, 4.21 mmol) and solid NaOMe (0.478 g, 8.85 mmol) in MTBE (5 mL) at room temperature. The mixture was stirred for 20 min and cooled to 0 °C for another 10 min. Freshly prepared *n*BuMgCl 0.8 M in MTBE (10.3 mL, 8.20 mmol) was added dropwise to the zinc methoxide solution with vigorous stirring over 5-10 min at 0 °C and the heterogenous mixture was left to stir for 2 h at room temperature. The freshly prepared dibutylzinc solution was left to settle for a few hours resulting in the precipitation of white inorganic salts. The dibutylzinc solution was then gently filtered via cannula in a flame dried Schlenk flask under argon (7 mL, 0.18 M).

The enantio-enriched cyclopentadienyl ligand was prepared according to general procedure C from 1-(cyclopenta-2,4-dien-1-ylidenemethyl)-2-methoxybenzene **51a** (55.0 mg, 0.3 mmol) and freshly prepared dibutylzinc (3.3 mL, 0.6 mmol, 2 equivs.) to yield the crude product. Column chromatography (pentane/CH_2Cl_2, 6:1) afforded the title compound as a colourless oil (42.0 mg, 58%, 90:10 *er*). $\boldsymbol{R_f}$ = 0.34 (pentane/CH_2Cl_2, 6:1). The individual α/β tautomer (0.8:1.2 ratio) signals could not be uniquely identified and are referred to as tautomer 1 and tautomer 2 and integrated on this basis. **^{1}H NMR** (400.1 MHz, CDCl3, 25 °C): δ = 7.20–7.10 (m, 2.0 H, Ar, both tautomers), 6.94–6.85 (m, 2.0 H, Ar, both tautomers), 6.47–6.36 (m, 1.6 H, Cp,

both tautomers), 6.27–6.21 (m, 0.8 H, Cp, tautomer 1), 6.12–6.06 (m, 0.6 H, Cp, tautomer 2), 4.27–4.18 (m, 1.0 H, C*H*Bu, both tautomers), 3.84 (s, 1.8 H, OMe, tautomer 2) *overlapped by* 3.84 (s, 1.2 H, OMe, tautomer 1), 3.01-2.95 (m, 1.2 H, CH_2, tautomer 2), 2.85–2.80 (m, 0.8 H, CH_2, tautomer 1), 2.00-1.75 (m, 2.0 H, $CH_2C_3H_7$, both tautomers), 1.39-1.17 (m, 4.0 H, C_2H_4Me, both tautomers), 0.88 (t, J = 7.0 Hz, 3.0 H, CH_2Me, both tautomers) ppm. **^{13}C NMR** (100.6 MHz, $CDCl_3$, 25 °C): δ = 157.1 (*C*OMe, tautomer 2), 157.0 (*C*OMe, tautomer 1), 153.0 (Cp*C*CH, tautomer 1), 150.1 (Cp*C*CH, tautomer 2), 134.6 (Cp, tautomer 2), 133.9 (Cp, tautomer 1), 133.2 (Cp, tautomer 2), 133.1 (Cp, tautomer 2), 132.1 (Cp, tautomer 1), 130.7 (Cp, tautomer 2), 128.0 (Ar, tautomer 2), 127.9 (Ar, tautomer 1), 126.7 (Ar, both tautomers), 126.2 (Cp, tautomer 1), 125.7 (Cp, tautomer 2), 120.6 (Ar, both tautomers), 110.6 (Ar, both tautomers), 55.5 (OMe, both tautomers), 42.6 (CH_2, tautomer 1), 41.0 (CH_2, tautomer 2), 38.5 (*C*HBu, tautomer 1), 37.7 (*C*HBu, tautomer 2), 34.6 (*C*$H_2C_3H_7$, tautomer 1), 34.1 (*C*$H_2C_3H_7$, tautomer 2), 30.1 (*C*$_2H_4$Me, tautomer 1), *overlapped by* 30.0 (*C*$_2H_4$Me, tautomer 2), 22.7 (*C*$_2H_4$Me, both tautomers), 14.0 (CH_2Me, both tautomers) ppm. **IR** ($CHCl_3$): $\tilde{\nu}$ = 3065, 3009, 2959, 2933, 2861, 2838, 1598, 1491, 1464, 1439, 1369, 1341, 1289, 1243, 1163, 1116, 1052, 1032, 949, 900, 821 cm^{-1}. **HRMS** (EI+): calcd. for $C_{17}H_{22}O$ $[M]^+$ 242.1671; found 242.1670. **CHN** Anal. calcd. for $C_{17}H_{22}O$: calcd. C 84.25, H 9.15; found C 84.27, H 9.10. **GC:** (Chirasil-DEX-CB); T_{inj} = 250 °C, T_{det} = 280 °C, flow = 2.0 mL min^{-1}, t_i = 100 °C (100 min), t_f = 170 °C (1.0 °C min^{-1}): (*R*)-enantiomer: t_R = 139.9 min, (*S*)-enantiomer: t_R = 140.5 min. **$[\alpha]_D^{25}$:** -43.5 (*c* = 1.0 in $CHCl_3$).

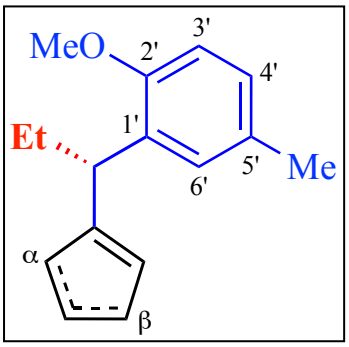


Time [Min]	Quantity [% Area]	Height [uV]	Area [uV.Min]	Area % [%]
139.68	49.89	67232.9	16726.3	49.893
140.20	50.11	65033.7	16797.7	50.107
	100.00	132266.6	33524.0	100.000



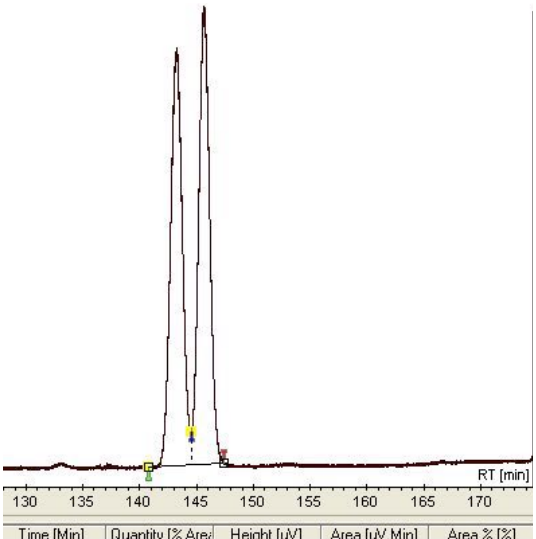
Time [Min]	Quantity [% Area]	Height [uV]	Area [uV.Min]	Area % [%]
139.92	10.34	3022.3	672.1	10.336
140.47	89.66	24904.6	5830.3	89.664
	100.00	27926.9	6502.3	100.000

(*S*)-1-(1-(cyclopenta-1,3-dien-1-yl)propyl)-2-methoxy-5-methylbenzene and (*S*)-1-(1-(cyclopenta-1,4-dien-1-yl)propyl)-2-methoxy-5-methylbenzene (*S*)-50ba

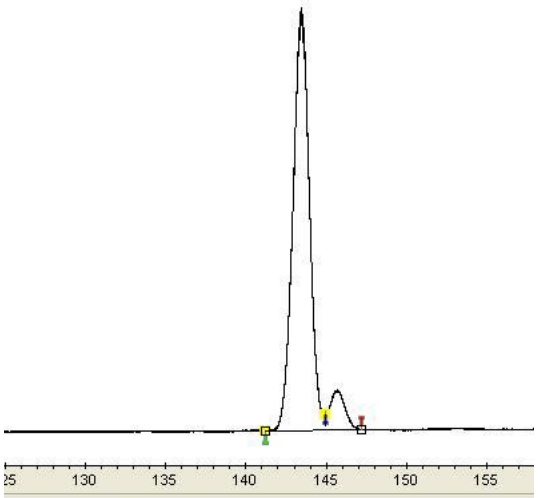


Prepared according to general procedure C from 1-(cyclopenta-2,4-dien-1-ylidenemethyl)-2-methoxy-5-methylbenzene **51b** (59.0 mg, 0.3 mmol) to yield the crude product. Column chromatography (pentane/CH_2Cl_2, 6:1) afforded the title compound as a colourless oil (39.0 mg, 56%, 92:8 *er*). $\mathbf{R_f}$ = 0.50 (pentane/CH_2Cl_2, 6:1). The individual α/β tautomer (1 : 1 ratio) signals could not be uniquely identified and are referred to as tautomer 1 and tautomer 2 and integrated on this basis. **^{1}H NMR** (400.2 MHz, $CDCl_3$, 25 ^{o}C): δ 6.99-6.89 (m, 2 H, H-4' and H-6'), 6.79

(d, 0.5 H, *J* = 8.2 Hz, H-3' tautomer 2) *overlapped by* 6.78(d, *J* = 8.2 Hz, 0.5 H, H-3' tautomer 1), 6.48-6.35 (m, 1.4 H, Cp both tautomers), 6.22-6.29 (m, 0.9 H Cp tautomer 1 or 2), 6.12-6.08 (m, 0.5 H, Cp tautomer 1 or 2), 4.15-4.05 (m, 1.0 H, *CH*Et both tautomers), 3.82 (s, 1.6 H, O*Me* tautomer 2) *overlapped by* 3.81 (s, 1.4 H, O*Me* tautomer 1), 3.00-2.97 (br, 1 H, CH_2 in Cp tautomer 2), 2.85-2.82 (br, 1 H, CH_2 in Cp tautomer 1), 2.27 (br, 3.0 H, CH_3-Ar, both tautomers), 2.05-1.78 (m, 2 H, CH_2Me both tautomers), 0.90 (t, 1.6 H, *J* = 7.3 Hz, CH_2*Me* tautomer 2) *overlapped by* 0.89 (t, 1.4 H, *J* = 7.3 Hz, CH_2*Me* tautomer 1) ppm. **^{13}C NMR** (100.6 MHz, $CDCl_3$, 25 ^{o}C): δ 155.4 (*C*-O-Me tautomer 2), 155.2 (*C*-O-Me tautomer 1), 153.1 (Cp-*C*-CHEt tautomer 1 or 2), 150.2 (Cp-*C*-CHEt tautomer 1 or 2), 134.8 (Cp tautomer 2), 133.5 (Ar *C*-1' tautomer 2), 133.3 (Cp tautomer 1), 132.9 (Ar *C*-1' tautomer 1), 132.3 (Cp tautomer 2), 130.9 (Cp tautomer 1), 129.9 (Ar *C*-5' tautomer 1), 129.8 (Ar *C*-5' tautomer 2), 128.9 (Ar *C*-4' or *C*-6' tautomer 2), 128.7 (Ar *C*-4' or *C*-6' tautomer 1), 127.3 (Ar *C*-4' or *C*-6' tautomer 2), 127.2 (Ar *C*-4' or *C*-6' tautomer 1), 126.3 (Cp tautomer 1), 125.8 (Cp tautomer 2), 110.9 (Ar *C*-3' both tautomers), 55.9 (O*Me* both tautomers), 42.8 (*C*H_2 in Cp tautomer 1), 41.1 (*C*H_2 in Cp tautomer 2), 40.6 (*C*HEt tautomer 1), 39.8 (*C*HEt tautomer 2), 27.9 (Me*C*H_2 tautomer 1), 27.4 (Me*C*H_2 tautomer 2), 20.9 (H_3*C*-Ar both tautomers), 12.7 (CH_2*Me* both tautomers) ppm. **IR** ($CHCl_3$): $\tilde{\nu}$ = 3064, 3008, 2963, 2932, 2875, 2837, 2736, 1603, 1500, 1464, 1368, 1338, 1287, 1243, 1183, 1155, 1120, 1079, 1036, 985, 951, 900, 821821 cm^{-1}. **HRMS (EI+)**: calcd. for $C_{16}H_{22}O$ $[M]^+$ 228.1514; found 228.1506. **GC:** (octakis(2,6-di-*O*-methyl-3-*O*-pentyl)-gamma-cyclodextrin) T_{inj} = 250 ^{o}C, T_{det} = 280 ^{o}C, flow = 2.0 mL min^{-1}, t_i = 90 ^{o}C (80 min), t_f = 160 ^{o}C (0.5 ^{o}C min^{-1}): (*S*)-enantiomer: t_R = 143.4 min, (*R*)-enantiomer: t_R = 145.7 min. **$[\alpha]_D^{25}$:** -17.0 (c = 1.0 in $CHCl_3$).

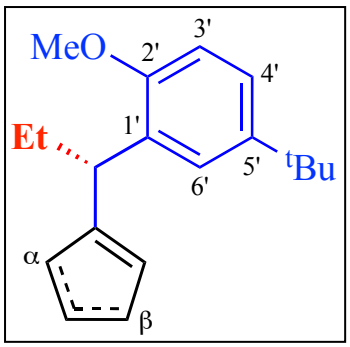


Time [Min]	Quantity [% Area]	Height [uV]	Area [uV.Min]	Area % [%]
143.22	49.63	6480.0	7818.3	49.635
145.69	50.37	7091.0	7933.4	50.365
	100.00	13571.0	15751.7	100.000



Time [Min]	Quantity [% Area]	Height [uV]	Area [uV.Min]	Area % [%]
143.44	92.16	18136.9	21337.0	92.164
145.67	7.84	1729.9	1814.1	7.836
	100.00	19866.8	23151.1	100.000

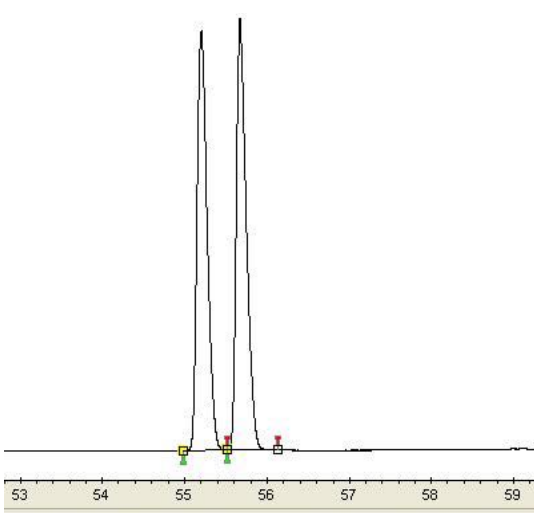
(*S*)-5-(*tert*-butyl)-1-(1-(cyclopenta-1,3-dien-1-yl)propyl)-2-methoxybenzene and (*S*)-5-(*tert*-butyl)-1-(1-(cyclopenta-1,4-dien-1-yl)propyl)-2-methoxybenzene (*S*)-50ca



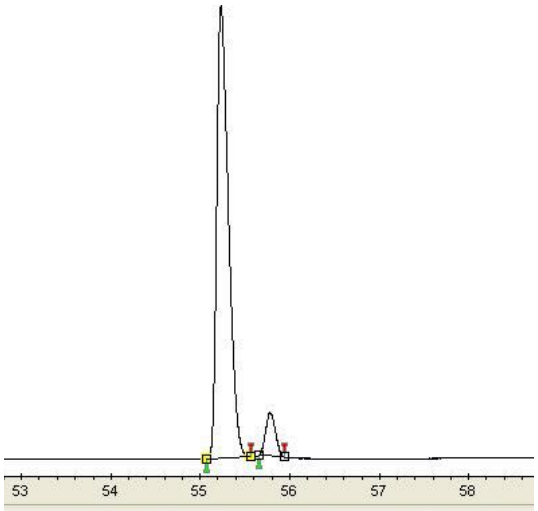
Prepared according to general procedure C from 5-(*tert*-butyl)-1-(cyclopenta-2,4-dien-1-ylidenemethyl)-2-methoxybenzene **51c** (72.0 mg, 0.3 mmol) to yield the crude product. Column chromatography (pentane/Et_2O, 4:1) afforded the title compound as a colourless oil (50.0 mg, 62%, 93:7 *er*). $\mathbf{R_f}$ = 0.70 (pentane/Et_2O, 4:1). The individual α/β tautomer (1.0 : 0.9 ratio) signals could not be uniquely identified and are referred to as tautomer 1 and tautomer 2 and integrated on this basis. **^{1}H NMR** (400.2 MHz, $CDCl_3$, 25 ^{o}C): 7.19-7.15 (m, 2 H, H-4' and H-6' both

tautomers), 6.83-6.77 (m, 1 H, H-3' both tautomers), 6.46-6.41 (m, 1 H Cp tautomer 1 or 2), 6.40-6.35 (m, 0.5 H, Cp tautomer 1 or 2), 6.27-6.22 (m, 1 H Cp tautomer 1 or 2), 6.10-6.07 (m, 0.5 H, Cp tautomer 1 or 2), 4.05-4.17 (m, 1 H, *CH*Et both tautomers), 3.81 (2 overlapping s, 3 H, O*Me* both tautomers), 3.00-2.97 (br, 0.9 H, CH_2 in Cp tautomer 2), 2.86-2.82 (br, 1 H, CH_2 in Cp tautomer 1), 2.05-1.80 (m, 2 H, CH_2Me both tautomers), 1.28 (2 overlapping s, C_4H_9-*Ar*, both tautomers), 0.90 (t, 1.4 H, *J* = 7.3 Hz, CH_2*Me* tautomer 2) *overlapped by* 0.89 (t, *J* = 7.3 Hz, 1.6 H, CH_2*Me* tautomer 1). **^{13}C NMR** (100.6 MHz, $CDCl_3$, 25 °C): δ 155.2 (*C*-O-Me tautomer 2), 155.1 (*C*-O-Me tautomer 1), 153.1 (Cp-*C*-CHEt tautomer 1), 150.1 (Cp-*C*-CHEt tautomer 1), 143.2 (Ar *C*-5' tautomer 1 or 2), 143.1 (Ar *C*-5' tautomer 1 or 2), 134.7 (Cp tautomer 1), 133.2 (Cp tautomer 2), 132.9 (Ar *C*-1' both tautomers), 132.3 (Cp tautomer 1), 130.8 (Cp tautomer 2), 126.5 (Ar *C*-4' or *C*-6' tautomer 1 or 2), 126.1 (Ar *C*-4' or *C*-6' tautomer 1 or 2), 125.5 (Ar *C*-4' or *C*-6' tautomer 1 or 2), 125.3 (Ar *C*-4' or *C*-6' tautomer 1 or 2), 123.3 (Cp tautomer 2), 123.2 (Cp tautomer 1), 110.2 (Ar *C*-3' both tautomers), 55.8 (O*Me* both tautomers), 42.6 (*C*H_2 in Cp tautomer 1 or 2), 41.1 (*C*H_2 in Cp tautomer 1 or 2), 41.0 (*C*HEt tautomer 1 or 2), 40.2 (*C*HEt tautomer 1 or 2), 34.2 (-*C*-C_3H_9, both tautomers), 31.7 (-C-*C*$_3$H$_9$, both tautomers), 28.0 (Me*C*H_2 tautomer 1), 27.5 (Me*C*H_2 tautomer 2), 12.7 (CH_2*Me* both tautomers) ppm. **IR** ($CHCl_3$): $\tilde{\nu}$ = 3011, 2964, 2905, 2874, 2837, 1606, 1500, 1464, 1394, 1364, 1296, 1246, 1178, 1136, 1108, 1079, 1035, 952, 890, 821 cm^{-1}. **HRMS** (EI+): calcd.

for $C_{19}H_{26}O$ $[M]^+$ 270.1984; found 270.1985. **GC**: (Chirasil-DEX-CB); T_{inj} = 250 °C, T_{det} = 280 °C, flow = 2.0 mL min^{-1}, t_i = 130 °C (50 min), t_f = 170 °C (5.0 °C min^{-1}): (*S*)-enantiomer: t_R = 55.2 min, (*R*)-enantiomer: t_R = 55.8 min. $[\alpha]_D^{25}$: +5.1 (*c* = 1.0 in $CHCl_3$).

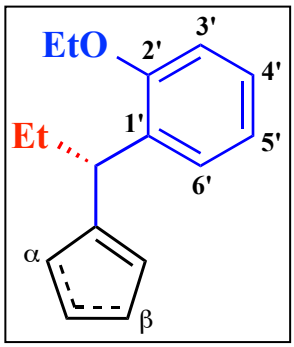


Time [Min]	Quantity [% Area]	Height [uV]	Area [uV.Min]	Area % [%]
55.20	49.80	84201.6	12050.1	49.800
55.67	50.20	86625.5	12146.6	50.200
	100.00	170827.0	24196.7	100.000



Time [Min]	Quantity [% Area]	Height [uV]	Area [uV.Min]	Area % [%]
55.23	92.52	96665.8	14580.9	92.525
55.78	7.48	9320.7	1178.1	7.475
	100.00	105986.5	15759.0	100.000

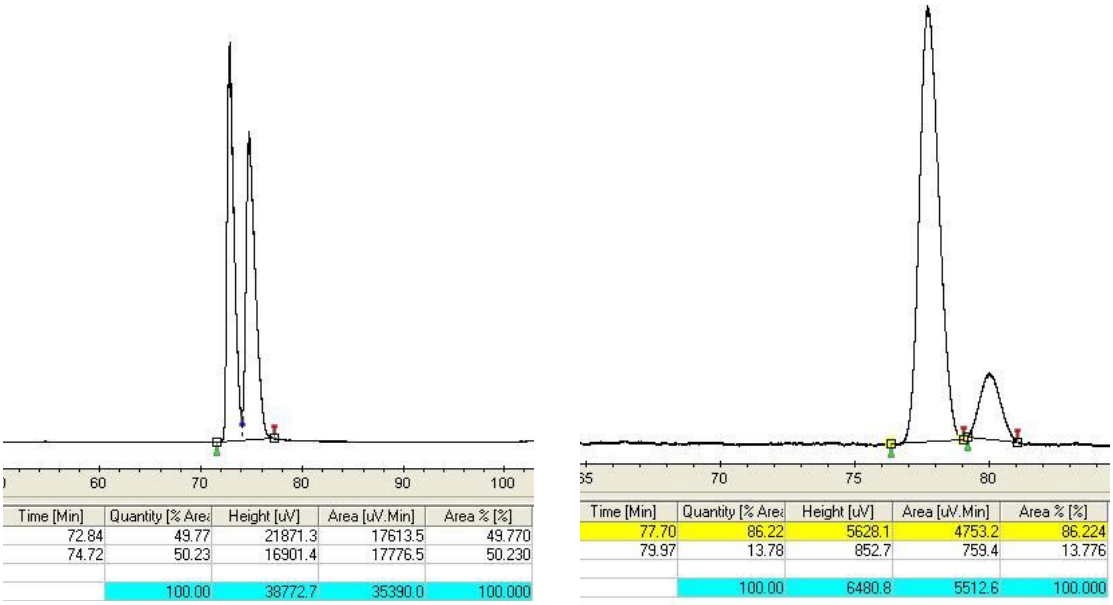
(*S*)-1-(1-(cyclopenta-1,3-dien-1-yl)propyl)-2-ethoxybenzene and (*S*)-1-(1-(cyclopenta-1,4-dien-1-yl)propyl)-2-ethoxybenzene (*S*)-50da



Prepared according to general procedure C from 1-(cyclopenta-2,4-dien-1-ylidenemethyl)-2-ethoxybenzene **51d** (59.0 mg, 0.3 mmol) to yield the crude product. Column chromatography (pentane/CH_2Cl_2, 8:1) afforded the title compound

as a colourless oil (45.0 mg, 62%, 86:14 *er*). $\mathbf{R_f}$ = 0.36 (pentane/CH_2Cl_2, 8:1). The individual α/β tautomer (0.8 : 1.1 ratio) signals could not be uniquely identified and are referred to as tautomer 1 and tautomer 2 and integrated on this basis. **^{1}H NMR** (400.2 MHz, $CDCl_3$, 25 ^{o}C): δ 7.16-7.07 (m, 2 H, H-4' and H-6' both tautomers), 6.91-6.81 (m, 2 H, H-3' and H-5' both tautomers), 6.44-6.33 (m, 1.5 H, Cp both tautomers), 6.27-6.20 (m, 0.8 H, Cp tautomer 1 or 2), 6.12-6.08 (m, 0.6 H, Cp tautomer 1 or 2), 4.18-4.10 (m, 1 H, *CH*Et both tautomers), 4.07-3.98 (m, 2 H, -O-C*H*$_2$Me both tautomers), 2.97-2.96 (br, 1.1 H, C*H*$_2$ in Cp tautomer 2), 2.82-2.80 (br, 0.8 H, C*H*$_2$ in Cp tautomer 1), 2.05-1.78 (m, 2 H, *CH*$_2$Me both tautomers), 1.41 (2 overlapping t, *J* = 7.0 Hz, 3 H, -O-CH$_2$*Me* both tautomers), 0.89 (t, 1.7 H, *J* = 7.3 Hz, -CH-CH$_2$*Me* tautomer 2) *overlapped by* 0.88 (t, *J* = 7.3 Hz, 1.3 H CH$_2$*Me* tautomer 1) ppm. **^{13}C NMR** (100.6 MHz, $CDCl_3$, 25 ^{o}C): δ 156.9 (*C*-O-Me tautomer 1 or 2), 156.7 (*C*-O-Me tautomer 1 or 2), 153.1 (Cp-*C*-CHEt tautomer 1 or 2), 150.2 (Cp-*C*-CHEt tautomer 1), 134.8 (Cp tautomer 2), 134.0 (Ar *C*-1' tautomer 1), 133.2 ((Ar *C*-1' tautomer 2), 133.2 (Cp tautomer 1), 132.3 (Cp tautomer 1), 130.9 (Cp tautomer 2), 128.2 (Ar *C*-4' or *C*-6' tautomer 1 or 2), 128.0 (Ar *C*-4' or *C*-6' tautomer 1 or 2), 126.9 (Ar *C*-4' or *C*-6' tautomer 1), 126.8 (Ar *C*-4' or *C*-6' tautomer 2), 126.3 (Cp tautomer 2), 125.8 (Cp tautomer 1), 120.6 (Ar *C*-5' both tautomers), 111.8 (Ar *C*-3' both tautomers), 63.9 (-O-*C*H$_2$Me both tautomers), 42.8 (*C*H$_2$ in Cp tautomer 2), 40.8 (*C*HEt tautomer 1), 41.1 (*C*H$_2$ in Cp tautomer 1), 40.0 (*C*HEt tautomer 2), 27.8 (Me*C*H$_2$ tautomer 2), 27.4 (Me*C*H$_2$ tautomer 1), 15.1 (-O-CH$_2$*Me* both tautomers), 12.7 (-CH-CH$_2$*Me* both tautomers) ppm. **IR** ($CHCl_3$): $\tilde{\nu}$ = 3072, 3007, 2967, 2932, 2876, 1597, 1491, 1477, 1451, 1392, 1368, 1341, 1288, 1242, 1160, 1122, 1078, 1048, 985, 951, 928, 902, 826. **HRMS** (EI+): calcd. for $C_{16}H_{20}O$ $[M]^+$ 228.1514; found 228.1513. **GC**: (Chirasil-DEX-CB); T_{inj} = 250 ^{o}C, T_{det} = 280 ^{o}C, flow = 2.0

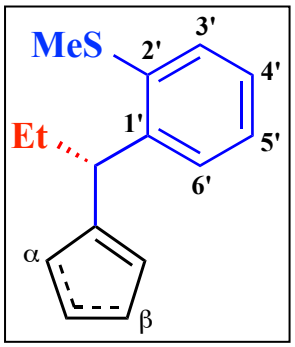
mL min^{-1}, t_i = 110 °C (100 min), t_f = 170 °C (10.0 °C min^{-1}): (*S*)-enantiomer: t_R = 77.7 min, (*R*)-enantiomer: t_R = 80.0 min. $[\alpha]_D^{25}$: -32.1 (*c* = 1.0 in $CHCl_3$).



Time [Min]	Quantity [% Area]	Height [uV]	Area [uV.Min]	Area % [%]
72.84	49.77	21871.3	17613.5	49.770
74.72	50.23	16901.4	17776.5	50.230
	100.00	38772.7	35390.0	100.000

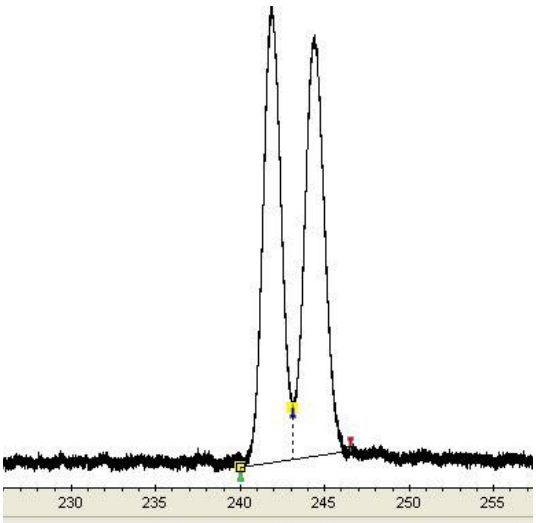
Time [Min]	Quantity [% Area]	Height [uV]	Area [uV.Min]	Area % [%]
77.70	86.22	5628.1	4753.2	86.224
79.97	13.78	852.7	759.4	13.776
	100.00	6480.8	5512.6	100.000

(*S*)-1-(1-(cyclopenta-1,3-dien-1-yl)propyl)-2-(methylthio)benzene and (*S*)-1-(1-(cyclopenta-1,4-dien-1-yl)propyl)-2--(methylthio)benzene (*S*)-50ea

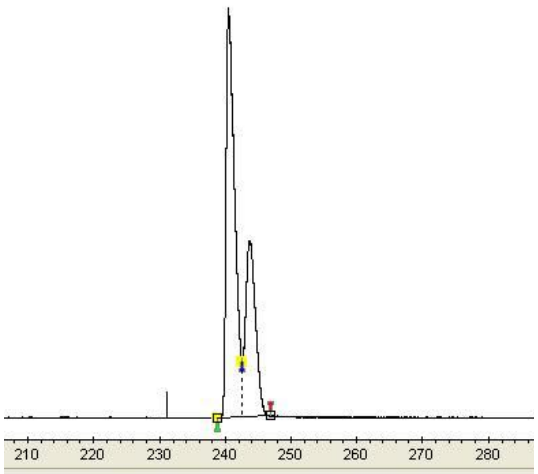


Prepared according to general procedure C from 1-(cyclopenta-2,4-dien-1-ylidenemethyl)-2-(methylthio)benzene **51e** (60.0 mg, 0.3 mmol) to yield the crude product. Column chromatography (pentane/CH_2Cl_2, 3:1) afforded the title compound as a colourless oil (29.0 mg, 42 %, 66:34 *er*). $\mathbf{R_f}$= 0.58 (pentane/CH_2Cl_2, 3:1). The individual α/β tautomer (0.7 : 1.3 ratio) signals could not be uniquely identified and are referred to as tautomer 1 and tautomer 2 and integrated on this basis. **^{1}H NMR**

(400.2 MHz, $CDCl_3$, 25 °C): δ 7.26-7.08 (m, 4 H, Ar both tautomers), 6.44-6.35 (m, 1.6 H, Cp tautomer 1 or 2), 6.28-6.22 (m, 0.6 H, Cp tautomer 1 or 2), 6.12-6.08 (m, 0.7 H, Cp tautomer 1 or 2), 4.25-4.12 (m, 1 H, *CH*Et both tautomers), 3.01-2.95 (m, 1.3 H, C*H*$_2$ in Cp tautomer 2), 2.89-2.75 (m, 0.7 H, C*H*$_2$ in Cp tautomer 1), 2.45 (2 x s, S-*Me* both tautomers), 2.09-1.80 (m, 2 H, *CH*$_2$Me both tautomers), 0.89 (t, *J* = 7.3 Hz, 2 H -CH$_2$*Me* tautomer 2) *overlapped by* 0.90 (t, *J* = 7.3 Hz, 1 H CH$_2$*Me* tautomer 1) ppm. **^{13}C NMR** (100.6 MHz, $CDCl_3$, 25 °C): δ 152.1 (Cp-*C*-CHEt tautomer 1), 149.5 (Cp-*C*-CHEt tautomer 2), 143.5 (*C*-S-Me, or Ar *C*-1' tautomer 1), 142.8 (*C*-S-Me, or Ar *C*-1' tautomer 2), 137.6 (C-S-Me, or Ar *C*-1' tautomer 2), 137.5 (*C*-S-Me, or Ar *C*-1' tautomer 1), 134.4 (Cp tautomer 2), 133.6 (Cp tautomer 2), 132.2 (Cp tautomer 1), 131.3 (Cp tautomer 1), 127.4 (Ar *C*-4' or *C*-6' tautomer 2), 127.2 (Ar *C*-4' or *C*-6' tautomer 1), 127.0 (Ar *C*-4' or *C*-6' tautomer 1), 126.7 (Ar *C*-4' or *C*-6' tautomer 2), 126.6 (Cp tautomer 2), 126.5 (Cp tautomer 1), 126.4 (Ar *C*-5' tautomer 1), 126.3 (Ar *C*-5' tautomer 2), 125.5 (Ar *C*-3' tautomer 1), 125.4 (Ar *C*-3' tautomer 2), 63.9 (-O-*C*H$_2$Me both tautomers), 44.6 (*C*HEt tautomer 1), 43.7 (*C*HEt tautomer 2), 42.6 (*C*H$_2$ in Cp tautomer 1), 41.2 (*C*H$_2$ in Cp tautomer 2), 28.5 (Me*C*H$_2$ tautomer 1), 27.9 (Me*C*H$_2$ tautomer 2), 16.6 (S-*Me* both tautomers), 12.6 (CH$_2$*Me* both tautomers) ppm. **IR** ($CHCl_3$): $\tilde{\nu}$ = 3062, 3008, 2965, 2927, 2876, 1619, 1587, 1467, 1439, 1366, 1242, 1085, 1042, 968, 952, 890 cm^{-1}. **HRMS** (EI+): calcd. for $C_{15}H_{18}S$ $[M]^+$ 230.1129; found 230.1126. **GC**: (Chirasil-DEX-CB); T_{inj} = 250 °C, T_{det} = 280 °C, flow = 2.0 mL min^{-1}, t_i = 100 °C (120 min), t_f = 130 °C (0.1 °C min^{-1}): (*S*)-enantiomer: t_R = 240.4 min, (*R*)-enantiomer: t_R = 243.6 min. **$[\alpha]_D^{25}$**: -32.3 (c = 1.0 in $CHCl_3$).

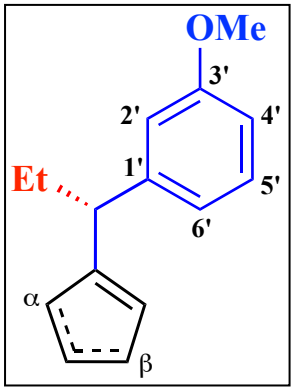


Time [Min]	Quantity [% Area]	Height [uV]	Area [uV.Min]	Area % [%]
241.87	50.02	769.7	962.3	50.01
244.38	49.98	705.1	961.6	49.98
	100.00	1474.8	1923.9	100.00



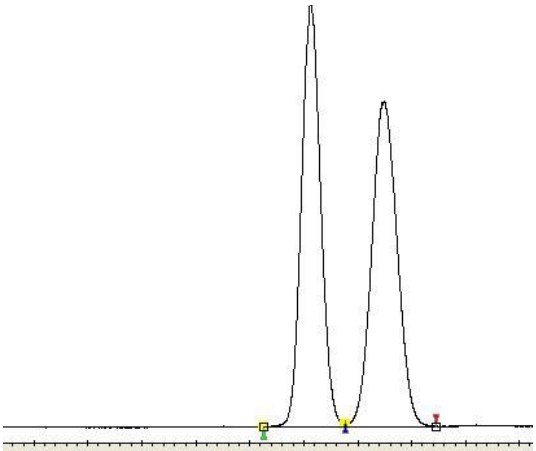
Time [Min]	Quantity [% Area]	Height [uV]	Area [uV.Min]	Area % [%]
240.43	66.22	8496.0	12789.8	66.219
243.64	33.78	3652.7	6524.7	33.781
	100.00	12148.7	19314.5	100.000

(*S*)-1-(1-(cyclopenta-1,3-dien-1-yl)propyl)-3-methoxybenzene and (*S*)-1-(1-(cyclopenta-1,4-dien-1-yl)propyl)-3-methoxybenzene (*S*)-50fa

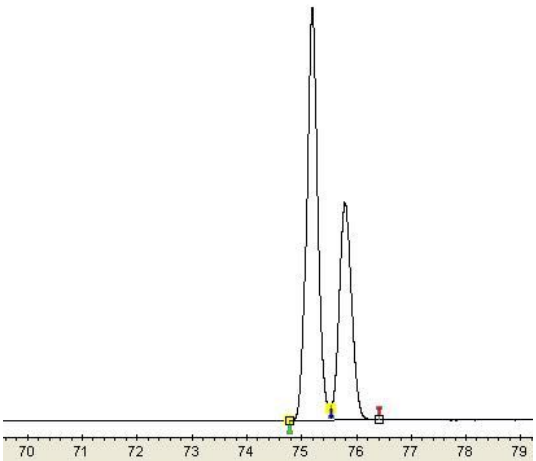


Prepared according to general procedure C from 1-(cyclopenta-2,4-dien-1-ylidenemethyl)-3-methoxybenzene **51f** (55.0 mg, 0.3 mmol) to yield the crude product. Column chromatography (pentane/CH_2Cl_2, 2:1) afforded the title compound as a colourless oil (35.0 mg, 54 %, 63:37 *er*). $\mathbf{R_f}$= 0.62 (pentane/CH_2Cl_2, 2:1). The individual α/β tautomer (1.0 : 1.0 ratio) signals could not be uniquely identified and are referred to as tautomer 1 and tautomer 2 and integrated on this basis. **^{1}H NMR**

(400.2 MHz, $CDCl_3$, 25 °C): δ 7.23-7.17 (m, 1 H, H-5'), 6.82-6.70 (m, 3 H, H-4', H-6' and H-2'), 6.44-6.40 (m, 0.5 H, Cp tautomer 1 or 2), 6.40-6.36 (m, 0.9 H, Cp tautomer 1 or 2), 6.28-6.22 (m, 1.0 H, Cp tautomer 1 or 2), 6.11-6.08 (m, 0.5 H Cp tautomer 1 or 2), 3.79 (2 overlapping s, 3 H, O*Me* both tautomers), 3.57-3.46 (m, 1.0 H, *CH*Et both tautomers), 2.99-2.96 (m, 1 H, C*H*$_2$ in Cp tautomer 2), 2.81-2.78 (m, 1 H, C*H*$_2$ in Cp tautomer 1), 2.06-1.78 (m, 2 H, *CH*$_2$Me both tautomers), 0.90 (t, 1.4 H, J = 7.3 Hz, CH_2*Me* tautomer 2) *overlapped by* 0.87 (t, 1.6 H, J = 7.3 Hz, CH_2*Me* tautomer 1) ppm. **^{13}C NMR** (100.6 MHz, $CDCl_3$, 25 °C): δ 159.6 (*C*-O-Me both tautomers), 152.6 (Cp-*C*-CHEt tautomer 2), 149.9 (Cp-*C*-CHEt tautomer 2), 146.8 (Ar *C*-1' tautomer 2), 146.1 (Ar *C*-1' tautomer 1), 134.0 (Cp tautomer 2), 133.6 (Cp tautomer 1), 132.1 (Cp tautomer 2), 131.2 (Cp tautomer 1), 129.2 (Ar C-5' both tautomers), 126.4 (Cp tautomer 1), 125.9 (Cp tautomer 2), 120.6 (Ar *C*-6' tautomer 2), 120.4 (Ar *C*-6' tautomer 1), 114.1 (Ar *C*-2' tautomer 1), 113.9 (Ar *C*-2' tautomer 2), 111.0 (Ar *C*-4' both tautomers), 55.1 (O*Me* both tautomers), 49.4 (*C*HEt tautomer 1), 48.4 (*C*HEt tautomer 2), 42.3 (*C*H$_2$ in Cp tautomer 1), 41.1 (*C*H$_2$ in Cp tautomer 2), 28.3 (Me*C*H$_2$ tautomer 2), 27.8 (Me*C*H$_2$ tautomer 1), 12.6 (CH_2*Me* both tautomers) ppm. **IR** ($CHCl_3$): $\tilde{\nu}$ = 3011, 2964, 2934, 2875, 2838, 1599, 1584, 1489, 1465, 1454, 1436, 1365, 1315, 1259, 1151, 1049, 997, 952, 890 cm^{-1}. **HRMS** (EI+): calcd. for $C_{15}H_{18}O$ $[M]^+$ 214.1358; found 214.1356. **GC:** (Chirasil-DEX-CB); T_{inj} = 250 °C, T_{det} = 280 °C, flow = 2.0 mL min^{-1}, t_i = 100 °C (40 min), t_f = 160 °C (1.0 °C min^{-1}): (*S*)-enantiomer: t_R = 75.2 min, (*R*)-enantiomer: t_R = 75.8 min. **$[\alpha]_D^{25}$:** -9.7 (*c* = 0.5 in $CHCl_3$).

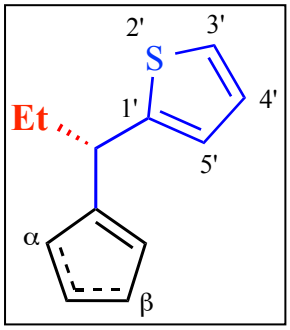


Time [Min]	Quantity [% Area]	Height [uV]	Area [uV.Min]	Area % [%]
75.56	49.64	9939.8	2039.6	49.642
76.24	50.36	7597.5	2069.0	50.358
	100.00	17537.2	4108.6	100.000



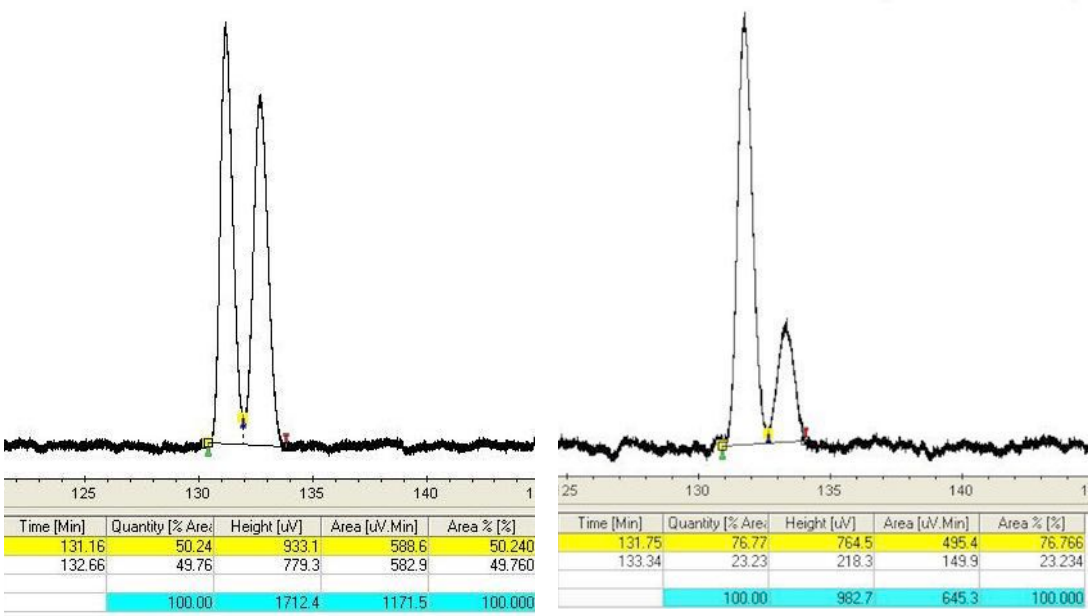
Time [Min]	Quantity [% Area]	Height [uV]	Area [uV.Min]	Area % [%]
75.20	62.81	20301.7	4716.6	62.813
75.78	37.19	10739.9	2792.3	37.187
	100.00	31041.6	7508.8	100.000

(*S*)-1-(1-(cyclopenta-1,3-dien-1-yl)propyl)-2-thiophene and (*S*)-1-(1-(cyclopenta-1,3-dien-1-yl)propyl)-2-thiophene (*S*)-50ga

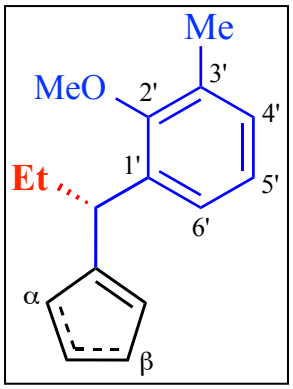


Prepared according to general procedure C from 1-(cyclopenta-2,4-dien-1-ylidenemethyl)-2-thiophene **51g** (57.0 g, 0.3 mmol) to yield the crude product. Column chromatography (pentane/CH_2Cl_2, 19:1) afforded the title compound as a colourless oil (17.0 mg, 30 %, 77:23 *er*). $\mathbf{R_f}$ = 0.46 (pentane/CH_2Cl_2, 19:1). The individual α/β tautomer (0.7 : 1.3 ratio) signals could bnot be uniquely identified and are referred to as tautomer 1 and tautomer 2 and integrated on this basis. **^{1}H NMR** (400.2 MHz, $CDCl_3$, 25 ^oC): δ 7.16-7.11 (m, 1 H, H-3' or H-5'), 6.96-6.90 (m, 1 H, H-4'), 6.85-6.80 (m, 1 H, H-3' or H-5'), 6.50-6.40 (m, 1.5 H, Cp both tautomers),

6.33-6.26 (m, 0.7 H, Cp both tautomers), 6.17-6.12 (m, 0.6 H, Cp tautomer 2), 3.96-3.82 (m, 1.0 H, *CH*Et both tautomers), 3.03-2.97 (br, 1.3 H, C*H*$_2$ in Cp tautomer 2), 2.90-2.87 (br, 0.7 H, C*H*$_2$ in Cp tautomer 1), 2.05-1.89 (m, 2 H, *CH*$_2$Me both tautomers), 0.93 (2 overlapping t, *J* = 7.4 Hz, 3 H, CH$_2$*Me* both tautomers) ppm. **^{13}C NMR** (100.6 MHz, $CDCl_3$, 25 ^{o}C): δ 151.9 (Cp-*C*-CHEt or Het Ar *C*-1' tautomer 1), 149.6 (Cp-*C*-CHEt or Het Ar *C*-1' tautomer 1), 149.5 (Cp-*C*-CHEt or Het Ar *C*-1' tautomer 2), 148.8 (Cp-*C*-CHEt or Het Ar *C*-1' tautomer 2), 134.0 (Cp tautomer 2), 133.4 (Cp tautomer 2), 132.1 (Cp tautomer 1), 131.6 (Cp tautomer 1), 127.4 (Cp tautomer 1), 126.7 (Cp tautomer 2), 126.6 (Het Ar *C*-4' both tautomers), 124.0 (Het Ar *C*-3' or *C*-5' tautomer 2), 123.7 Het Ar *C*-3' or *C*-5' tautomer 1), 123.3 (Het Ar *C*-3' or *C*-5' tautomer 2), 123.2 (Het Ar *C*-3' or *C*-5' tautomer 1), 44.4 (*C*HEt tautomer 1), 43.6 (*C*HEt tautomer 2), 41.7 (*C*H$_2$ in Cp tautomer 1), 41.2 (*C*H$_2$ in Cp tautomer 2), 29.9 (Me*C*H$_2$ tautomer 1), 29.3 (Me*C*H$_2$ tautomer 2), 12.7 (CH$_2$*Me* tautomer 1), 12.6 (CH$_2$*Me* tautomer 2) ppm. **IR** ($CHCl_3$): $\tilde{\nu}$ = 3116, 3073, 3007, 2966, 2932, 2902, 2875, 2733, 2451, 2366, 2345, 1793, 1719, 1686, 1655, 1638, 1602, 1560, 1542, 1524, 1509, 1460, 1438, 1368, 1303, 1262 cm^{-1}. **HRMS** (EI+): calcd. for $C_{15}H_{18}O$ $[M]^+$ 190.0816; found 190.0807. **GC:** (Chirasil-DEX-CB); T_{inj} = 250 ^{o}C, T_{det} = 280 ^{o}C, flow = 2.0 mL min^{-1}, t_i = 70 ^{o}C ramp at 0.2 ^{o}C min^{-1} t_f = 130 ^{o}C: (*S*)-enantiomer: t_R = 131.8 min, (*R*)-enantiomer: t_R = 133.3 min. **$[\alpha]_D^{25}$:** +22.1 (*c* = 1.0 in $CHCl_3$).

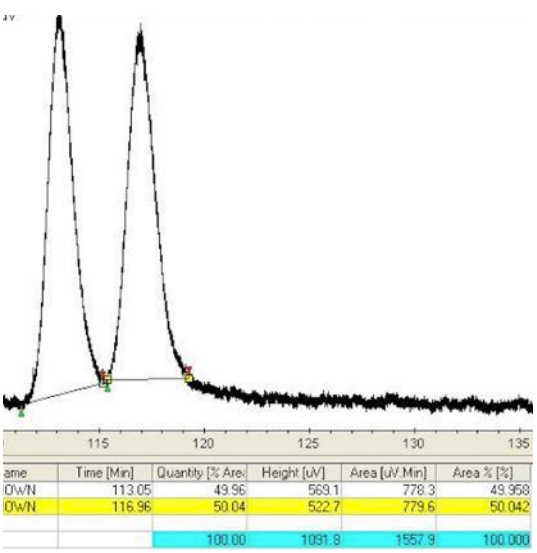


(*S*)-1-(1-(cyclopenta-1,3-dien-1-yl)propyl)-2-methoxy-3-methylbenzene and (*S*)-1-(1-(cyclopenta-1,4-dien-1-yl)propyl)-2-methoxy-3-methylbenzene (*S*)-50ha

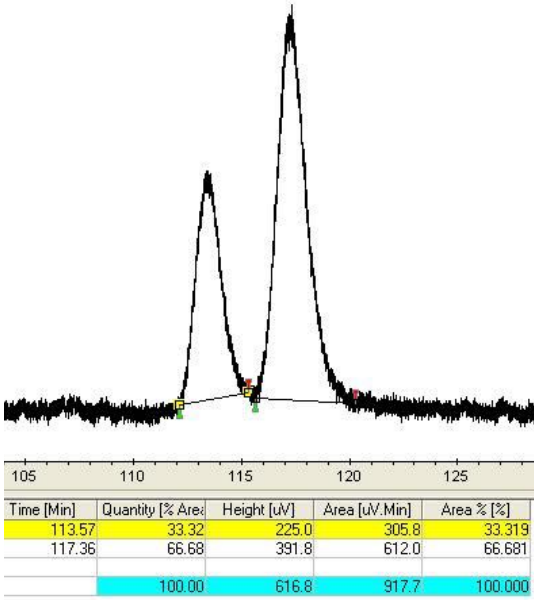


Prepared according to general procedure C from 1-(cyclopenta-2,4-dien-1-ylidenemethyl)-2-methoxy-3-methylbenzene **51h** (59.0 mg, 0.3 mmol) to yield the crude product. Column chromatography (pentane/Et_2O, 9:1) afforded the title compound as a colourless oil (30.0 mg, 43%, 67:33 *er*). $\mathbf{R_f}$ = 0.64 (pentane/Et_2O, 9:1). The individual α/β tautomer (1.2 : 0.8 ratio) signals could not be uniquely identified and are referred to as tautomer 1 and tautomer 2 and integrated on this basis. **^{1}H NMR** (400.2 MHz, $CDCl_3$, 25 ^{o}C): δ 7.08-6.95 (m, 3 H, H-4', H-5' and H-

6'), 6.46-6.35 (m, 1.3 H, Cp tautomer 1 or 2), 6.34-6.11 (m, 1.4 H, Cp tautomer 1 or 2), 6.07-6.01 (m, 0.4 H, Cp tautomer 1 or 2), 4.11-4.01 (m, 1 H, *CH*Et both tautomers), 3.72 (2 overlapping s, 3 H, O*Me* both tautomers), 2.99-2.93 (m, 0.8 H, C*H*$_2$ in Cp tautomer 2), 2.92-2.76 (m, 1.2 H, C*H*$_2$ in Cp tautomer 1), 2.32 (s, 3 H, Ar-C*H*$_3$), 2.08-1.74 (m, 2 H, *CH*$_2$Me both tautomers), 0.89 (t, 1.2 H, *J* = 7.3 Hz, CH$_2$*Me* tautomer 2) *overlapped by* 0.87 (t, 1.8 H, *J* = 7.3 Hz, CH$_2$*Me* tautomer 1) ppm. **^{13}C NMR** (100.6 MHz, $CDCl_3$, 25 ^{o}C): δ 156.8 (*C*-O-Me tautomer 2), 156.7 (*C*-O-Me tautomer 1), 153.1 (Cp-*C*-CHEt tautomer 1), 150.5 (Cp-*C*-CHEt tautomer 2), 138.0 (Ar *C*-1' tautomer 1), 137.3 (Ar *C*-1' tautomer 2), 134.4 (Cp tautomer 2), 133.6 (Cp tautomer 2), 132.2 (Cp tautomer 1), 131.1 (Cp tautomer 1), 131.0 (Ar *C*-3'-CH_3 both tautomers), 129.1 (Ar *C*-4' or *C*-6' tautomer 1), 129.0 (Ar *C*-4' or *C*-6' tautomer 1), 126.7 (Cp tautomer 1), 126.2 (Cp tautomer 2), 126.1 (Ar *C*-4' or *C*-6' tautomer 2), 126.0 (Ar *C*-4' or *C*-6' tautomer 1), 124.2 (Ar *C*-5' tautomer 1), 124.1 (Ar *C*-5' tautomer 2), 60.9 (O*Me* tautomer 1), 60.8 (O*Me* tautomer 2), 42.6 (*C*H$_2$ in Cp tautomer 1), 41.2 (*C*H$_2$ in Cp tautomer 2), 41.1 (*C*HEt tautomer 1), 40.3 (*C*HEt tautomer 2), 28.8 (Me*C*H$_2$ tautomer 1), 28.2 (Me*C*H$_2$ tautomer 2), 16.6 (Ar-*C*H$_3$ both tautomers), 12.8 (CH$_2$*Me* both tautomers) ppm. **IR** ($CHCl_3$): $\tilde{\nu}$ = 3065, 3011, 2964, 2935, 2875, 2828, 1602, 1467, 1423, 1366, 1334, 1253, 1168, 1093, 1011, 952, 899, 875, 821 cm^{-1}. **HRMS** (EI+): calcd. for $C_{16}H_{22}O$ $[M]^+$ 228.1514; found 228.1523. **GC:** (Astec CHIRALDEX B-TA); T_{inj} = 250 ^{o}C, T_{det} = 280 ^{o}C, flow = 2.0 mL min^{-1}, t_i = 70 ^{o}C ramp at 0.2 ^{o}C min^{-1} t_f = 130 ^{o}C: (*R*)-enantiomer: t_R = 113.6 min, (*S*)-enantiomer: t_R = 117.4 min. **$[\alpha]_D^{25}$:** -28.9 (*c* = 1.0 in $CHCl_3$).

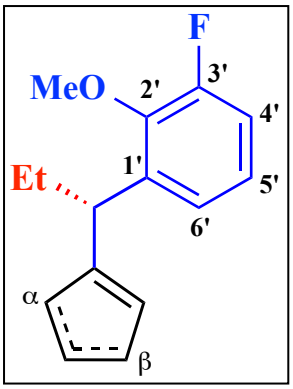


ame	Time [Min]	Quantity [% Area]	Height [uV]	Area [uV.Min]	Area % [%]
OWN	113.05	49.96	569.1	778.3	49.958
OWN	116.96	50.04	522.7	779.6	50.042
		100.00	1091.8	1557.9	100.000



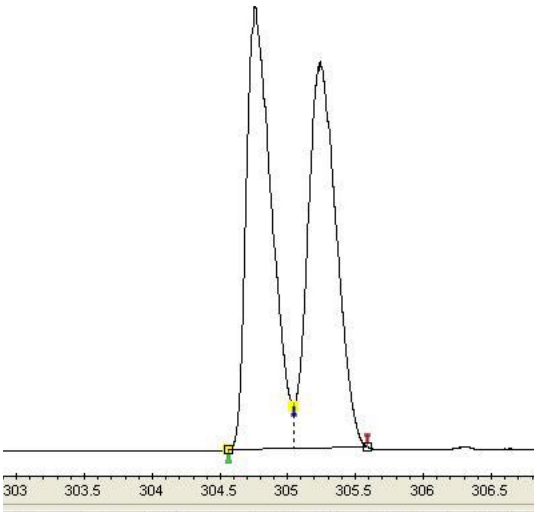
Time [Min]	Quantity [% Area]	Height [uV]	Area [uV.Min]	Area % [%]
113.57	33.32	225.0	305.8	33.319
117.36	66.68	391.8	612.0	66.681
	100.00	616.8	917.7	100.000

(*S*)-1-(1-(cyclopenta-1,3-dien-1-yl)propyl)-3-fluoro-2-methoxybenzene and (*S*)-1-(1-(cyclopenta-1,4-dien-1-yl)propyl)-3-fluoro-2-methoxybenzene (*S*)-50ia

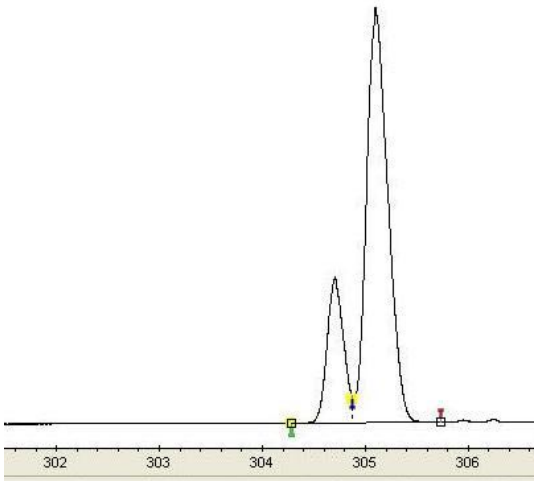


Prepared according to general procedure C from 1-(cyclopenta-2,4-dien-1-ylidenemethyl)-3-fluoro-2-methoxybenzene **51i** (61.0 mg, 0.3 mmol) to yield the crude product. Column chromatography afforded the title compound as a colourless oil (27.0 mg, 39%, 79:21 *er*). $\mathbf{R_f}$ = 0.50 (pentane/CH_2Cl_2, 4:1). The individual α/β tautomer (1.1 : 0.9 ratio) signals could not be uniquely identified and are referred to as tautomer 1 and tautomer 2 and integrated on this basis. **^{1}H NMR** (400.2 MHz, $CDCl_3$, 25 ^{o}C): δ 6.97-6.87 (m, 3 H, H-4', H-5' and H-6'), 6.44-6.36 (m, 1.3 Cp tautomer 1 or 2), 6.26-6.23 (m, 1.0 H, Cp tautomer 1 or 2), 6.09-6.05 (m, 0.4 H, Cp

tautomer 1 or 2), 4.13-4.03 (m, 1 H, *CH*Et both tautomers), 3.89-3.85 (m, 3 H, O*Me* both tautomers), 2.99-2.95 (m, 0.9 H, C*H*$_2$ in Cp tautomer 2), 2.88-2.74 (m, 1.1 H, C*H*$_2$ in Cp tautomer 1), 2.07-1.75 (m, 2 H, *CH*$_2$Me both tautomers), 0.88 (t, 1.4 H, *J* = 7.3 Hz, CH$_2$*Me* tautomer 2) *overlapped by* 0.87 (t, 1.6 H, *J* = 7.2 Hz, CH$_2$*Me* tautomer 1) ppm. **^{13}C NMR** (100.6 MHz, $CDCl_3$, 25 ^{o}C): δ 155.9 (d, *J* = 246 Hz, C-F both tautomers), 152.4 (Cp-*C*-CHEt tautomer 1), 149.9 (Cp-*C*-CHEt tautomer 2), 145.9 (d, *J* = 10.5 Hz, *C*-O-Me tautomer 2), 145.7 (d, *J* = 10.5 Hz, *C*-O-Me tautomer 1), 139.9 (d, *J* = 1.7 Hz, Ar C-1' tautomer 1), 139.3 (d, *J* = 1.7 Hz, Ar C-1' tautomer 2), 134.3 (Cp tautomer 2), 133.7 (Cp tautomer 2), 132.2 (Cp tautomer 1), 131.2 (Cp tautomer 1), 126.8 (Cp tautomer 1), 126.2 (Cp tautomer 2), 123.6-123.8 (m, Ar *C*-5' both tautomers), 123.5 (d, *J* = 3.1 Hz, Ar *C*-6' tautomer 2), 123.3 (d, *J* = 3.1 Hz, Ar *C*-6' tautomer 1), 114.4 (d, *J* = 19.3 Hz, Ar *C*-4' tautomer 2), 114.3 (d, *J* = 19.3 Hz, Ar *C*-4' tautomer 1), 61.5 (app. t, O*Me* both tautomers), 42.6 (*C*H$_2$ in Cp tautomer 1), 41.2 (*C*H$_2$ in Cp tautomer 2), 41.1 (d, *J* = 2.3 Hz, *C*HEt tautomer 1), 40.4 (d, *J* = 2.3 Hz, *C*HEt tautomer 2), 28.1 (Me*C*H$_2$ tautomer 1), 27.6 (Me*C*H$_2$ tautomer 2), 12.7 (CH$_2$*Me* both tautomers) ppm. **^{19}F NMR** (376.6 MHz, $CDCl_3$) δ = -130.48 ppm. **IR** ($CHCl_3$): $\tilde{\nu}$ = 3065, 3009, 2966, 2936, 2903, 2876, 2837, 2734, 1603, 1585, 1521, 147, 1434, 1366, 1327, 1273, 1173, 1104, 1063, 1035, 1008, 961, 896, 880, 821 cm^{-1}. **HRMS** (EI+): calcd. for $C_{15}H_{17}OF$ $[M]^+$ 232.1263; found 232.1263. **GC:** (Chirasil-DEX-CB); T_{inj} = 250 ^{o}C, T_{det} = 280 ^{o}C, flow = 2.1 mL min^{-1}, t_i = 80 ^{o}C ramp at 3.0 ^{o}C min^{-1} to 130 ^{o}C, then ramp at 10.0 ^{o}C min^{-1} t_f = 150 ^{o}C: (*R*)-enantiomer: t_R = 304.7 min, (*S*)-enantiomer: t_R = 305.1 min. **$[\alpha]_D^{25}$:** -26.3 (*c* = 1.0 in $CHCl_3$).

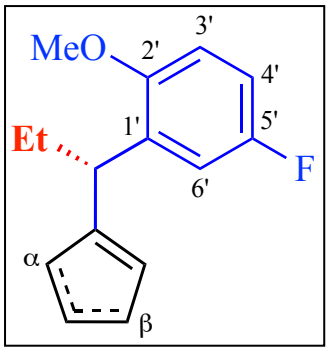


Time [Min]	Quantity [% Area]	Height [uV]	Area [uV.Min]	Area % [%]
304.76	50.31	24596.6	5258.0	50.313
305.24	49.69	21390.5	5192.6	49.687
	100.00	45987.1	10450.6	100.000



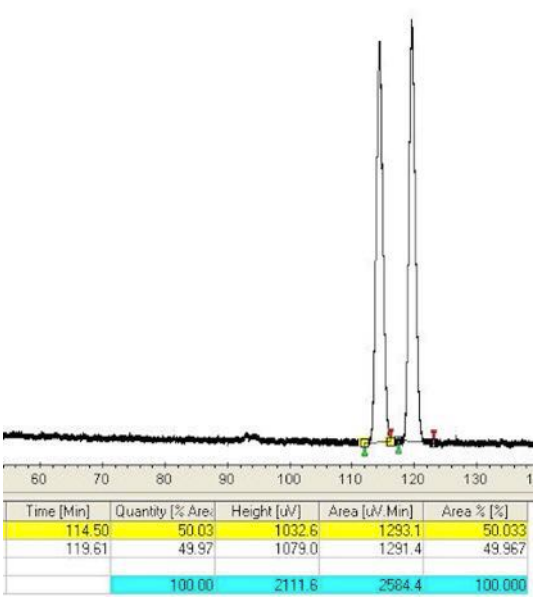
Time [Min]	Quantity [% Area]	Height [uV]	Area [uV.Min]	Area % [%]
304.71	21.21	7014.6	1289.7	21.208
305.10	78.79	20029.7	4791.6	78.792
	100.00	27044.4	6081.3	100.000

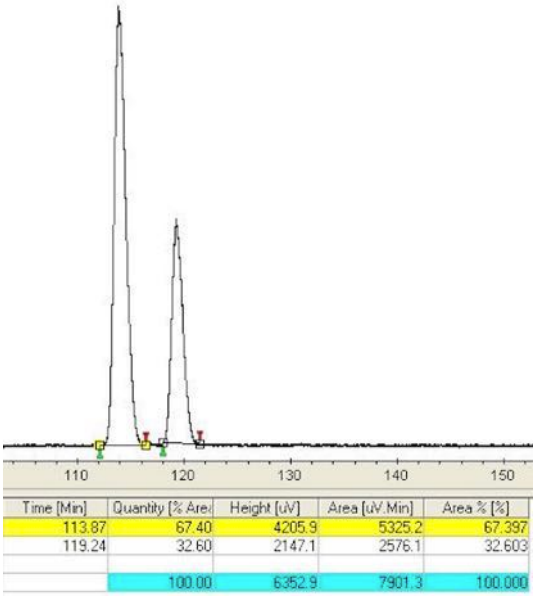
(*S*)-1-(1-(cyclopenta-1,3-dien-1-yl)propyl)-5-fluoro-2-methoxybenzene and (*S*)-1-(1-(cyclopenta-1,4-dien-1-yl)propyl)-5-fluoro-2-methoxybenzene (*S*)-50ja



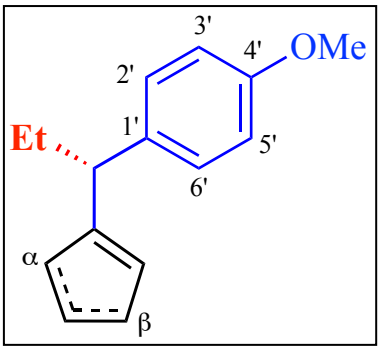
Prepared according to general procedure C from 1-(cyclopenta-2,4-dien-1-ylidenemethyl)-5-fluoro-2-methoxybenzene **51j** (61.0 mg, 0.3 mmol) to yield the crude product. Column chromatography (pentane/CH_2Cl_2, 4:1) afforded the title compound as a colourless oil (49.0 mg, 69%, 67:33 *er*). $\mathbf{R_f}$ = 0.48 (pentane/CH_2Cl_2, 4:1). The individual α/β tautomer (0.9 : 1.1 ratio) signals could not be uniquely identified and are referred to as tautomer 1 and tautomer 2 and integrated on this basis.

^{1}H NMR (400.2 MHz, $CDCl_3$, 25 ^{o}C): δ 6.87-6.72 (m, 3 H, H-3', H-4' and H-6'), 6.45-6.34 (m, 1.5 Cp tautomer 1 or 2), 6.28-6.23 (m, 0.9 H, Cp tautomer 1 or 2), 6.12-6.06 (m, 0.5 H, Cp tautomer 1 or 2), 4.15-4.06 (m, 1 H, *CH*Et both tautomers), 3.81 (s, 1.6 H, OMe tautomer 2), 3.80 (s, 1.4 H, OMe tautomer 1), 3.02-2.95 (m, 1.1 H, C*H*$_2$ in Cp tautomer 2), 2.83-2.77 (m, 0.9 H, C*H*$_2$ in Cp tautomer 1), 2.02-1.72 (m, 2 H, *CH*$_2$Me both tautomers), 0.89 (t, 1.6 H, *J* = 7.3 Hz, CH_2*Me* tautomer 2) *overlapped by* 0.88 (t, 1.4 H, *J* = 7.2 Hz, CH_2*Me* tautomer 1) ppm. **^{13}C NMR** (100.6 MHz, $CDCl_3$, 25 ^{o}C): δ 155.9 (d, *J* = 238 Hz, C-F both tautomers), 153.5 (d, *J* = 2.3 Hz, *C*-O-Me tautomer 2), 153.3 (d, *J* = 2.3 Hz, *C*-O-Me tautomer 1), 151.9 (Cp-*C*-CHEt tautomer 1), 149.3 (Cp-*C*-CHEt tautomer 2), 135.6 (d, *J* = 6.8 Hz, Ar C-1' tautomer 1), 135.0 (d, *J* = 6.8 Hz, Ar C-1' tautomer 2), 134.4 (Cp tautomer 2), 133.5 (Cp tautomer 2), 132.1 (Cp tautomer 1), 131.0 (Cp tautomer 1), 126.7 (Cp tautomer 1), 126.2 (Cp tautomer 2), 114.8 (t, Ar *C*-4' or C-6' both tautomers), 112.7 (d, *J* = 4.6 Hz, C-5' tautomer 1), 112.5 (d, *J* = 4.6 Hz, C-5' tautomer 2), 111.6 (m, Ar *C*-4' or C-6' both tautomers), 56.2 (O*Me* both tautomers), 42.6 (*C*H_2 in Cp tautomer 1), 41.2 (*C*H_2 in Cp tautomer 2), 41.1 (*C*HEt tautomer 1), 40.4 (*C*HEt tautomer 2), 27.8 (Me*C*H_2 tautomer 1), 27.3 (Me*C*H_2 tautomer 2), 12.5 (CH_2*Me* tautomer 1), 12.4 (CH_2*Me* tautomer 2) ppm. **^{19}F NMR** (376.6 MHz, $CDCl_3$) δ = -123.72 ppm. **IR** ($CHCl_3$): $\tilde{\nu}$ = 3065, 3009, 2965, 2934, 2876, 2837, 1599, 1495, 1465, 1442, 1424, 1368, 1340, 1273, 1242, 1178, 1148, 1109, 1075, 1035, 955, 900, 876, 821 cm^{-1}. **HRMS** (EI+): calcd. for $C_{15}H_{17}OF$ $[M]^+$ 232.1263; found 232.1263. **GC:** (Chirasil-DEX-CB); T_{inj} = 250 ^{o}C, T_{det} = 280 ^{o}C, flow = 2.0 mL min^{-1} t_i = 100 ^{o}C (150 min), t_f = 170 ^{o}C (1.0 ^{o}C min^{-1}): (*S*)-enantiomer: t_R = 113.7 min, (*R)*-enantiomer: t_R = 119.2 min. **$[\alpha]_D^{25}$:** -21.9 (*c* = 1.0 in $CHCl_3$).





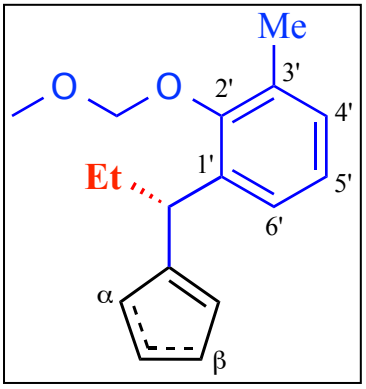
(*S*)-1-(1-(Cyclopenta-1,3-dien-1-yl)propyl)-4-methoxybenzene and (*S*)-1-(1-(cyclopenta-1,4-dien-1-yl)propyl)-4-methoxybenzene 50ka



Prepared according to general procedure C from 1-(cyclopenta-2,4-dien-1-ylidenemethyl)-4-methoxybenzene **51k** (55.0 mg, 0.3 mmol) to yield the crude product. Column chromatography (pentane/CH_2Cl_2, 4:1) afforded the title compound as a colourless oil (47.0 mg, 73%, 50:50 *er*). $\mathbf{R_f}$ = 0.40 (pentane/CH_2Cl_2, 4:1). The individual α/β tautomer (0.9 : 1.1 ratio) signals could not be uniquely identified and are referred to as tautomer 1 and tautomer 2 and integrated on this basis. **^{1}H NMR** (400.2 MHz, $CDCl_3$, 25 ^{o}C): δ 7.05-7.15 (m, 2 H, H-2' and H-6'), 6.77-6.89 (m, 2 H, H-5' and H-3'), 6.33-6.45 (m, 1.2 H, Cp tautomer 1 or 2), 6.22-6.28 (m, 0.8 H, Cp

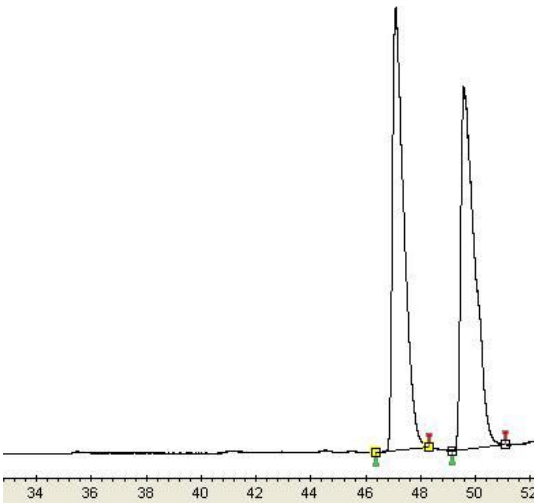
tautomer 1 or 2), 6.04-6.11 (m, 0.5 H Cp tautomer 1 or 2), 3.78 (2 overlapping s, 3 H, O*Me* both tautomers), 3.40-3.55 (m, 1.0 H, *CH*Et both tautomers), 2.87-3.02 (m, 1.1 H, C*H*$_2$ in Cp tautomer 2), 2.71-2.85 (m, 0.9 H, C*H*$_2$ in Cp tautomer 1), 1.75-2.05 (m, 2 H, *CH*$_2$Me both tautomers), 0.86 (t, 1.6 H, *J* = 7.0 Hz, CH$_2$*Me* tautomer 2) *overlapped by* 0.85 (t, 1.4 H, *J* = 7.0 Hz, CH$_2$*Me* tautomer 1) ppm. **^{13}C NMR** (100.6 MHz, $CDCl_3$, 25 ^{o}C): δ 158.0 (*C*-O-Me both tautomers), 153.4 (Cp-*C*-CHEt tautomer 1), 150.6 (Cp-*C*-CHEt tautomer 2), 137.4 (Ar *C*-1' tautomer 1), 136.6 (Ar *C*-1' tautomer 2), 134.2 (Cp tautomer 2), 133.7 (Cp tautomer 2), 132.2 (Cp tautomer 1), 131.3 (Cp tautomer 1), 129.1 (Ar C-2' and C-4' tautomer 2), 128.9 (Ar C-2' and C-4' tautomer 1), 126.2 (Cp tautomer 1), 125.7 (Cp tautomer 2), 113.8 (Ar C-3' and C-5' both tautomers), 55.3 (O*Me* both tautomers), 48.6 (*C*HEt tautomer 1), 47.6 (*C*HEt tautomer 2), 42.4 (*C*H$_2$ in Cp tautomer 1), 41.2 (*C*H$_2$ in Cp tautomer 2), 28.6 (Me*C*H$_2$ tautomer 1), 28.1 (Me*C*H$_2$ tautomer 2), 12.8 (CH$_2$*Me* tautomer 1), 12.7 (CH$_2$*Me* tautomer 2) ppm. **IR** ($CHCl_3$): $\tilde{\nu}$ = 3062, 3030, 2997, 2959, 2931, 2873, 2834, 1611, 1584, 1511, 1463, 1364, 1338, 1301, 1249, 1177, 1113, 1039, 985, 951, 930, 898, 833, 809, 740, 678 cm^{-1}. **HRMS** (EI+): calcd. for $C_{15}H_{18}O$ $[M]^+$ 214.1358; found 214.1367. **GC:** Racemic product obtained (Chirasil-DEX-CB); T_{inj} = 250 ^{o}C, T_{det} = 280 ^{o}C, flow = 2.0 mL min^{-1}, t_i = 110 ^{o}C (70 min), t_f = 170 ^{o}C (10.0 ^{o}C min^{-1}): enantiomer-1: t_R = 75.9 min, enantiomer-2: t_R = 76.1 min.

(*S*)-1-(1-(cyclopenta-1,3-dien-1-yl)propyl)-2-(methoxymethoxy)-3-methyl-benzene and (*S*)-1-(1-(cyclopenta-1,4-dien-1-yl)propyl)-2-(methoxymethoxy)-3-methylbenzene (*S*)-50la

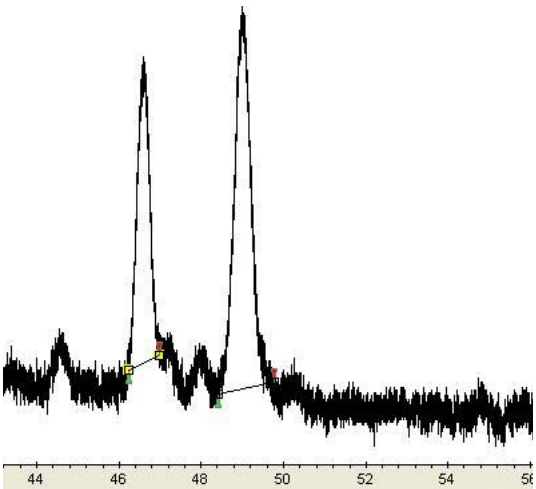


Prepared according to general procedure C from 1-(cyclopenta-2,4-dien-1-ylidenemethyl)-2-(methoxymethoxy)-3-methylbenzene **51l** (68.0 mg, 0.3 mmol) to yield the crude product. Column chromatography (pentane/Et_2O, 4:1) afforded the title compound as a colourless oil after column chromatography (11.0 mg, 15%, 63:37 *er*). $\mathbf{R_f}$ = 0.64 (pentane/Et_2O, 4:1). The individual α/β tautomer (1.1 : 0.9 ratio) signals could not be uniquely identified and are referred to as tautomer 1 and tautomer 2 and integrated on this basis. **^{1}H NMR** (400.2 MHz, $CDCl_3$, 25 ^{o}C): δ 7.08-6.92 (m, 3 H, H-4', H-5' and H-6'), 6.47-6.35 (m, 1.3 H, tautomer 1 and 2), 6.27-6.20 (m, 1 H, tautomer 1 or 2), 6.07-6.00 (m, Cp tautomer 1 or 2), 4.98-4.90 (m, 2 H, -O-C*H*$_2$-O- both tautomers), 4.15-4.04 (m, 1 H, *CH*Et both tautomers), 3.62 (2 overlapping s, 3 H, O*Me* both tautomers), 2.98-2.92 (m, 0.8 H, C*H*$_2$ in Cp tautomer 2), 2.90-2.75 (m, 1.1 H, C*H*$_2$ in Cp tautomer 1), 2.32 (s, 3 H, Ar-C*H*$_3$), 2.08-1.74 (m, 2 H, *CH*$_2$Me both tautomers), 0.88 (t, 1.4 H, *J* = 7.3 Hz, CH_2*Me* tautomer 2) *overlapped by* 0.87 (t, 1.6 H, *J* = 7.3 Hz, CH_2*Me* tautomer 1) ppm. **^{13}C NMR** (100.6 MHz, $CDCl_3$, 25 ^{o}C): δ 154.5 (*C*-O-Me tautomer 2), 154.3 (*C*-O-Me tautomer 1),

153.0 (Cp-*C*-CHEt tautomer 1), 150.4 (Cp-*C*-CHEt tautomer 2), 138.2 (Ar *C*-1' tautomer 1), 137.5 (Ar *C*-1' tautomer 2), 134.5 (Cp tautomer 2), 133.7 (Cp tautomer 1), 132.2 (Cp tautomer 1), 131.3 (Ar C-3' tautomer 1), 131.2 (Cp tautomer 2), 129.1 (Ar C-3' tautomer 2), 129.0 (Cp tautomer 2), 126.7 (Cp tautomer 1), 126.2 (Ar C-4' or C-6' tautomer 1), 126.2 (Ar C-4' or C-6' tautomer 2), 126.1 (Ar C-4' or C-6' both tautomers), 124.6 (Ar C-5' tautomer 1), 124.5 (Ar C-5' tautomer 2), 99.8 (-O-*C*H_2-O- tautomer 1), 99.7 (-O-*C*H_2-O- tautomer 2), 57.5 (O*Me* both tautomers), 42.7 (*C*H_2 in Cp tautomer 1), 41.2 (*C*HEt tautomer 1), 41.1 (*C*H_2 in Cp tautomer 2), 40.4 (*C*HEt tautomer 2), 29.0 (Me*C*H_2 tautomer 1), 28.3 (Me*C*H_2 tautomer 2), 17.3 (Ar-*C*H_3 both tautomers), 12.7 (CH_2*Me* tautomer 2) ppm. **IR** ($CHCl_3$): $\tilde{\nu}$ = 3011, 2964, 2934, 2876, 1602, 1465, 1401, 1366, 1246, 1157, 1069, 979, 926, 900 cm^{-1}. **HRMS** (EI+): calcd. for $C_{17}H_{22}O_2$ $[M]^+$ 258.1620; found 258.1630. **GC:** MOM deprotection (H^+/H_2O) was carried out in diethyl ether at room temperature. (Chirasil-DEX-CB); T_{inj} = 250 °C, T_{det} = 280 °C, flow = 2.0 mL min^{-1}, t_i = 130 °C (90 min), t_f = 170 °C (10.0 °C min^{-1}): (*R*)-enantiomer: t_R = 46.6 min, (*S*)-enantiomer: t_R = 49.0 min. **$[\alpha]_D^{25}$:** -5.1 (*c* = 0.5 in $CHCl_3$).

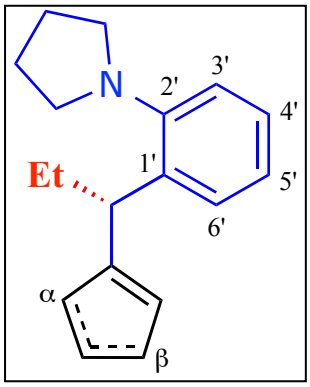


Time [Min]	Quantity [% Area]	Height [uV]	Area [uV.Min]	Area % [%]
47.09	49.78	21271.7	10205.7	49.784
49.57	50.22	17427.2	10294.1	50.216
	100.00	38698.9	20499.8	100.000



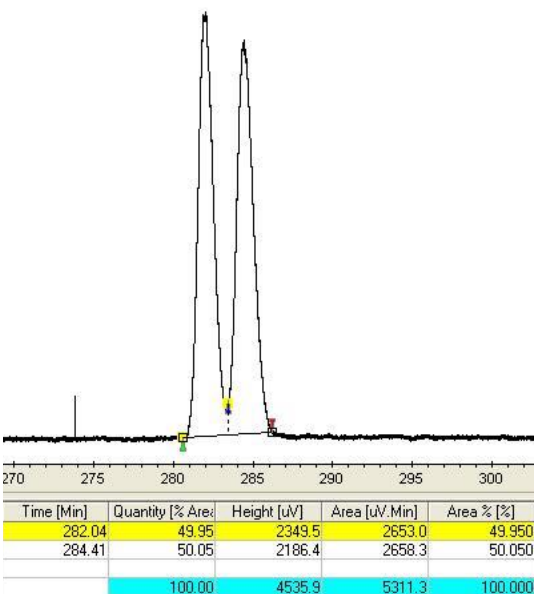
Time [Min]	Quantity [% Area]	Height [uV]	Area [uV.Min]	Area % [%]
46.60	37.45	104.6	36.3	37.454
49.01	62.55	129.4	60.5	62.546
	100.00	234.0	96.8	100.000

(*S*)-1-(2-(1-(cyclopenta-1,3-dien-1-yl)propyl)phenyl)pyrrolidine and (*S*)-1-(2-(1-(cyclopenta-1,4-dien-1-yl)propyl)phenyl)pyrrolidine 50ma

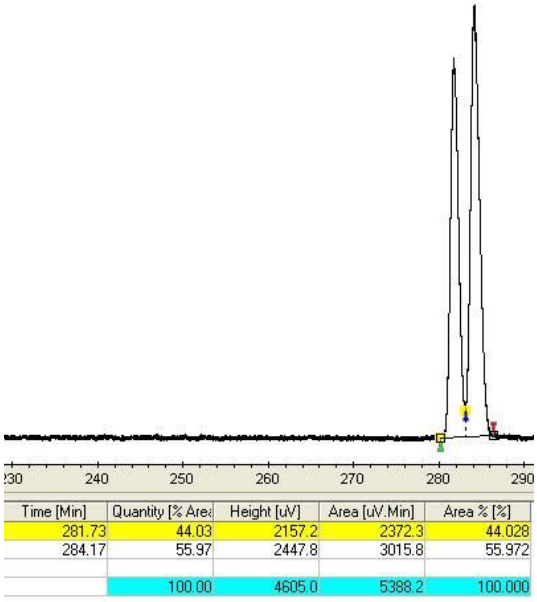


Prepared according to general procedure C from 1-(2-(cyclopenta-2,4-dien-1-ylidenemethyl)phenyl)pyrrolidine **51m** (67.0 mg, 0.3 mmol) to yield the title compound as a colourless oil after column chromatography (29.0 mg, 38%, 56:44 *er*). $\mathbf{R_f}$ = 0.60 (pentane/MTBE, 19:1). The individual α/β tautomer (1.2 : 0.8 ratio) signals could not be uniquely identified and are referred to as tautomer 1 and tautomer 2 and integrated on this basis. **^{1}H NMR** (400.2 MHz, $CDCl_3$, 25 ^{o}C): δ 7.17-7.07 (m, 3 H, H-4', H-5' and H-6'), 7.02-6.95 (m, 1 H, H-3'), 6.46-6.33 (m, 1.3 H, Cp tautomer 1 or 2), 6.25-6.18 (m, 1.2 H, Cp tautomer 1 or 2), 6.08-6.02 (m, 0.4 H, Cp tautomer 1 or 2), 4.27-4.22 (m, 0.6 H, *CH*Et tautomer 1), 4.22-4.15 (m, 0.4 H, *CH*Et tautomer 2), 3.21-3.10 (m, -C*H*$_2$-N-C*H*$_2$- both tautomers), 3.03-2.95 (m, 2 H, -C*H*$_2$-N-C*H*$_2$- both tautomers), 2.95-2.92 (m, 0.8 H, C*H*$_2$ in Cp tautomer 2), 2.90-2.75 (m, 1.2 H, C*H*$_2$ in Cp tautomer 1), 2.07-1.95 (m, 1 H, *CH*$_2$Me both tautomers), 1.95-1.84 (m, 4 H, -N-CH$_2$-C*H*$_2$-C*H*$_2$-), 1.82-1.70 (m, 1 H, *CH*$_2$Me both tautomers), 0.85 (t, 1.2 H, *J* = 7.3 Hz, CH$_2$*Me* tautomer 2) *overlapped by* 0.83 (t, 1.8 H, *J* = 7.3 Hz, CH$_2$*Me* tautomer 1) ppm. **^{13}C NMR** (100.6 MHz, $CDCl_3$, 25 ^{o}C): δ 153.9 (C-2'-N tautomer 1), 151.1 (C-2'-N tautomer 2), 149.7 (Cp-*C*-CHEt tautomer 2), 149.6 (Cp-*C*-CHEt tautomer 1), 140.0 (Ar *C*-1' tautomer 2), 139.1 (Ar *C*-1' tautomer 1), 135.0

(Cp tautomer 2), 133.3 (Cp tautomer 2), 132.3 (Cp tautomer 1), 130.9 (Cp tautomer 1), 128.4 (Cp tautomer 2), 128.3 (Cp tautomer 1), 126.5 (Ar C-4' or C-6' tautomer 2), 126.4 (Ar C-4' or C-6' both tautomers), 125.7 (Ar C-4' or C-6' tautomer 2), 123.0 (Ar C-5' tautomer 1), 122.9 (Ar C-5' tautomer 2), 119.3 (Ar C-3' tautomer 1), 119.1 (Ar C-3' tautomer 2), 53.3 (-C*H*$_2$-N-C*H*$_2$- tautomer 1), 53.2 (-C*H*$_2$-N-C*H*$_2$- tautomer 2), 43.0 (*C*H$_2$ in Cp tautomer 1), 42.0 (*C*HEt tautomer 1), 41.2 (*C*HEt tautomer 2), 41.1 (*C*H$_2$ in Cp tautomer 2), 29.5 (Me*C*H$_2$ tautomer 2), 28.9 (Me*C*H$_2$ tautomer 2), 24.9 (N-CH$_2$-*C*H$_2$-*C*H$_2$- both tautomers), 12.7 (CH$_2$*Me* both tautomers) ppm. **HRMS** (EI+): calcd. for $C_{18}H_{23}N$ $C_{18}H_{23}N$ $[M]^+$ 253.1830; found 253.1837. **GC:** (Chirasil-DEX-CB); T_{inj} = 250 °C, T_{det} = 280 °C, flow = 2.0 mL min^{-1}, t_i = 100 °C (60 min isothermal), 130 °C (0.1 °C min^{-1} – 20 min) t_f = 170 °C (5.0 °C min^{-1}): enantiomer-1: t_R = 281.7 min, enantiomer-2: t_R = 284.2 min.



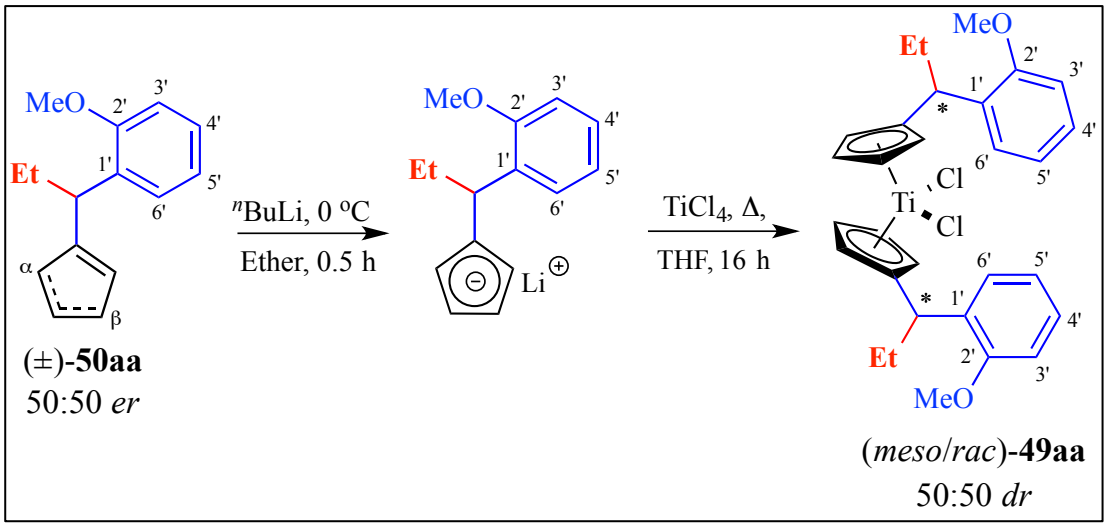
Time [Min]	Quantity [% Area]	Height [uV]	Area [uV.Min]	Area % [%]
282.04	49.95	2349.5	2653.0	49.950
284.41	50.05	2186.4	2658.3	50.050
	100.00	4535.9	5311.3	100.000



Time [Min]	Quantity [% Area]	Height [uV]	Area [uV.Min]	Area % [%]
281.73	44.03	2157.2	2372.3	44.028
284.17	55.97	2447.8	3015.8	55.972
	100.00	4605.0	5388.2	100.000

4.1.4 Preparation of chiral titanocene derivatives

(*Meso/rac*)-dichloridobis(1-propyl-1'-(2-methoxyphenyl)-η^5-cyclopentadienyl)-titanium (*meso/rac*)-49aa

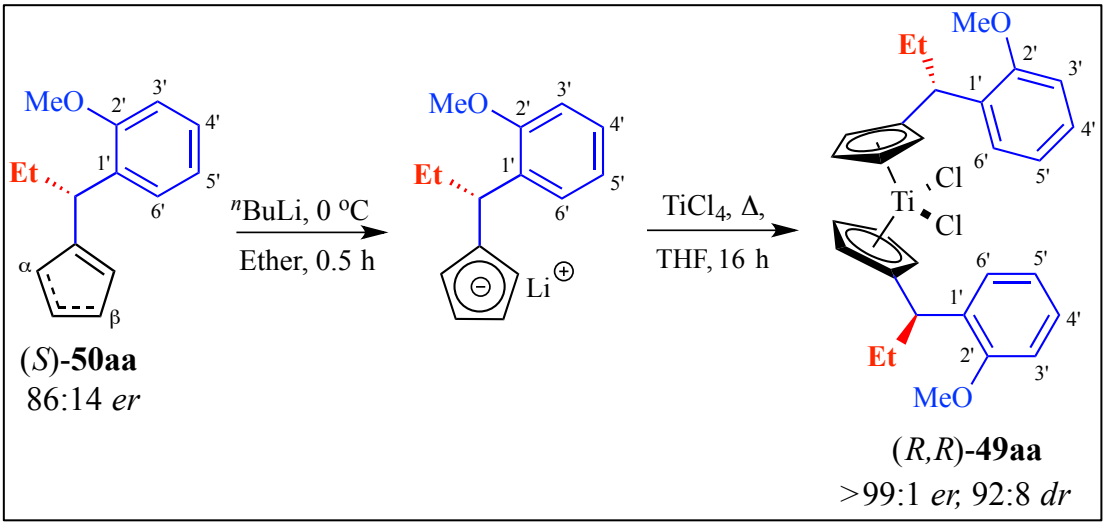


A flame-dried Schlenk tube was left to cool under vacuum for 30 min and then weighed under vacuum. Under a stream of argon, (±)-**50aa** (0.535 g, 2.50 mmol, 1.0 equiv.) was added, followed by dry diethyl ether (10 mL). The mixture was cooled to 0 °C, and ^{n}BuLi (1.7 mL, 2.75 mmol, 1.1 equiv., 1.6 M in hexane) was added. The solution was left to stir for 30 min at 0 °C to yield a white precipitate of the lithium substituted-cyclopentadienide in a faint yellow solution. The latter solution was removed by cannula filtration, and the solid was washed twice with dry ether (2 x 3 mL) and refiltered under argon. The white lithium substituted-cyclopentadienide precipitate was dried under vacuum at 0.1 Torr for 1 h and then weighed under vacuum (0.410 g, 1.86 mmol, 74%). This intermediate (1.86 mmol, 2.0 equiv.) was dissolved in dry THF (7.5 mL) to give a colourless solution. In another Schlenk tube, titanium tetrachloride (0.93 mL, 0.93 mmol, 1.0 equiv., 1.0 M in toluene) was dissolved in dry THF (7.5 mL) to give a yellow solution. The solution of titanium tetrachloride was added to the solution of the EtArCpLi by cannula under argon at room temperature to give a dark red solution, which was heated to reflux for 16 h at

85 °C. The resultant solution was then cooled, and the solvent was removed under reduced pressure. The remaining brown residue was extracted with chloroform, which was filtered through a long thick pad of Celite to remove LiCl. The solvent was removed in vacuo to yield the crude solid material. Purification was performed by direct infusion of pentane on top of a saturated solution of the crude titanocene in CH_2Cl_2 (final mixture ca. 5:1 pentane/CH_2Cl_2). After purification, a red solid was obtained (0.359 g, 71% - based on titanium). The individual *rac*- and *meso*-diastereomers (1:1 ratio) signals were identified via the enantiopure titanocenes and integrated on this basis. **M.p.** 173-174 ^oC. **^{1}H NMR** (500.1 MHz, $CDCl_3$, 22 ^oC): δ 7.25 (ddd, J = 7.5, 7.0, 1.0 Hz, 1 H, H-4') *overlapped by* 7.19 (ddd, J = 7.5, 7.0, 1.0 Hz, 1 H, H-4'), 7.03 (br d, J = 6.9 Hz, 2 H, H-6' both isomers), 6.92-6.85 (m, 4 H, H-3' and H-5', both isomers), 6.72 (AB, J_{AB} = 2.5 Hz, 1 H, Cp *rac*-isomer), 6.70 (AB, J_{AB} = 2.5 Hz, 1 H, Cp *meso*-isomer), 6.45 (AB, J_{AB} = 2.5 Hz, 1 H, Cp *rac*-isomer), 6.39 (AB, J_{AB} = 2.5 Hz, 1 H, Cp *meso*-isomer), 6.16 (AB, J_{AB} = 2.5 Hz, 1 H, Cp *meso*-isomer), 6.05 (AB, J_{AB} = 2.5 Hz, 1 H, Cp *rac*-isomer), 6.00 (AB, J_{AB} = 2.0 Hz, 1 H, Cp *meso*-isomer), 5.96 (AB, J_{AB} = 2.0 Hz, 1 H, Cp *rac*-isomer), 4.41 (br, 2 H, *CH*Et both isomers), 3.77 (s, 6 H, 2 x OMe, both isomers), 2.23-2.08 (m, 2 H, CH_2Me both isomers), 2.02-1.86 (br, 2 H, CH_2Me both isomers), 0.75 (t, J = 7.5 Hz, 3 H, CH_2*Me meso*-isomer) *overlapped by* 0.75 (t, J = 7.5 Hz, 3 H, CH_2*Me rac*-isomer) ppm. **^{13}C NMR** (125.8 MHz, $CDCl_3$, 25 ^oC): δ 157.7 (C-2' Ar both isomers), 142.7 (C-1' Ar *meso*-isomer), 142.4 (*C*(2) Ar *rac*-isomer), 131.9 (br, *ipso*-Cp *meso* or *rac*-isomer), 130.2 (br, *ipso*-Cp *meso* or *rac*-isomer), 127.8 (C-4' Ar both isomers), 123.2 (Cp *rac*-isomer), 122.0 (Cp *meso*-isomer), 120.9 (C-5' or C-6') both isomers Ar), 120.8 (C-5' or C-6' Ar both isomers), 119.3 (Cp *rac*-isomer), 118.9 (Cp *meso*-isomer), 118.4 (Cp *rac*-isomer), 117.6 (Cp *meso*-isomer), 116.5 (br, Cp *meso*-

isomer), 115.5 (br, Cp *rac*-isomer), 111.1 (C-3' Ar both isomers), 55.6 (OMe both isomers), 42.1 (*CH*Et both isomers), 26.4 (*C*H_2Me both isomers), 12.0 (CH_2*Me* both isomers) ppm. **IR** (ATR.): $\tilde{\nu}$ = 3118, 2962, 2933, 2875, 2835, 1597, 1583, 1490, 1459, 1434, 1379, 1334, 1290, 1242, 1183, 1157, 1117, 1080, 1048, 1025, 908, 838, 829, 797 775, 752, 740, 712 cm^{-1}. **HRMS** (ESI^+): Calcd. for $C_{30}H_{34}Cl_2NaO_2Ti^+$ $[M+Na]^+$ 567.1308, found: 567.1319. **CHN** Anal. calcd. for $C_{30}H_{34}Cl_2O_2Ti$: C, 66.07; H, 6.28; found: C, 65.94; H, 6.28. Data as in literature.[112]

(*R*,*R*)-dichloridobis[1-propyl-1'-(2-methoxyphenyl)-η^{5}cyclopentadienyl]-titanium (*R*,*R*)-49aa

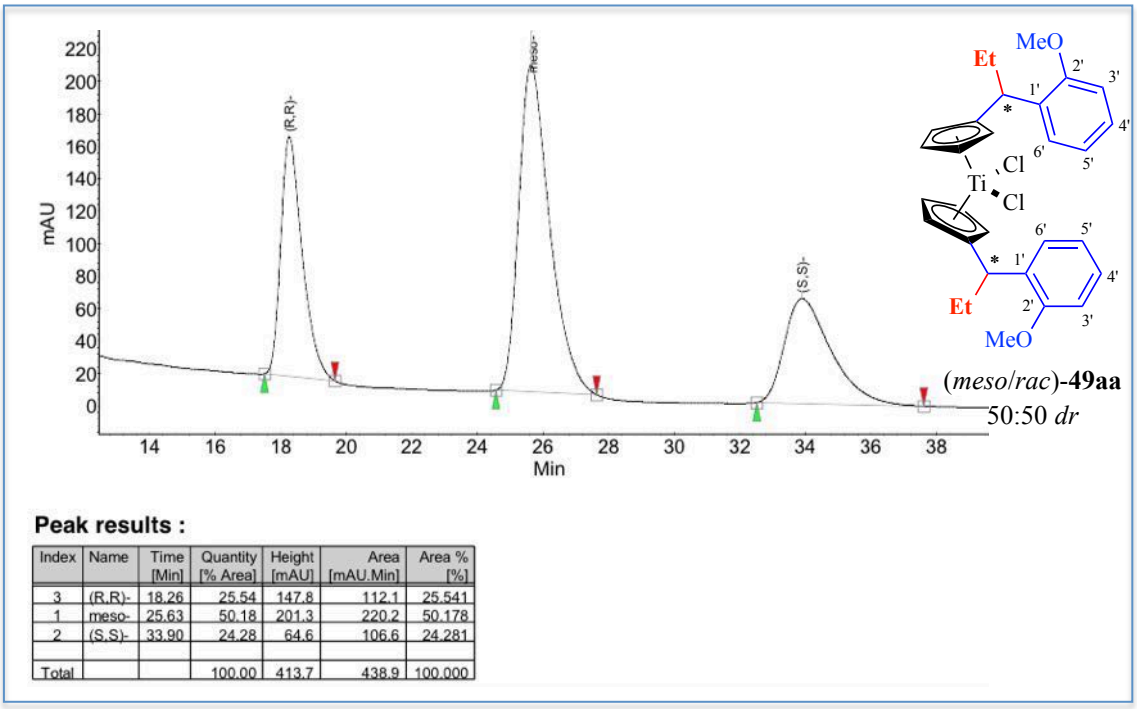


A flame-dried Schlenk tube was left to cool under vacuum for 30 min and then weighed under vacuum. Under a stream of argon, (*S*)-**50aa** (86:14 *er*) (0.50 g, 2.34 mmol, 1.0 equiv.) was added, followed by dry ether (9 mL). The mixture was cooled to 0 °C, and *n*BuLi (1.65 M in hexane, 1.6 mL, 2.6 mmol, 1.1 equiv.) was added. The solution was left to stir for 30 min at 0 °C to yield a white precipitate of the lithium substituted cyclopentadienide in a faint yellow solution. The solvent was removed from the EtArCpLi by cannula filtration, and the solid was washed with dry ether (4 mL) and refiltered under argon. The precipitate was dried under vacuum at 0.1 Torr

for 1 h and weighed under vacuum. The lithium substituted-cyclopentadienide (0.465 g, 2.11 mmol, 2.0 equiv.) was dissolved in dry THF (8 mL) to give a colourless solution. In another Schlenk tube, titanium tetrachloride (1 mL, 1.0 mmol, 0.95 equiv., 1 M in toluene) was dissolved in dry THF (8.0 mL) to give a yellow solution. The solution of titanium tetrachloride was added to the solution of EtArCpLi by cannula under argon at room temperature to give a dark red solution, which was heated to reflux for 16 h at 85 °C. The resultant solution was then cooled, and the solvent was removed under reduced pressure. The remaining brown residue was extracted with chloroform, which was filtered through a long narrow (10cm x 4.5 cm) thick pad of Celite to remove LiCl. The solvent was removed *in vacuo* to yield the crude oil, which solidified on standing (0.512 g, 95% - based on titanium, 0.75:0.25 *dr*). The solid was dissolved in dichloromethane (2.5 mL) and was transferred to a vial 4 dram, followed by the layering of hexane (5.0 mL). The solutions were left to diffuse for 30 h at 5 ^{o}C. A light red solid was obtained (178 mg, 33% - based on titanium, 0.60:0.40 *dr*). The filtrate was passed through a small plug of celite in a glass needle pipette, to remove any remaining solid, which could co-precipitate the next crop. Argon was then bubbled gently through the top of the filtrate solution until the oily edge of the vial started to become partially soluble. The solution was then placed at 5 ^{o}C for another 30 h to yield red single crystals of titanocene (76 mg, 14% - based on titanium, 0.92:0.08 *dr*). **^{1}H NMR** (400.2 MHz, $CDCl_3$, 22 ^{o}C): δ 7.20 (ddd, 2 H, J = 7.5, 7.0, 1.0 Hz, H-5), 7.03 (br d, 2 H, J = 6.9 Hz, H-3), 6.92-6.84 (m, 4 H, H-4' and H-6'), 6.73 (AB, J_{AB} = 2.5 Hz, 2 H, Cp), 6.45 (AB, J_{AB} = 2.5 Hz, 2 H, Cp), 6.05 (AB, J_{AB} = 2.5 Hz, 2 H, Cp), 5.95 (AB, J_{AB} = 2.0 Hz, 2 H, Cp), 4.41 (br, 2 H, *CH*Et), 3.77 (s, 6 H, OMe, both isomers), 2.23-2.08 (m, 2 H, CH_2Me), 2.03-1.85 (br, 2 H, CH_2Me), 0.76 (t, J = 7.5 Hz, 3 H, CH_2*Me*) ppm.

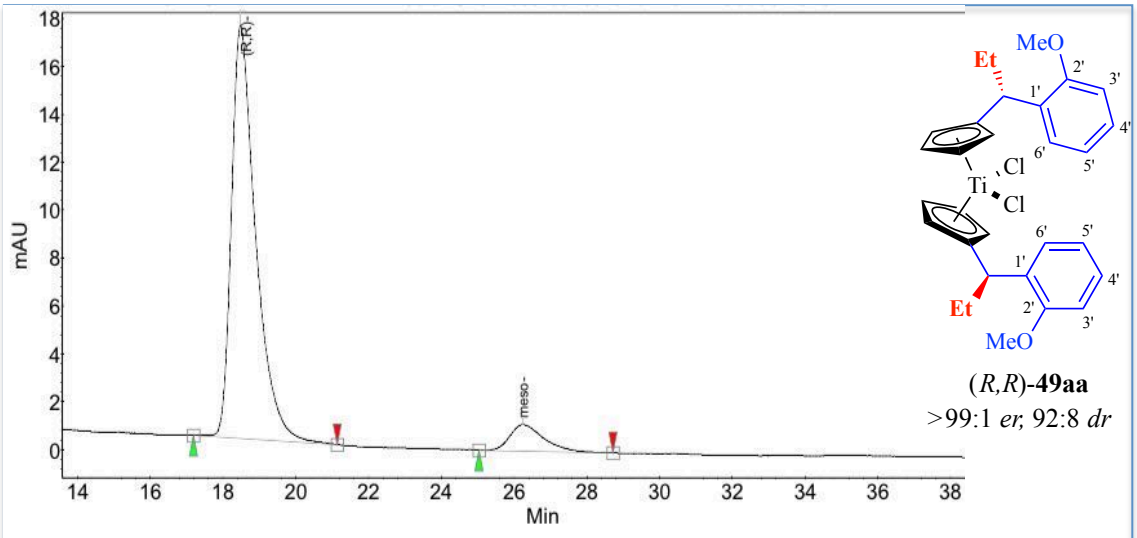
^{13}C NMR (100.6 MHz, $CDCl_3$, 25 °C): δ 157.7 (C-2'), 142.4 (C-1'), 130.2 (br, *ipso*-Cp), 127.8 (C-4'), 123.3 (Cp), 120.9 (C-5' and C-6'), 119.0 (Cp), 118.5 (Cp), 115.5 (br, Cp), 111.2 (C-3'), 55.6 (OMe), 42.1 (*CH*Et), 26.5 (CH_2Me), 12.0 (CH_2*Me*) ppm.

HPLC: (Chiracel OD); sample dissolved in MTBE, eluent 25% isopropanol / 75% hexane, 0.5 mL/min, 254 nm: (*R*,*R*)-enantiomer t_R = 18.26 min, (*meso*)-enantiomer t_R = 25.63 min, (*S*,*S*)-enantiomer t_R = 33.90 min.



Peak results :

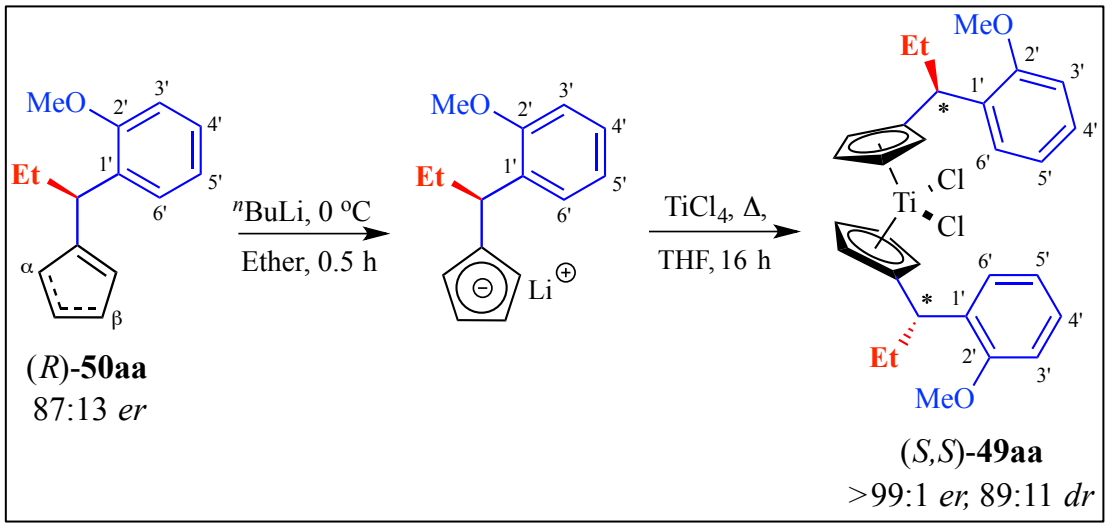
Index	Name	Time [Min]	Quantity [% Area]	Height [mAU]	Area [mAU.Min]	Area % [%]
3	(R,R)-	18.26	25.54	147.8	112.1	25.541
1	meso-	25.63	50.18	201.3	220.2	50.178
2	(S,S)-	33.90	24.28	64.6	106.6	24.281
Total			100.00	413.7	438.9	100.000



Peak results :

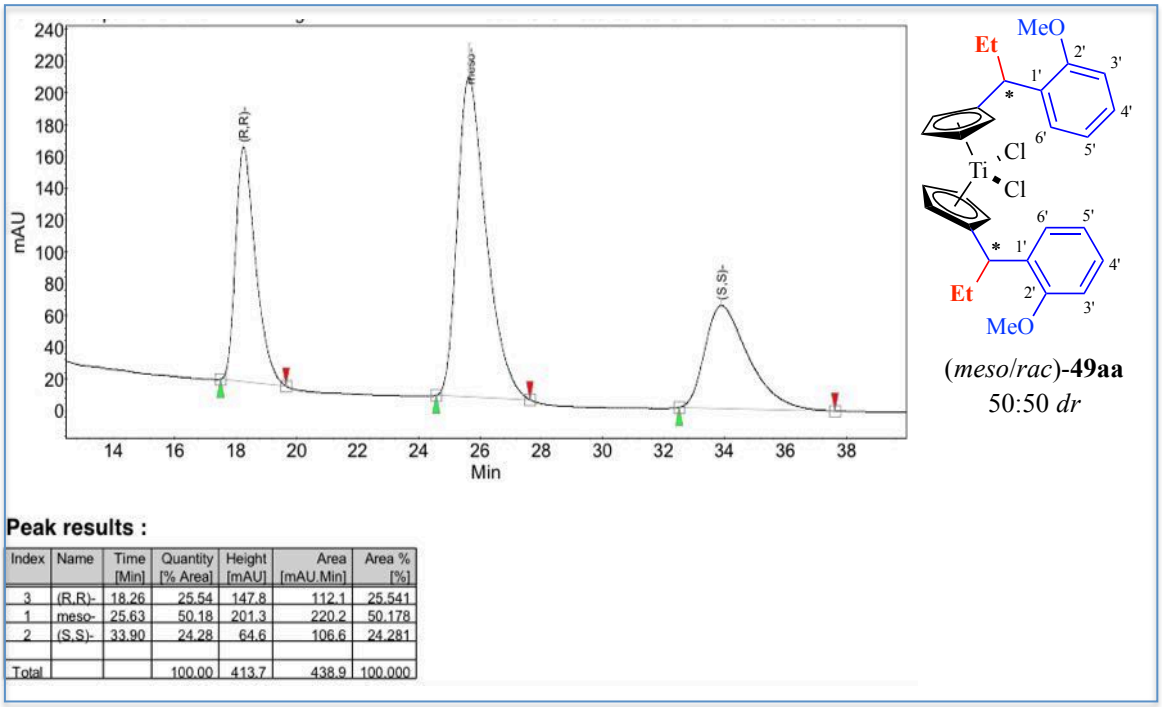
Index	Name	Time [Min]	Quantity [% Area]	Height [mAU]	Area [mAU.Min]	Area % [%]
1	(R,R)-	18.48	91.79	17.2	13.3	91.793
2	meso-	26.23	8.21	1.1	1.2	8.207
Total			100.00	18.3	14.5	100.000

(*S*,*S*)-dichloridobis[1-propyl-1'-(2-methoxyphenyl)-η^5-cyclopentadienyl]-titanium; (*S*,*S*)-49aa



A flame-dried Schlenk tube was left to cool under vacuum for 30 min and then weighed under vacuum. Under a stream of argon, (*R*)-EtArCp **50aa** (87:13 *er*) (0.70 g, 3.27 mmol, 1.0 equiv.) was added, followed by dry ether (13 mL). The mixture was cooled to 0 °C, and *n*BuLi (1.65 M in hexane, 2.2 mL, 3.60 mmol, 1.1 equiv.) was added. The solution was left to stir for 30 min at 0 °C to yield a white precipitate of the lithium substituted cyclopentadienide in a faint yellow solution. The solvent was removed from the EtArCpLi by cannula filtration under argon, and the solid was washed with dry ether (5 mL) and refiltered under argon. The precipitate was dried under vacuum at 0.1 Torr for 1 h and weighed under vacuum. The lithium substituted-cyclopentadienide (0.623 g, 2.83 mmoles, 2.0 equiv.) was dissolved in dry THF (11 mL) to give a colourless solution. In another Schlenk tube, titanium tetrachloride 1.00 M in toluene (1.4 mL, 1.4 mmol, 0.99 equiv.) was dissolved in dry THF (11 mL) to give a yellow solution. The solution of titanium tetrachloride was added to the solution of EtArCpLi by cannulation at room temperature to give a dark red solution, which was heated to reflux for 16 h at 85 °C. The resultant solution was then cooled, and the solvent was removed under reduced

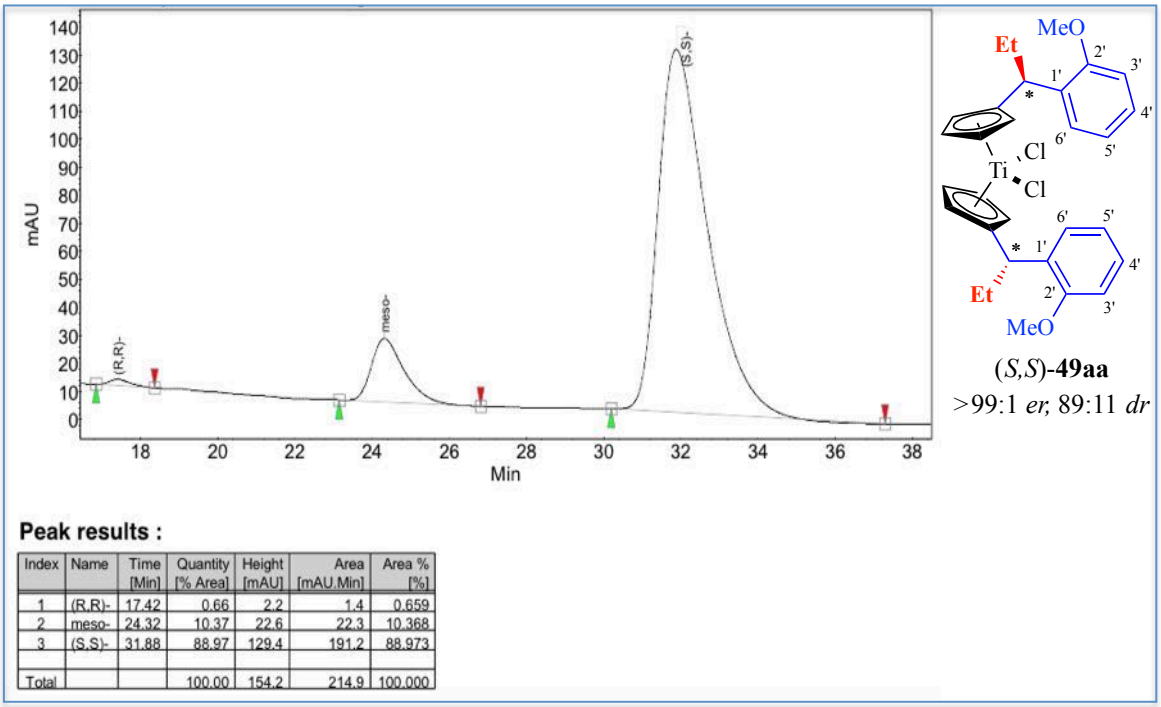
pressure. The remaining brown residue was extracted with chloroform, which was filtered through a long narrow (10cm x 4.5 cm) thick pad of Celite to remove LiCl. The solvent was removed in vacuo to yield the crude oil, which solidified on standing (642 mg, 84% - based on titanium, 0.77:0.23 *dr*,). The solid was dissolved in dichloromethane (2.5 mL) and was transferred to an 8 mL vial, followed by the layering of hexane (5.0 mL). The solutions were left to diffuse for 20 h at 20 ^{o}C. A light red solid was obtained (26 mg, 0.55:0.45 *dr*). The filtrate was passed through a small plug of celite in a glass needle pipette to a vial 4 dram, to remove any remaining solid which could co-precipitate the next crop. Argon was then bubbled gently through the top of the filtrate solution until the oily edge of the vial started to become partially soluble. The solution was then placed at 5 ^{o}C for 20 h to yield red/orange crystals (single enantiomer) and traces of brown dark spheres (meso) (228 mg, 30% - based on titanium, 0.88:0.12 *dr*,). **^{1}H NMR** (400.2 MHz, $CDCl_3$, 22 ^{o}C): δ 7.20 (ddd, *J* = 7.5, 7.0, 1.0 Hz, 2 H, H-4'), 7.03 (br d, *J* = 6.9 Hz, 2 H, H-6'), 6.92-6.84 (m, 4 H, H-3' and H-5'), 6.73 (AB, J_{AB} = 2.5 Hz, 2 H, Cp), 6.45 (AB, J_{AB} = 2.5 Hz, 2 H, Cp), 6.05 (AB, J_{AB} = 2.5 Hz, 2 H, Cp), 5.95 (AB, J_{AB} = 2.0 Hz, 2 H, Cp), 4.41 (br, 2 H, *CH*Et), 3.77 (s, 6 H, OMe, both isomers), 2.23-2.08 (m, 2 H, CH_2Me), 2.03-1.85 (br, 2 H, CH_2Me), 0.76 (t, *J* = 7.5 Hz, 3 H, CH_2*Me*) ppm. **^{13}C NMR** (100.6 MHz, $CDCl_3$, 25 ^{o}C): δ 157.7 (C-2'), 142.4 (C-1'), 130.2 (br, *ipso*-Cp), 127.8 (C-4'), 123.3 (Cp), 120.9 (C-5' and C-6'), 119.0 (Cp), 118.5 (Cp), 115.5 (br, Cp), 111.2 (C-3'), 55.6 (OMe), 42.1 (*CH*Et), 26.5 (CH$_2$Me), 12.0 (CH$_2$*Me*) ppm. **HPLC:** (Chiracel OD); sample dissolved in MTBE, eluent 25% isopropanol / 75% hexane, 0.5 mL/min, 254 nm: (*R*,*R*)-enantiomer t_R = 18.26 min, (*meso*)-enantiomer t_R = 25.63 min, (*S*,*S*)-enantiomer t_R = 33.90 min.



(*meso*/*rac*)-**49aa**
50:50 *dr*

Peak results :

Index	Name	Time [Min]	Quantity [% Area]	Height [mAU]	Area [mAU.Min]	Area % [%]
3	(R,R)-	18.26	25.54	147.8	112.1	25.541
1	meso-	25.63	50.18	201.3	220.2	50.178
2	(S,S)-	33.90	24.28	64.6	106.6	24.281
Total			100.00	413.7	438.9	100.000

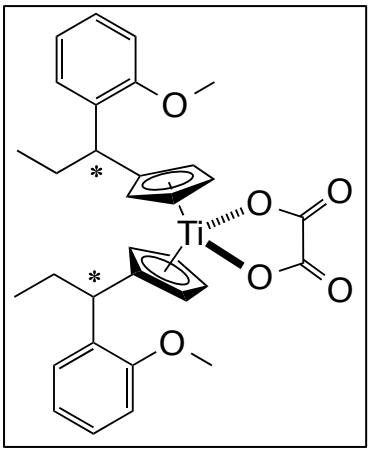


(*S*,*S*)-**49aa**
>99:1 *er*, 89:11 *dr*

Peak results :

Index	Name	Time [Min]	Quantity [% Area]	Height [mAU]	Area [mAU.Min]	Area % [%]
1	(R,R)-	17.42	0.66	2.2	1.4	0.659
2	meso-	24.32	10.37	22.6	22.3	10.368
3	(S,S)-	31.88	88.97	129.4	191.2	88.973
Total			100.00	154.2	214.9	100.000

***Rac*/*meso*-oxalatobis(1-propyl-1'-(2-methoxyphenyl)-η^5-cyclopentadienyl)-titanium; (*rac*/*meso*)-119**



Silver oxalate (0.064g, 0.21 mmol) and (*rac*/*meso*)-**49aa** (0.082g, 0.15 mmol) were added to a round bottomed flask under a stream of argon atmosphere shielded from light. Acetone (40 mL) was then added and the solution was left to stir for 48 h. The resulting mixture was then cannula-filtered. After recrystallization ($CHCl_3$/pentane 1:4) of the crude orange solid, a yellow orange solid was obtained (68 mg, 71% - based on titanium). **^{1}H NMR** (500.1 MHz, $CDCl_3$, 22 ^{o}C): δ_H 0.76 (t, 3 H, J = 7.5 Hz, CH_2*Me rac*-isomer) *overlapped by* 0.76 (t, 3 H, J = 7.5 Hz, CH_2*Me meso*-isomer), 1.81-1.95 (m, 4 H, *CH_2*Me both isomers), 3.85 (s, 6 H, 2 x OMe, both isomers), 4.01 (br, 2 H, *CH*Et both isomers), 6.17-6.19 (m, 2H, Cp), 6.23-6.25 (m, 2H, Cp), 6.38 (AB, 1 H, J_{AB} = 2.5 Hz, Cp), 6.44 (AB, 1 H, J_{AB} = 2.5 Hz, Cp), 6.51-6.53 (m, 2H, Cp), 6.85-6.90 (m, 4 H, *H*-C(4) and *H*-C(6) Ar, both isomers), 6.94-6.97 (m, 2H, Ar), 7.18-7.23 (m, 2 H, Ar both isomers). **^{13}C NMR** (125.8 MHz, $CDCl_3$, 25 ^{o}C): δ_C 11.9 (CH_2*Me* both isomers), 26.3 (*C*H_2Me both isomers), 42.1 (*CH*Et both isomers), 55.4 (OMe both isomers), 111.1 (*C*(6) Ar both isomers), 117.9, 119.1, 119.9, 120.8, 121.0, 121.8, 122.3, 128.1, 129.6, 130.2, 147.0, 147.2, 157.4, 157.5, 163.0, 163.1 **HRMS** (ESI$^+$) Calcd. for $C_{32}H_{34}O_6TiH^+$ $[M+H]^+$ 563.1908, found: 563.1895.

4.2 Biology Section

4.2.1 Cell culture

All carcinoma cell lines were sourced from the American Type Tissue Cell Culture Collection (ATCC) and cultured in RPMI 1640 nutrient medium supplemented with 10% foetal bovine serum (FBS). Cells were passaged twice weekly to maintain logarithmic growth and incubated at 37 °C in an atmospheric environment constituting 5% CO_2. Cell stocks were cryopreserved (-155 °C in liquid nitrogen) and upon re-introduction to culture were used in experiments ≤ 30 passages to minimise phenotypic/genotypic drift. Milligram quantities of titanocene were weighed using an Ultra Micro Balance. Titanocene compound stocks (20 mM) were prepared freshly in DMSO directly before use. Dilution procedures were conducted adopting identical procedures taking < 1 h followed by immediate use. This procedure is important to ensure reproducibility and correlation with the active hydrolysis of **49aa** as described in section 1.2. MRC-5, normal lung fibroblast cells were cultured in ATCC-formulated Eagle's Minimum Essential Medium, Catalog No. 30-2003 supplemented with 10% foetal bovine serum (FBS). Cell cultures were mycoplasma free.

4.2.2 Growth inhibitory studies *in vitro*

The antiproliferative activity was performed by MTT [3-(4,5-dimethyl-thiazol-2-yl)-2,5-diphenyltetrazolium bromide] assay on three different human carcinoma cell lines; colon (HCT-116), pancreas (MiaPaCa-2), and breast (MDA-MB-468) and MRC-5 non-malignant fibroblasts line. Carcinoma cell lines were maintained in RPMI 1640 medium supplemented with 10% (v/v) FBS (foetal bovine serum). Fibroblasts were maintained in Eagle’s minimum essential medium. Cells were

seeded into 96-well plates at a density of 3 x 10^3 per well (180 µL per well) and allowed to adhere for 24 h at 37 ^oC / 5% CO_2. A 20 mM top stock solution of agent **4** in DMSO was then freshly made. Serial dilutions were prepared in RMPI 1640 medium supplemented with 10% FBS. Control wells received vehicle alone (20 µL per well). The final concentrations in the wells were; 0.5 µM, 1 µM, 2 µM, 5 µM, 10 µM, 20 µM, 50 µM and 100 µM. The final concentration of DMSO in the wells never exceeded 1% v/v. Vehicle control assays were performed. Experimental plates were incubated for a further 72 h period at 37 ^oC / 5% CO_2. Cell viability was recorded at the time of agent addition (T_0) and following 72 h exposure: following addition of MTT solution (2 mg/mL in PBS - 50 µL per well), experimental plates were incubated for 3 h to allow reduction of MTT to insoluble dark purple formazan crystals. The supernatant in each well was then aspirated and cellular formazan solublised by addition of DMSO (150 µL per well). Absorbance was read at wavelength 550 nm using an Anthos Labtec systems plate reader. Measured intensity is proportional to metabolic activity, which correlates to cellular viability. Estimated GI_{50} values (the concentration of agent which inhibits growth by 50%) were calculated by performing MTT assays at time of drug addition as well as after 24 h or 72 h exposure.

4.2.3 Clonogenic assays

Clonogenic assays were performed to measure the ability of single cells to survive a brief exposure to test agent and maintain proliferative potential to form colonies. A small number of cells/well; 300 (HCT-116), 400 (Mia PaCa-2) were seeded in 6-well plates with 2 mL medium and were allowed to attach for 24 h. Treatments were guided by GI_{50} concentrations obtained from the MTT assays. After 24 h exposure to

titanocenes, the medium was removed, cells gently washed (2 x sterile PBS, 37 °C) before incubation in agent-free medium for 7 – 9 days (HCT-116), or 14 days (Mia PaCa-2). Experiments were terminated when colonies of more than 50 cells were visible in control wells. Colonies were washed (x3) with PBS, fixed with 100% methanol for 15 min, stained 0.5% methylene blue (1:1 water:methanol; 15 min), washed (distilled water), air dried and counted.

4.2.4 Annexin V-FITC/PI apoptosis assay

Cells were seeded in 6 well plates (2 x 10^5 cells/well for 24 h and 1 x 10^5 cells/well for 72 h in 2 ml complete medium), allowed to attach overnight and subsequently treated for up to 72 h as required. Following treatment, medium containing any floating cells was decanted to a labelled FACS tube and kept on ice. Cells were trypsinised and, once detached, pooled together with the appropriate medium and floating cells. Cells were then pelleted in a Beckman Coulter Allegro centrifuge at 1,200 rpm for 5 min, 4 ^{o}C. The supernatant was discarded and the pellet broken up by gently flicking the tube. Cold, complete medium (2 mL) was added to the cells; samples were then kept on ice for 10 min, whilst cell counts were performed.

All cells were included in the cell count for these experiments; 1 x 10^5 cells were then transferred to a fresh FACS tube, 1 mL PBS added and the cells pelleted as before. The supernatant was discarded, ensuring all the PBS had been removed and the pellet broken up by gentle flicking of the tube. Annexin binding buffer (100 µL; 1x) and 5 µL annexin V-FITC was added to each tube. The tube was briefly vortexed and incubated at RTP in the dark for 15 min. Annexin binding buffer (400µL; 1x) and 10 µL 50 µg/mL PI solution was added to each tube which was vortexed and kept on ice for 10 min in the dark prior to analysis on the flow cytometer. Samples

were analysed within 1 h to avoid deterioration of the cells. Gates were set up on a dual colour dot plot for vehicle and treated samples and the percentages of early apoptotic cells (annexin V–FITC positive, PI negative) or late apoptotic/necrotic cells (annexin V–FITC positive, PI positive) recorded.

4.2.5 Cell cycle & Dual DNA damage (γh2ax) / cell cycle analysis

Cells were seeded in Corning® tissue-culture treated culture dishes (100mm x 20 mm). For MDA-MB-468, 1 x 10^6 cells were seeded per culture dish for 24 h treatment whilst 5 x 10^5 cells were seeded per culture dish for 72 h treatment in 10 mL complete medium. For the rapidly dividing cell line HCT-116, 6 x 10^5 cells were seeded per culture dish for 24 h treatment whilst 3 x 10^5 cells were seeded per culture dish for 72 h treatment in 10 mL complete medium. Cells were then allowed to attach overnight and treated for up to 72 h as required. Following treatment, medium containing any floating cells was decanted to a labelled falcon tube and kept on ice. Cells were then washed with 1 mL PBS and placed into the respective falcon tube.

Cells were trypsinised (500mL Trypsin/EDTA solution), incubated at 37 ^oC and, once detached, all cells were flushed from the bottom of the Petri dish (using a 200 mL pipette), and transferred to the appropriate falcon tube. Cells were then pelleted in a centrifuge at 1,250 rpm for 10 min, at room temperature. The supernatant was then aspirated, leaving a small amount in the bottom of the tube to avoid disturbing the pellet. The pellet was then resuspended by gently flicking the tube. PBS (1 mL) was then added to each falcon tube and the tube containing the suspension was then centrifuged, the supernatant liquid was aspirated and cells resuspended. Cells were then fixed in a vented class II cabinet, 500 mL 1% methanol-free formaldehyde in PBS was added to each falcon tube. The suspension was pipetted up and down

several times to ensure a single cell suspension. The suspension was then incubated for 5 min at room temperature, gently flicking the tube occasionally.

Cells were then permeabilised by adding 500 mL 0.4% Triton X-100 in PBS, with gentle mixing. Once added to all tubes, tubes were left at room temperature for 1 min and then, tubes containing suspensions were then centrifuged, the supernatant liquid was aspirated and cells resuspended. FBS (1 mL; 1%) in PBS was then added to cells, contents were gently mixed and incubated for 30 min at room temperature. Samples can be stored for up to 1 week – Falcon tubes were capped and placed in the fridge until all samples were collected.

Cell cycle analysis (24 h after agent addition)

Following centrifugation, the supernatant liquid was aspirated and cells resuspended in PBS containing 300 mL of 50 mg/mL propidium iodide (PI)/0.1 mg/mL RNaseA. At least 10 min incubation was allowed prior to flow cytometric analysis of cell cycle distribution.

Dual DNA damage (γH2AX) / cell cycle analysis (72 h after agent addition)

Cell suspensions were centrifuged and supernatant aspirated. During centrifugation, primary antibody (anti γH2AX - Millipore 05-636) dilution was prepared (1:3333 in 1% FBS in PBS). Cells were resuspended in the primary antibody solution (200 mL), the suspension was gently mixed and incubated for 1.5 h at room temperature. PBS (1 mL) was then added and the tube containing the suspension was centrifuged and supernatant discarded. During centrifugation, secondary antibody (goat anti-mouse AlexaFluor 488 (Molecular Probes A 10684) dilution was prepared (1:1750 in 1% FBS in PBS). Cells were resuspended in secondary antibody solution (200 mL), the suspension was then mixed gently and incubated for 1 h at room temperature. PBS (1

mL) was then added and tubes centrifuged and supernatant discarded. For cell cycle analysis, 300 mL of 50 mg/mL PI/0.1 mg/mL RNaseA in PBS was then added. At least 10 min incubation was allowed prior to flow cytometric analysis, followed by the transfer of cell/liquid suspension in a FACS tube / samples analysed on the flow cytometer.

4.2.6 Confocal microscopy - live imaging

MDA-MB-468 cells (3 x 10^5 cells) were seeded in glass-bottomed petridishes with a #1.5 thickness coverslip glued into the bottom of the Petri dish (MatTek Corp. Part No P35G-1.5-20-C) in 2 mL RMPI medium supplemented with 10% FBS. Cells were left to attach for 24 h. Medium was then aspirated, cells washed twice with HBSS and then stained with 4 uM Hoechst 33342 DNA stain (Sigma Aldrich CAS no. 23491-52-3) followed by incubation at 37 ^oC for 30 min. Staining solution was then aspirated, cells washed with HBSS and then re-stained with 1 mM ER-Tracker Red (BODIPY® TR Glibenclamide, E34250, Invitrogen) for 20 min. Staining solution was then aspirated, washed with medium, aspirated again and replaced with medium. Cells were then viewed under the fluorescence microscope. Fluorescent images (ex. 405nm / em. 410-500 nm for Hoechst 33342 and ex. 594nm / em. 600-730nm for ER-Tracker Red) were captured using a Zeiss LSM710 confocal on a Zeiss Observer with a PlanApo 40x / 1.30 oil objective running Zen software.

4.2.7 Relative protein phosphorylation

Relative protein phosphorylation levels of 24 kinases were detected simultaneously using the Human Phospho-Mitogen-activated Protein Kinase (MAPK) Antibody Array (Catalog # ARY002B) from R&D systems according to the manufacturer's instructions. Briefly, cells were seeded in Corning® tissue-culture treated culture

dishes (100mm x 20 mm). For MDA-MB-468, 1 x 10^6 cells were seeded per culture dish. Cells were then allowed to attach overnight and left untreated or treated with (*S*,*S*)-**4**, 20 μM, for 24 h. Cells were rinsed with PBS followed by solubilisation in lysis buffer by gently rocking the lysates at 4°C (30 min). The cell lysates were then microcentrifuged at 14,000 x g (5 min) and then the supernatant was transferred into a clean eppendorf tube. Quantitation of sample protein concentration was carried out using QuickStart Bradford Assay (Bio-Rad, Hemel Hempstead). Aliquots of the lysates were then stored frozen at −80°C. Membranes were blocked with the kit's blocking buffer at room temperature for 1 hour on a rocking platform shaker. Whilst membrane blocking, the 2 cell lysate samples (MDA-MB-468 – 24 h control and 24 h (*S*,*S*)-**4**, 20 μM) were diluted with array buffer followed by a cocktail of biotinylated detection antibodies. The sample was mixed and incubated at room temperature for 1 h. The sample/antibody mixture was placed on the membrane and the dish containing the membrane was incubated overnight at 4°C on a rocking platform shaker. Thereafter, cocktails of biotinylated detection antibodies were added at room temperature for 1 h. Phosphorylated proteins were revealed using streptavidin-HRP/Chemi Reagent Mix and autoradiography films (Amersham Hyperfilm ECL, GE Healthcare Life Sciences, Buckinghamshire, UK).

4.2.8 Western Blot analysis

MDA-MB-468 and HCT-116 cells were lysed in NP-40 lysis buffer supplemented with PhosSTOP Phosphatase Inhibitor Cocktail (Roche Applied Science) and COMPLETE-mini Protease Inhibitor Cocktail (Roche Applied Science). Cell debris was removed by centrifugation at 14,000 x g for 5 min. Protein concentrations were determined using QuickStart Bradford Assay (Bio-Rad, Hemel Hempstead, UK). Cell lysate proteins (50 μg) were separated by SDS-polyacrylamide gel

electrophoresis and then transferred to a nitrocellulose membrane. Membranes were probed with the following antibodies, all purchased from Cell Signaling Technologies: p-EGFR (Tyr1068), total-EGFR, p-AKT (Ser473), total-AKT, p-GSK3β (Ser9), total-GSK3β, p-ERK1/2(Thr202/Tyr204), total-ERK1/2 and GAPDH.

4.2.9 ICP-MS studies

Cells were grown as described (Section 4.2.1) in 5 ml of RPMI-1640 medium supplemented with 10% v/v foetal bovine serum (FBS). No titanium above background levels (0.3 ppb) could be detected in either of these components. Typically a known quantity of MDA-MB-468 cells (around 5×10^5) were grown in the presence (*S*,*S*)-**49aa** (30 μM), or its absence (control). Higher concertation-time loadings of (*S*,*S*)-**49aa** could not be used without engendering degradative lysis. At the end of 4 h, the growth medium of each sample was removed to a separate vial and the cells, now very close to paraptotic death, were washed with 2 × 2ml PBS, and the washings added to the vial containing the separated supernatant medium. The remaining cells were then treated with trypsin solution (1mL), spun to a pellet, the supernatant trypsin solution removed and added to the washing vial. The cell pellet was once more washed with PBS (1 ml). The pelleted cells were digested (16% w/w HNO_3, 3 mL, 95 ^oC, 2 h) and diluted with MilliQ water up to a final volume of 15 mL. The combined wash solutions were similarly digested. Analyses were conducted on a Thermo Scientific iCAP QC and indicated treated cells contained 3.3 ± 0.3 femtomol Ti per cell. Cells untreated with (*S*,*S*)-**49aa** showed only background levels (0.3-0.35 femtomol Ti per cell). If complete hydrolysis to TiO_2 of standard density (4.23 g cm^{-3}) was attained at 3.3 femtomol/cell the titanium would have to be

present in the cell as $>10^7$ aggregates of maximum 1-2 nm dimensions to have avoided detection in our TEM studies (Section 4.3). Analyses of the wash samples from (*S*,*S*)-**49aa** (30 μM) 4 h treated MDA-MB-468 cells indicates that the majority (>99.9%) of the applied titanium dose is recovered.

4.3 TEM studies

4.3.1 Instrument / cell culture

A JEOL 2100F TEM instrument equipped with Gatan Orius high sensitivity cameras was used. Atomic contrast HAADF imaging was performed using the JEOL Digital STEM system and Electron Energy Loss Spectroscopy (EELS) was via a Gatan Tridiem Filter. The TEM was also equipped with a state-of-the-art windowless X-MaxN 100TLE EDX detector, on loan from Oxford Instruments. This detector had been optimised for fast acquisition and improved light element detection, and so is significantly more suited to analysis of biological samples than previous generations of EDX detector. The system was also equipped with a Gatan 914 liquid nitrogen cooled holder, for stabilising heat-sensitive samples.

This configuration allows for analysis down to the nanometer (nm) scale at concentrations down to 0.01 at% for the typical sample thickness and acquisition time used in this study. Concentrations of Ti to 1 part in 10,000 C, or Ti content aggregates of greater than 1nm, would therefore be expected to be detectable if present within the cell.

MDA-MB-468 cells were cultured as per section 3.1 in thermanox coverslips in 6 well plates. Cells were left to attach for 24 h followed by exposure of 50 μM **49aa**

for up to 6 h. In order to achieve maximum dose-time exposure and to maximise the opportunity for uptake and detection of titanium, *meso/rac*-**49aa** was utilised. Untreated control cells and titanocene treated cells were fixed with 3% EM glutaraldehyde in 0.1 M cacodylate buffer for 1 h at 4 ^{o}C. Fixed cells were then washed with 0.1 M cacodlyate buffer followed by post-fixation with 1% aqueous osmium tetraoxide for 30 minutes. Samples were then washed with distilled water (5 min) followed by dehydration in graded ethanol series from 50% to 70% to 90% to 100%. The coverslips were then transferred to a clean porcelain dish and washed (2 x 5 min) with 100% propylene oxide. Resin (25 mL araldite CY212 resin, 15 mL agar 100 resin, 55 mL DDSA, 2 mL dibutyl phthalate and 1.5 mL DMP 30) was prepared and the samples were then infiltrated with this resin mixture. Samples were then embedded by inverting the coverslip on a BEEM capsule filled with the resin so that only the cell layer is embedded in the resin. The sample was then left in an embedding oven for 48 hours at 60 ^{o}C. The resin sample was then sectioned using an ultramicrotome (200 nM thickness) and embedded in a copper mesh grid and stained with uranyl acetate/lead citrate.

Imaging and elemental analysis in the TEM was performed on microtomed sections, both on sections supported on copper mesh grid only – i.e. sample against vacuum – or on sections additionally supported on newly commercially available graphene oxide support grids (Agar Scientific) that became available during this study. The graphene oxide films provide a charge and heat conductive support that stabilises the sample under the electron beam, allowing longer acquisition times.[141]

References

1. National Cancer Institute. http://www.cancer.gov/cancertopics/what-is-cancer (accessed April 3, 2015).
2. Ferlay, J.; Soerjomataram, I.; Dikshit, R.; Eser, S.; Mathers, C.; Rebelo, M.; Parkin, D. M.; Forman, D.; Bray. F. *Int. J. Cancer*. **2015**, *136,* 359-386.
3. Bauer, K. R.; Brown, M.; Cress, R. D.; Parise, C. A.; Caggiano. V. *Cancer*. **2007**, *109,* 1721-1728.
4. Agranat, I.; Caner, H.; Caldwell. J. *Nat Rev Drug Discov*. **2002**, *1*, 753-768.
5. Smith. S. W. *Toxicol. Sci.* **2009**, *110,* 4-30.
6. McConathy, J.; Owens. M. J. *J. Clin Psychiatry*. **2003**, *5,* 70-73.
7. Chhabra, N.; Aseri, M. L.; Padmanabhan. D. *Int. J. Appl Basic Med Res*. **2013**, *3*, 16-18.
8. Hutt, A. J.; Valentova. J. *Acta Facult. Pharm. Univ. Comenianae*. **2003**, *50,* 7-23.
9. Dlorea, A.; Busselberg. D. *Cancers*. **2011**, *3,* 1351-1371.
10. Ozols. R. F. *Cancer Treat. Rev*. **1991**, *18,* 77-83.
11. Ozols. R. F. Hematol. *Oncol. Clin. N. Am*. **1992**, *6,* 879-894.
12. Abu-Surrah, A.; Kettunen. M. *Curr. Med. Chem*. **2006**, *13,* 1337-1357.
13. Siddik. Z. H. *Oncogene*. **2003**, *22*, 7265-7279.
14. Eastman. A. *Pharmacol. Ther*. **1987**, *34,* 155-156.
15. Reedijk. J. *Platinum Metals Rev.* **2008**, *52*, 2-11.
16. Fichtinger-Schepman, A. M. J.; van der Veer, J. L.; den Hartog, J. H. J.; Lohman, P. H. M.; Reedijk. J. *Biochem.* **1985**, *24*, 707.

17. Bellon, S. F.; Coleman, J. H.; Lippard. S. J. *Biochem*. **1991**, *30,* 8026-8035.

18. Shi, L.; Nishioka, W. K.; Thing, J.; Bradbury, E. M.; Litchfield, D. W.; Greenberg. A. H. *Science*. **1994**, *263,* 1143-1145.

19. He, G.; Siddik. Z. H. *Proc. Am. Assoc. Cancer Res*. **2001**, *42,* 901.

20. Appella, E.; Anderson. C. W. *Eur. J. Biochem*. **2001**, *268,* 2764-2772.

21. Delmastro, D. A.; Vaisman, A.; Solle, M.; Chaney. S. G. *Cancer Chemother. Pharmacol.* **1997**, *39,* 245-243.

22. Dent, P.; Grant. S. *Clin. Cancer Res*. **2001**, *7,* 775-783.

23. Ormerod, M. G.; O'Neill, C.; Robertson, D.; Kelland, L. R.; Harrap. K. R. *Cancer Chemother. Pharmacol.* **1996**, *37,* 463-471.

24. Henkels, K. M.; Turchi. J. J. *Cancer Res.* **1999**, *59,* 3077-3083.

25. Cui, Y.; Konig, J.; Buchholz, J. K.; Spring, H.; Leier, I.; Keppler. D. *Mol. Pharmacol.* **1999**, *55,* 929-937.

26. Koike, K.; Kawabe, T.; Tanaka, T.; Toh, S.; Uchiumi T. et. al. *Cancer Res*. **1997**, *57,* 5475-5479.

27. Komatsu, M.; Sumizawa, T.; Mutoh, M.; Chen, Z. S.; Terada K. et. al. *Cancer Res*. **2000**, *60,* 1312-1316.

28. Arnesano, F.; Pannuzio, A.; Coluccia, M.; Natile. G. *Coord. Chem. Rev.* **2015**, *284*, 286-297.

29. Stordal, B.; Pavlakis, N.; R. Davey. *Cancer Treat. Rev.* **2007**, *33,* 347-357.

30. Kopf, H.; Kopf-Maier. P. *Angew. Chem. Int. Ed. Eng.* **1979**, *18*, 477-478.

31. Kopf-Maier, P.; Kopf, H.; Wagner, W.; Hesse. B. *Eur. J. Cancer.* **1981**, *17,* 665-669.

32. Kopf-Maier, P.; Kopf. H. In *Metal Compounds in Cancer Therapy,* Fricker, S. P., Chapman & Hall, London, 1994; pp 109-146.

33. Kopf-Maier, P.; Klapotke. T. *Arzneim-Forsch.* **1987**, *37*, 532-534.

34. Kopf-Maier, P.; Klapotke, T.; Kopf, H.; Preiss, F.; Marx. T. *Anticancer Res.*, **1986**, *6*, 33-37.

35. Kopf-Maier, P.; Hesse, B.; Kopf. H.; *J. Cancer Res. Clin. Oncol.*, **1980**, *96*, 43-51.

36. Kopf-Maier. P.; *Cancer Chemother. Pharmacol.*, **1989**, *23*, 225-230.

37. Christodoulou, C. V.; Ferry, D. R.; Fyfe, D. W.; Young, A.; Doran, J.; Sheehan T. M. et. al.. *J. Clin. Oncol.*, **1998**, *16*, 2761-2769.

38. Korfel, A.; Scheulen, M. E.; Schmoll, H. J.; Grundel, O.; Harstrick A.; et. al. *Clin. Can. Res*. **1998**, *4,* 2701-2708.

39. Muller, B. W.; Muller R.; Lucks S.; Mohr W; Patent 5296237 A, 1994.

40. Kroger, N.; Kleeberg, U. R.; Mross, K.; Edler, L.; Hossfeld. D. K.; *Onkologie*. **2000**, *23,* 60-62.

41. Lummen, G.; Sperling, H.; Luboldt, H.; Otto, T.; Rubben. H.; *Cancer Chemo. Pharm.* **1998**, *42,* 415-417.

42. Buettner, K. M.; Valentine. A. M. Chem. Rev. **2012,** *112,* 1863-1881.

43. Dabrowiak. J. C. In *Metals in Medicine;* Wiley, Chichester, 2009; pp 176.

44. Mendelez. E. *Crit. Rev. Oncol. Haem*. **2002**, *42,* 309-315.

45. Kopf-Maier, P.; Krahl. D. *Naturwissenshaften*. **1981**, *68,* 273-274.

46. Kopf-Maier, P.; Krahl. D. *Chem Biol Interactions*. **1983**, *44,* 317-328.

47. Guo, M.; Guo, Z.; Sadler. P. J. *J. Biol. Inorg. Chem* **2001**, *6,* 698-707.

48. Mokdsi, G.; Harding. M. M. *J. Organomet. Chem* **1998**, *565,* 29-35.

49. Toney, J. H.; Marks. T. J. *J. Am. Chem. Soc.* **1995**, *107,* 947-953.

50. Doppert. K. *Naturwissenschaften*. **1990**, *77,* 19-24.

51. Erxleben, A.; Claffey, J.; Tacke. M. *J. Inorg. Biochem.* **2010**, *104,* 390-396.

52. Tacke. M. *Lett. Drug Design Discov.* **2008**, *5,* 322-335.

53. Kuo, L. Y.; Liu, A. H.; Marks. T. J. In *Metal ions in biological systems;* A. Sigel, H. S., Ed.; New York: Marcel Dekker, 1996; pp 53-85.

54. Harding, M. M.; Mokdsi. G. *Curr. Med. Chem*. **2000**, *7,* 1289.

55. Abeysinghe, P. M.; Harding. M. M. *Dalton Trans.* **2007**, *32,* 3474-3482.

56. Pizarro, A. M.; Habtemariam, A.; Sadler. P. J. *Top. Organomet. Chem*. **2010**, *32,* 21-56.

57. Gao, L. M.; Hernandez, R.; Matta, J.; Melendez. E. *J. Biol. Inorg. Chem*. **2007**, 959-967.

58. Guo, M.; Sun, H.; McArdle, H. J.; Gambling, L.; Sadler. P. J. *Biochemistry*. **2000**, *39,* 10023-10033.

59. Hernandez, R.; Lamboy, J.; Gao, L. M.; Matta, J.; Roman, F. R.; Melendez. E.; *J. Biol Inorg Chem*. **2008**, *13*, 685-692.

60. Tshuva, E. Y; Ashenhurst. J. A. *Eur J. Inorg. Chem*. **2009**, *2009,* 2203-2218.

61. Tshuva, E. Y.; Peri. D. *Coord. Chem. Rev*. **2009**, *253,* 2098-2115.

62. Immel, T. A.; Groth, U.; Huhn. T. *Chemistry*. **2010**, *16,* 2775-2789.

63. Schur, J.; Manna, C. M.; Deally, A.; Koster, R. W.; Tacke M. et. al. *Chem. Commun*. **2013**, *49,* 4785-4787.

64. Osella, D.; Ravera, M.; Cassino, C.; Monti, E.; Gariboldi M. et. al. *J. Inorg.*

Biochem. **2005**, *99,* 2264-2269.

65. Vessieres, A.; Plamont, M. A.; Cabestaing, C.; Claffey J. et. al. *J. Organomet. Chem*. **2009**, *694,* 874-879.
66. Sarsam, S. W.; Nutt, D. R.; Strohfeldt, K.; Watson. K. A. *Metallomics* **2011**, *3,* 152-161.
67. Bowman. D. C. *J. Chem Educ*. **2006**, *83,* 735-740.
68. Cuenca. T. In *Comprehensive Organometallic Chemistry III;* Elsevier; Vol. 4, 2007; pp 323-695.
69. Halterman. R. L. *Chem. Rev*. **1992**, *92,* 965-994.
70. Hogan, M.; Tacke. M. *Topics in Organometallic Chemistry;* Springer, Vol. 32, New York, 2010; pp 119-140.
71. Strohfeldt, K.; Tacke. M. *Chem Soc. Rev.* **2008**, *37,* 1174-1187.
72. Allen, O. R.; Croll, L.; Gott, A. L.; Knox, R. J.; McGowan. P. C. *Organometallics*. **2004**, *23,* 288-292.
73. Neuenschwander. M. The Chemistry of Double-bonded Functional Groups. Patai, S., Ed.; Vol. 2, Wiley, Unwin Brothers Limited, 1989; pp 1131-1268.
74. Stone, K. J.; Little. R. D. *J. Org. Chem*. **1984**, *49,* 1849-1853.
75. Moise, C.; Leblanc, J. C.; Tirouflet. J. *Tetrahedron Lett*. **1974**, *19,* 1723-1724.
76. Pampillon, C.; Claffey, J.; Strohfeldt, K.; Tacke. M. *Eur. J. Med Chem*. **2008**, *43,* 122-128.
77. Eisch, J. J.; Shi, X.; Owuor. F. A. *Organometallics*. **1998**, *17,* 5219-5221.
78. Tacke, M.; Cuffe, L. P.; Gallagher, W. M.; Lou, Y.; Mendoza O. et. al. *J. Inorg. Biochem*. **2004**, *98,* 1987-1994.

79. Rehmann, F. J. K.; Rous, A. J.; Mendoza, O.; Sweeney, N. J.; Strohfeldt. K. *Polyhedron*. **2005**, *24,* 1250-1255.

80. Rehmann, F. J. K.; Cuffe, P.; Mendoza, O.; Rai, D. K.; Sweeney. N. *App. Organomet. Chem*. **2005**, *19,* 293-300.

81. Strohfeldt, K.; Muller Bunz, H.; Pampillon, C.; Sweeney, N. J.; Tacke. M. *Eur. J. Inorg. Chem*. **2006**, 4621-4628.

82. Vos, D.; Jutzi. P. *Synthesis*. **2000**, *3,* 357-359.

83. Qing-Hui, Z.; Yu-Long, L.; Zheng-Jie, H.; Shou-Shan. C. *Chem. J. Chinese Univ*. **1995**, *16,* 1706-1709.

84. Suttil, J. A.; McGuinness, D. S.; Evans. S. J. *Dalton Transactions*. **2010**, *39,* 5278-5285.

85. Ceron, D. P.; Ruiz, S. G.; Prashar, S.; Fajardo, M.; Antinoio, A.; Otero. A. *Chem. Commun*. **2007**, *72,* 747-763.

86. Ceballos-Torres, J.; Gomez-Ruiz, S.; Kaluderovic, G. N.; Fajardo, M.; Paschke, R.; Prashar. S. *J. Organomet. Chem*. **2012**, *700,* 188-193.

87. Erker, G.; R. Nolte, R. Aul, S. Wilker, C. Kruger, R. Noe. *J. Am. Chem. Soc.* **1991**, *113,* 7594-7602.

88. Welker, M.; Woodward, S.; Alexakis. A. *Org. Lett*. **2010**, *12,* 576-579.

89. Tang, X.; Blake, A. J.; Lewis, W.; Woodward. S. *Tetrahedron: Asym*. **2009**, *20,* 1881-1891.

90. Tang, X.; Woodward, S.; Krause. N. *E. J. Org. Chem*. **2009**, 2836-2844.

91. Edwards, A. J.; Paver, M. A.; Raithby, P. R.; Rennie, M. A.; Russell, C. A.; Wright. D. S. *Organometallics.* **1994**, *13,* 4967-4972.

92. Johnson, A. L.; Willcocks, A. M.; Raithby, P. R.; Warren, M. R.; Kingsley, A. J.; Odedra. R. *Dalton Trans.* **2009**, 922-924.

93. Swart. M. *Inorg. Chim. Acta*. **2007**, *360,* 179-189.

94. Shoshkin, A. N.; Bochkarev, L. N.; Khorshev. S. Y. *Russ. J. Gen. Chem*. **2002**, *72,* 715-716.

95. Honzicek, J.; Klepalova, I.; Vinklarek, J.; Padelkova, Z.; Cisarova I. et. al. *Inorg. Chim. Acta*. **2011**, *373,* 1-7.

96. Woodward. S. *Tetrahedron*. **2002**, *58,* 1017-1050.

97. Claffey, J.; Hogan, M.; Bunz, H. M.; Pampillon, C.; Tacke. M. J. *Organomet. Chem*. **2008**, *693,* 526-536.

98. Cambridge Crystallographic Data Centre (CCDC, www.ccdc.cam.ac.uk). Structures used were: ECUHEQ, ECUJAO, KEDKEJ, MAJMAM and VATWAO.

99. Keltera, G.; Sweeney, N. J.; Strohfeldt, K.; Fiebig, H. H.; Tacke. M. *Anti-Cancer Drugs*. **2005**, *16,* 1091-1098.

100. Gomez-Ruiz, S.; Maksimovic-Ivanic, D.; Mijatovic, S.; Kaluoerovic. G. N. *Bioinorg. Chem. and Appl*. **2012**, 1-14.

101. Olszewski, U.; Hamilton. G. *Anti-Cancer Agents Med. Chem.* **2010**, *10,* 302-311.

102. Zhao, Y. H.; Abraham, M. H.; Zissimos. A. M. *J. Org. Chem*. **2003**, *68*, 7368-7373.

103. Alexakis, A.; Krause N.; Woodward S. Ed. In *Copper-Catalyzed Asymmetric Synthesis;* Wiley-VCH Verlag GmbH & Co., Weinheim, Germany, 2014

104. Brintzinger, H. H.; Fisher, D.; Mulhaupt, R.; Reiger, B.; Waymouth. R. M. *Angew. Chem. Int. Ed. Engl.* **1995**, *34,* 1143-1170.

105. Didier, D.; Marek. I. In *Copper-Catalyzed Asymmetric Synthesis;* A. Alexakis, N. K. S. W., Ed.; Wiley-VCH; pp 273-274.

106. Nakamura, M.; Hirai, A.; Nakamura. E. *J. Am. Chem. Soc.* **2000**, *112,* 978-979.

107. Kramer, K.; Leong, P.; Lautens. M. *Org. Lett.* **2011**, *13,* 819-821.

108. Lautens, M.; Hiebert. S. *J. Am. Chem. Soc.* **2004**, *126,* 1437-1447.

109. Mintz, E. A. PCT Int. Appl. WO 9212112 A1 19920723, 1992.

110. Abbenhuis, H. C. L.; Burckhardt, U.; Gramlich, V.; Togni, A.; Albinati, A.; Mullers. B. *Organometallics* **1994**, *13,* 4481-4493.

111. Suzuka, T.; Ogasawara, M.; Hayashi. T. *J. Org. Chem* **2002**, *67,* 3355-3359.

112. Cini, M.; Bradshaw, T. D.; Lewis, W.; Woodward. S. *Eur. J. Org. Chem* **2013**, 3997-4007.

113. Teichert, J. F.; Feringa. B. L. *Angew. Chem. Int. Ed.* **2010**, *49,* 2486-2528.

114. Coskun, N.; Erden. I. *Tetrahedron* **2011**, *67,* 8607-8614.

115. Claffey, J.; Hogan, M.; Bunz, H. M.; Pampillon, C.; Tacke. M. *Chem Med Chem* **2008**, *3,* 729-731.

116. Moore, J. W.; Pearson. R. G. Kinetics and Mechanism. Wiley-Interscience New York, 1981; Vol. 3rd Ed.

117. Billo. E. J. Excel for Chemists: A Comprehensive Guide. Ed. John Wiley & Sons Inc. New York, 2011; Vol. 3rd Ed..

118. Potter. G. D. *A novel series of titanocene dichloride derivatives: synthesis,*

characterization and assessment of their cytotoxic properties; Queen's University Canada, 2008.

119. Tannock, I. F.; Rotin. D. *Cancer Res*. **1989**, *49,* 4373-4384.

120. Ravera, M.; Cassino, C.; Monti, E.; Gariboldi, M.; Osella. D. *J. Inorg. Biochem*. **2005**, *99,* 2264-2269.

121. Cuffe, S.; Dowling, C.M.; Claffey, J.; Pampillon, C.; Hogan, M.; Fitzpatrick, J.M.; Carty, M.P.; Tacke, M.; Watson. R.W. *The Prostate* **2011**, *71,* 111-124.

122. O'Connor, K.; Gill, C.; Tacke, M.; Rehmann, F. J.; Strohfeldt, K.; Sweeney, N.; Fitzpatrick, J. M.; Watson. R. W. *Apoptosis*. **2006**, *11,* 1205-1214.

123. Christodoulou, C. V.; Eliopoulos, A. G.; Young, L. S.; Hodgkins, L.; Ferry, D. R.; Kerr. D. J. *Br. J. Cancer*. **1998**, *77,* 2088-2097.

124. Kuo, L. J.; Yang. L. X. *In Vivo*. **2008**, *22,* 305-309.

125. Rieger, A. M.; Nelson, K. L.; Konowalchuk, J. D.; Barreda. D. R. *J. Vis. Exp.* **2011**, 1-4.

126. Vermes, I.; Haanen, C.; Steffens-Nakken, H.; Reutelingsperger. C. A. *J. Immun. Meth*. **1995**, *184,* 39-51.

127. Winey, M.; Meehl, J. B.; O'Toole, E. T.; Giddings Jr. T. H. *Mol. Bio. Cell*. **2014**, *25,* 319-323.

128. Heckman. C. *Nat. Prot*. **2008**, Protocol 251.

129. Kitambi, S. S.; Toledo, E. M.; Usoskin, D.; Wee, S.; Harisanker A. et. al. *Cell*. **2014**, *157,* 313-328.

130. Rashkow, J. T.; Patel, S. C.; Tappero, R.; Sitharaman Soc. B. *J. R. Soc. Interface*. **2013**, *94*, 1152.

131. Speradino, S.; Poksay, K.; De Belle, I.; Lafuente, M. J.; Liu, B.; Nasir, J.; Bredesen. D. E. *Cell Death Differ*. **2004**, *11,* 1066-1075.

132. Eombonne, J.; Padron, L.; Enjalbert, A.; Krantic, S.; Torriglia. A. *Apoptosis*. **2006**, *11,* 367-375.

133. Wang Y, Li X; Wang, L.; Ding, P.; Zhang, Y.; Han W. Ma D. *J. Cell Sci*. **2004**, *117,* 1525-1532.

134. Zhang, J.; Zhang, L.; Shen L. Xu X-M *Oncology Lett*. **2013**, *5,* 756-760.

135. Roy, H. K.; Olusola, B. F.; Clemens, D. L.; Karolski, W. J.; Ratashak, A.; Lynch, H. T.; Smyrk. T. C. *Carcinogenesis*. **2002**, *23,* 201-205.

136. Wortzel, I.; Seger. R. *Genes Cancer*. **2011**, *2,* 195-209.

137. Park, E-J.; Lee, S. Y.; Lee, G-H.; Kim, D-W.; Kim, Y.; Cho, M-H.; Kim. J-H. *Toxicology Lett*. **2014**, *230,* 69-79.

138. Ritter. S. K. *Chem. Eng. News*. **2012**, *90,* 9.

139. Ren, W.; Liu, Z.; Wen, Y.; Zhang, R.; Lu. X. *J. Am. Chem. Soc*. **2009**, *131,* 11509-11518.

140. Tzur, E.; Szadkowska, A.; Ben-Asuly, A.; Makal, A.; Goldberg, I.; Wozniak, K.; Grela, K.; Lemcoff. N. *Chem. Eur. J*. **2010**, *16,* 8726-8737.

141. Pantelic, R. S.; Meyer, J. C.; Kaiser, U.; Stahberg. H. *Solid Stat Commun*. **2012**, *152,* 1375-1382.

Appendix

A1.1: Mass spectrometry

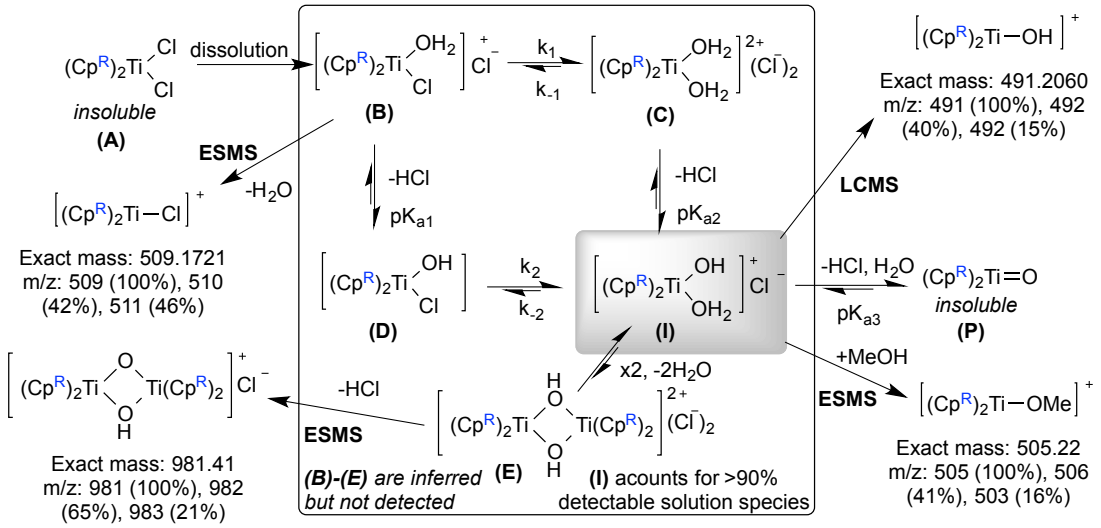
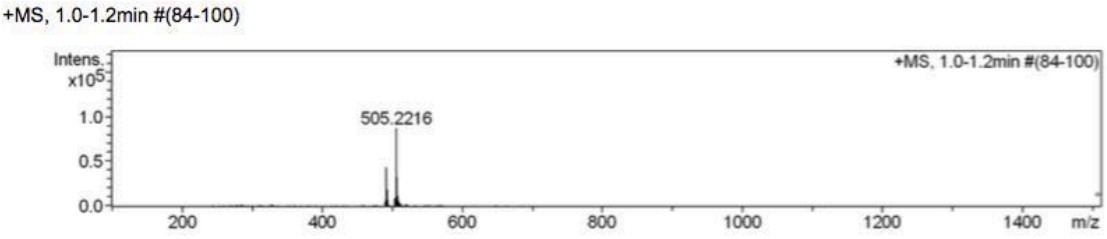
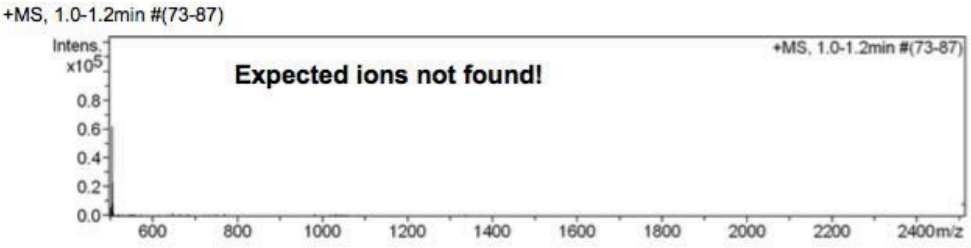


Figure A1: ESMS (in 1% DMSO/99% D_2O) and LCMS studies (in 1% DMSO/99% D_2O or RPMI 1640 medium alone) point to a single major homogeneous species whose daughter ions are consistent with the presence of $[(Cp^R)_2Ti(OH)(OH_2)]Cl$ (**I**) being the major soluble intermediate attained upon dissolution of (*S,S*)-**49aa**.



#	m/z	I %
1	285.2068	1.4
2	327.0829	1.1
3	457.2364	0.7
4	489.2106	4.6
5	490.2116	5.8
6	491.2068	49.5
7	492.2091	20.2
8	493.2087	7.7
9	494.2093	1.7
10	503.2268	8.6
11	504.2271	10.7
12	505.2216	100.0
13	506.2251	36.9
14	507.2221	12.5
15	508.2179	3.0
16	509.1745	5.7
17	510.1763	2.3
18	511.1718	2.6
19	512.1747	0.8
20	519.2018	1.7

Figure A2: ESMS spectrum of (*S,S*)-**49aa** in 1% DMSO / 99% D_2O. The molecular ion peak $[(Cp^R)2Ti(OMe)]^+$ is due to the presence of methanol from the 'sipper' robot in the MS system.

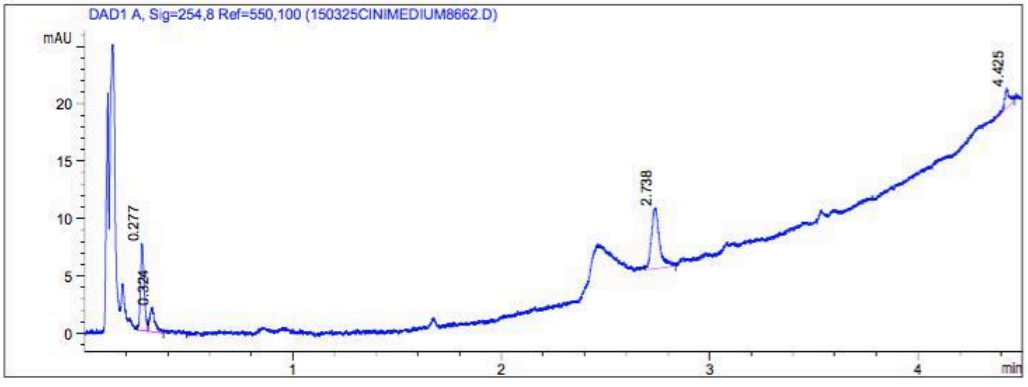


#	m/z	I %
1	503.2265	8.5
2	504.2271	10.8
3	505.2219	100.0
4	506.2254	36.6
5	507.2233	13.2
6	508.2248	3.0
7	509.2197	0.6
8	519.2027	1.4
9	520.2053	0.6
10	531.2007	0.8
11	545.2171	1.1
12	546.2186	0.5
13	548.5061	0.5
14	553.4606	1.3
15	554.4655	0.5
16	647.4605	1.4
17	648.4648	0.6
18	769.4874	0.9
19	770.4879	0.5
20	981.4082	0.4

Figure A3: GC-MS spectrum of (*S,S*)-**49aa** in 1% DMSO / 99% D_2O after 20 h (presence of dimer).

University of Nottingham- HPLC-MS report for CiniMedium

Data File name: D:\WALKUP\PCZSW\15-03\150325CINIMEDIUM8662.D
Standard Bradshaw lab growth medium as supplied by M. Cini
Walkup method: 'F9505A'
Data acquired by: Admin
on: 3/25/2015 at 2:23:11 PM
Method: C:\Chem32\1\METHODS\F9505A-RESEARCH.M
Injection Vol : 2.0 ul
Column: 30.00MM Sunfire
Vial: Vial 11

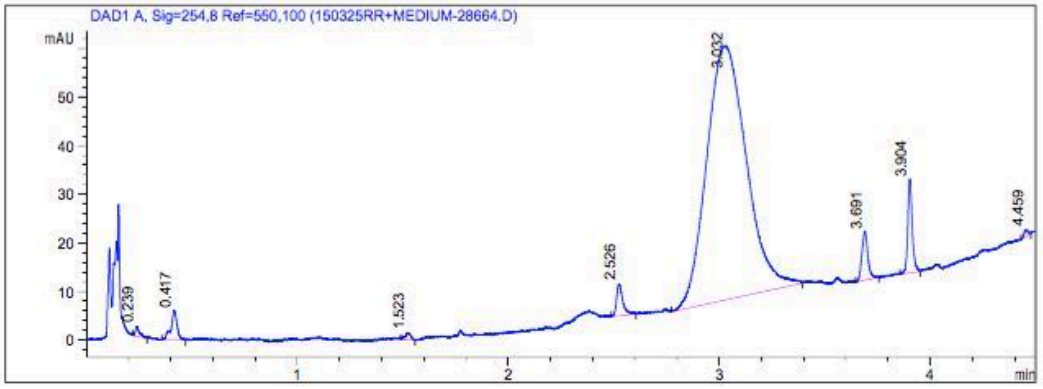


#	Meas. RT	Peak Type	Height	Width	Area	Area %
1	0.277	BV	7.424	0.020	9.347	30.836
2	0.324	VB	2.022	0.024	3.601	11.880
3	2.738	BB	5.176	0.038	14.259	47.042
4	4.425	BB	1.589	0.026	3.105	10.242

Figure A4: LC-MS spectrum of RPMI-1640 medium only

University of Nottingham- HPLC-MS report for RR+Medium-2

Data File name: D:\WALKUP\PCZTM\15-03\150325RR+MEDIUM-28664.D
Re-run RR+Medium now looking for 491
Walkup method: 'F9505A-MASS'
Data acquired by: Admin
on: 3/25/2015 at 2:39:44 PM
Method: C:\Chem32\1\METHODS\F9505A-MASS.M
Injection Vol : 2.0 ul
Column: 30.00MM Sunfire
Vial: Vial 13



#	Meas. RT	Peak Type	Height	Width	Area	Area %
1	0.239	BB	2.019	0.019	2.805	0.365
2	0.417	BB	6.061	0.030	12.680	1.651
3	1.523	BB	1.448	0.024	2.901	0.378
4	2.526	BB	6.620	0.031	13.998	1.822
5	3.032	BB	52.282	0.154	685.152	89.198
6	3.691	BB	10.006	0.030	19.871	2.587
7	3.904	BB	19.225	0.023	28.720	3.739
8	4.459	BB	1.340	0.022	2.002	0.261

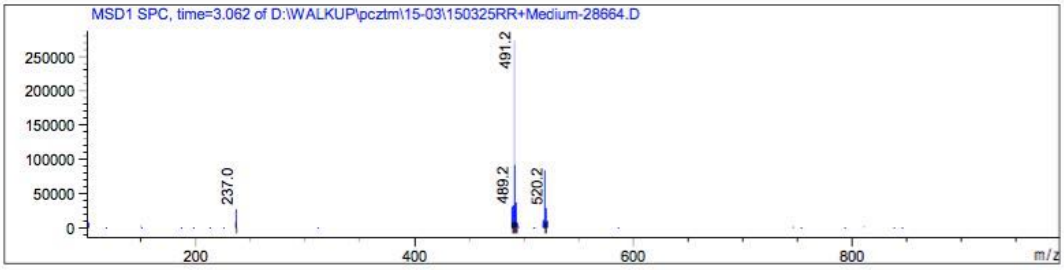


Figure A5: LC-MS spectrum of RPMI-1640 medium + (*S*,*S*)-**49aa**.

A1.2: Hydrolysis NMR spectroscopy

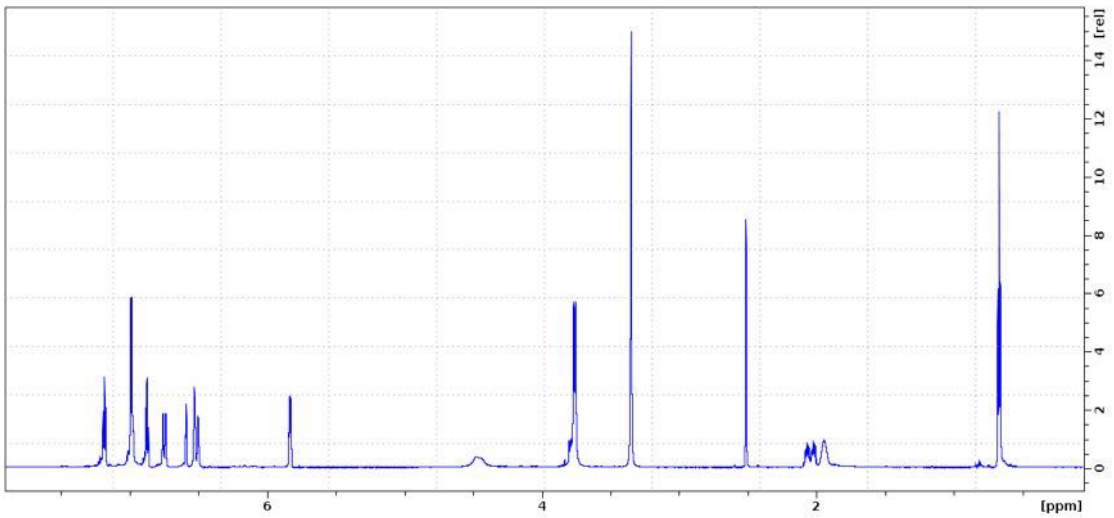


Figure A6: NMR spectrum of (*rac/meso*)-**49aa** in D_6-DMSO

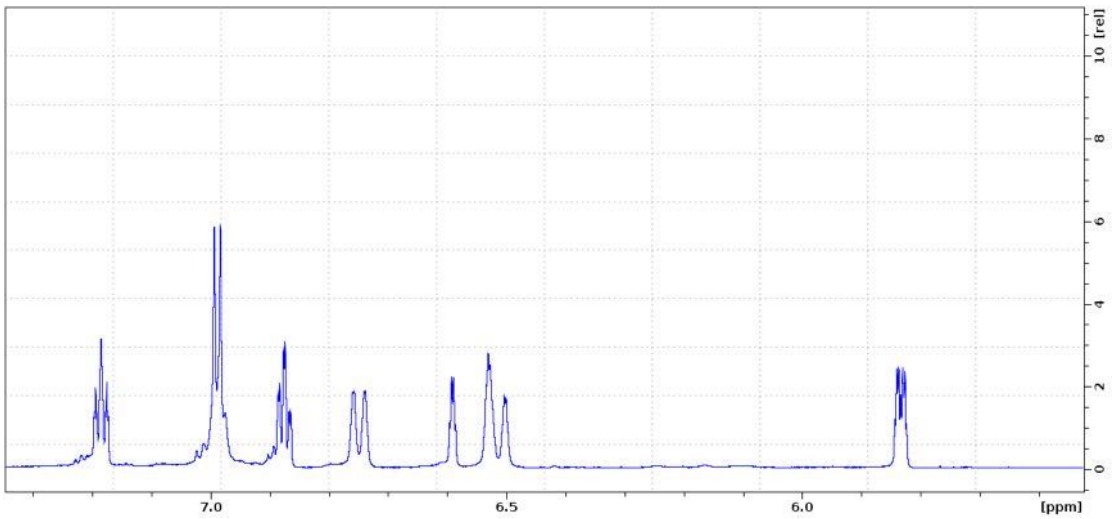


Figure A7: Aromatic region NMR spectrum of (*rac/meso*)-**49aa** in D_6-DMSO.

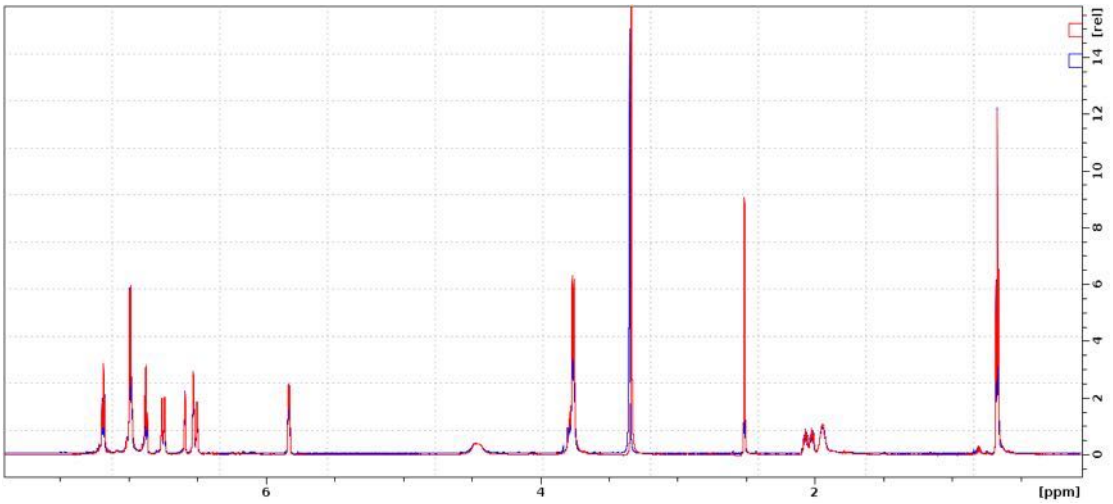


Figure A8: NMR spectrum of (*rac/meso*)-**49aa** at 0 h (blue) and 48 h (red) from dissolution of sample in D_6-DMSO.

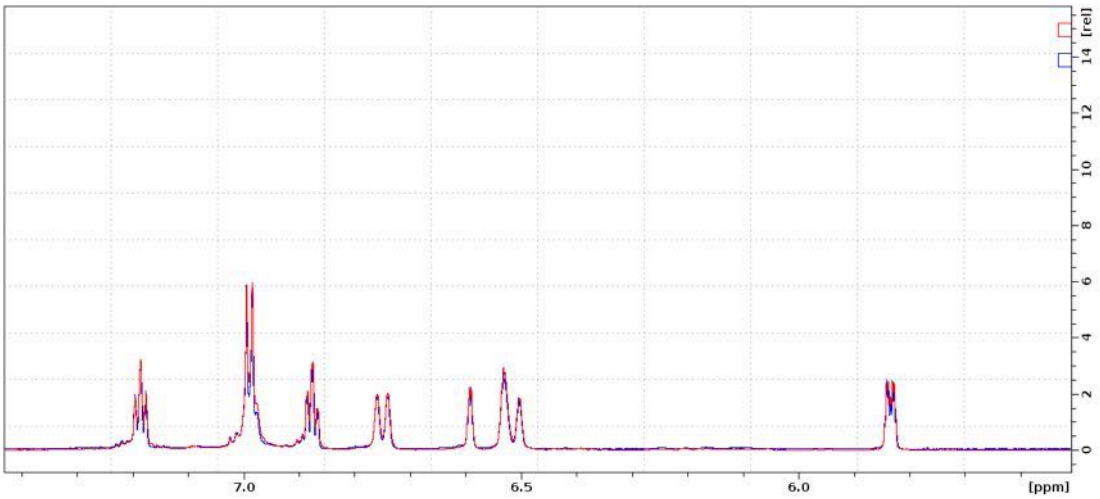


Figure A9: Ar region NMR spectrum of (*rac/meso*)-**49aa** at 0 h (blue) and 48 h (red), from dissolution of sample in D_6-DMSO.

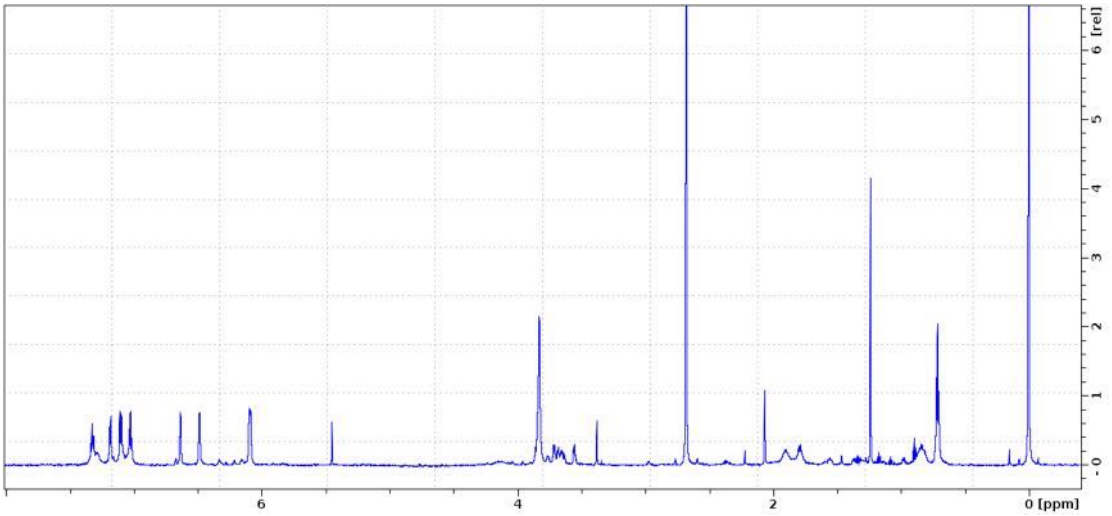


Figure A10: NMR spectrum of (*R,R*)-**49aa** in 1% D_6-DMSO / 99% D_2O at $[\mathbf{I}]_{max}$

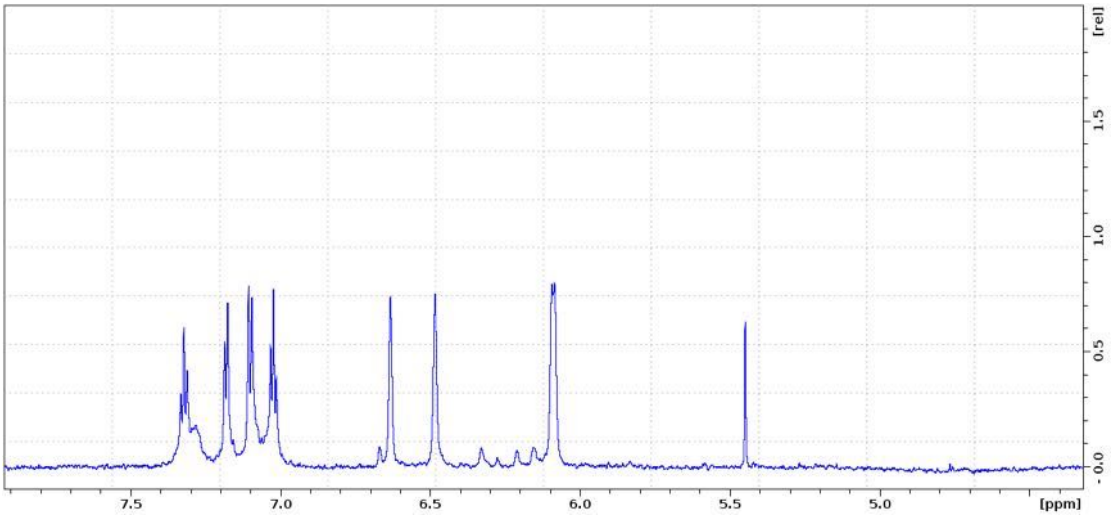


Figure A11: NMR spectrum of (*R,R*)-titanocene in 1% D_6-DMSO / 99% D_2O at $[\mathbf{I}]_{max}$

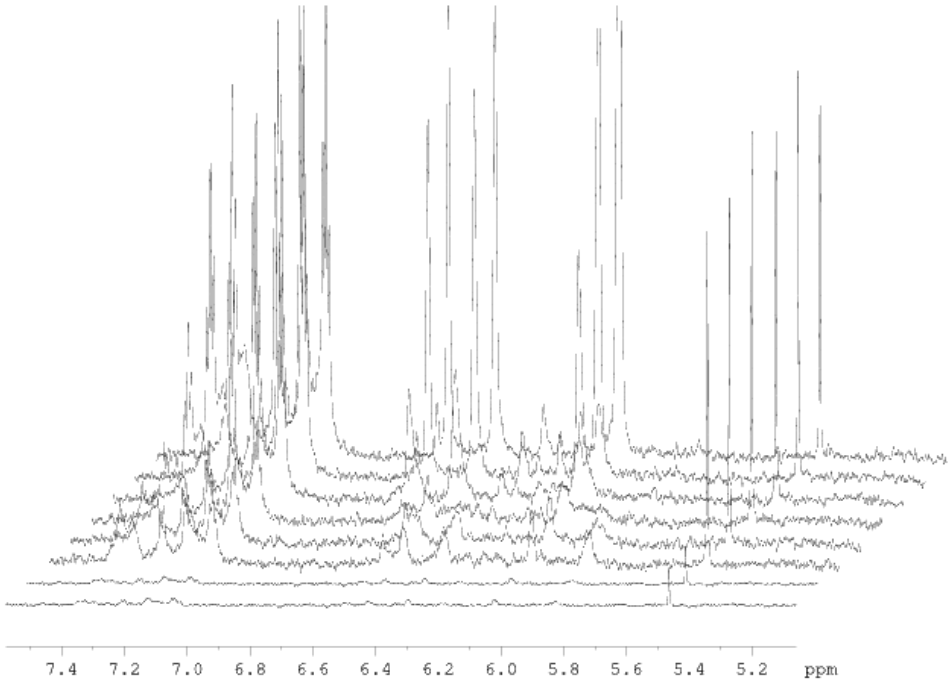


Figure A12: NMR spectra stack of (*R,R*)-**49aa** aromatic region in 1% D_6-DMSO / 99% D_2O at [**A**] to $[\mathbf{I}]_{max}$.

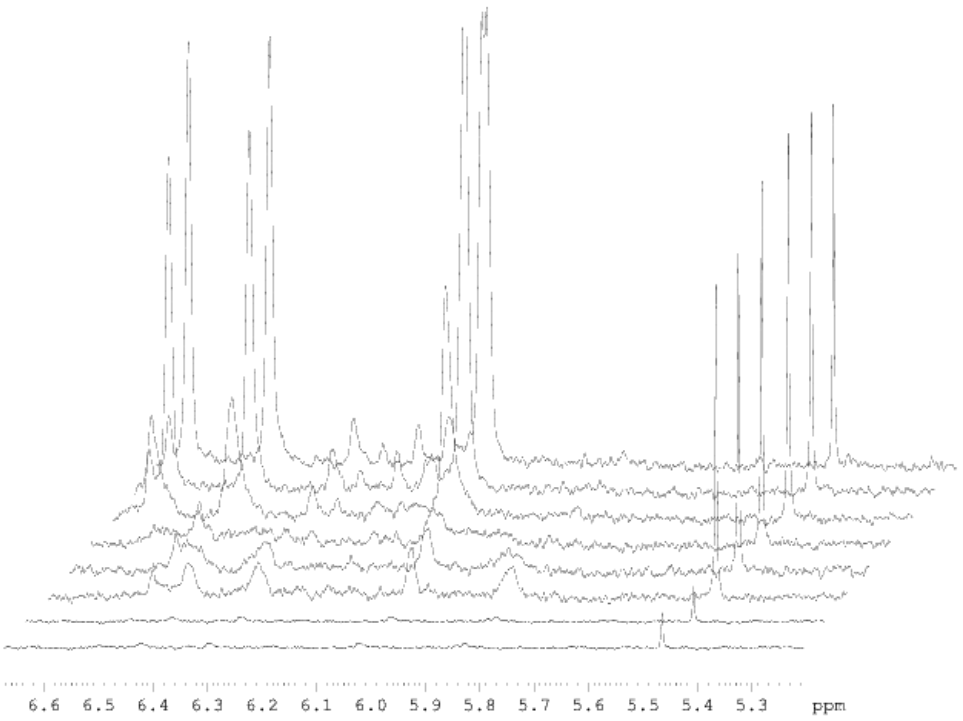


Figure A13: NMR spectra stack of (*R,R*)-**49aa** aromatic region in 1% D_6-DMSO / 99% D_2O at [**A**] to $[\mathbf{I}]_{max}$.

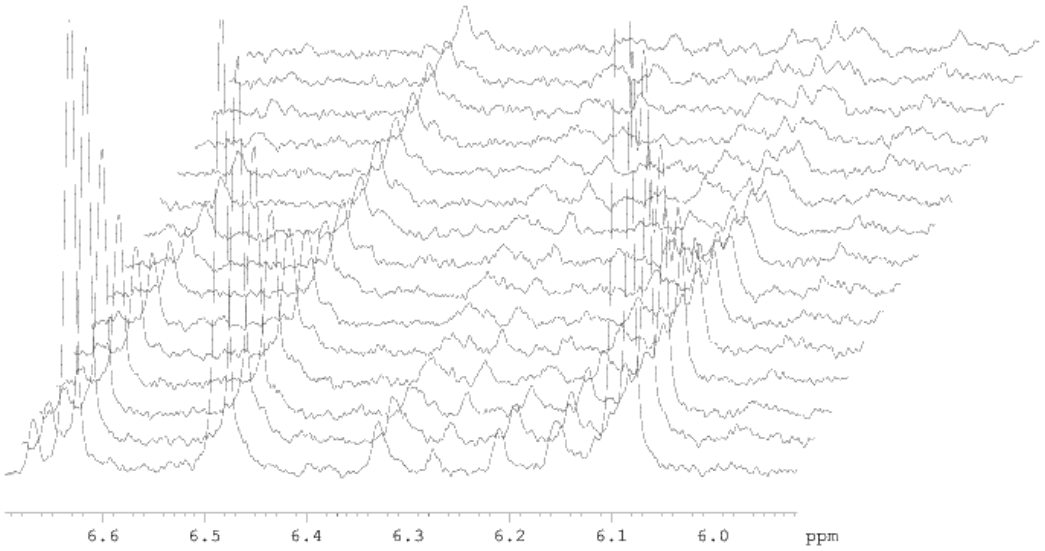


Figure A14: NMR spectra stack of (*R,R*)-**49aa** cyclopentadienyl region in 1% D_6-DMSO / 99% D_2O at $[\mathbf{I}]_{max}$ to [**P**].

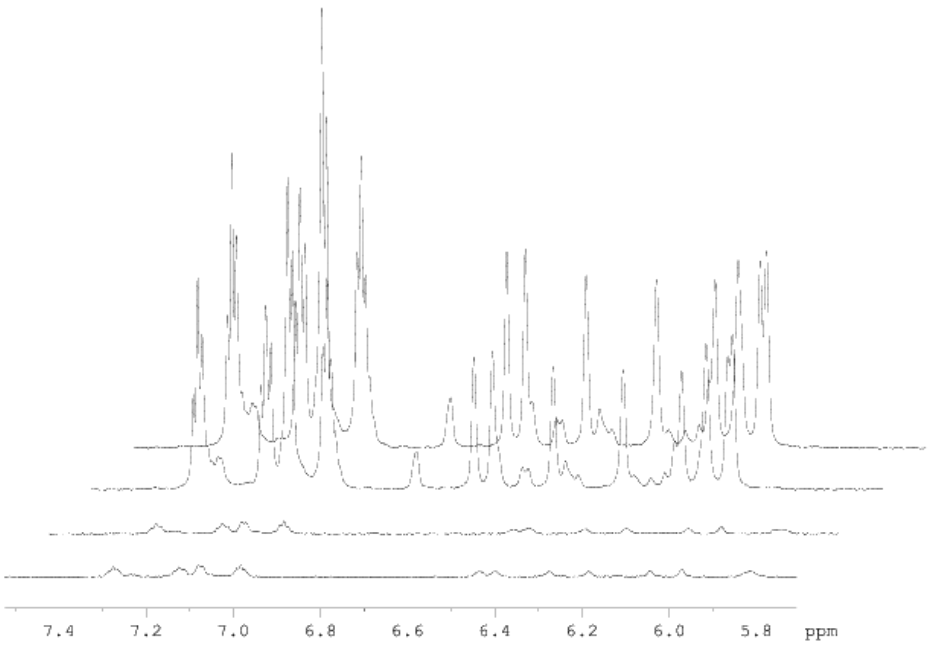


Figure A15: NMR spectra stack (*R,R*)-**49aa** aromatic region 20% D_6-DMSO / 80% D_2O [**A**] to $[\mathbf{I}]_{max}$

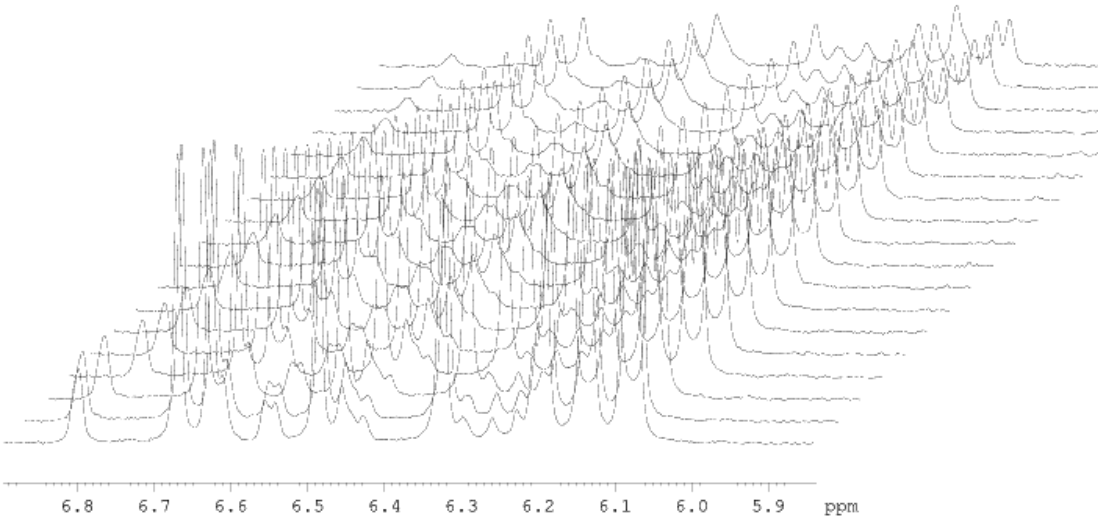


Figure A16: NMR spectra stack (*R,R*)-**49aa** aromatic region 20% D_6-DMSO / 80% D_2O $[\mathbf{I}]_{max}$ to [**P**].

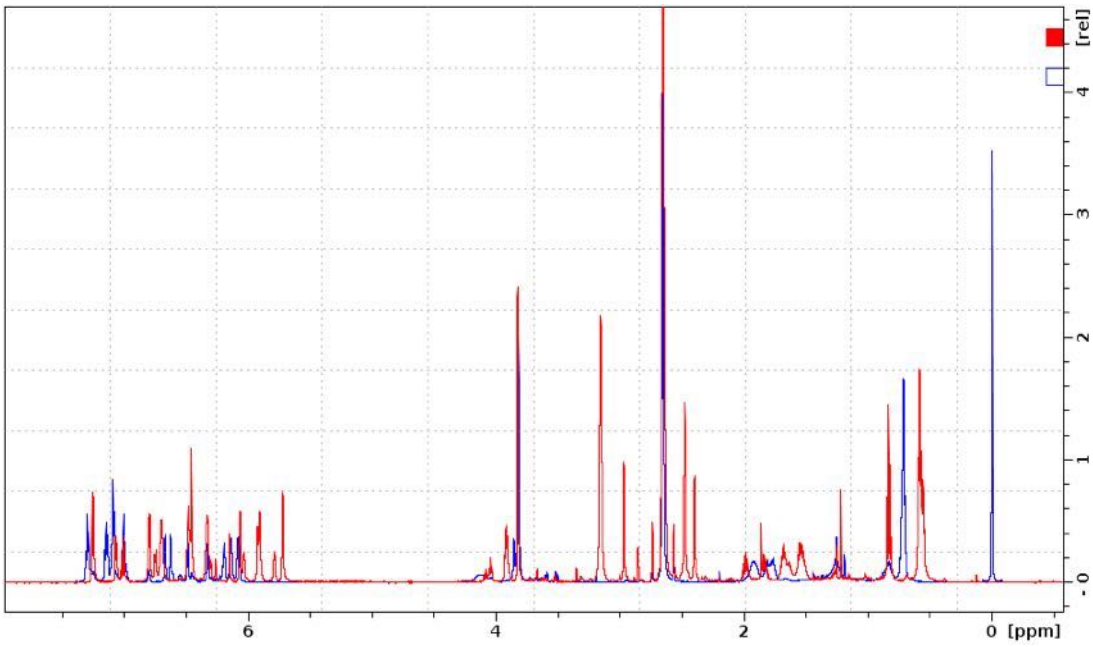


Figure A17: NMR spectrum stack (*rac/meso*)-**49aa** (blue line) at $[\mathbf{I}]_{max}$ *vs* free cyclopentadienyl tautomers (red line) in 20% D_6-DMSO / 80% D_2O.

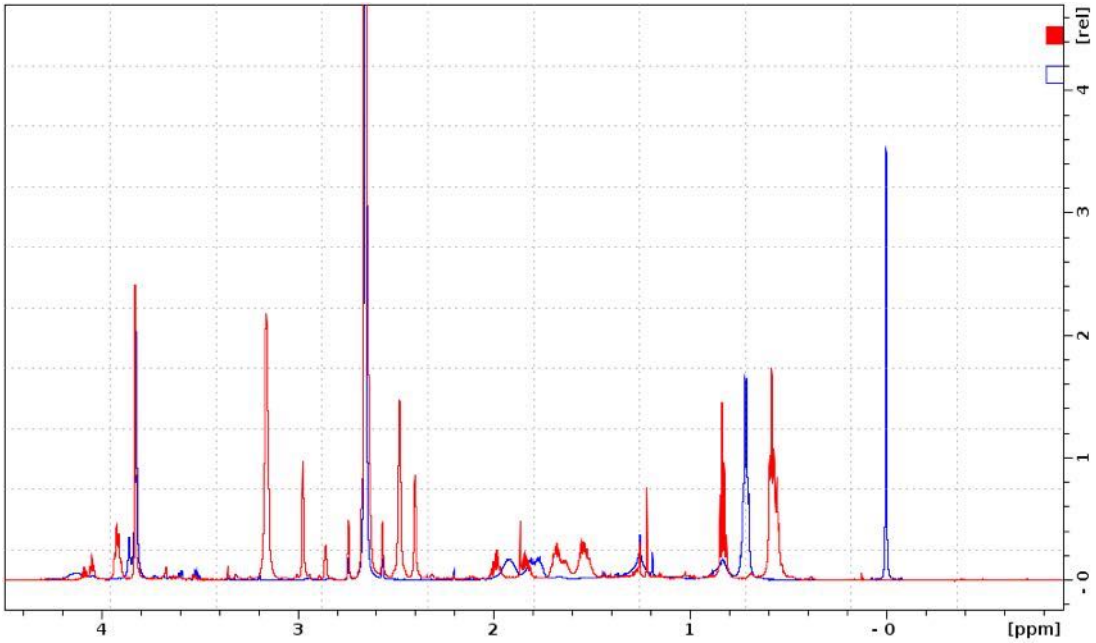


Figure A18: NMR spectrum stack 0 ppm – 4.5 ppm (*rac/meso*)-**49aa** (blue line) at $[\mathbf{I}]_{max}$ *vs* free cyclopentadienyl tautomers (red line) in 20% D_6-DMSO / 80% D_2O.

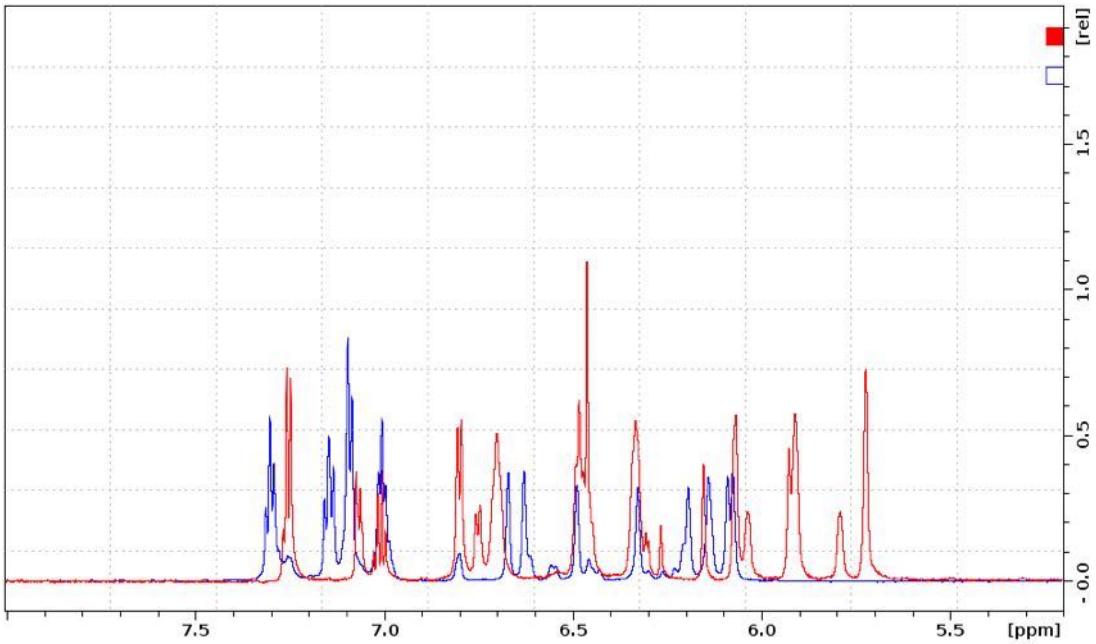


Figure A19: NMR spectrum stack 5 ppm – 8 ppm (*rac/meso*)-**49aa** (blue line) at $[I]_{max}$ *vs* free Cp tautomers (red line) in 20% D_6-DMSO / 80% D_2O.

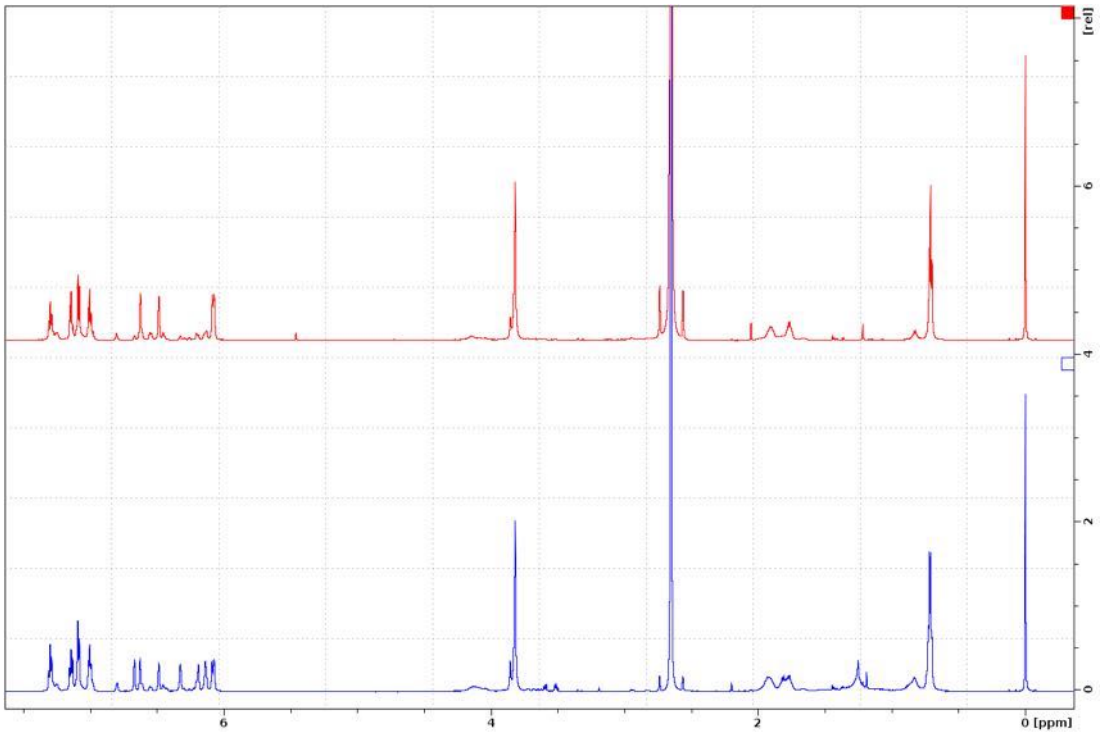


Figure A20: NMR spectra (*rac/meso*)-**49aa** (blue line) at $[\mathbf{I}]_{max}$ *vs* (*R/R*)-**49aa** at $[\mathbf{I}]_{max}$ (red line) in 20% D_6-DMSO / 80% D_2O.

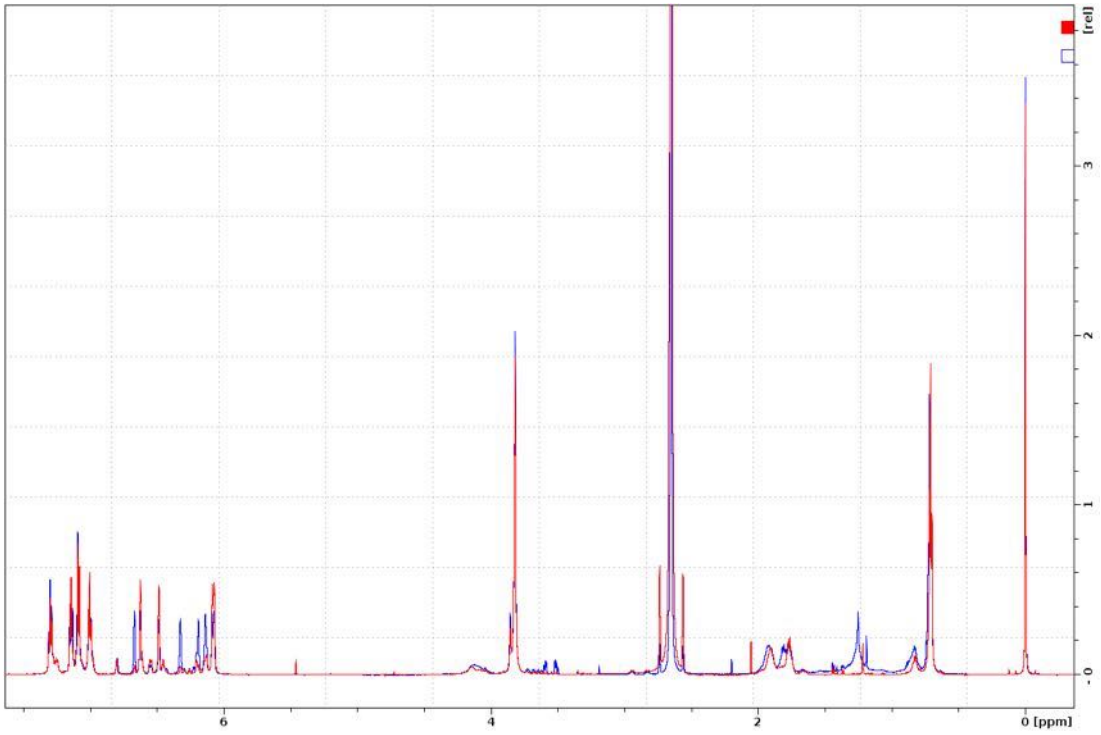


Figure A21: NMR spectrum stack (*rac/meso*)-**49aa** (blue line) at $[\mathbf{I}]_{max}$ *vs* (*R/R*)-**49aa** at $[\mathbf{I}]_{max}$ (red line) in 20% D_6-DMSO / 80% D_2O.

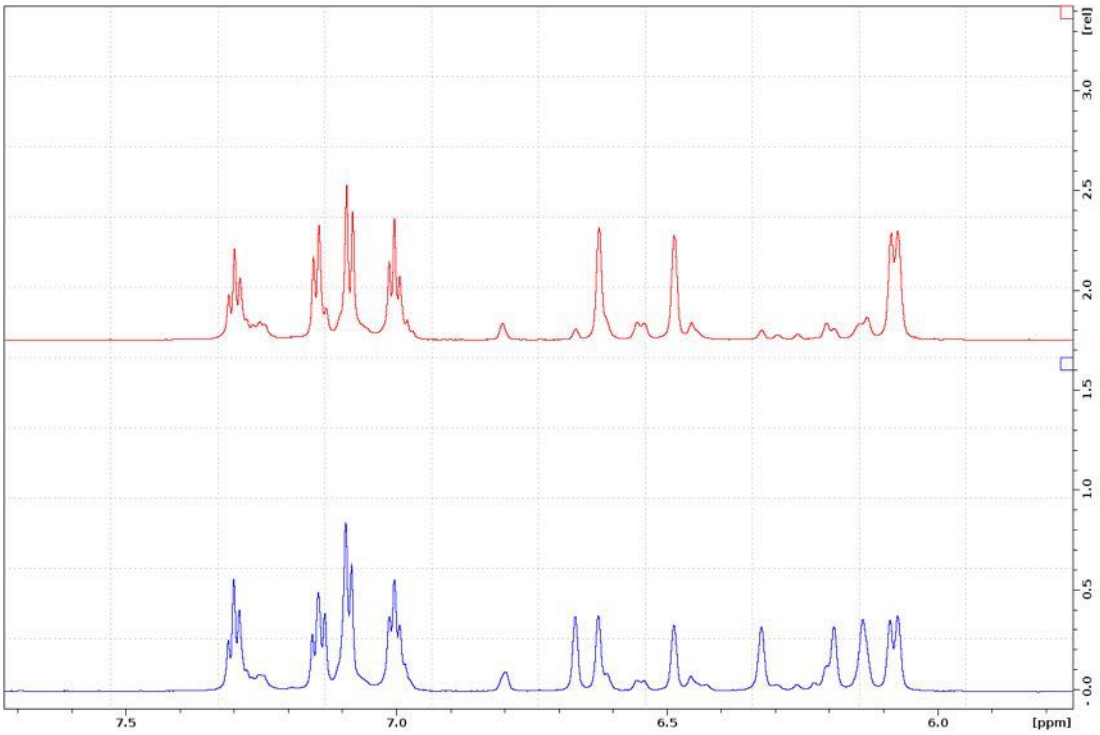


Figure A22: NMR spectra aromatic region (*rac/meso*)-**49aa** (blue line) at $[\mathbf{I}]_{max}$ *vs* (*R/R*)-**49aa** at $[\mathbf{I}]_{max}$ (red line) in 20% D_6-DMSO / 80% D_2O.

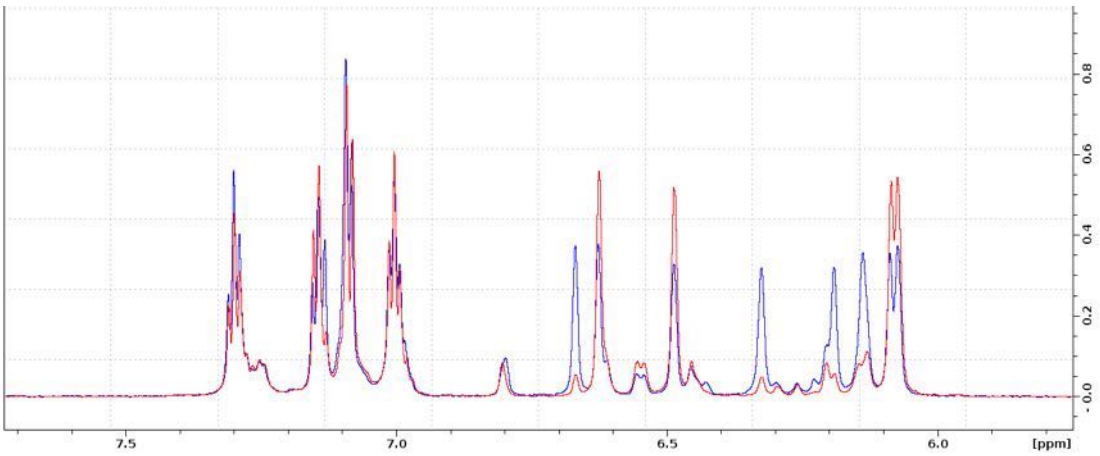


Figure A23: NMR spectra stack aromatic region (*rac/meso*)-**49aa** (blue line) at $[\mathbf{I}]_{max}$ *vs* (*R/R*)-**49aa** at $[\mathbf{I}]_{max}$ (red line) in 20% D_6-DMSO / 80% D_2O.

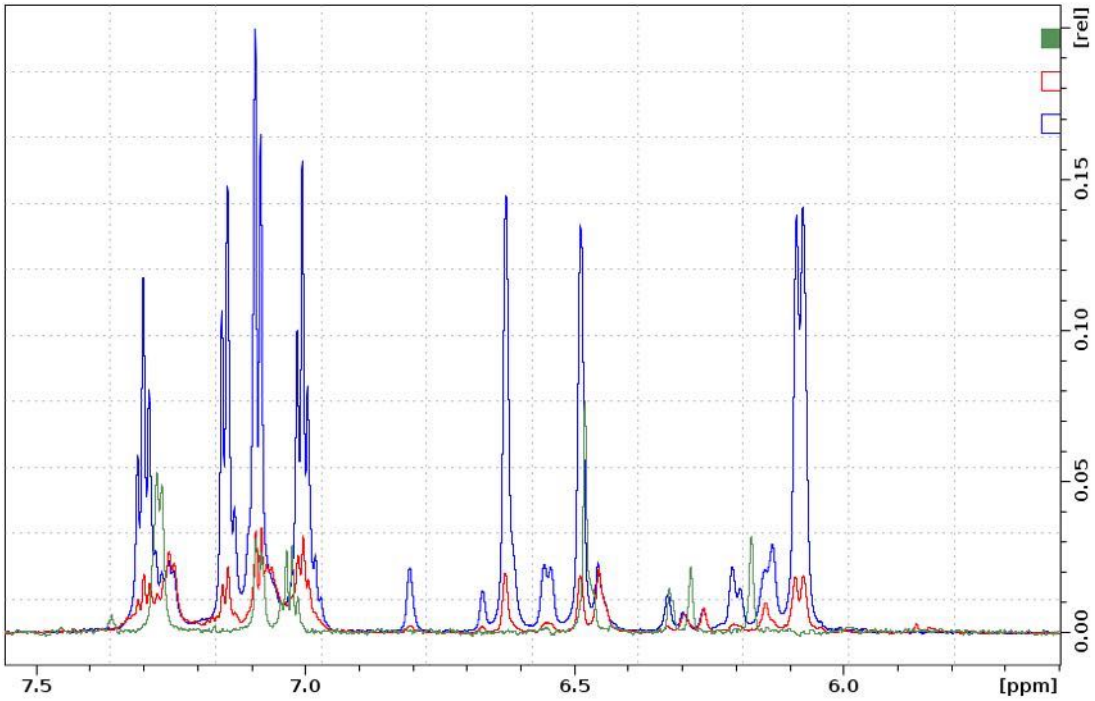


Figure A24: NMR spectra stack aromatic region (*R,R*)-**49aa** (blue line) at $[I]_{max}$ *vs* (*R/R*)-**49aa** at $[I]_p$ (red line) *vs* free cyclopentadienyl tautomers (green line) in 20% D_6-DMSO / 80% D_2O.